



**Water–swellable Rubber Based on Hydroxyethylcellulose Grafted
Polyacrylamide and Epoxidized Natural Rubber Blends**

Ajaman Adair

**A Thesis Submitted in Partial Fulfillment of the Requirements for
the Degree of Doctor of Philosophy in Polymer Technology**

Prince of Songkla University

2022

Copyright of Prince of Songkla University



**Water–swellable Rubber Based on Hydroxyethylcellulose Grafted
Polyacrylamide and Epoxidized Natural Rubber Blends**

Ajaman Adair

**A Thesis Submitted in Partial Fulfillment of the Requirements for
the Degree of Doctor of Philosophy in Polymer Technology**

Prince of Songkla University

2022

Copyright of Prince of Songkla University

Thesis Title Water–swellable Rubber Based on Hydroxyethylcellulose
Grafted Polyacrylamide and Epoxidized Natural Rubber Blends

Author Mr. Ajaman Adair

Major Program Polymer Technology

Major Advisor:

.....
(Assoc. Prof. Azizon Kaesaman)

Examining Committee:

.....Chairperson
(Asst. Prof. Dr. Surat Areerat)

Co-advisors:

.....
(Assoc. Prof. Dr. Pairote Klinpituksa)

.....Committee
(Assoc. Prof. Azizon Kaesaman)

.....Committee
(Assoc. Prof. Dr. Pairote Klinpituksa)

.....Committee
(Asst. Prof. Dr. Sitisaiyidah Saiwari)

.....Committee
(Asst. Prof. Dr. Bencha Thongnuanchan)

The Graduate School, Prince of Songkla University, has approved this thesis as partial fulfillment of the requirements for the Doctor of Philosophy Degree in Polymer Technology

.....
(Prof. Dr. Damrongsak Faroongsarng)
Dean of Graduate School

This is to certify that the work here submitted is the result of the candidate's own investigations. Due acknowledgment has been made of any assistance received.

.....Signature

(Assoc. Prof. Azizon Kaesaman)

Major Advisor

.....Signature

(Mr. Ajaman Adair)

Candidate

I hereby certify that this work has not been accepted in substance for any other degree, and is not being currently submitted in candidature for any degree.

.....Signature

(Mr. Ajaman Adair)

Candidate

ชื่อวิทยานิพนธ์	ยางบวมน้ำจากไฮดรอกซีเอทิลเซลลูโลสกราฟต์ด้วยพอลิอะคริลาไมด์ผสม ยางธรรมชาติอีพอกซีไดซ์
ผู้เขียน	นายอชมาน อาแด
หลักสูตร	เทคโนโลยีพอลิเมอร์
ปีการศึกษา	2564

บทคัดย่อ

วัตถุประสงค์ของการวิจัยคือการเตรียมยางบวมน้ำจากการผสมกราฟต์โคพอลิเมอร์ของไฮดรอกซีเอทิลเซลลูโลส (HEC) กับพอลิอะคริลาไมด์ (PAM) และยางธรรมชาติอีพอกซีไดซ์ (ENR) ซึ่งประกอบด้วย 2 ส่วนหลักคือ 1) สังเคราะห์กราฟต์โคพอลิเมอร์ในสภาวะสารละลาย พอลิเมอร์บวมน้ำสูง (SAPs) และพอลิเมอร์บวมน้ำสูงคอมพอสิต (SAPCs) สามารถเตรียมได้จากปฏิกิริยากราฟต์โคพอลิเมอร์เซชันของพอลิอะคริลาไมด์บนไฮดรอกซีเอทิลเซลลูโลส โดยใช้พอแทสเซียมเปอร์ซัลเฟต (KPS) เป็นสารริเริ่มปฏิกิริยาและ เอ็น เอ็น เมทิลีนบิสอะคริลาไมด์เป็นสารเชื่อมขวางขอบเขตของปฏิกิริยาการกราฟต์โคพอลิเมอร์เซชันสามารถประเมินจากปริมาณร้อยละผลผลิตการกราฟต์ (%GY) และร้อยละประสิทธิภาพการกราฟต์ (%GE) ที่อัตราส่วนไฮดรอกซีเอทิลเซลลูโลสต่อพอลิอะคริลาไมด์ (HEC/AM) ต่าง ๆ โดยกำหนดอัตราส่วนไฮดรอกซีเอทิลเซลลูโลสต่อพอลิอะคริลาไมด์ที่บวมน้ำสูงสุด ศึกษาอิทธิพลของพารามิเตอร์อื่นๆ ในปฏิกิริยาการกราฟต์ เช่น ปริมาณสารริเริ่มและความเข้มข้นของสารเชื่อมขวาง รวมถึงอุณหภูมิและเวลาของปฏิกิริยาการกราฟต์โคพอลิเมอร์เซชัน นอกจากนี้มีการทดสอบผลของปริมาณฟิลเลอร์ต่อความสามารถในการบวมน้ำของพอลิเมอร์บวมน้ำสูงและพอลิเมอร์บวมน้ำสูงคอมพอสิต ข้อมูลทางฟูเรียสทรานสฟอร์มอินฟราเรดใช้ยืนยันการกราฟต์ของพอลิอะคริลาไมด์บนไฮดรอกซีเอทิลเซลลูโลส โดยที่สัญญาณช่วงกว้างของการสั่นแบบยืดของ -OH ใน HEC ที่ 3560-3320 cm^{-1} เปลี่ยนเป็นสัญญาณแคบขึ้นผนวกกับแถบไหล่ที่ 3195 cm^{-1} เนื่องจากการยืดแบบสั่น -NH ในเอไมด์ ของโคพอลิเมอร์ สัญญาณสูงของ HEC ที่ 1020 และ 1059 cm^{-1} หายไปเนื่องจาก -C-OH เปลี่ยนเป็น -C-O-C- ในกราฟต์โคพอลิเมอร์ ความสามารถในการบวมน้ำของ SAPs และ SAPCs ขึ้นอยู่กับพารามิเตอร์ที่แตกต่างกันและความสามารถในการบวมน้ำสูงสุดคือ 426 กรัมต่อกรัมและ 538 กรัมต่อกรัมสำหรับ SAPs และ SAPCs ตามลำดับ 2) เตรียมยางบวมน้ำด้วยการผสมเชิงกลของยางธรรมชาติอีพอกซีไดซ์ (ENR) และ SAPC กับชุดสารวัลคาไนซิงในเครื่อง

ผสมแบบปิด (Brabender Plasticorder) ที่ 40° C และความเร็วโรเตอร์ 60 รอบต่อนาที ในกรณีนี้ SAPC ได้สังเคราะห์มาจาก SAP และเบนโทไนท์ ศึกษาพฤติกรรมการบวมของน้ำลำดับที่หนึ่งของยางบวมน้ำจากยางธรรมชาติอีพอกซีไดซ์ที่มีระดับอีพอกซีเดชันแตกต่างกัน พบว่า ยางบวมน้ำที่มีอีพอกซีเดชันโมลร้อยละ 50 (ENR-50) ให้การบวมน้ำสูงกว่าและน้ำหนักหลังบวมน้ำน้อยกว่า ดังนั้นจึงเลือก ENR-50 เป็นเมทริกซ์ในการเตรียมยางบวมน้ำในการศึกษาผลของปริมาณ SAPC (0, 5, 10, 15 และ 20 phr) ผลการวิจัยพบว่า การบวมน้ำและน้ำหนักที่หายไปเพิ่มขึ้นตามปริมาณ SAPC ที่เพิ่มขึ้น ในขณะที่ความต้านทานแรงดึง การยืดตัว ณ จุดขาด และความหนาแน่นของการเชื่อมขวางลดลงตามปริมาณ SAPC ที่เพิ่มขึ้น อย่างไรก็ตามพบว่าค่าโมดูลัสเพิ่มขึ้นตามการเพิ่มปริมาณ SAPC จากนั้นนำยางบวมน้ำจาก ENR-50/SAPC และสารวัลคาไนซ์ ที่ให้ผลพฤติกรรมการบวมน้ำดีที่สุดมาผสมกับพอลิไวนิลแอลกอฮอล์ (PVA) ที่ปริมาณ PVA เท่ากับ 0, 0.5, 1, 5, 10 phr ผลการทดสอบพบว่า การบวมน้ำของยางบวมน้ำเพิ่มขึ้น แต่การหายไปของน้ำหนักลดลง ตามปริมาณ PVA ที่เพิ่มขึ้น นอกจากนี้พบว่าคุณสมบัติเชิงกลของยางบวมน้ำลดลงตามปริมาณ PVA ที่เพิ่มขึ้น

Thesis Title	Water–swellable Rubber Based on Hydroxyethyl cellulose Grafted Polyacrylamide and Epoxidized Natural Rubber Blends
Author	Ajaman Adair
Major Program	Polymer Technology
Academic Year	2021

ABSTRACT

The aim of research was to prepare water-swellable rubber (WSR) based on hydroxyethyl cellulose (HEC) grafted polyacrylamide (PAM) and epoxidized natural rubber (ENR) blends. Research was consisted mainly of 2 parts, 1) to synthesize of grafted copolymer by means of solution radical copolymerization. Superabsorbent polymers (SAPs) and superabsorbent polymers composites (SAPCs) were prepared successfully by solution graft copolymerization of polyacrylamide onto hydroxyethyl cellulose, using potassium persulfate (KPS) as an initiator, and *N, N'*-methylenebisacrylamide (MBA) as a crosslinker. The extent of grafting was evaluated from grafting yield percentage (%GY) and grafting efficiency percentage (%GE) at various HEC/AM ratios and determined optimal ratio. Influences of preparation parameters such as HEC/AM ratios, amount of initiator and crosslinker's concentration, reaction temperature and time, and amount of filler on water swelling capacity of SAPs and SAPCs were also investigated. FTIR determination confirmed that the PAM was successfully grafted onto the HEC backbone, broad band for stretching vibration of –OH (HEC) at 3560-3320 cm^{-1} was changed into sharper with a shoulder band at 3195 cm^{-1} due to -NH stretching vibration in amide of grafted copolymer. The strong band of HEC at 1020 and 1059 cm^{-1} were disappeared due to -C-OH changes to -C-O-C- grafted copolymer. The swelling capacity of SAPs and SAPCs depended strongly on different parameters, and the maximum swelling capacity was 426 g/g and 538 g/g for the SAPs and SAPCs, respectively. 2) to compound the water-swellable rubber by mechanical blending of ENR and SAPC with curative package in an internal mixer (Brabender Plasticorder) at 40° C and rotor speed of 60 rpm. In this case, the SAPC was

synthesized from SAP and bentonite clay. The WSRs with different epoxidation levels were investigated for first water swelling behaviors. It was found that the WSR with 50% mole epoxidation gave higher water absorbency, and lower in weight loss. Therefore, ENR-50 was chosen as the rubber matrix to prepare WSR by blending with SAPC at 0, 5, 10, 15, and 20 phr. The results found that water absorbency, weight loss and modulus increased with increasing SAPC contents, while the tensile strength, elongation at break and crosslink density decreased. Furthermore, a selective WSR prepared from ENR-50, SAPC, and curatives package have been compounded with polyvinyl alcohol (PVA) at 0, 0.5, 1, 5, 10 phr. The results found that increasing PVA content resulted in increased water absorbency but decreased weight loss. Nevertheless, the mechanical properties of the WSR was decreased with increasing PVA contents.

ACKNOWLEDGEMENT

First and foremost, the researcher offers our sincerest gratitude to our adviser, Assoc. Prof. Azizon Kaesaman and Assoc. Prof. Dr. Pairote Klinpituksa co-advisor, whose always encouragement, guidance and support from the initial to the final level of research and enabled me to develop an understanding of the criteria of polymer technology. Without their guidance with persistent and longtime help this research would probably not have been achievable and practicable. The head of polymer technology program for giving a convenient and providing the tool without any confusedness, giving me the biggest opportunity to investigate an information system in polymer technology, and the processed that was discussed to me, thanks to all lecturers in polymer technology for having preferable guidance. To my parents, I would like to thank to them for supporting satisfied my daily lives, for always standing beside me at nearly all times of my need, even under un-condition state, their prosperity and love for me. Thanks to Head program Asst. Prof. Dr. Sitisaiyidah Saiwari, for always reminding what professional ethics is that made me a better individual, for the suggestions that has given to me and her encourages to be global competitive students. To all polymer technology students for guiding me and making my research successful and reliable

Ajaman Adair

TABLE OF CONTENTS

	Page
บทคัดย่อ	v
ABSTRACT	vii
ACKNOWLEDGEMENT	ix
TABLE OF CONTENTS	x
LIST OF TABLES	xiv
LIST OF FIGURES	xvi
CHAPTER 1 INTRODUCTION	1
1.1 Generals	1
1.2 Objectives	4
1.3 Scope of Research Work	5
1.4 Expected Advantages.....	6
CHAPTER 2 LITERATURE SURVEY	7
2.1 Introduction.....	7
2.2 Definition and preparation superabsorbent polymer and composite	11
2.3 Natural rubber	23
2.4 Modified Natural Rubber.....	27
2.5 Epoxidised Natural Rubber.....	29
2.6 Superabsorbent polymer and superabsorbent polymer composite	32
2.7 Cellulose and hydroxyethyl cellulose	37
2.8 Grafting of hydroxyethyl cellulose	39
2.9 Vinyl monomers grafted hydroxyethyl cellulose	43
2.10 Initiator system for graft copolymerization of cellulose and cellulose ethers	44
2.11 Water-swellaable rubbers	47
2.12 Blends of SAP or SAPC with rubber.....	51

TABLE OF CONTENTS (Cont.)

	Page
CHAPTER 3 MATERIALS AND METHODOLOGY	61
3.1 Materials	61
3.1.1 Hydroxyethyl cellulose.....	61
3.1.2 Acrylamide (AM)	62
3.1.3 Potassium persulfate (KPS).....	62
3.1.4 <i>N, N'</i> -methylenebisacrylamide (MBA)	62
3.1.5 Acetone.....	63
3.1.6 Toluene	63
3.1.7 Epoxidized natural rubber (ENR-25) and (ENR-50).....	64
3.1.8 Zinc oxide	64
3.1.9 Stearic acid	64
3.1.10 <i>N</i> -tert-butyl-2-benzothiazyl sulfonamide (TBBS)	65
3.1.11 Sulfur	65
3.1.12 Polyvinyl alcohol (PVA)	65
3.1.14 Methanol.....	65
3.1.15 Ethanol.....	66
3.1.16 Sodium hydroxide	66
3.2 Instruments	66
3.2.1 Internal mixer	66
3.2.2 Mooney Viscometer	67
3.2.3 Fourier Transform Infrared Spectrometer (FTIR)	67
3.2.4 X-ray diffraction.....	68
3.2.5 Thermogravimetry (TGA)	68
3.2.6 Scanning electron microscope	69
3.2.7 Moving Die Reometer (MDR)	69
3.2.8 Testing Machine	70
3.2.10 Thermogravimetric Analyzer (TGA)	70
3.2.11 Hardness Tester	71

TABLE OF CONTENTS (Cont.)

	Page
3.3 Methodology	71
3.3.1 Preparation and characterization of SAP and SAPC	71
3.3.2 Effect of bentonite clay for preparation of superabsorbent polymer composite (SAPC)	79
3.4 Preparation of water-swellaable rubber (WSR)	81
3.4.1 Effect of ENR and ENR/SAPC blends	81
3.4.2 Effect of ENR and SAPC blend ratios on swelling capacity of WSR..	84
3.4.3 Effect of PVA as compatibilizer on swelling capacity of WSR.....	84
3.5 Swelling measurements	85
3.6 Tensile properties.....	86
3.7 Determination of the crosslink density	86
3.8 Cure characterization	87
3.9 Morphological properties.....	88
3.10 Thermal properties.....	88
CHAPTER 4 RESULTS AND DISCUSSION.....	89
4.1 Preparation of superabsorbent polymer	89
4.1.1 Effect of HEC/AM ratio on grafting and water swelling capacity	94
4.1.2 Infrared spectroscopy	98
4.1.3 Effect of initiator amount on swelling capacity	102
4.1.4 Effect of crosslinking agent concentration on swelling capacity	103
4.1.5 Influences of alkaline hydrolysis temperature and time on swelling capacity	104
4.1.6 Effect of bentonite clay loading on swelling capacity.....	105
4.2 Preparation of WSR.....	106
4.2.1 Types of Rubber and SAPC contents of various WSR	106
4.2.2 Effect of compatibilizer on swelling behaviors and mechanical properties.....	120

TABLE OF CONTENTS (Cont.)

	Page
CHAPTER 5 CONCLUSIONS.....	131
5.1. Generals	131
5.2 Preparation of SAP and SAPC	131
5.2 Formulation of Water Swellable Rubber (WSR).....	132
REFERENCES.....	134
APPENDIX	146
VITAE	179

LIST OF TABLES

		Page
Table 2.1	Composition of components in raw natural rubber	24
Table 2.2	Classification of modification reactions of the cis-1,4-polyisoprene chain	26
Table 2.3	Typical properties of ENR and SMR L	30
Table 2.4	Comparative air permeability of general rubber at 30° C	31
Table 3.1	Various parameters on graft copolymerization	72
Table 3.2	HEC/ AM ratios of graft copolymerization	73
Table 3.3	Conditions for the saponification of SAP and SAPC	76
Table 3.4	Parameters of saponified of SAPs.	76
Table 3.5	Various contents of KPS incorporate on graft copolymerization	78
Table 3.6	Various concentration of MBA parameter on graft copolymerization of SAPs	79
Table 3.7	Bentonite loading on graft copolymerization of SAPC	80
Table 3.8	Conditions for alkaline hydrolysis of SAPC	81
Table 3.9	Formulation of water-swellaable rubber with different types of epoxidized natural rubber	82
Table 3.10	Formulation of WSR with varying SAPC loadings	84
Table 3.11	Compounding formulation of WSR with varying amounts of PVA as compatibilizers	85
Table 4.1	Effect of HEC/AM ratios on the grafting form of SAP	95
Table 4.2	Formulation of WSR with varying SAPC loadings	108
Table 4.3	Cure characteristics (ts1, tc90, CRI, M _L , M _H and M _H -M _L) of WSR with and without SAPC	117
Table 4.4	Shore A hardness of WSR recipes at different loading of SAPC	120

LIST OF TABLES (Cont.)

	Page
Table 4.5 ts1, tc90, CRI, M _L , M _H and M _H -M _L from WSR at different contents of PVA, SAPC 15 phr, ZnO 6 phr, Stearic acid 0.5 phr, TBBS 1 phr and Sulfur 2 phr	125
Table 4.6 Tensile properties of WSR filled with different PVA contents	126
Table 4.7 Shore A hardness of WSR with PVA formulation, WSR prepared by blending ENR-50 and SAPC 15 phr, ZnO 6 phr, Stearic acid 0.5 phr, TBBS 1 phr and Sulfur 2 phr	127
Table 4.8 Shows cross-linked density of WSR at different PVA contents	128

LIST OF FIGURES

		Page
Figure 2.1	Hydrogel classification based on their original sources	13
Figure 2.2	Mechanism of grafted polymerization polyacrylamide onto Guaran using ceric ammonium initiation	14
Figure 2.3	Mechanism of graft copolymerization poly-2-hydroxyethylmethacrylate onto carrageenan backbone inducing by ceric ammonium nitrate	15
Figure 2.4	Preparation of chitin-PAA hydrogel	16
Figure 2.5	Hydrogel classification	18
Figure 2.6	Beta-1,4-glycosidic linkage of cellulose and alpha-1,4-glycosidic linkage of starch	19
Figure 2.7	Mechanism of cellulose-g-P(AA-co-AM-co-AMPS)/MMT superabsorbent hydrogel	21
Figure 2.8	Three-dimensional polymerization hydrogel	22
Figure 2.9	Ready-made water-soluble polymer hydrogel	23
Figure 2.10	Chemical structure of natural rubber	24
Figure 2.11	Natural rubber to epoxidized natural rubber (ENR)	28
Figure 2.12	Types of modified NR	29
Figure 2.13	Mechanism of epoxidation	30
Figure 2.14	Oil resistance of ENR-25 and ENR-50 compared to NR after 70 hours in ASTM No.1, 2, and 3 oils	32
Figure 2.15	Swelling mechanism of superabsorbent polymer	33
Figure 2.16	SAP chains (a) before and after swelling and (b) sodium polyacrylate networks	34
Figure 2.17	Reactant and pathways to prepare synthetic SAP	35
Figure 2.18	Structure of hydroxyethyl cellulose	39
Figure 2.19	Reaction of toluene diisocyanate to synthesize monoblocked diisocyanate	41

LIST OF FIGURES (Cont.)

	Page
Figure 2.20 Modified HEC-g- <i>N</i> -isopropylacrylamide temperature sensitive hydrogel	42
Figure 2.21 Mechanism of grafting acrylonitrile onto starch by ceric ion	45
Figure 2.22 Thermal initiated KPS to generate free radical	46
Figure 2.23 Mechanisms of interaction between CR and silica surface	49
Figure 3.1 Molecular structure of HEC	61
Figure 3.2 Molecular structure of acrylamide	62
Figure 3.3 Molecular structure of KPS	62
Figure 3.4 Molecular structure of MBA	62
Figure 3.5 Molecular structure of acetone	63
Figure 3.6 Molecular structure of toluene	63
Figure 3.7 Molecular structure of ENR-25 and ENR-50	64
Figure 3.8 Molecular structure of stearic acid	64
Figure 3.9 Molecular structure of TBBS	65
Figure 3.10 Molecular structure of PVA	65
Figure 3.11 Internal mixer Brabender plasticorder	66
Figure 3.12 Mooney viscometer	67
Figure 3.13 Fourier transform Infrared spectrophotometer	67
Figure 3.14 X-ray diffractometer	68
Figure 3.15 Thermogravimeter analysis	68
Figure 3.16 Scanning electron microscope	69
Figure 3.17 Moving Die Rheometer	69
Figure 3.18 Testing machine	70
Figure 3.19 Thermogravimetric analyzer	71
Figure 3.20 Hardness tester	71
Figure 3.21 Grafted copolymerization and separation steps	74

LIST OF FIGURES (Cont.)

		Page
Figure 3.22	Compounding procedures for WSR preparation without compatibilizer (A) and with compatibilizer (B)	83
Figure 4.1	Graft copolymerization of PAM onto HEC without crosslinker	92
Figure 4.2	Graft copolymerization of PAM onto HEC in the presence of crosslinker (a) inter-cellulose chains crosslinking and (b) intra-cellulose chains crosslinking	94
Figure 4.3	Effects of HEC/AM ratio on swelling capacity before and after hydrolysis by 2 M NaOH, [KPS] = 1 g/1.2 g HEC, [MBA] = 0.1 mmol/100 g HEC, temperature = 70o C, time 2 h, agitation speed 100 rpm, and washing 3 times with distilled water	96
Figure 4.4	Hydrogel in amide form prepared from 1/10 HEC/AM ratio, [KPS] = 1 g/1.2 g HEC, [MBA] = 0.1 mmol/100 g HEC, temperature = 70o C, time 120 minutes, agitation speed 100 rpm	97
Figure 4.5	HEC-g-PAM in carboxylate form after hydrolysis with 2M NaOH at 70o C for 60 minutes	97
Figure 4.6	HEC-g-PAM in assortment of functional forms after hydrolysis with 2M NaOH at 70o C for 60 minutes and washing several times with distilled water	98
Figure 4.7	FTIR spectra of (a) HEC and (b) HEC-g-PAM before alkaline hydrolysis	99
Figure 4.8	Propose grafting copolymerization reaction between HEC and PAM	100

LIST OF FIGURES (Cont.)

		Page
Figure 4.9	FTIR spectra of (a) HEC-g-PAM and HEC-g-PAM after alkaline hydrolysis were affected by wash cycles with distilled water: (b) washing 1, (c) washing 2, and (d) washing 3	101
Figure 4.10	Effects of KPS on Sw and %GF of SAP at HEC/AM =1/10, MBA = 0.1 mmol/100 g HEC, reaction temperature 60 oC and reaction time 2 hours	102
Figure 4.11	Effects of MBA concentration on swelling capacity at 24 hours of an immersion time	103
Figure 4.12	The influence of hydrolysis temperature on swelling capacity of SAP prepared at HEC/AM =1/10, KPS = 1 g /1.2 g HEC, MBA = 0.1 mmol/100 HEC, and reaction time 120 mins	104
Figure 4.13	Influence of reaction time for alkaline hydrolysis on water swelling capacity of SAP prepared through HEC/AM =1/10, KPS = 1 g /1.2 g HEC, MBA = 0.1 mmol/100 HEC, and reaction time 2 hours.	105
Figure 4.14	Effects of bentonite clay loading on water swelling capacity. HEC/AM (g/g) = 1/10, KPS = 1 g/(1.2 g HEC), [MBA] = 0.1 mmol/(100 g HEC), temperature = 70o C	106
Figure 4.15	Swelling behaviors of WSR-25 and WSR-50 at 30 days of soaking time	107
Figure 4.16	Plot of first water absorbency of WSR containing various SAPC loading with soaking time	109
Figure 4.17	Graphical difference of SAPC loading affecting (%) weight loss of WSR prepared by blending of ENR-50 with various loadings of SAPC after having first water immersion	109
Figure 4.18	Second water absorbency of WSR at various SAPC loading with soaking time	110

LIST OF FIGURES (Cont.)

	Page
Figure 4.19 FTIR spectra of (a) ENR-50, (b) WSR before water absorption and (c) WSR after water absorption, WSR prepared by SAPC loading 15 phr	111
Figure 4.20 Relationship of modulus at 100% and 300% strain for the WSR filled with different SAPC contents	112
Figure 4.21 Tensile strength and elongation at break for the WSR filled with different SAPC contents	113
Figure 4.22 Crosslink density of WSR at different SAPC contents	114
Figure 4.23 Tentative multifunctional groups structure appearing in SAPC	115
Figure 4.24 Cure-curves of WSR at different contents of SAPC	116
Figure 4.25 SEM micrographs of WSR with 15 phr SAPC (A) surface and (B) cross section before and after immersion in water	118
Figure 4.26 SEM micrographs of WSR with 15 phr SAPC: (a) surface (fracture images; magnification x250; scale bar 250 μ m), and (b and c) SEM/EDX of WSR with X-ray mapping of O	119
Figure 4.27 Plot of water absorbency of WSR containing various PVA loading with soaking time, prepared from mechanical blending of 100 phr ENR-50, 15 phr SAPC, 6 phr ZnO, 0.5 phr stearic acid, 1 phr TBBS and 2 phr sulfur	121
Figure 4.28 Weight loss (%) at PVA contents of WSR after first water swelling capacity	122
Figure 4.29 FTIR spectra of (a) ENR-50, (b) WSR with SAPC, (c and d) WSR with PVA loading 5 phr before and after water absorption, WSR prepared by blending ENR-50 and SAPC loading 15 phr, ZnO 6 phr, Stearic acid 0.5 phr, TBBS 1 phr and Sulfur 2 phr	123

LIST OF FIGURES (Cont.)

	Page
Figure 4.30 Cure-curves of WSR at different contents of PVA	124
Figure 4.31 SEM micrographs of WSR with 10 phr PVA (A) surface and (B) cross section before and after immersion in water	129
Figure 4.32 TGA and DGT curves water swellable rubber with 5 phr of PVA	130

CHAPTER 1

INTRODUCTION

1.1 Generals

Natural rubber (NR) is one of the most important natural occurring polymers with a green renewable feedstock which is obtained from the trees of *Hevea Brasiliensis* species. The plants are tapped by producing an incision in the bark of the rubber tree and collecting the sticky milk-like latex which is then refined into usable rubber. The purified form of natural rubber is the chemical structure mostly composed of *cis*-1,4-polyisoprene, which can also be produced synthetically (Hamzah *et al.*, 2012). Natural rubber is generally very stretchy, flexible and extremely waterproof which is allowed to be utilized for various applications and products, as is synthetic rubber.

Water-swallowable rubber (WSR) is a functional material with elastic sealing and water-swelling properties. It is mainly compounded from natural rubber, modified natural rubber or synthetic rubber with super-absorbent polymers (SAP) and organic/inorganic salts and/or any saline materials. The SAP is a vital ingredient to raise the absorption of water into the rubber matrix to cause swelling (Kim, 2014). The swelling mechanism of swallowable rubbers in aqueous fluids is illustrated with SAPs or SAPCs that is dispersed into elastomers. The SAP is a polyelectrolyte and swells due to osmotic pressure effects (Elliott, 2003). Water molecules placed around polymer migrate into the network across a diffusion gradient of the polymer backbone. The polymer chains cannot be straightened due to the cross-linking, the polymers expand as water moves into the network leading to swelling of the rubber matrix. There are two main procedures possible to prepare WSR, firstly by means of graft polymerization of hydrophilic/loving water monomers onto natural rubber or synthetic rubber (Wang *et al.*, 2015). The second procedure mostly used to prepare SWR, is by means of mechanical mixing of hydrophobic rubbers with hydrophilic superabsorbent polymers (SAPs) or superabsorbent polymer composites (SAPCs). Poor dispersion amongst phase of hydrophilic SAP or SAPC and hydrophobic rubber is one of the general problems that always occur in the blending system due to different polarities. However,

the problems can be solved by increasing the polarity of rubber and/or decreasing hydrophilicity of polymers. This conforms with various studies which report that the introduction of compatibilizer can improve phase dispersion through covalently bonding between rubber and hydrophilic polymers (Nakason *et al.*, 2013; Zhang *et al.*, 2001).

In the 1980s, water absorption materials were derived from cellulosic or fiber-based products. Choices were tissue paper, cotton, sponge, and fluff pulp. These types of materials had a low water absorption capacity up to 20 times their initial weight. In the 1960s, the water conservation materials were firstly invented by the United States Department of Agriculture for soils amendment. They worked hard and developed a polymer based on the grafting of polyacrylonitrile onto starch backbone. This new material can absorb a large volume of water more than 400 times its weight without releasing liquid fluids even under high pressure (Kiatkamjornwong, 2007). The SAPs were originally synthetic crosslinked polyacrylic acid and polyacrylated derivatives of petroleum products which have a tendency of increasing cost and endless lack. They are able to absorb large quantities of water without dissolving, even exceeding 1,000 folds their dry weight (Wack *et al.*, 2007). Due to its excellent swelling behaviors, the SAPs have prompted much attention on both fields of academic and industries to produce SAP for utilizing worldwide. For example, they are widely proposed for horticultural purposes over the last five decades with the idea to improve water availability for plants (Zohuriaan-Mehr *et al.*, 2008). Several benefits of SAPs have been described corresponding to applications such as in disposable baby diapers, in agriculture as a soil amendment (Cannazza *et al.*, 2014), in controlled release of drugs as a carrier (Chang, 2011), in coal dewatering (Peer *et al.*, 2003; Devasahayam *et al.*, 2015), in waste water treatment (Wang *et al.*, 2011) and in cosmetic and absorbent pads (Todd *et al.*, 2008), as well as in gel electrolyte membranes (Navarra *et al.*, 2015). Various SAP or SAPC have been used to prepare water swellable rubber by dispersing them into natural rubber or synthetic rubber (Nakason *et al.*, 2012, Li *et al.*, 2013; Zhang *et al.*, 1999; Wang *et al.*, 2002; Liu *et al.*, 2006; Dehbari *et al.*, 2015). According to their original resources SAPs are definitely divided into three main types, namely natural polymers (polysaccharide derivatives and amino acid derivatives), semi-synthetic polymers (cellulosic primitive derivatives), and synthetic polymers

(Mikkelsen, 1994). Various SAPs have been commercialized, but most of these are synthetic polyacrylate-based products, non-degradable and are considered as potential pollutants for the environments. Due to much attention to environment protecting issues, biodegradable SAPs stand actively as a point of interest for potential commercial application in various fields. Biodegradable SAP has attracted more attention in both academics and industries after the first biodegradable SAP from starch grafted polyacrylate was introduced and showed excellent water-swelling capabilities (Kiatkamjornwong, 2007). Although all types of SAP have no direct threat to human life, systematically disposal of synthetic SAPs waste is still a source of environmental pollutants (Nnadi *et al.*, 2011). This problem has prompted polymer technologist to produce SAP with reducing the need to have an actual disposal system. The naturally occurring SAPs are attractive options due to their unique renewability and biodegradability. Amongst them, polysaccharides have been employed due to availability in large feedstock, renewability and biodegradability. Hydroxyethyl cellulose (HEC) is modified cellulose with abundant reactive hydroxyl groups, where they can be grafted with hydrophilic vinyl monomers to produce materials with an excellent property (Lin *et al.*, 2004). HEC is a cellulose ether which is the most readily available in trade. Because one or more hydroxyl protons on the backbone are substituted by ethylhydroxyl group, HEC is expected to have a high level of water retention when compared with cellulose. Various types of SAPs prepared from graft copolymerization of polyacrylamide or polyacrylic acid onto HEC have been reported (Yang *et al.*, 2007; Samaha *et al.*, 2015), but there are no research reports on SAPC preparation from HEC-g-polyacrylamide (PAM)/bentonite and no report on the use of SAPC as a dispersing particle in rubber for a preparation of WSR.

The main aim of this research is to investigate the water swelling capacity and other properties of WSRs prepared by mechanical mixing of epoxidized natural rubber and hydroxyethyl cellulose grafted polyacrylamide/bentonite (SAPC). This thesis consists of two parts involving the following:

- 1) Preparation of SAP and SAPC from HEC-graft-polyacrylamide and bentonite clay filled composite. The HEC was used as a polymer backbone for grafting with polyacrylamide (PAM) in the presence of potassium persulfate (KPS) a thermally radical initiator under solution polymerization. The polymer networks were

constructed using *N, N'*-methylene bisacrylamide (MBA) and overall reaction took place under nitrogen gas atmosphere. The influence of HEC/AM ratios on the percentage of grafting yield (%GY) and grafting efficiency (%GE) was investigated and tested for water swelling capacity. The HEC/AM ratios that gave the highest water swelling capacities were further experimented for an initiator and cross-linker concentration and were measured for water swelling capacity. To enhance the swelling capacity of all final SAP and SAPC, the alkaline hydrolysis was performed using 2M NaOH solution. The influences of reaction time and reaction temperature on water swelling capacity of all final SAP and SAPC were also investigated. FTIR determination was used to confirm the polyacrylamide grafted onto HEC backbone.

2) Preparation of water-swellaable rubber by mechanical blending of ENR, SAPC with other ingredients and the blending procedures were studied. The effect of WSR component on water swelling capacity and mechanical properties were investigated. The level of epoxide mole percentage of rubber, SAPC content and the content of compatibilizer (PVA) on water swelling capacity of WSR were also investigated.

1.2 Objectives

The research aims to achieve the following objectives:

1.2.1 To prepare the superabsorbent polymer (SAP) and bentonite filled composite (SAPC) by means of graft copolymerization of PAM onto HEC backbone.

1.2.2 To prepare the superabsorbent polymer composite (SAPC) at different contents of bentonite clay and to investigate the effect of bentonite clay on water swelling capacity and morphology of SAPC.

1.2.3 To prepare a new water-swellaable rubber (WSR) from the blends of epoxidized natural rubber (ENR) and superabsorbent polymer composite (SAPC) in which the morphology of the blends, water swelling behaviors, and mechanical properties were focused intensively.

1.3 Scope of Research Work

The following is the scope of the research in details:

1.3.1 Synthesis and characterization of superabsorbent polymer and its composite by means of solution graft copolymerization of PAM onto HEC and FTIR determination were used to confirm the successful graft copolymer by comparing the data between the spectra of HEC and its grafted copolymer.

1.3.2 Investigation of the effect of HEC/AM on grafting percentage and grafting efficiency, as well as on water swelling capacity before and after alkaline hydrolysis.

1.3.3 Investigation of the influence of initiator concentration of graft copolymerization on water swelling capacity before and after treating with 2 M NaOH.

1.3.4 Investigation of the cross-linker concentration of graft copolymerization on water swelling capacity before and after treating with 2 M NaOH.

1.3.5 Investigation of the influence of temperature and time for alkaline hydrolysis under the condition of 2 M NaOH, on water swelling capacity.

1.3.6 Investigation of the influence of neutralization of SAP and SAPC after alkaline hydrolysis, by using HCl and distilled water on water swelling capacity.

1.3.7 Investigation of the effect of bentonite clay loading on water swelling capacity.

1.3.8 Preparation of WSR by mechanical blending of ENR with SAPC and other ingredients including ZnO, Stearic acid, TBBS and sulfur vulcanizing agent using internal mixer Brabender plasticorder.

1.3.9 Investigation of the effect of ENR grade (ENR-25 and ENR-50) WSR on swelling behaviors and some mechanical properties.

1.3.10 Investigation of the effect of SAPC loading on swelling behaviors and mechanical properties.

1.3.11 Investigation of the influence of compatibilizer (PVA) and its loading on swelling behaviors and mechanical properties of WSR.

1.4 Expected Advantages

The following are the expected advantages of the research:

1.4.1 To gain new superabsorbent polymer and superabsorbent polymer composite from grafting copolymerization of polyacrylamide onto hydroxyethyl cellulose and bentonite clay incorporation.

1.4.2 To develop new biodegradable water-swellaable natural rubber based on ENR and SAPC blends with a desire water swelling behaviors and mechanical properties.

1.4.3 To evaluate and estimate a new application of water-swellaable rubber based on ENR and SAPC blends.

CHAPTER 2

LITERATURE SURVEY

2.1 Introduction

The definition of the term polymer blend refers to a mixture of at least two macromolecules which are usually polymers or copolymers. The estimation of polymer blends production was 20% of the total consumption of invention polymers, and marketing worldwide for these materials was expected to enhance up to 50 million tons per year (Piorowska, 2013). The blends are usually classified into two types, depending on their structural form as either miscible or immiscible; the miscible blends are defined as homogenous as they have negative free energy of mixing. The blends normally have a dispersion phase sizes in ranges of 2 to 4 nm calculation. Immiscible blends are always mentioned in polymer alloy and have been defined as the blends that are compatibilized with modified surface and stabilized morphologies (Utracki *et al.*, 1989). Compatibilization is a process of modification by means of adding a chemical substance to decrease the interfacial properties of an immiscible polymer blend that results in increasing the stability of their blends. This method is an important process that converts polymer blends into a mixture with the desired set of performance characteristics. The general advantages of the polymer blend can be described in the form of (1) Creating the lowest cost of materials with desired properties. (2) Enhancing the application of engineering materials. (3) Improving the important properties of the blends. (4) Offering the means for industrial polymers and /or another polymer segment, to manage polymer waste (Utracki, 2002). The expansion of polymer application has largely created polymer waste by increasing the need for disposal management. The environmental issue in recent years, global warming has affected directly not only to human, but also plants, animals and other microorganisms. There are many initial causes that have been promoting the change of global temperature, greenhouse effect and destructive ozone and these two are important phenomenon produced mainly by population. The disposal of polymer waste with improper

treatment, can possibly form initial precursor, especially poisonous gas, which has promoted the change of global temperature.

The factors affecting the properties of blended polymers include (Pusca *et al.*, 2010).

1. Particle size, size distribution, and filler content.
2. Particle shape and surface structure.
3. Mechanical properties of the other ingredients (stiffness, strength etc.).
4. Compounding and molding methods used.
5. The bond strength between another ingredient and polymer.
6. Polymer properties

Polymer blends can be classified into various groups, depending on their kind of polymeric materials, whether plastic or polymeric rubber such as rubber-rubber blends, plastic-rubber blends, and plastic-plastic blends. The rubber-rubber blends play an important role in the recent year due to their applications of about 75 % by volume derived from this form of the blends. Apart from that polymer blends, it can be classified according to different parameters such as compatibility, production methods, nature of polymer architecture and a number of the polymer components (Utracki, 2002).

The composite rubbers reinforce rubbers that usually consist of an important rubber matrix including natural rubbers, modified natural rubbers or synthetic rubbers which can be vulcanized at temperatures of up to 150 °C. Generally, the chemical structure of all rubber types consists mainly long chain hydrocarbon with low polarity and is inferior in water swelling capacity. The difference in polarity of rubber phase and water resulting rubber could not be swollen or dissolved in water and other high polarity solvents. To improve water swelling of rubber, a superabsorbent or hydrogels filler is preferably introduced in loading amount of 10 to 120 mass-percentage, based on the mass of the rubber matrix (Nakason *et al.*, 2012; Wang *et al.*, 1997; Jiang *et al.*, 2013; Dehbari *et al.*, 2015; Zhang *et al.*, 1998; Li *et al.*, 2013). In addition, rubbers have an excellent water swelling capacity when its surface was chemically modified by means of graft copolymerization with such hydrophilic monomers (Wang *et al.*, 2015; He *et al.*, 2007). In this work WSRs are targeted to investigate their water swelling behaviors as well as mechanical properties. The factors influencing WSR on water swelling behaviors and mechanical properties include ENR grades, SAPC contents, and

content of compatibilizer. WSRs are compounded using ENR matrix, TBBS, ZnO, stearic acid and superabsorbent polymer composite (SAPC) under sulfur vulcanization. SAPC with high water swelling capacity is produced by grafting copolymerization of acrylamide onto HEC backbone using KPS as an initiator, MBA as a crosslinker and its composite is formed using bentonite clay as a filler. Generally mechanical mixing of polymers results in well dispersed of loving water resin in the rubber matrix and formed homogeneously, but it has poor mechanical properties due to the weak compatibility between rubber and loving water resin. In addition, studies indicated that SAP or SAPC was migrated exactly after having water immersion experiment (Ren *et al.*, 2004; Nakason *et al.*, 2013; Li *et al.*, 2016). To reduce these inferiors, many attempts have been done by researchers, for example, by introducing an obtained grafted copolymer of chloroprene rubber with poly (ethylene glycol) which can improve the compatibility between chloroprene rubber and crosslinked poly (sodium acrylate) (Wang *et al.*, 1998). WSR is prepared by blending chlorinated polyethylene rubber with poly (acrylic acid + acrylic amide) and compatibilized by amphiphilic graft copolymer of chlorinated polyethylene graft polyethylene glycol (CPE-*g*-PEG), and the results indicated that at the proper contents of compatibilizer, the blends had increased the equilibrium swelling ratio and decreased the weight loss ratio, additionally, the mechanical behaviors of the blends were definitely improved (Zhang *et al.*, 2004). According to Nakason and coworkers, three types of WSRs were prepared separately by mechanical blending of natural rubber, Epoxidized NR and melted NR with SAPC, the results indicated that both WSRs from modified NR gave higher water swelling capacities than those of unmodified NR, while they had inferiors to tensile strength, elongation and elongation at break. However, the optimized content of PEO introduction into WSRs lead to give higher water swelling capacity and acceptable tensile strength (Nakason *et al.*, 2013). WSRs were prepared completely by mechanical mixing of chloroprene rubber, precipitated silica, crosslinked sodium polyacrylate, PEO and vulcanizing agent using Banburi two roll mill. The special interaction between CR and precipitated silica had increased water swelling capacity of WSRs, on the other hand, at the proper loading of PEO, water swelling capacity of WSRs was increased as significant as a content of crosslinked sodium polyacrylate (Wang *et al.*, 1998; Wang *et al.*, 1999). The attempt to make dispersion well of the blends can be done by the

following steps, the adjustment of different gaps amongst rubber and SAPC phase, especially in their polarity. The ENR and SAPC had more lesser polarity gaps than NR which forecast the blends having better in compatibility. In order to improve their interaction amongst the phase of the blends, a compatibilizing agent was generally introduced, they worked as a right hand combining to rubber phase and another one to another phase by forming physical interaction and/or chemical reaction through covalent bond and/or hydrogen bond depending on their equivalent structure. In this work, PVA was chosen as a compatibilizer to stabilize the morphology of the blends. The good interaction amongst phase of compatibilizing agent in WSRs, it might be influenced on both water swelling behaviors and mechanical properties. Most of WSRs were prepared by mechanical blending of rubber and SAP or SAPC, generally their properties functioned mainly under the control of all ingredients such as rubber, SAPC and/ or other fillers. Studies indicated SAP or SAPC contents played significant role in influencing water swelling capacities of WSRs, the results showed that the water swelling capacity was strongly increased with increasing SAP or SAPC contents while their mechanical properties decreased. The introduction of fillers, for example, precipitate silica, polyethylene oxide, or other inorganic could sometimes cause a chemical reaction or physical interaction which had led to form great bonding amongst WSRs' phase and occasionally improved both swelling capacity and mechanical property (Wang *et al.*, 1998; Wang *et al.*, 1999; Wang *et al.*, 2002; Nakason *et al.*, 2013). This research aims to produce WSRs from mechanical mixing of ENR, SAPC and other fillers with expectation in high water swelling capacity and great mechanical properties. The main criteria of this research however, is that there were many reasons that the researcher could briefly described, firstly, there is no publication reported about using of SAPC prepared from the grafting copolymerization of PAM onto HEC backbone, as a superabsorbent polymer in compounding WSRs. The second, the poor dispersion of SAPC in polymer blends is an important constraint that is of concern to the researcher, the difference in their polarity between rubber and SAPC, they might have aggregated and phase separation leading have inferiors to water swelling and mechanical properties. To avoid this obstacle, the ENR has been chosen instead of NR for producing WSRs with finally expecting to gain in greatest properties. The chemical modification of NR through converting C=C double bond into the tricyclic either by

means of epoxidation, or by forming epoxidized natural rubber (ENR). The presence of oxygen atom in molecule leading ENR had higher polarity than those of original natural rubber, and it should have an excellent interaction with SAPC, finally they would be given a superior water swelling capacity as well as mechanical properties.

2.2 Definition and preparation superabsorbent polymer and composite

The definition of SAP or SAPC has been defined comprehensively by several researchers, for instance:

A material that has a loosely cross-linked with three-dimensional networks of flexible polymer chains that carry dissociated, ionic functional groups. (Kiatkamjornwong, 2007)

A material that has three-dimensional network of polymers formed by either chemical or physical cross-linking in water (Adel, 2010)

A material that is characterized by network structure with a suitable degree of crosslinking (Ahmed, 2013)

A polymer networks that take in and keep huge quantities of water (Akhtar, 2015)

A material that has crosslinked hydrophilic polymers insoluble in water, but capable of absorbing large amounts of water through a swelling process (Demitri, 2008)

A SAP as hydrogels that can absorb water more than hundred times of their own volume, which was not dissolved but was swollen with water, as they were three-dimensionally crosslinked with hydrophilic functional groups such as alcohol, carboxylic acid, amine, and sulfuric acid (Sohn, 2003).

A material with three-dimensional networks of hydrophilic polymers is connected by chemical and/or physical crosslinking. These networks are composed of homopolymers or copolymers and can absorb and hold a significant amount of water (Kuang *et al.*, 2011).

A material that was a crosslinked network of a hydrophilic polymer that is insoluble in water. In the presence of abundant water, a hydrogel absorbs water to swell to a size much larger than its original size (Chen *et al.*, 1998).

A material that has a particular class of macromolecular gels, obtained by chemical stabilization of hydrophilic polymers in a three-dimensional network, in which the dispersed phase is water, present in substantial quantity (Demitri *et al.*, 2013).

From the overall definition, it can be concluded that superabsorbent polymer (SAP) is a new kind of functional material, usually polymers or copolymers that is a unique crosslinked hydrophilic polymer with three-dimensional networks of loosening polymer chains, obtained through various processes and techniques. The SAPs structure generally contain carboxylic acid, partially neutralized carboxyl groups, carboxamide and carboxylate salt (Kiatkamjornwong, 2007; Wage *et al.*, 2007). They work when the surrounding water is drawn into the polymer network across a diffusion gradient of the polymer backbone. The polymer chains want to straighten but unable due to the cross-linking. Thus, the polymers expand as water moves into the network. The SAPs possess not only a high fluid absorbing capacity but also long period retaining of absorbed fluid even under high temperature and pressure conditions. They are able to absorb large quantities of water to more than 1,000 times of their original weight without dissolving (Nnadi *et al.*, 2011). By right of this, SAPs have attracted continuously attention and annually produced for utilizing in many fields of application, for example, disposable baby diapers, soil amendment in agriculture, wound dressing application in medicine (Tanodekaew *et al.*, 2004; Calo *et al.*, 2015), controlled release of drug carrier, coal dewatering, wastewater treatment (Wang *et al.*, 2011), cosmetic and absorbent pads (Todd and Daniel, 2008). The SAPs originally are synthetic crosslinked polyacrylic acid and polyacrylates which is derived from petroleum products. The production cost depends directly on petroleum management charged, on one hand, the estimation of using a tendency to increase in cost and unstable due to it exhaust and unrenewable characteristics.

SAP hydrogels can be classified into various types, based on different parameters, according to their resource they were classified widely into two categories including natural hydrogel and synthetic hydrogel, the details of each type are shown in Figure 2.1. Furthermore, based on this parameter, some researchers classified sharply into three categories such as a natural hydrogel, synthetic hydrogel, and semi-synthetic hydrogel. According to Mikkelsen (1999) the SAP hydrogel is divided widely into three

types including natural (polysaccharide and their derivatives), semi-artificial or semi-synthetic (cellulosic based their derivatives) and artificial or fully synthetic.

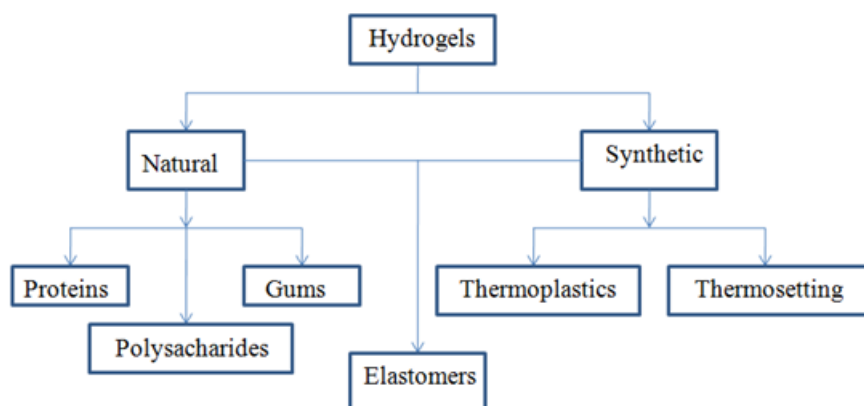
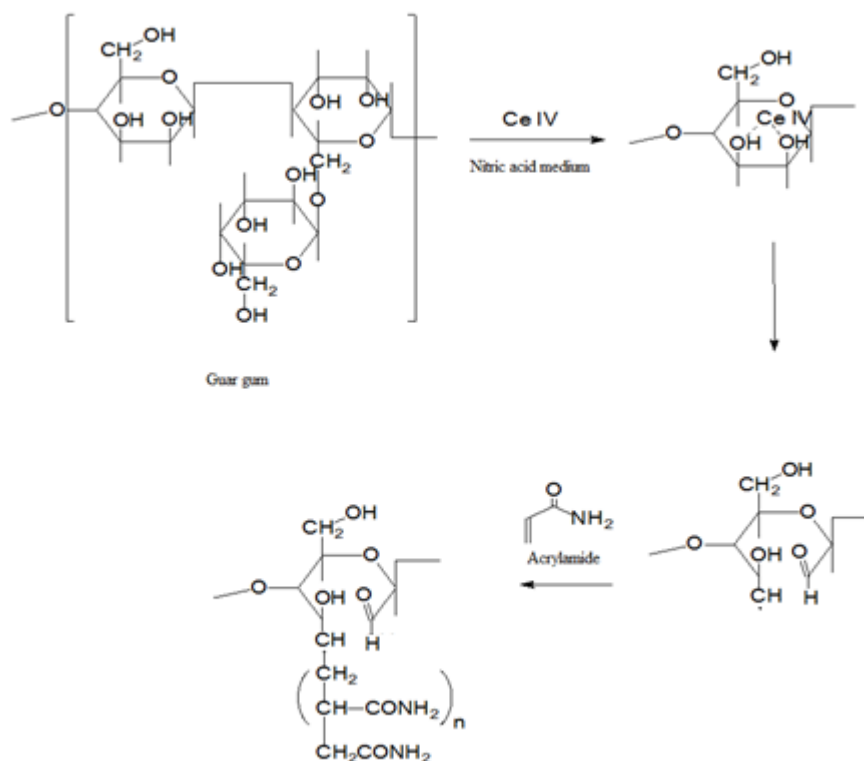


Figure 2.1 Hydrogel classification based on their original sources

For natural SAP hydrogel, they are mostly derived from the naturally occurring polysaccharide such as starch, alginate, and agarose, and proteins such as collagen and gelatin. However, various SAP hydrogel is derived from gums including guar gum, its polysaccharide that composed mainly of galactose and mannose, but its structure is quite different from all those polysaccharides which arranged of linear chain backbone of 1,4- β -linked mannose residues with galactose residues linked to 1,6- β of at every second mannose. Gum has shorter side chain than those polysaccharides leading it to modify easily. Hydrogel microsphere is formed when grafting polyacrylamide onto the guar gum in the presence of glutaraldehyde crosslinker (Soppirath *et al.*, 2002). The obtained hydrogel from grafting polyacrylamide onto guar gum has been introduced by a number of researchers, using Ce (IV) as initiators in the presence of nitric acid medium. The important change in which guar gum transformed into grafted copolymer is proposed briefly in Figure 2.2.



Grafted copolymer

Figure 2.2 Mechanism of grafted polymerization polyacrylamide onto Guaran using ceric ammonium initiation (Soppirath *et al.*, 2002)

According to Sadeghi, (2010) and coworkers, kappa carrageenan grafted poly-2-hydroxymethacrylate was chemically performed through grafting copolymerization of 2-hydroxymethacrylate onto kappa carrageenan backbone using ceric ammonium nitrate as initiator in aqueous solution. There was no difference in reaction mechanism that affected by ceric ion, initially formed a complex between Ce⁴⁺ with two adjacent hydroxyl groups at C₂-C₃ of polymer backbone and further cleaved to form carboxal and reactive macroradical where the graft reaction was propagated forming grafted copolymer. The proposed mechanism is illustrated in Figure 2.3

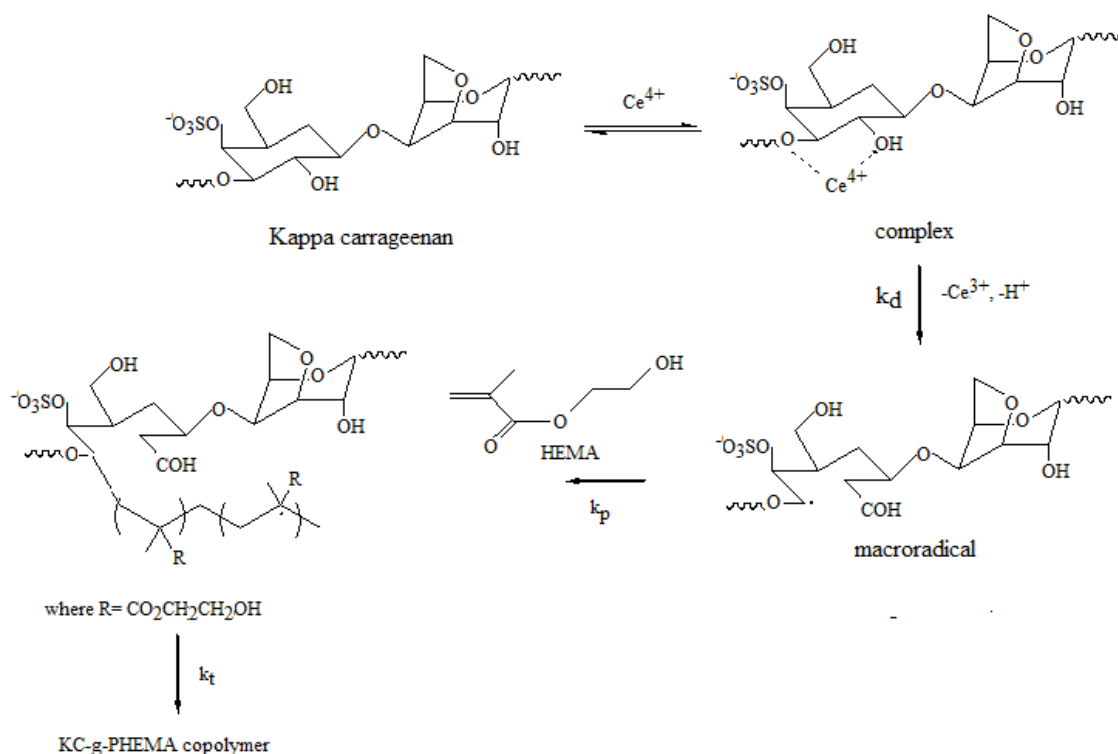


Figure 2.3 Mechanism of graft copolymerization poly-2-hydroxyethylmethacrylate onto carrageenan backbone inducing by ceric ammonium nitrate (Sadeghi et al., 2010)

This important mechanism is also found when polyacrylamide is grafted onto *cassia tora* gum in the presence of ceric ammonium nitrate initiator (Sharma *et al.*, 2002) and sago starch graft with methyl methacrylate using ceric ammonium nitrate and potassium persulfate as a redox reaction (Fakhrul-Razi *et al.*, 2001).

Cross-linked hydrogels prepared by means of graft copolymerization of acrylic acid onto guar gum and incorporated polyaniline chains can be absorbed by large contents of water within their structure (Sharma *et al.*, 2015). Graft copolymerization of acrylic acid on rice starch using potassium permanganate with various acids as a redox system was monitored.

Acrylic acid, acrylamide, and their carboxylate salts are generally an important monomers that are employed to produce traditional synthetic hydrogels by means of chemical polymerization. Studies indicated that grafting of acrylic acid, acrylamide, and their carboxylated salt onto naturally occurring polymer backbone have been successfully done by many researchers. The obtained grafted copolymer showed not

only highest water swelling capacity but also biodegradability. Graft copolymerization of polyacrylic acid onto chitin completely produced a wound dressing material with better for wound care. The reaction scheme of chitin graft polyacrylic acid has imaged in figure 2.4.

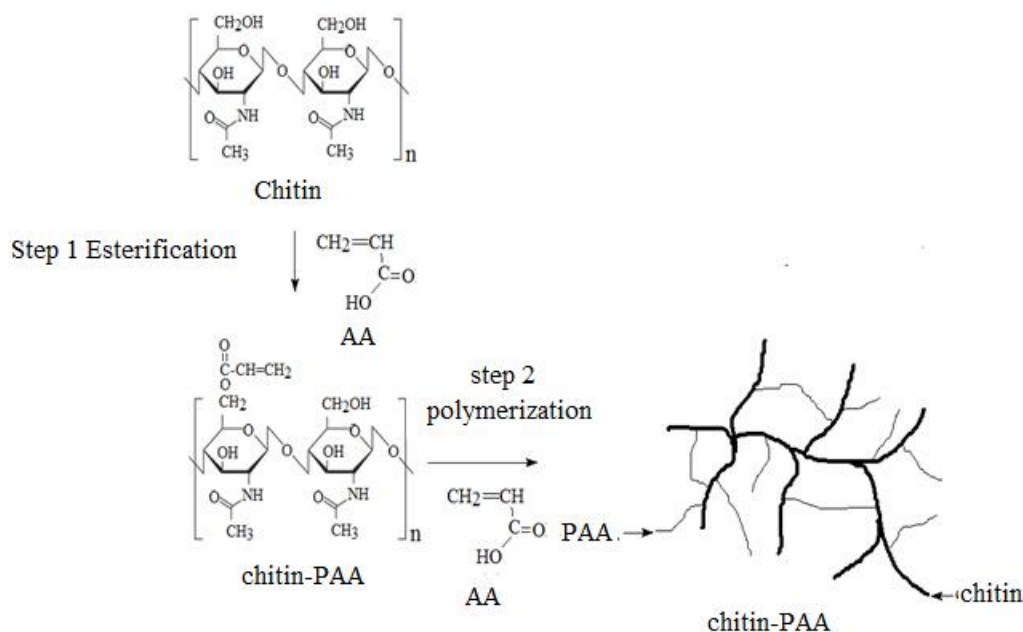


Figure 2.4 Preparation of chitin-PAA hydrogel (Thanoekaew *et al.*, 2004)

Chitin grafted polyacrylic acid copolymer with superior's water absorption properties have been produced by many of researchers. The obtained chitin grafted polyacrylic acid copolymer could enhanced the water absorption ability and actsd as a biomedical materials for short-lived replacing skin (Thanoekaew *et al.*, 2004; Ahmed and Ikram, 2016; Anitha *et al.*, 2014)

Besides their resources, SAP hydrogel can be classified fundamentally on their different polymeric composition. The preparation procedure is the most important factor that affects their composition which lead to formations of some important types of materials. According to polymeric composition, SAP hydrogel can yet be classified into three types; 1). Homopolymer hydrogels, which is usually mentioned to a polymer that is derived from a single species of monomer, it might have crosslinked structure depending on monomer polymerized and preparation method 2). Copolymeric hydrogels, are always referred to a polymer that polymerized through two or more

species of, in which identical or different monomers. This type of hydrogel would be composed for at least one of the hydrophilic components arranged in random, block or alternative conformation through a polymer chain network 3). Multipolymer interpenetrates polymeric hydrogels (IPNs), this is a hydrogel that is produced from two independent crosslinked synthetic or natural polymer contained in the network structure.

According to its physical structure and chemical composition, the SAP hydrogel can be classified into three types including amorphous (non-crystalline), semicrystalline and crystalline, respectively. Hydrogel, if finely considered to their durability, can be classified into two categories including durable hydrogel and biodegradable hydrogel. Durable hydrogel is generally composed mostly of the polyacrylate-based hydrogels, this type when considered to its resources is also called a synthetic hydrogel and biodegradable hydrogel such as polysaccharides-based hydrogels. Biodegradable hydrogel is sometimes called natural hydrogel which can be degraded under biological factor such as water, enzyme, or etc, forming simplest and harmless molecule releasing to the surrounding. In recent years, an environmental stimulus is an important factor that has led to classify SAP hydrogel into different categories, for example, pH stimuli, temperature stimuli, ionic strength or electric field stimuli (El-Sherbiny *et al.*, 2013). The overall classification of hydrogel is described as it shown in Figure 2.5.

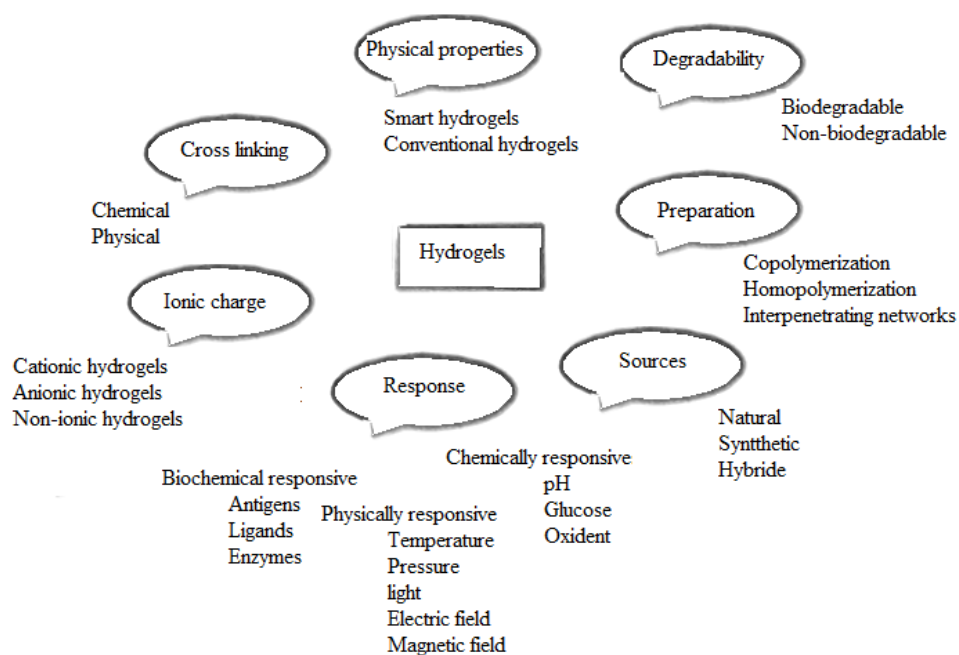


Figure 2.5 Hydrogel classification (modified from Ullah *et al.*, 2015)

Mostly SAPs are synthetically produced through radical polymerization of polyacrylic acid, polyacrylamide and polyacrylate salt which are mainly derived from petroleum product, unrenewable and has tendency to increase in cost. Albeit all kinds of SAP have no direct threat to human life, the disposal of synthetic waste can cause a large range of environmental pollution (Akhter *et al.*, 2004; Nakason *et al.*, 2010; Nnadi *et al.*, 2011). This problem has largely motivated polymer technologist of both fields of academic and manufacturing industries to produce SAP that reduces the need for creating a disposal system. The naturally occurring SAPs have attracted more attention due to their unique renewable and biodegradable properties. They are degraded as a result of the natural biological process, including the action of enzyme, micro-organisms, and water, forming simplest gaseous which is environmentally safe. The factor attracting more interest to natural occurring SAPs is the fact that they can be produced in large scale at a low price. Polysaccharides and proteins are employed due to having a large feedstock, renewability, and biodegradability. Studies indicated that grafting hydrophilic monomer onto starch have led to form SAP hydrogel with highest water swelling capacity. (Kiatkamjornwong and Faullimmel, 1991; Kiatkamjornwong and Mechai, 1997; Kiatkamjornwong, 2007; Nakason *et al.*, 2008; Faullimmel *et al.*,

1988; Sangsirimongkolying *et al.*, 1999; Ahmed 2015; Hérold and Fouassier 1981; Mostafa 1995; Jyothi 2010; Hu and Zhang 2002; Sadeghi *et al.*, 2015; El Sayed 2015).

Cellulose is the main component of the cell wall in a lignocellulosic plant that is embedded in a gel matrix composed of hemicellulose, lignin, and other polymers. (Abdul halim, 2012). Cellulose is polysaccharide with arrangement in the linear form of generally glucose unit. The main different forms between cellulose and starch is beta 1,4-glycosidic linkage while starch form alpha-1,4-glycosidic linkage. The difference between beta-1,4 and alpha-1,4 glycosidic linkage results in different digestibility in humans. The structures of cellulose and starch are shown in Figure 2.6.

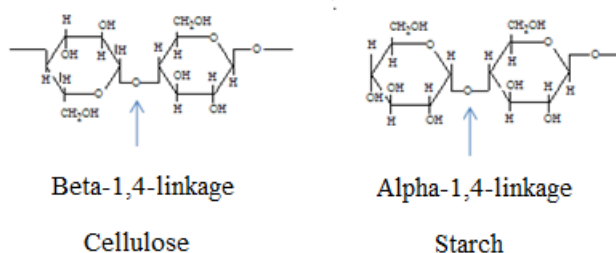


Figure 2.6 Beta-1,4-glycosidic linkage of cellulose and alpha-1,4-glycosidic linkage of starch (Nakason *et al.*, 2008; Faullimmel *et al.*, 1988)

Cellulosic microfiber when grafted with polyacrylic acid forms grafted copolymer with improving ion exchange and fluid absorbency on the fibers (Loría-Bastarrachea *et al.*, 2002). Grafting of polyacrylic acid onto cellulose membrane form grafted copolymer which is applied as a taste sensor for absorbing lipids into Millipore filter paper, the results indicated that grafted copolymer can improve the taste sensing efficiency of the membrane (Majumdar *et al.*, 2006). Grafting polyacrylic acid onto a cellulose derivative forms hydrogel which applied worldwide for soil amendment, the results indicate that it could significantly enhance the water retention capacity of the soil and could sustain release of water for a long time without additional water needed (Demitri *et al.*, 2013).

Cellulose derivatives, besides cellulose acetate and nitrocellulose, recognizes carboxymethyl cellulose (CMC) and hydroxyethyl cellulose (HEC), and they are two

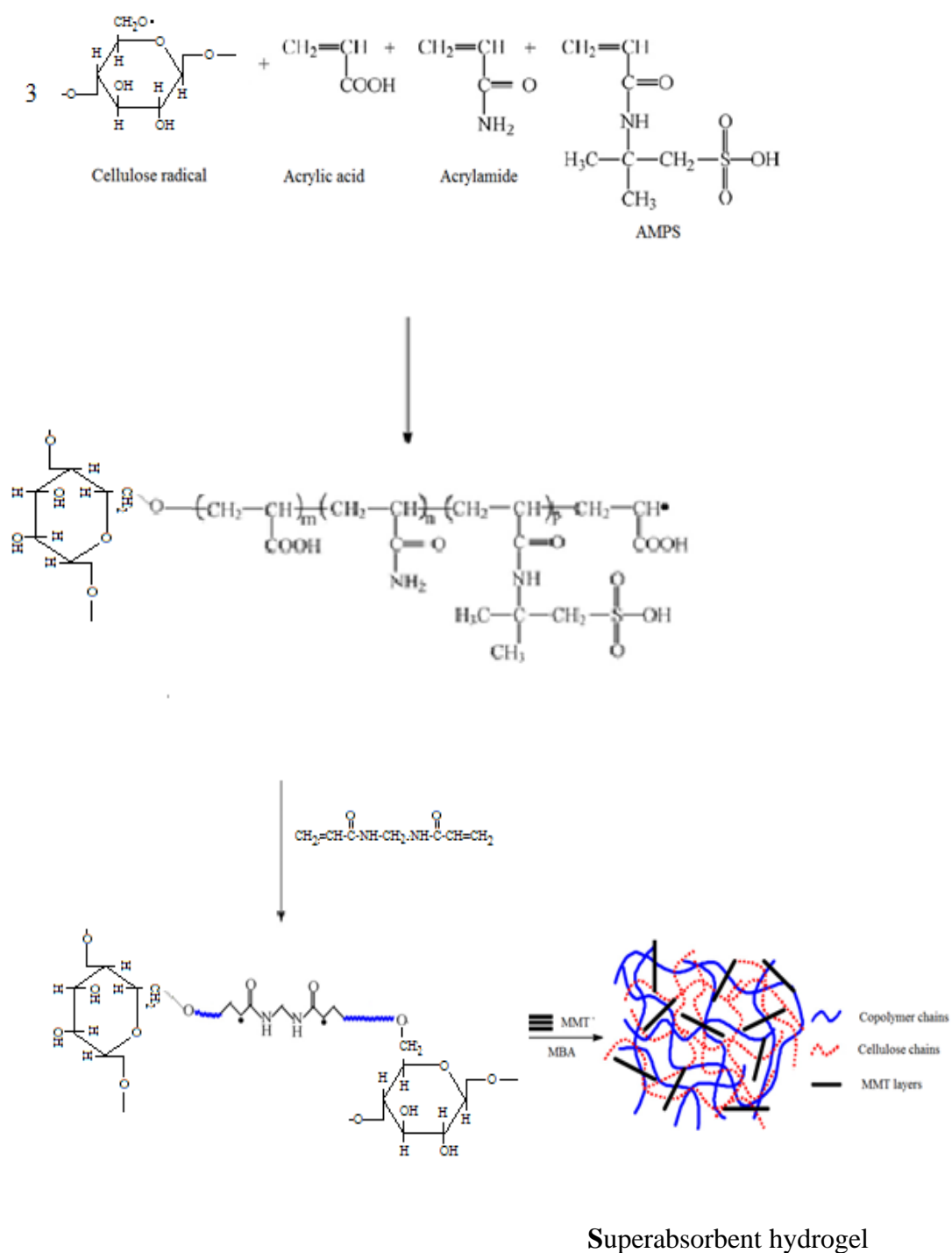


Figure 2.7 Mechanism of cellulose-g-P(AA-co-AM-co-AMPS)/MMT superabsorbent hydrogel (Bao *et al.*, 2011)

Chemical hydrogels are generally synthesized through formation of three-dimensional networks via water-soluble monomer and polyfunctional crosslinker as shown in Figure 2.8

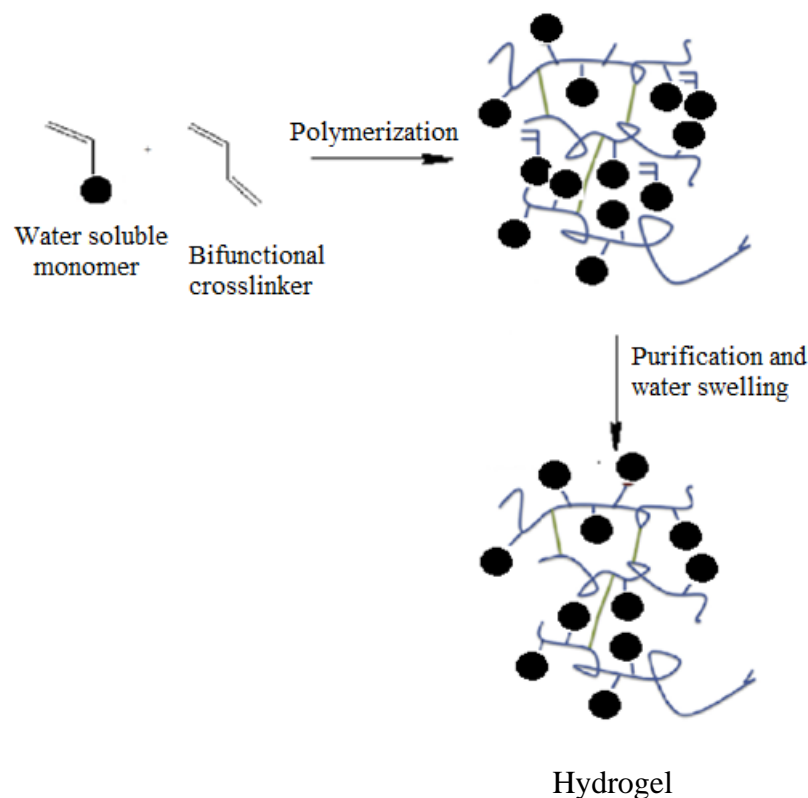


Figure 2.8 Three-dimensional polymerization hydrogel (Calo *et al.*, 2015)

The novel methods for synthesizing hydrogels from ready-made water-soluble polymers were discovered by using heat treatment or microwave radiation under condition of aqueous solution polymerization. Poly (methyl vinyl ether-alt-maleic anhydride) as a water-soluble polymer is together mixed with poly (vinyl alcohol) at room temperature and then crosslinked by thermal process under autoclaving with high pressure or microwave radiation. The process on how to understand the hydrogel forming is indicated in Figure 2.9

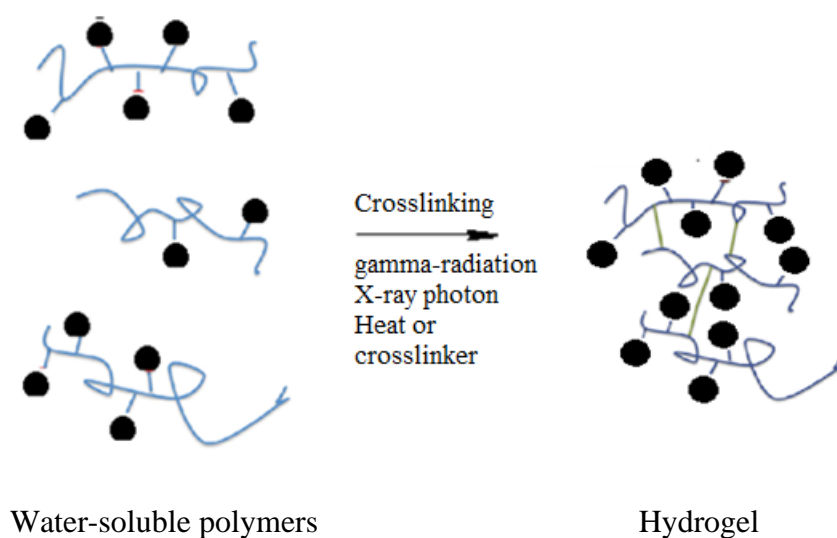


Figure 2.9 Ready-made water-soluble polymer hydrogel (Cook *et al.*, 2012)

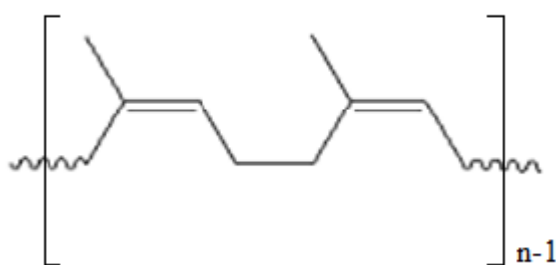
2.3 Natural rubber

Natural rubber (NR) is the most abundance of naturally occurring polymer which usually mentions to product from rubber tree of *Hevea brasilliensis*. The plant is tapped by producing an incision in the bark of the rubber tree and collecting the sticky milk-like latex which is then refined into a usable rubber. The purified form of natural rubber is the structure chemically composed of *cis*-1,4-polyisoprene with an empirical formula C_5H_8 that is a structure of isoprene unit (Figure 2.8) (Hamzah *et al.*, 2012). Isoprene was a repeating unit of natural rubber where one of the double bonds remains for each isoprene unit (Kohjiya *et al.*, 2014). Natural rubber is generally very stretchy, flexible and extremely waterproof. Therefore, it allows to utilize for large range of applications and products available, as is a synthetic rubber. Beside the polyisoprene as the main polymer, natural rubber latex generally consists of other impurities of organic compounds including protein, carbohydrate, fatty acid and water as the detail indicated in Table 2.1.

Table 2.1 Composition of components in raw natural rubber (Eng and Ong, 2000)

Components	Percentage (%) ^a
Rubber hydrocarbon	93.7
Proteins	2.2
Lipids	3.4
Carbohydrates	0.4
Ash	0.2
Others	0.1

a : Based on 100 grams total solid content (TSC) by weight



cis-1,4-Polyisoprene

Figure 2.10 Chemical structure of natural rubber

Recent years, Thailand is one of the leading manufacturers of NR in the world, but forms of *cis*-1,4-polyisoprene that mostly uses natural rubber classified as elastomers. NR is used extensively by many manufacture companies for producing rubber products, either alone or in combination with other materials. In most of its practical forms, NR possesses excellent properties, it has a large stretch ratio and high resilience and is extremely waterproof. By right of this, various production derived from NR has been marketed worldwide in all countries around the world such as clothes, condom, balloon, parts of automobile, aircraft, building, sealing material, living place decoration and etc. Notwithstanding NR chemical structure hich consists of unsaturated C=C double bond chain, it still has some drawbacks especially with the

factors that are strongly affected to double bond by converting into single bond such as ozone, oxidizing agents, concentrated acids, bases and so forth. On the other hand, the hydrophobic chain structure leads natural rubber to be intensively inferior to petroleum-based oils and also has the lowest water swelling capacity which has a limitation for few applications. Various publications have offered the best process of how to remove and fulfill the drawbacks of natural rubber. Rubber modification is a process of chemical or physical that is used specially to form modified rubber with improving the inferior properties of rubber. NR is chemically modified through a special reaction or physically interact to form a kind of modified NR.

It is well-known that NR hydrocarbon composes entirely is *cis*-1,4-Polyisoprene in which the reactive chemical is placed of at least one double bond between C2 and C3 of each isoprene unit. It has seven allylic protons on carbon C1, C4 and C methyl. All five carbon atoms are possible sites for chemical modification. The hyperconjugation of double bond with methyl and methylene group are influenced double bond to become a reactive position for selecting chemical reaction with reagents. Five types of NR modification include 1) isomerization, rearrangement and molecular weight reduction, 2) addition to double bond, 3) substitution to allylic proton, 4) cyclo addition and 5) ene addition, as indicated in Table 2.2. However, graft copolymerization of vinyl monomers onto polyisoprene do not appear at this area but it will be separately detailed in the section of WSR preparation.

Table 2.2 Classification of modification reactions of the cis-1,4-polyisoprene chain
(based on Gelling and Porter, 1988)

Reaction types	Reagents used
1. Isomerization, rearrangement and molecular weight reduction	Thiol acid isomerization Sulphur dioxide isomerization Photo- and radiation-induced isomerization Cyclization Mechanical chain scission Oxidative chain scission Photochemically initiated chain scission (nitrobenzene)
2. Simple addition to the double bond	Hydrogenation Hydroformylation Halogen addition Halogen acid addition Halocarbon addition Sulphenyl halide addition Hydroboration Hydrosilylation Peroxide and accelerated sulphur crosslinking
3. Substitution of allylic hydrogen	Autoxidation (primary steps) Maleic anhydride reaction (radical initiated) Quinoneimine and quinonediimine reaction Epoxidation (1 + 2)
4. Cycloaddition	Carbene addition (1+2) Nitrene addition (1+2) Photolytic carbonyl addition (2+2) Chlorosulphonyl isocyanate addition (predominantly 2 + 2) Ozone reaction (primary step) (3 + 2) Nitrite oxide addition (3 + 2) Nitrene addition (3+2) Nitrilimine addition (3+2) Sydnone addition (3 + 2) Azide addition (primary step) (3 + 2) Sulphur diimide addition (3 + 2) o-Quinonemethide addition (resin cure) (4+2) Singlet oxygen addition
5. Ene addition	Activated carbonyl and thiocarbonyl addition Maleic anhydride addition (high temperature) Chlorosulphonyl isocyanate addition (minor reaction) C-Nitroso addition Azodicarbonyl addition

Epoxidation of NR is a reaction which responds readily to electron availability at the double bond via bicyclic transition state. Studies indicated that the introduction of oxirane ring onto NR via epoxidation uses organic peracid, forming epoxidized natural rubber (ENR) with improving the resistance to ozone, oils, solvents, concentrated acid-base and gas permeability (Heping *et al.*, 1999). Hydrogenated natural rubber (HNR) is completely formed when natural rubber is treated with hydrogen gas under an effective catalyst, and the obtained HNR can improve the resistance to oxidation, degradation of the ozone and long-term heat resistance (Mahittikul *et al.*, 2009). Vulcanized NR is formed when treated with sulfur or related material under the heating condition, and they lost all original properties effected by temperature, softening with heat and hardening with cold. The chemical crosslinking of NR to each other by means of the addition of vulcanizing agent leading NR to be superior to mechanical properties (Ariyawiriyanan *et al.*, 2013). According to Arayapranee *et al.*, (2013) natural rubber is grafted separately with acrylonitrile, methyl methacrylate and styrene, forming grafted natural rubber (GNRs). The obtained grafted natural rubber is found to increase in polarity and provide good resistance to thermal, petroleum-based oils, and ozone while the mechanical properties are still maintained.

2.4 Modified Natural Rubber

Since as early as 1801, natural rubber has been modified in various methods, the term modified natural rubber can assign to the degree of chemical modification from a small mole percent to a large mole percent depending on its applications. Higher levels of modification tend to transform the nature polyisoprene from a rubber to plastic-like material. Because natural rubber has fixed cis-polyisoprene structure and unable to have its polymerization process tailored like that of the synthetic rubber industry to provide suitable pendant groups. Natural rubber has been modified with a variety of groups for a whole cross section of purpose. To improve the low-temperature properties and for crosslinking of natural rubber, the thiols and related material are added. The double bond existing within natural rubber are simultaneously converted into the tricyclic ether when treating with organic peroxide under proper conditions and forming epoxidized natural rubber (ENR).

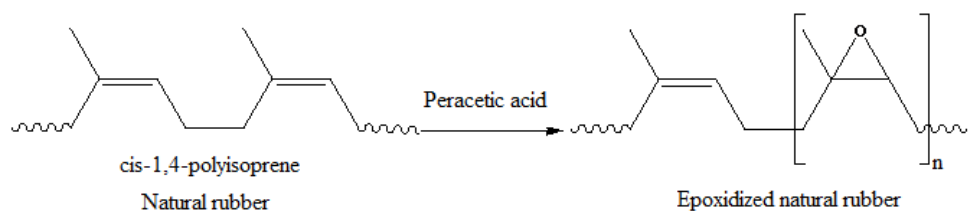


Figure 2.11 Natural rubber to epoxidize natural rubber (ENR) (Ratnam *et al.*, 2001b)

The introduction of oxirane ring into natural rubber can improve the gas permeability and oil resistance property. Studies indicated both ENR-25 and ENR-50 grades exhibits good wet grip characteristics and have been examined as tire tread materials. The addition of maleic anhydride and maleimides by means of graft copolymerization has enhanced the interaction between the nylon fibers and the NR matrix (Dong *et al.*, 2013). The modified form to be realized will include hydrogenated NR, chlorinated natural rubber, hydrohalogenation natural rubber, cyclized natural rubber, resin-modified natural rubber, poly (methyl methacrylate)-grafted natural rubber, superior-processing natural rubber, N-phenyl carbamoyl azidoformate-modified natural rubber, polystyrene-grafted natural rubber, epoxidized natural rubber (ENR), degraded natural rubber and thermoplastic natural rubber. All types of modified natural rubber will be detailed and focused, especially, on epoxidized natural rubber due to their usage as a rubber matrix for preparing water swellable natural rubber.

NR can be modified in multi forms through physical and/or chemical reaction, for example, the mechanical blending of natural rubber with plastic forming thermoplastic elastomer which can meet both the desired properties and economic cost. The modified forms of natural rubber are indicated in Figure 2.12.

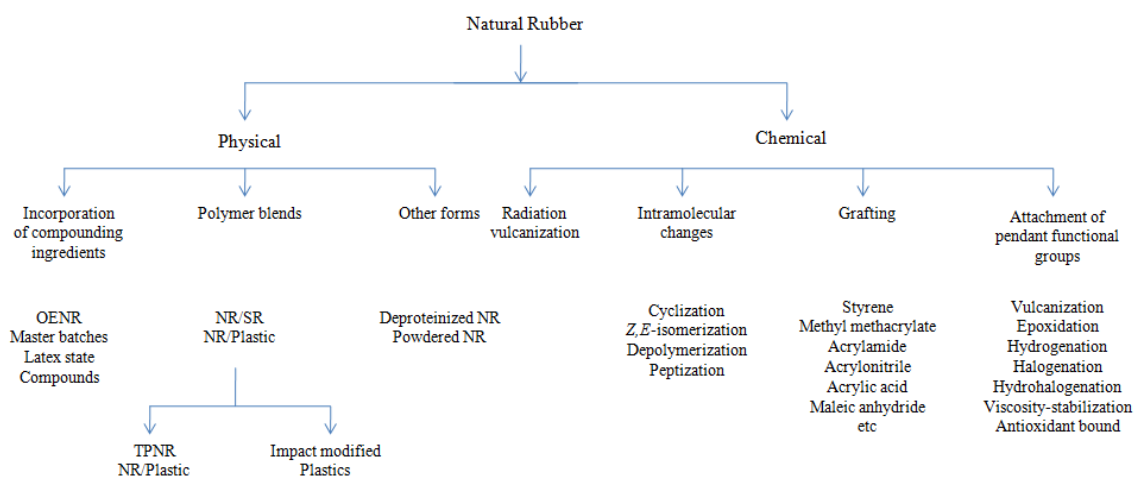


Figure 2.12 Types of modified NR

2.5 Epoxidised Natural Rubber

Epoxidised natural rubber (ENR) is a derivative of natural rubber produced by chemical reaction of natural rubber with organic peracids such as peracetic acid or performic acid. It is realized that the pure form of ENRs sample was firstly synthesized at the mid-1980s and their properties fully recorded (Gelling, 1985). The tentative reaction mechanism is illustrated briefly in Figure 2.13. Generally, natural rubber has unique superior mechanical properties to those of synthetic rubber. However, NR cannot compete with the specialty of synthetic rubbers with regards to such properties as gas permeability and oil resistance. The epoxidation reactions establish an important criterion for the chemical modification of NR, which lead to the development of clean epoxidised natural rubber. These new polymers have improved oil resistance and decrease gas permeability, whilst retaining many of NR properties and also exhibit some novel features better than natural rubber alone. Natural rubber when treated with peracid usually peracetic acid or performic acid forms some substituents oxirane ring into cis-1,4-polysoprene chain. The level of epoxide group substituents is an important factor that will directly define properties of obtained rubber.

From Table 2.3 it is found that the distribution of oxirane groups along the polymer backbone strongly determines the physical properties of the ENR. The content of oxirane group implantation on NR is affected directly by Tg, specific gravity, and mooney viscosity. Both ENR-25 and ENR-50 have Mooney viscosities in the range of 75-90 on production. Studies also found that epoxidation of NR increases the polarity, and the solubility of ENR depending on the nature of the solvent and the content of epoxidation comprised. They found that the glass transition temperature of ENR is increased by approximately 1° C for every 1 mol % epoxidation adding. The polarity of ENR increases with an increase in the level of epoxide groups. At high levels of epoxide groups, these materials became more resistant to hydrocarbons while decreasing their resistance to polar solvents (Baker and Gelling, 1987). The epoxide groups in ENR have also been investigated as routes to new crosslinking systems and rubber bound anti degradants and as intermediates for further chemical modification (Gelling, 1999).

As mentioned earlier the slightly change in chemical structure by implanting randomly of oxirane groups on double bond of 1,4-cis polyisoprene leading ENR has an excellent property such as oil resistance, gas impermeability, good wet grip, and high damping characteristics (Muhamad *et al.*, 2006). The oil resistance of ENR is due to the polarity of the oxirane group. The air permeability of NER decreases with increasing level of oxirane group, this is due to more compatability nature. There are already some examples of ENR properties with improving resistance to oil and gas permeability as shown in Table 2.4 and Figure 2.14.

Table 2.4 Comparative air permeability of general rubber at 30° C (Matador, 2007)

Rubber types	Air permeability
NR	100
ENR-25	32
ENR-50	8
SBR-500	48
NBR (34% acrylonitrile)	4

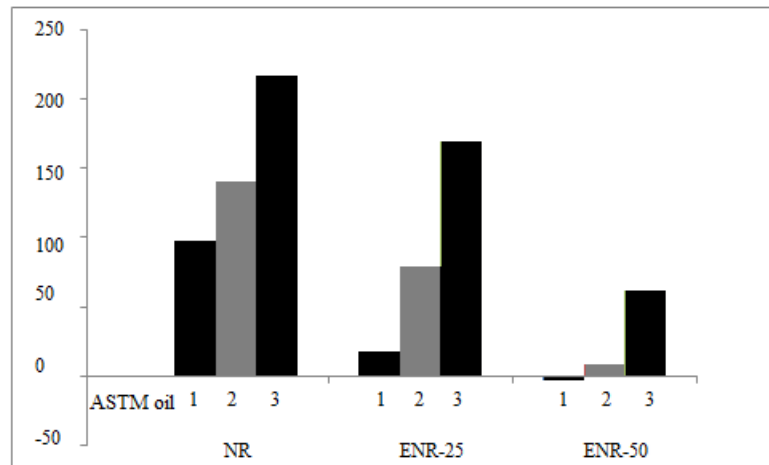


Figure 2.14 Oil resistance of ENR-25 and ENR-50 compared to NR after 70 hours in ASTM No.1, 2, and 3 oils (Matador, 2007)

Studies have indicated that the resistance to oil is affected directly with an increasing amount of epoxide level in natural rubber. The mechanical blending of ENR-50 with EVA at 50:50 blend ratios indicate the most stable blend which leads to the improvement the thermal stability and has the greatest mechanical properties (Muhamad *et al.*, 2006).

2.6 Superabsorbent polymer and superabsorbent polymer composite

Superabsorbent polymers (SAPs) are crosslinked hydrophilic polymer with three-dimensional networks of polymer chains that generally contain carboxylic acid, partially neutralized carboxyl groups, carboxamide, and sodium carboxylate. They can absorb large quantities of water to more than 1,000 times of their original weight without dissolving (Wage *et al.*, 2007). In the late 1960s, the long water retention SAP based on natural polymers was first invented by United States Department of Agriculture for soil amendment (Kiatkamjornwong, 2007). They developed a polymer based on starch-g-polyacrylonitrile with a greater water absorption more than 400 times of its original weight. In the middle of 1970s, SAPs were developed in Japan for use in personal care and hygienic products such as disposable diapers, sanitary napkins, surgical pads and others. In addition to these applications, SAPs are also used

in soil conditioning as a controlled release agent for agrochemicals or pharmaceuticals. The important factors that provide empower absorbing to superabsorbent polymers are osmotic pressure and affinity between polymer electrolyte and fluids. High crosslink density of polymer networks in contrast plays the main factor that suppresses the absorbing strength of fluids. Thus, SAPs possess not only a high fluid absorbing capacity, but also a limitation ability to release the absorbed fluid. Basically, superabsorbent polymers are crosslinked polyacrylates which mostly derive from petrochemical resources. Therefore, polyacrylate is not environmental green, non-renewable and its future cost tends to be high depending on the petroleum industry (Nnadi *et al.*, 2011).

Due to super-swelling capacities, SAPs can be used in various applications such as disposable diapers, water conservative agriculture, cosmetic and absorbent pads (Todd and Daniel, 2008). Swelling mechanisms of SAP can be explained as shown in Figure 2.15.

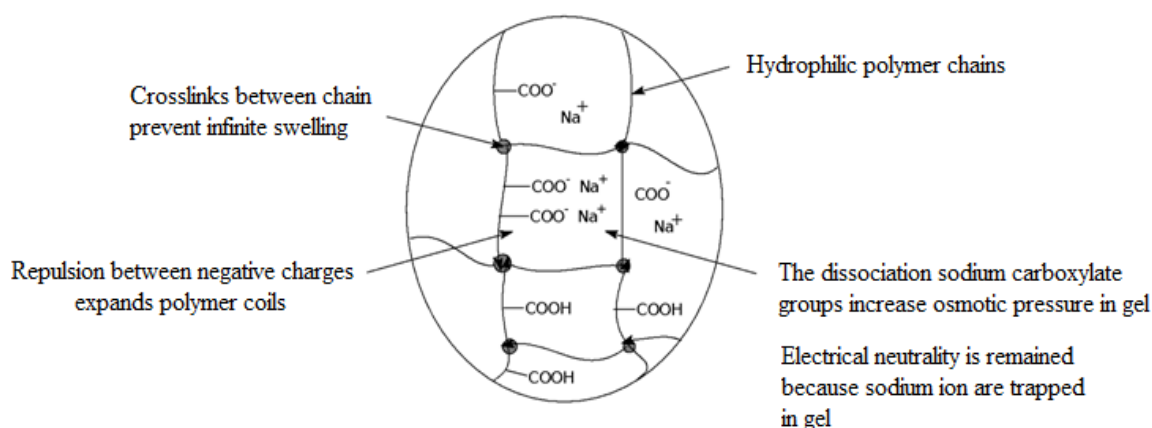


Figure 2.15 Swelling mechanism of superabsorbent polymer (Elliott, 2004)

Figure 2.15 shows a crosslinked network of superabsorbent polymers that contain carboxyl group partially neutralized by sodium to form carboxylate ions and sodium carboxylate. Water molecules that place around polymer are drawn into the network across a diffusion gradient of the polymer backbone. The polymer chains want to straighten but cannot due to the cross linking. Thus, the polymers expand as water moves into the network.

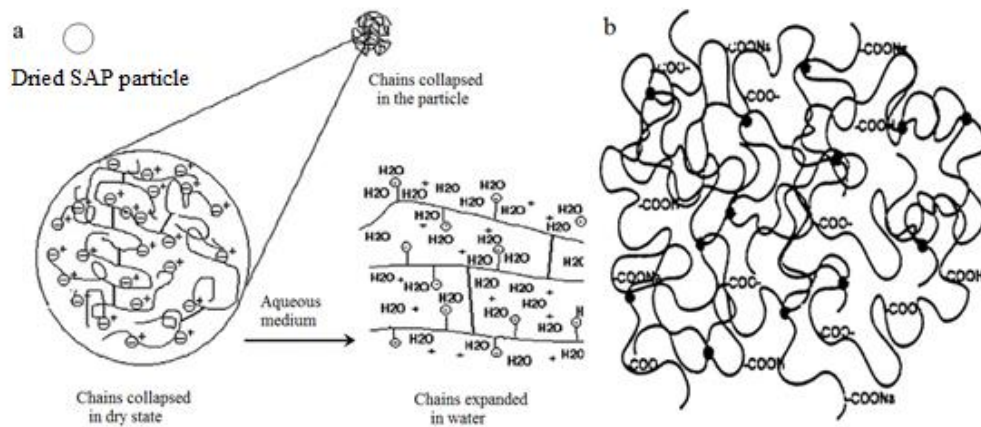
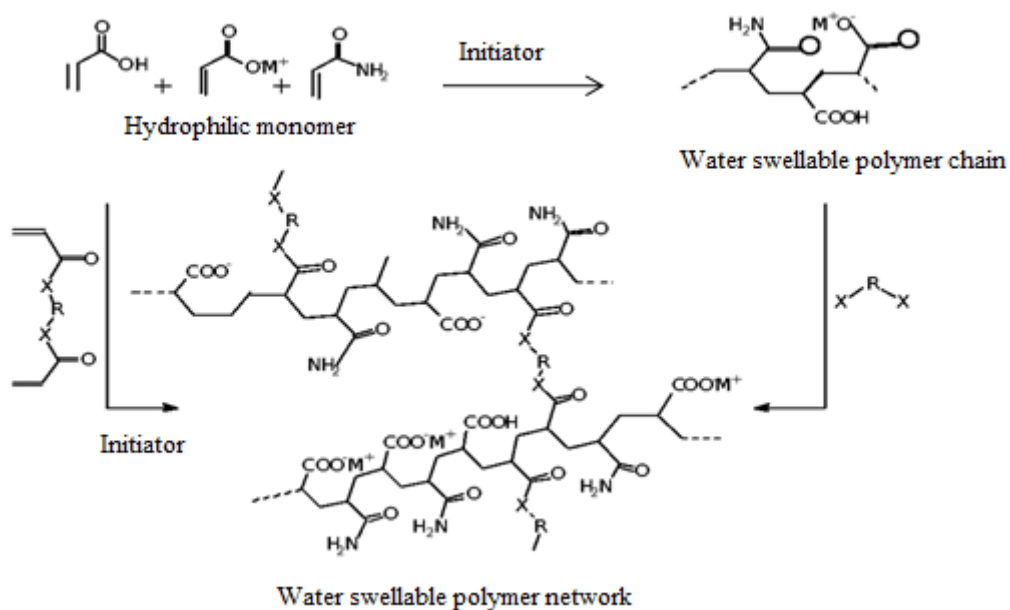


Figure 2.16 SAP chains (a) before and after swelling and (b) sodium polyacrylate networks (Dehbari and Tang, 2015)

Hydrophilic polymers are divided into three types including natural (e.g. polysaccharide and polysaccharide derivatives), semi synthetic (e.g. cellulosic derivatives) and synthetic polymers (e.g. crosslink polyacrylate) (Mikkelsen, 1999). Synthetic polymers are typically crosslinked acrylic acid homopolymer, sodium neutralized acrylate ion and acrylamide. General synthetic pathways of SAP are shown in Figure 2.17.



Where $\text{CH}_2=\text{CH}-\text{X}-\text{R}-\text{X}-\text{CH}_2=\text{CH}$ and $\text{X}-\text{R}-\text{X}$ are polyvinyl and polyfunctional crosslinkers

Figure 2.17 Reactant and pathways to prepare synthetic SAP (Mohammad *et al.*, 2008)

Amongst them, the synthetic polymers are most commonly used due to their high stability against environmental function and hard breaking down (Shooshtarian *et al.*, 2011). However, all types of superabsorbent polymer do not directly threaten the human life (Akhter *et al.*, 2004; Sunny Gils *et al.*, 2009). In early SAP invention, superabsorbent polymers are used for disposable hygienic products, mainly disposable diapers, feminine sanitary napkins and adult incontinence products (Todd *et al.*, 2008). Rapid development of superabsorbent technology and performance has been largely led by demands in disposable hygiene segment. The advances in absorption of materials have attracted and allowed to next development of ultra- thin baby diapers which use a less portion of materials.

Recently, the extended use of synthetic polymers has led to a large environmental pollution caused by disposal of those synthetic polymer wastes (Nakason *et al.*, 2010). The increase in environmental problems has been stimulated and turned attention of the scientists both in academic and industry to produce biodegradable polymer from naturally occurring resources. Biodegradable polymers

are polymers that can be degraded as a result of natural biological process including action of enzyme, micro-organisms and water, then transforming into harmless and simplest substances releasing to surroundings. Moreover, biodegradable polymers are able to eliminate the need to create a disposal system which can cause environmental damage. Because of environmental concern, biodegradable polymers have motivated great attention to both polymer and environmental fields for developing a new material with the desired property and safe environment.

The preparation method of biodegradable SAP includes blending of polymer with naturally occurring materials which are the most general procedure due to ease and lower cost (Nakason *et al.*, 2010); copolymerizing natural hydrophilic polymers with a crosslinking agent (Yu *et al.*, 2006) and grafting a synthetic vinyl monomer onto naturally occurring materials. The latter is a promising way due to its side chain connection built by covalent bond leading to high stability of copolymer product.

Wide varieties of naturally occurring polymers such as starch, cellulose and cellulose derivatives are utilized as a polymer backbone for grafting with hydrophilic monomers. The deep detail will be reviewed in the next sections. Hydroxyethyl cellulose (HEC) is the most well-known cellulose derivative that is used to prepare biodegradable superabsorbent polymer by grafting with acrylic acid or acrylamide monomers. Various monomers both using alone or mixture are grafted onto starch, cellulose, and cellulose derivatives. Some fillers have been combined to form a superabsorbent polymer composites with a superior swelling capability. Superabsorbent polymer composite (SAPC) is formed when incorporating the inorganic fillers such as silica, medicinal stone (Wang *et al.*, 2011), china clay, bentonite, kaolin, montmorillonite, attapulgite, and mica (Li *et al.*, 2004; Wu *et al.*, 2001). The results found that the SAPC could improve not only water swellability but also mechanical properties. The initiation system is one of the important factors for grafting copolymerization, a wide variety of initiators has been manipulated to prepare grafted copolymers with different levels of water swellability, for example, potassium persulfate, ammonium persulfate and ceric ammonium nitrate (Nakason *et al.*, 2010; Lanthong *et al.*, 2006; Jasmin *et al.*, 2010; Lui *et al.*, 1998). Superabsorbent polymer hydrogel is formed when cassava starch grafted with polyacrylamide under ammonium persulfate initiator and *N, N*-methylenebisacrylamide crosslinker. The obtained

hydrogel is further treated with 1 M NaOH, neutralized with 0.5 M HCl and are tested for water swelling capacity. The result shows that the hydrogel has water swelling capacity higher than 500 g/g of initial weight (Nakason, 2010).

2.7 Cellulose and hydroxyethyl cellulose

Cellulose is the most abundant renewable naturally occurring polymers. It is a major component in the rigid cell walls of plants with a linear polysaccharide and glucose units. Cellulose is one of the most favorable raw materials for producing biodegradable materials due to its natural abundant availabilities and low cost. Cellulose possesses several attractive properties with a benefit for the environment, for example, biodegradability and biocompatibility due to their structural arrangement with the ability to form suprastructure (Heinze and Liebert, 2001). Cellulose consists of plenty of reactive hydroxyl groups that can be easily abstracted to form oxygen radicals. They can then be polymerized in the presence of vinyl monomer to produce cellulose derivatives. The cellulose acetate is a modified natural polymer that has unique properties to enable a great variety of end-use applications such as fabrics, films, cigarette filters, separation technology and other special applications. The graft copolymerization is the most effective route used to modify both structure and properties of the cellulose. Many applications of grafted cellulose have been reported. Cellulose-graft-poly (butyl acrylate) copolymers is used for moisture, chemical and thermal resistant materials (Thakur et al., 2013a). Lignocellulose-graft-polyacrylate is eco-friendly used for green composite applications (Thakur *et al.*, 2013b). Sunn hemp fibers-graft-ethyl acrylate and binary monomers (ethyl acrylate (EA) + methyl methacrylate (MMA), EA+ acrylic acid (AA) are found to increase thermal stabilities of polyhydroxybutyrate biocomposite (Kalia *et al.*, 2011). Grafting of polystyrene onto cellulose create a new wood-plastic material with improving mechanical and physical properties. The adhesion tests show that these graft copolymers can function effectively as compatibilizers or interface agents to bond the hydrophobic plastic material to wood, evolving into a new class of composites. (Ranayan *et al.*, 1989). A graft copolymer of *N, N'*-dimethyl-acrylamide and cellulose has been used for protein adsorption resistance (Yan *et al.*, 2008). By conventional method, grafting

copolymerization of vinyl monomer onto cellulose usually shows some disadvantages, for instance, the presence of unwanted product together with desired graft copolymer, chain degradation, and large amount of ungrafted cellulose contaminated in the product (Yan *et al.*, 2008). In addition, cellulose does not dissolve in general solvents and so the grafting reaction occurs in heterogeneous medium. This is different from the synthesized graft copolymers that are prepared in a homogeneous medium. Generally, there are 3 most possible ways to modify the chemical property of cellulose. Amongst them, converting cellulose into cellulose ether or cellulose ester is the most promising methods since the polarity increases, leading to dissolve well in water and general solvents. The next is to prepare a crosslinking derivative of cellulose, and last method is graft copolymerization of cellulose with monomers in order to introduce a branched chain onto cellulose skeleton. In addition to cellulose, cellulose ethers such as carboxymethyl cellulose, ethyl hydroxyethyl cellulose and hydroxyethyl cellulose (Roy *et al.*, 2009; Bikales *et al.*, 1879), are used as the polymer backbone for grafting copolymerization. Monomers such as acrylic acid (Loria-Bastarrachea *et al.*, 2002), acrylamide (Bicak *et al.*, 1999; Yoshinobu *et al.*, 1992), *N,N*-dimethyl acrylamide (Yan *et al.*, 2008), methyl methacrylate (Canché-Escamilla *et al.*, 1997) and methacrylonitrile (Gaylord *et al.*, 1972), have been grafted onto cellulose and cellulose derivative. In the last decade, new solvents for cellulose are disclosed and thereafter increase the use of homogeneous condition for the grafting copolymerization of cellulose. This condition expands the synthesis pathway for cellulose modifications. The homogeneous condition gives better control of heat and mass transfer, degree of substitution and the distribution pattern along the polymer chain (El Seoud *et al.*, 2005). Recently, the growth in living radical polymerization (LRP) technology has prompted a potential pathway to create a new cellulose grafted copolymer. Fortunately, most monomers that are always polymerized with conventional radical polymerization can be properly applied for living radical polymerizations. Although LRP method is developed in grafting reaction, but their management cost is still high compared to those conventional methods.

The most well-known modified cellulose is hydroxyethyl cellulose (HEC) which is readily available cellulose ether. It is a water-soluble polymer with non-ionic character. The HEC has been utilized for various applications, such as a thickener, suspender, binder, emulsifier, film's former, stabilizer, dispersing agent, water retaining agent and protective colloid agent. It is readily soluble in hot or cold water and can be used to prepare solutions with a broad level of viscosities. It has a greater tolerance for dissolved electrolytes. HEC is synthesized from the reaction of cellulose and sodium hydroxide to firstly form swollen alkali cellulose, then reacts with ethylene oxide to form hydroxyethyl cellulose. The replacement of one or more hydrogen atom of hydroxyl groups by ethylhydroxyl group can alter both physical and chemical properties. Especially, for SAP and SAPC preparation, the increasing of oxygen atom in structural molecule is expected to enhance high water retention.

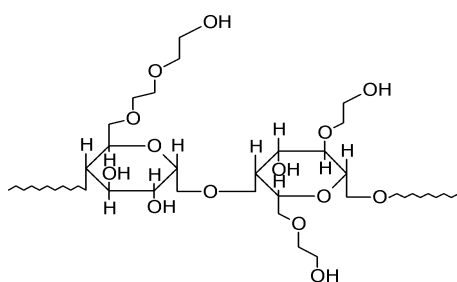


Figure 2.18 Structure of hydroxyethyl cellulose (Hercules, 1997)

2.8 Grafting of hydroxyethyl cellulose

Graft copolymerization is a chemical process for synthesizing of the branch copolymers, so called graft copolymers, in which the branches are structurally distinct from natural polymer backbone. Graft copolymer contains a long sequence of one monomer with one or more side chains of long sequences of another monomers. However, individual side chains of graft copolymers might be homopolymers or copolymers. Note that the different of second monomer side chains had more influenced to define product behaviors. For examples, grafting polyacrylic acid or polyacrylamide onto starch backbone formed grafted copolymer with an excellent

water swelling capacities. The obtained starch grafted copolymer has been introduced in various fields of application such as baby diapers, waste water treatment, controlled release of drug and so forth. Biodegradable plastic was formed when introducing poly (vinyl acetate) as a side chains on starch backbone through graft copolymerization of vinyl acetate onto starch. The obtained grafted copolymer was tested for water swelling capacity and water solubility. The results indicated that the grafted copolymer increased water swelling capacity while water solubility decreased. The obtained grafted copolymer is further tested against the function of temperature, they found that water swelling capacity increases with increasing temperature (Qu *et al.*, 2013). Starch grafting with acrylate esters, methacrylate esters and styrene monomers result in the form of thermoplastic grafted copolymer which is used worldwide as a starch-filled plastic. The addition of hydrophobic branches would be made more compatible with the plastic matrix and they were easily decomposed by the microorganisms. In addition, the biodegradable plastics also show an excellent tensile strength and images better in appearance. These polymers, for example, is starch-g-poly(methacrylate-co-acrylonitrile). The granule of starch-g-poly (methyl methacrylate) when extruded yield tough, leathery and translucent plastics and still held its integrity even under long periods of time water immersion (Jyothi, 2010).

The fundamental properties of HEC based superabsorbent polymer such as viscosity, the water swelling behaviors and moisture absorption have been compared with some commercial superabsorbent polymers. Various works related to the influence of grafting reaction of HEC including reaction methods, reaction conditions and applications have been reported. The HEC grafted with partially hydrolyzed acrylamide (HEC-g-(P-hyd) PAM) show high levels water swellabilities (Miyata *et al.*, 1995). The optimum conditions for HEC-g-PAA copolymer is prepared from grafting acrylic acid (AA) onto HEC, in the presence of potassium bromated/thiourea dioxide (TUD) as a redox initiator, with 30 mmol KBrO₃ and 30 mmol TUD/100 g HEC, 10-folds AA based on HEC weight at 50°C for 2 hours (Abdel-Halim, 2012). The HEC grafted with PAM by atom transfer radical polymerization (ATRP) is used as separation medium for double-stranded DNA fragmentation by capillary electrophoresis (Yang *et al.*, 2007). The HEC grafting with poly(4-vinylpyridine)

by ceric ammonium nitrate as initiator in aqueous nitric solution is applied as a physically absorbed coating of the fused silica capillaries and also has a great potential in the field of diagnosis and proteomics (Yang *et al.*, 2008). The HEC grafted poly(2-(dimethylamino) ethyl methacrylate) by ceric ammonium nitrate as initiator in aqueous nitric solution has been applied for a physically coating on capillary electrophoresis and, results found that grafted copolymer coating has great potentials in the field of diagnosis and proteomics (Cao *et al.*, 2009). The HEC grafted with poly(*N,N*-dimethyl acrylamide) copolymers by ATRP method is applied for separation of basic protein in capillary electrophoresis. The results show that this new multifunctional separation medium has a potential capacity in resisting basic protein adsorption (Yang *et al.*, 2010). However, HEC grafted copolymers as stated earlier are mostly applied for biochemical separation and a few of them are partly prepared by controlled/living radical polymerization.

The new superabsorbent polymers and composites based on hydroxyethyl cellulose have been reported by researchers. According to Peng *et al.* (2010), the temperature sensitive hydrogel is prepared by grafting *N*-isopropylacrylamide onto modified HEC backbone. Monoblocked diisocyanate is first synthesized through the reaction of toluene diisocyanate with defined terminal hydroxyl group as deduced in Figure 2.19

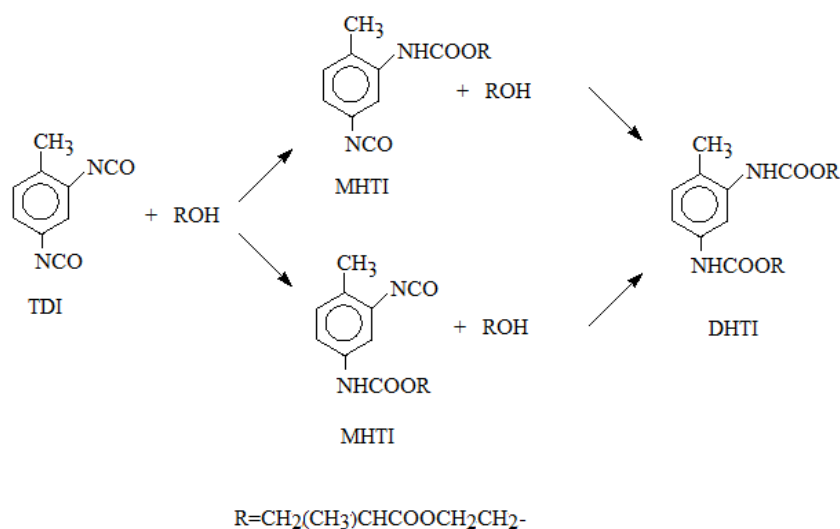


Figure 2.19 Reaction of toluene diisocyanate to synthesize monoblocked diisocyanate (Peng *et al.*, 2010)

The obtained monoblocked diisocyanate then reacts with HEC under catalyst of dibutyltin dilaurate to form modified HEC which further graft copolymerized with *N*-isopropylacrylamide to form targeted hydrogel as a detailed in Figure 2.20.

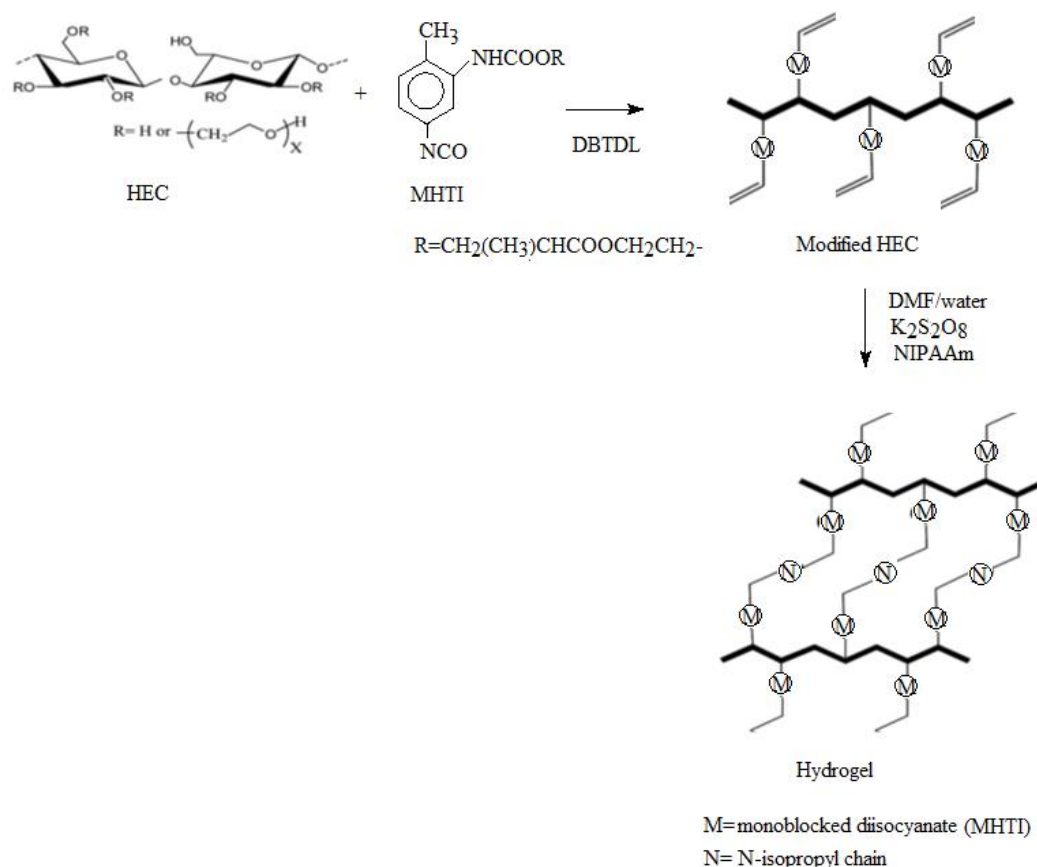


Figure 2.20 Modified HEC-g-*N*-isopropylacrylamide temperature sensitive hydrogel (Peng *et al.*, 2010)

The equilibrium swelling ratio of obtained temperature sensitive hydrogel was determined in buffer solution with pH 7.0 and temperature variable from 25.0 to 45.0 °C. The experimental data showed that they exhibited high sensitivity to temperature and the controlled drug release can be accomplished. The HEC grafted polyacrylic acid and associated attapulgite (HEC-g-PAA/APT) was prepared by grafting acrylic acid onto hydroxyethyl cellulose and combined with various wt% of attapulgite. The results showed that the introduction of 5 wt% attapulgite into

superabsorbent polymer (HEC-g-PAA) can be improved both water absorbency and water absorption rate, and can be retained high water absorbency over wide pH ranges (Wang *et al.*, 2010). New series of pH and saline-responsive superabsorbent composites were prepared from HEC grafted sodium acrylate and associated medicinal stone. The swelling tests revealed the presence of 10 wt% of medicinal stone greatly improved the swelling capacity up to 400% (Wang *et al.*, 2011). Water-soluble polymer containing sulfobetaine groups is synthesized from HEC grafted sulfobetaine-type zwitterionic monomer 3-dimethyl (methacryloyxy-ethyl) ammonium propane sulfonate (DMAPS), in the presence of a ceric ammonium nitrate (CAN)/ethylenediamine tetra acetic acid (EDTA) initiation system. The effects of grafting reaction are determined in terms of percentage of graft polymerization (%GP) and percentage of grafting conversion (%GC). The results found that %GP and %GC strongly depends on concentrations of CAN, EDTA and HEC. The %GP and %GC increases with increasing DMAPS concentration up to a certain value (Zhang *et al.*, 2002). Recently, superabsorbent nanocomposite series are prepared from HEC grafted partially neutralized acrylic acid by solution radical polymerization and incorporation with different fillers including raw vermiculite, acidified vermiculite and organo-vermiculite. (Wang *et al.*, 2011). The swelling capacity test shows that the use of vermiculite provided a great increase of water absorbency and the two latter fillers gave nanocomposites with higher swelling capabilities and swelling rate.

2.9 Vinyl monomers grafted hydroxyethyl cellulose

Either single or mixture types of monomers have been grafted onto hydroxyethyl cellulose and other components are incorporated to form composite materials with enhancing both mechanical properties and swelling capabilities. A partially hydrolyzed acrylamide (Miyata *et al.*, 1995), acrylic acid (Abdel-Halim, 2012; Sahama *et al.*, 2015), acrylamide (Yang *et al.*, 2007), mixtures of acrylic acid and acrylamide (Sahama *et al.*, 2015), 2-(dimethylamino) ethyl methacrylate (Cao *et al.*, 2009), 4-vinylpyridine (Yang *et al.*, 2008), *N,N'*-dimethyl acrylamide (Peng *et al.*, 2008; Yang *et al.*, 2010), *N*-isopropylacrylamide (Peng *et al.*, 2010) and 3-dimethyl-(methacryloy-

loxyethyl) ammonium propane sulfonate (DMAPS) (Zhang *et al.*, 2002) have been grafted onto hydroxyethyl cellulose backbone.

2.10 Initiator system for graft copolymerization of cellulose and cellulose ethers

The general method to synthesize biodegradable graft copolymers based on naturally occurring materials are through the formation of active sites on polymer molecules. The generation of free radicals or ions as reactive species is the most favorable method. The graft copolymerization of vinyl monomers such as acrylic acid, acrylamide and so forth, on to naturally occurring polymers is mostly performed by free radical polymerization due to their product chains which are much longer than the use of anionic polymerization (Kiatkamjornwong, 2007). There are two distinct experiments to generate free radicals on starch, cellulose or cellulose derivative backbone (Athawale *et al.*, 1999). The most general method is chemical initiation such as by using ceric ion system (L-Razi *et al.*, 2003; Huang *et al.*, 1968; Taghi *et al.*, 2006; Apopei *et al.*, 2012), potassium bromated/thiourea dioxide (Abdul-Halem, 2012), ammonium persulfate, potassium sulfate (Zhang *et al.*, 2002; Wang *et al.*, 2010; Wang *et al.*, 2011; Nakason *et al.*, 2010), Fenton reagent ($\text{Fe}^{2+}/\text{H}_2\text{O}_2$) (Witono *et al.*, 2012) and manganese (Mn^{4+}) (Mehrota *et al.*, 1978). The second method is to generate free radicals via photo irradiation on naturally occurring backbone such as by means of ultraviolet, gamma ray (Khanna *et al.*, 2011; Reyes *et al.*, 1968), and microwave (Singh *et al.*, 2006). For a chemical initiating system, ceric ion system is the most widely used because its reactions directly occur with the polymer backbones to generate free radicals at certain position where they can immediately start graft copolymerization. The proposed mechanism of grafting acrylonitrile onto starch in the presence of ceric ion to prepare starch-g-PAN is shown in Figure 2.21. Even though ceric ion system has provided several advantages, however the cost is so high that causes a problem for large scale applications. Various types of superabsorbent polymers have been synthesized by grafting starch, cellulose or cellulose derivatives with various hydrophilic monomers. Besides the ceric ion system, ammonium persulfate (Nakason *et al.*, 2010; Wang *et al.*, 2010; Wang *et al.*, 2011), potassium

persulfate (Quanxiao *et al.*, 2011; Feng *et al.*, 2010; Pandey *et al.*, 2012) have been utilized as a chemical initiator for generating free radical on natural polymer backbone.

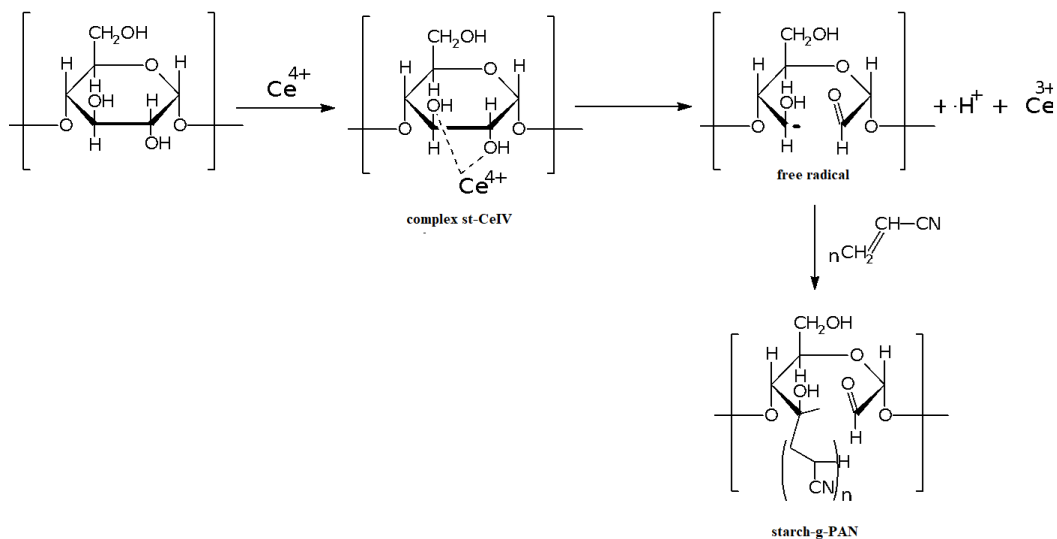


Figure 2.21 Mechanism of grafting acrylonitrile onto starch by ceric ion (Taghi *et al.*, 2006)

In this current research, potassium persulfate was used as chemically initiate reactive radical for grafting polyacrylamide onto hydroxyethyl cellulose. Polymer networking was produced by using *N, N'*-methylenebisacrylamide (MBA) as a crosslinking agent. The resultant SAPs with highest water swelling capacity was later incorporated with various loading of bentonite to form superabsorbent polymer composites (SAPC). The choice of using potassium persulfate as a chemical initiator was primarily considered by a number of following reasons.

The graft copolymerization reaction was carried out in homogeneous condition, the starting material was dissolved in distilled water. The advantages of the solution copolymerization were that all materials can be homogenized with ease to control and perform conditions.

In this reaction, an acrylamide monomer and crosslinker (MBA) were dissolved in distilled water, KPS was thermally initiated to generate reactive free radical which acted as an initiation step of radical graft copolymerization. The tentative thermally initiated KPS into reactive radical is illustrated in Figure 2.22.

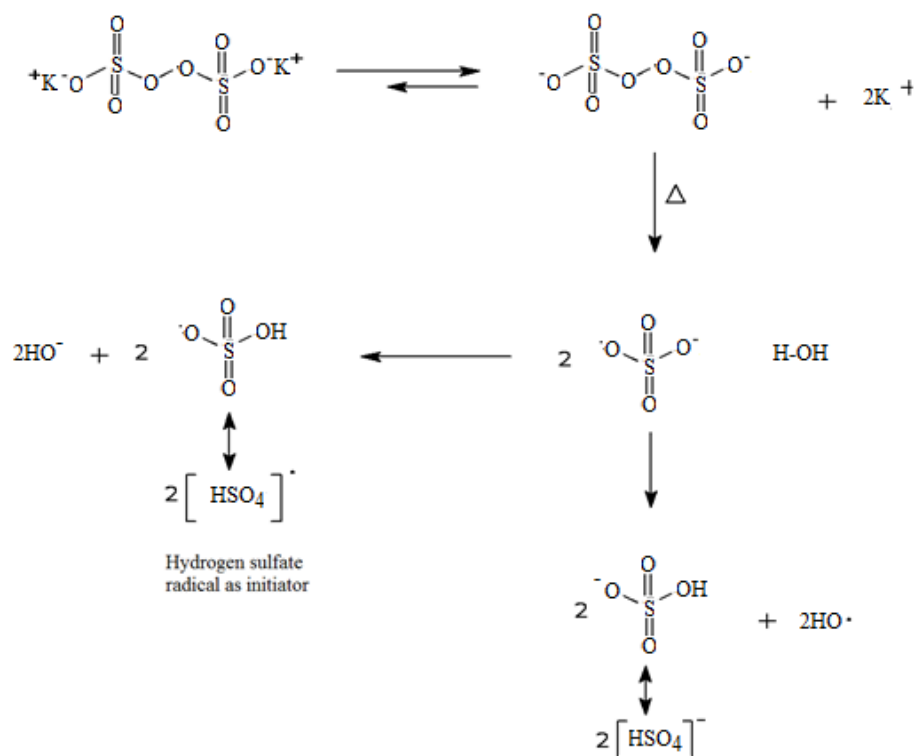


Figure 2.22 Thermal initiated KPS to generate free radical (Huang *et al.*, 2002)

The later, hydrogen of primary hydroxyl on ethyl cellulose was abstracted by reactive sulfate radical to form hydroxyethyl cellulose radical which acted as a propagation step for grafting copolymerization in the presence of acrylamide. The crude product with a mixture form was then purified by soxhlet extraction using acetone and 40% H₂O/EtOH as a solvent to remove unreacted acrylamide, crosslinker, initiator, and unwanted products. The resultant SAPs with carboxyl amide form were saponified using aqueous 2M NaOH and then neutralised by washing several times with distilled water. The final SAPs in proper form of carboxyl salt, carboxyl acid, and carboxamide were expected with enhancing water swelling properties.

2.11 Water-swollable rubbers

A kind of elastomeric material was prepared by mechanically blending rubber both natural and synthetic rubber, water absorbent polymer/composite with other fillers, also referred to water swollable rubbers (WSRs) or water swollable elastomers (WSEs). The end properties were to have a combination functions of both elastomeric materials as predominantly while achieving water swollability. The definition of water swollable rubber has been separately defined by many researchers, as a kind of elastomeric material prepared by blending rubber, water absorbent polymer and other fillers (Wang *et al.*, 1998) or as a new kind of elastomeric material, which possesses not only properties of general rubber (such as high resilience and good tensile strength), but also the water-swollability (Wang *et al.*, 1999). It is also described as a new kind of functional elastomer with elastic sealing and water-swelling properties (Zhang *et al.*, 1999) or as a functional polymer that expands its volume up to more than 1.5 times original by absorbing the surrounding water (Park *et al.*, 2001). Meanwhile it is also defined as a newly developed sealing material that has found broad application in underwater construction or as a new kind of functional elastomer with elastic sealing and water swelling properties (Zhang *et al.*, 2004) and another definition is as a new kind of functional elastomer with elastic sealing and water-swelling properties (Wang *et al.*, 2002). It is also defined as a new kind of functional product with elastic sealing and water-swelling properties (He *et al.*, 2007) and also as a functional polymer that expands its volume up to more than 1.5 times its original size by absorbing surrounding water (Saijun *et al.*, 2009). More definitions include a kind of elastomeric material, which possesses not only properties of general rubber (such as high resilience and good tensile strength), but also the water swollability (Zhang, 2012), a functional polymer that their volume is expanded up to more than 1.5 times their original weight by absorbing moisture or surrounding water (Nakason *et al.*, 2013), a new kind of elastomeric functional materials, and they possess both water-swelling ability and properties of general rubber such as outstanding resilience and excellent tensile strength (Li *et al.*, 2015). It is also known as a new type of functional material and composed of rubber and water-absorbent resin and it can be swollen with water several times its own weight and prevent water leakage from pipes and gaps at the same time (Wang *et*

al., 2015). Finally, it can be defined as a rubbery material which is fabricated from water-repellent products such as fabrics and coating, and they are usually applied for moisture sensitive products (Polgar *et al.*, 2017).

From the versatile definitions, it can be comprehensively concluded that water swellable rubber (WSR) is a new material with function of both elastic material and superabsorbent material, and it can be expanded more than 1.5 times of its mass when it gets swollen in water. It is also widely beneficial for caulking, sealing of gaps and waterproof materials. In recent years, various publications concerning water-swellable rubber have been published where it has been studied by many researchers both in the field of academic and field of industries. WSR contains mainly of rubber matrix, super absorbent resin and other fillers. Various methods have been modified to finally produce water swellable rubber with desiring properties such as, an important character of WSR, improving water swellable property as well as mechanical properties. Grafting hydrophilic polymer onto hydrophobic rubber is one feasible route that has been studied by many researchers, for example, a novel water swellable natural rubber has been produced through grafting polyacrylamide onto natural rubber using KPS/SHS oxidation-reduction as an initiation system with bentonite clay as an inorganic filler. The general properties of WSR both water swelling behaviors and mechanical properties have also been investigated. The change of grafting reaction that is affected by monomer ratio and initial dose is discussed. The results disclosed that at monomer to natural rubber ratio 0.8 and 0.75% of initiator the reaction exhibits the highest grafting ratio and grafting efficiency. The introduction of bentonite affects water absorption rate negatively while the capacity of resisting to salt increases. The results also found that repeat water absorption ratio and water retaining property of WSR with bentonite are better than those of WSR that is produced without bentonite. The free water content decreases when introducing bentonite, but bound water content increases (Bo-xiang, *et al.*, 2015). The water swellable natural rubber is prepared through the grafting of acrylamide onto natural rubber latex in the presence of formaldehyde crosslinker and under sulfur vulcanization. The water swelling property and repeat water swelling property of obtaining WSR was investigated as well as the mechanical property. The results indicated that the amount of crosslinker had effective both water swelling ratio and repeat water swelling ratio of WSR (Wang *et al.*, 2015). Graft

copolymerization of polyacrylic acid on to styrene butadiene rubber forming modified rubber which improved both morphology and mechanical properties of styrene butadiene rubber/polyurethane blends (Taheri *et al.*, 2016). However, the observation clearly displayed that the water swelling capacity of grafted rubber increases dramatically up to 258% when compared to those ungrafted SBR. This was due to the hydrophilic nature of the acrylic acid chains that enhanced the absorption of water within SBR matrix. The important evidence that confirmed the introduction of acrylic acid into SBR was an improving water swelling property when compared to SBR alone.

Studies indicated that the introduction of precipitated silica into WSR prepared by mechanical blending of chloroprene rubber with sodium polyacrylate, a certain chemical interaction occurs between rubber end group and silica leading WSR gave an excellent mechanical property (Wang *et al.*, 1998). The hydrogen bonding occurred between chlorine in chloroprene rubber and hydroxyl of silanol, later covalently formed by removing hydrochloride under heating condition. The proposed mechanism has been detailed in Figure 2.23

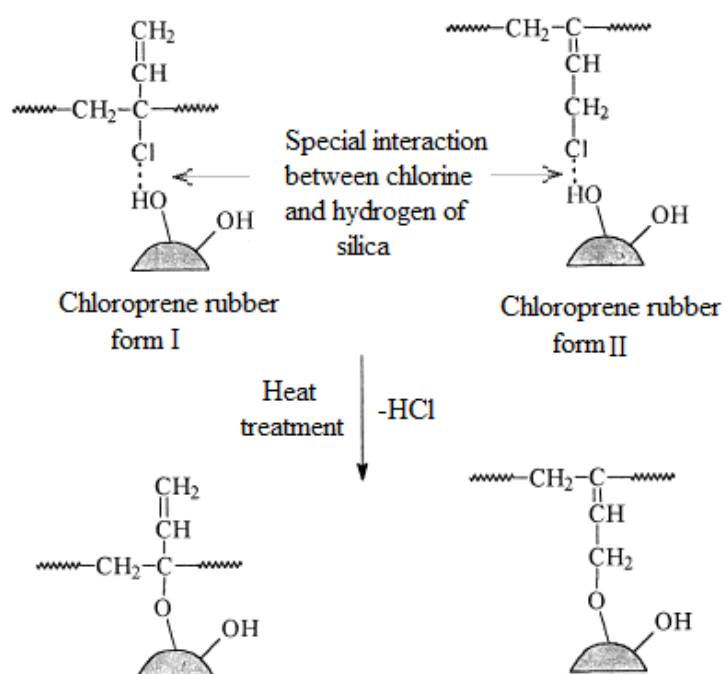


Figure 2.23 Mechanisms of interaction between CR and silica surface (Wang *et al.*, 1998)

According to Wang *et al.*, (1998), the results also found that the introduction of PEO at the proper content into WSR formulation, can positively effect both mechanical properties and water swelling capacity. The WSR prepared by mechanical blending of NR with crosslinked sodium polyacrylate (CSP) and compatibilized by amphiphilic block copolymers poly (ethylene oxide)-b-poly (butyl acrylate) (PEO-b-PBA). The results indicated that the NR and CSP combined together with PEO blocks bonded to CSP while terminating PBA bonded to NR. The specified interaction increased the adhesion between NR and CSP, leading CSP to not migrate from the rubber matrix (Wang *et al.*, 2002).

In order to improve the properties of WSR, some inorganic fillers such as carbon black, silica, and another nonblack filler, were also incorporated. The WSR was generally prepared through multicomponent mechanical blending of hydrophobic rubbers such as chloroprene rubber (Wang *et al.*, 1999; Liu *et al.*, 2006), epichlorohydrin rubber (Zhang *et al.*, 1999; Zhang *et al.*, 2000; Zhang *et al.*, 2001), natural rubber (Park and Kim, 2001; Wang *et al.*, 2002; Saijun *et al.*, 2009; Khongtong *et al.*, 2008), modified natural rubber including epoxidized natural rubber and maleated natural rubber (Nakason *et al.*, 2013) and synthetic rubbers such as chlorinated polyethylene (Ren *et al.*, 2004) with various kinds of superabsorbent polymer and other hydrophilic ingredients. Due to hydrophilic polar nature of superabsorbent polymers and hydrophobic nonpolar rubbers, the aggregation and poor dispersion of SAPs in rubber matrix is one of the serious problems that occurs during processing of WSR. This incompatibility problem often leads to the instability and degradation of WSR. The resulting blends have low water swelling capacity, poor mechanical properties and long-term water retention that causes limited use in practical applications.

The important behaviors of WSR are that they possess not only general rubber property but also water absorbing capacity. In addition, some inorganic fillers are added to improve water swelling capabilities of SAP. Non-black fillers including clay-based materials are of interest in recent years (Wang *et al.*, 2010). The incorporation of clay-based material in SAP not only reduces a production cost, but also improves the water swelling properties (Wu *et al.*, 2006; Zhang *et al.*, 2006). Various types of clays have been incorporated into SAP to form SAPC including diatomite, monmorillonite (Wang *et al.*, 2010), bentonite (Nakason *et al.*, 2004), and attapulgite (Li *et al.*, 2004).

There are two general methods used to prepare WSR; 1) chemical grafting of water swellable polymer such as polyacrylic, polyacrylamide, onto natural rubber, synthetic rubber and its derivatives, 2) mechanical mixing of hydrophobic rubbers with superabsorbent polymers. Herein, the mechanical mixing method is preferred due to its low production cost and easy to control.

2.12 Blends of SAP or SAPC with rubber

The composition of general rubber both natural rubber or synthetic rubber is a long chain hydrocarbon with nonpolar character, which is mostly inferior to water swelling capacity. The promising way to enhance water swelling capacity of rubber is to introduce some hydrophilic polymer into rubber either by mechanical blending or grafting methods. Generally, there are two principal methods used to improve water swelling capacity of rubber, i.e. by chemical grafting copolymerization of hydrophilic monomer onto rubber backbone or through mechanical blending of rubber with various types of superabsorbent polymer. The mechanical blending of rubber with superabsorbent polymer is an effective process due to its rapid processing method and relative ease (Wang *et al.*, 1997; Nakason *et al.*, 2013). The property of final products that is prepared by means of mechanical blending is usually under control. The combination of natural rubber or synthetic rubber and its derivatives with superabsorbent polymer has been investigated by a number of researchers. The final blend products are also called water-swellable rubber (WSR). The WSR has general rubber property and water swellability as they can expand their sizes or shape up to more than twice by absorbing the surrounding water or solution. This character provides a better function for sealing applications since the WSRs can importantly prevent water leak and air permeability.

There are a number of publications that report on preparation of WSR by using various types of rubber, superabsorbent polymers/composites, reinforcing fillers, compatibilizers, and other ingredients.

Blending polychloroprene synthetic rubber (CR) with crosslinked sodium polyacrylate (CSP), reinforces filler a precipitated silica, poly (ethylene oxide) (PEO) as water-soluble polymer and vulcanizing agents form WSR (Wang *et al.*, 1997). The

preparation of parameter and water-absorbent property of the blends were reported. This work aims mainly to study the preparation process of WSR and the optimum composition ranges of the blends were identified as CSP 25–75 phr; precipitated silica 10–50 phr; and PEO 5–30 phr. The effect of composition of the WSR on its water-absorbent properties such as degree of swelling, swelling rate and weight loss ratio of CSP was discussed. The results showed that the precipitated silica and water-soluble polymer (PEO) could improve the water-absorbent properties of WSR. The morphology of WSR was studied by scanning electron microscope (SEM) and micrographs showed a good dispersion of CSP and precipitated silica in the chloroprene rubber. However, later works have been done by Wang and co-researchers. They investigated the effects of fillers on mechanical properties of WSR prepared by blending polychloroprene rubber with crosslinked sodium polyacrylate, precipitated silica, polyethylene oxide and vulcanizing agents (Wang *et al.*, 1998). The mechanical properties of the water-swellingable rubber such as stress at break, strain at break modulus, energy at break, and hardness before and after swelling with water were determined. The results showed that the addition of precipitated silica increased the mechanical properties, while increasing quantity of crosslinked sodium polyacrylate the mechanical properties decreased. However, results also found that the addition of both of silica and CSP can improve water-absorbent properties of the obtained WSR. Furthermore, the addition of polyethylene oxide in ranges of 0-10 phr in the rubber formulation, the water-absorbent properties and the mechanical properties of WSR were also increased. But, the further increasing contents of polyethylene oxide had led to decrease the mechanical properties. The crosslink density of the WSR was calculated by using the Flory–Rehner equation. The mechanical strength of WSR was found to significantly increase with increasing crosslink density, while water-absorbent property decreased with increasing crosslink density. However, mechanical strength of WSR decreased after having first swelling in distilled water. The morphology of the blends was analyzed by SEM and the micrograph showed that both of precipitated silica and crosslinked sodium polyacrylate dispersed well in the rubber matrix.

Phase separation is one of the important obstacles that usually faced off and challenged to rubber technologist because it will generally lead the obtained WSR to have inferior both swelling in water and mechanical properties. This was due to strong

difference in their polarity amongst phase of hydrophobic rubber and hydrophilic SAPC. The promising choices for reducing gap are compatibilized by one which can be combined left to rubber and another one to SAPC (Zhang *et al.*, 1999). Polyvinyl alcohol when grafted with polybutyl acrylate form rubbery PVA-g-PBA which is an amphiphilic graft copolymer and used as compatibilizer for chlorohydrin water-swelling rubber. The synthetic parameters and characterization of polyvinyl alcohol grafted polybutyl acrylate were investigated comprehensively. WSR was compounded by blending chlorohydrin rubber (CHR) with hydrophilic crosslinked polyacrylate (CPA), precipitated silica (PSA), and poly (ethylene glycol) (PEG). The graft copolymerization of butyl acrylate onto poly (vinyl alcohol) was performed by using ceric ammonium nitrate as redox initiation system in aqueous medium. The formation of graft copolymer was confirmed by information of IR, SEM and wide-angle X-ray diffraction (WAXD). The percentages of monomer conversion and grafting were varied with concentrations of initiator, nitric acid, monomer, molecular weight ($X_n = 1750$, $\bar{M} = 80,000$), reaction temperature, and reaction time. The results showed an optimum condition for graft copolymerization reaction were $[Ce^{4+}] = 0.01$ mol/L; $[HNO_3] = 0.05$ mol/L; $[PVA] = 2.5 \times 10^{-4}$ mol/L; $[BA] = 0.702$ mol/L; temperature = $45^\circ C$; and reaction time = 3.5 hours. Moreover, the results also found that the introduction of some organic salts and organic solvents had a great influence upon grafting copolymerization. A series of WSRs were compatibilized by amphiphilic graft copolymer PVA-g-PBA, WSR prepared by blending of chlorohydrin rubber (CHR) with crosslinked polyacrylate (CPA), precipitated silica (PSA) as a reinforcing filler, and poly (ethylene glycol) (PEG) (Zhang *et al.*, 1999). The morphology of the blends was characterized by SEM. The dependence of the water-absorbing ratio by weight, the water-swelling ratio by volume, and the percentage loss by weight on PVA-g-PBA and crosslinked polyacrylate contents were investigated and informed. The results found that at fit contents of PVA-g-PBA affected water swelling behaviors and longterm water retention positively while it had negatively affected to first weight loss. It is very interesting that the percentage of weight loss was found to be less although under the increasing content of CPA. The SEM images indicated the blends had fine dispersion. However, another publication by Zhang and co-workers, shows that WSR was compounded through mechanical blending of chlorohydrin rubber with crosslinked

polyacrylate (CPA), precipitated silica and polyethylene glycol (PEG) (Zhang *et al.*, 2001). This work found that, poly (vinyl alcohol)-*g*-poly (butyl acrylate) (PVA-*g*-PBA) is also used as an amphiphilic compatibilizer for stabilizing the morphology of the blends. Various concentration of PEG loading in the blends was found to influence the swelling behaviors of WSR, and thus the PSA contents was investigated as well. To characterize morphology of the blends, the wide-angle X-ray diffraction (WAXD) technique confirmed the dispersion of PEG in the WSR. The dependence of the water absorbing ratio by weight, the water-swelling ratio by volume, and the percentage loss by weight on PEG and PSA contents were investigated. The effects of PEG and PSA on the second water-swelling behaviors and long-term water-retention behaviors were also determined. The results indicated that the optimum condition for the water-absorbing and water-swelling abilities within the range of the experiment were at 100 phr of CHR, 70-100 phr of CPA, 5-10 phr of compatibilizer PVA-*g*-PBA, 40-50 phr of PEG and the content of PSA at 40- 60 phr. The results also indicated that the first maximum water-swelling ratio by volume was 11.95, and the second maximum water-absorbing ratio by weight was 9.31, respectively.

Choices for removing the immiscible the blends were to basically introduce compatibilizing agent to combine rubber phase with others. Studies have reported the effect of amphiphilic block polymers based on poly-(ethylene oxide) and poly (butyl acrylate) as compatibilizers on the properties of water-swellaible rubber (Wang *et al.*, 2002). WSR was formulated by mechanical blending natural rubber with crosslinked sodium polyacrylate (CSP), poly (ethylene oxide)-*b*-poly (butyl acrylate) (PEO-*b*-PBA), poly (ethylene glycol) (PEG), precipitated silica as reinforcing filler, and under sulfur vulcanization. The preparation process was described and the water- swelling property of WSR was investigated. The results showed that the CSP resin plays the leading role in absorption behaviors. The increasing amounts of CSP resin 0-100 phr leads to have the higher expansion ratio of the rubber. The microphase structure of WSR was characterized by SEM. The results also found the addition of appropriate contents of poly (ethylene glycol) which acts as the pathway of water that can strongly enhance the water swellability. However, the poly (ethylene oxide) and poly (butyl acrylate) as compatibilizers play a dual role of improving compatibility in the system as the miscibility of CSP resin and NR matrix as well as PEG and NR matrix is

improved. The compatibilizing effect can be influenced by the quantity of poly (ethylene oxide)-b-poly (butyl acrylate) (PEO-b-PBA). The SEM images indicated that PEO-b-PBA distributed at the interface between CSP and NR. CSP and NR were linked together by PEO-b-PBA in which the PEO blocks were attached to CSP and PBA blocks were attached to NR.

A series of water swellable elastomers was compounded by mechanical blending of chlorinated polyethylene with super absorbent polymer derived from crosslinked of polyacrylic acid-co-polyacrylamide [P(AA-co-AM)] (Zhang *et al.*, 2004). In this work, the general properties including water swelling properties and mechanical behaviors of the blends were investigated. The results indicated that the equilibrium swelling ratio of the WSR increased with increasing the contents of superabsorbent polymer. The prepared water swelling elastomers were tested for temperature sensitivity, and the results disclosed that at testing temperature below 30° C, the swelling ratio increased with increasing of temperature, whereas at the temperature above 30° C, the swelling ratio decreased with an increase in testing temperature. In addition, WSR samples were tested for pH sensitivity which indicated that the water absorbency was strongly influenced by pH value. This study CPE-g-PEG was used as a compatibilizer and its effect on water swelling properties and percentage of weight loss were investigated. The results indicated that the introduction of compatibilizer has led to increase swelling ratio but decreased the percentage of weight loss while improving the mechanical property of the blends. The study also found that the mechanical property such as tensile strength was slightly decreased when large scale of compatibilizer added. Moreover, WSR was prepared entirely by mechanical blending of chlorohydrin rubber (CHR) with crosslinked poly sodium acrylate (CPA) poly (vinyl alcohol)-g-poly (butyl acrylate) (PVA-g-PBA), precipitated silica (PSA), and poly (ethylene glycol) (PEG) (Zhang *et al.*, 2004). Besides improving water swelling behaviors and mechanical property, the introduction of PVA-g-PBA into WSR affected the physical interaction of the blends. The results evidenced that the addition of PVA-g-PBA had increased the interfacial cohesion between CHR and CPA before and after water swelling and was able to improve water-swelling behavior while percentage loss by weight of sample decreased. The results also found that the

introduction of PVA-g-PBA, especially at the content of 5 phr had strongly influenced the mechanical property of WSR.

Mechanical mixing of chlorinated polyethylene (CPE) with Lithium polyacrylate salt forms WSR (Ren *et al.*, 2005). Lithium acrylate salt (LiAA) is *in situ* formed in a chlorinated polyethylene (CPE) matrix through the neutralization of lithium hydroxide (LiOH) and acrylic acid (AA) during mechanical mixing. The final compounds are vulcanized with dicumyl peroxide (DCP). The Fourier transform infrared spectrometry determination is utilized to characterize the *in-situ* preparation and polymerization of LiAA in CPE matrix. The crosslink density analysis results illustrate that the CPE/LiAA vulcanizates occupy both covalent bonds and ionic bonds. In this research, they were further examined with the effects of the DCP and LiAA contents on the mechanical properties and water-swelling properties of the CPE/LiAA vulcanizates. The relationship between the LiOH/AA molar ratio and the properties of the CPE/LiAA vulcanizates were also determined. The results indicated that LiAA can be improved by the mechanical and water-swelling properties of CPE/LiAA vulcanizates. Furthermore, the results also disclosed that the vulcanizates had an excellent water-swelling property, and their maximum water-swelling ratio was greater than 220% at the concentration of AA 50 phr and 1.0 phr of DCP crosslinker. The results also showed that the water-swelling ratio was increased with increasing LiAA content while increasing of DCP crosslinker had led to decrease in the water swelling ratio of WSR samples. Furthermore, the LiOH/AA molar ratio had strongly affected the water swelling ratio and it showed maximum value at the LiOH/AA molar ratio was 1.0. The *in-situ* preparation and polymerization of LiAA play important roles in the improvement of the mechanical properties and water-swelling properties of CPE/LiAA vulcanizates. It is very interesting to note that the research provided a novel process for the preparation of water-swelling elastomers.

A novel WSR was formulated through mechanical blending of chlorobutadiene rubber (CR) with crosslinked sodium polyacrylate (CSP), modified reactive clay and other additives. In this work, the CSP was firstly modified through interpenetrating polymer networks (IPNs) technology by using crosslinking of P(AA-*co*-BA). The morphology of WSRs sample was characterized by image from scanning electron microscope (SEM). The investigation of mechanical properties, water-swelling ratio

by mass, and the percentage loss of CSP in the WSR were examined. The results indicated that the modified CSP particles had dispersion well in the CR matrix and had led obtained WSR to increase of mechanical properties and water-swelling ratio. Furthermore, the results also found that the percentage of weight loss was significantly decreased, this was due to slightly migrate of CSP when compared with those unmodified sample. The results explored a maximum value of the tensile strength, elongation at break, and water-swelling ratio of WSR at where the percentage content of crosslinked P(AA-*co*-BA) used to modify CSP reached to 30% whereas a minimum percentage loss of CSP was exhibited. On the other hand, the results also found that at the content of modified CSP in WSR at around of 30 phr, the maximum tensile strength was 7.7 MPa, elongation at break was 1530, water-swelling ratio was 438 and it showed a minimum percentage loss of CSP 2.5% (Liu *et al.*, 2006). The highest water absorbent rubber was successfully prepared through mechanical blending of styrene butadiene rubber (SBR) as a matrix, with crosslinked poly sodium polyacrylate (PAANa) as a high absorbent water resin (Zhang *et al.*, 2012). To prevent phase separation in obtained WSR, the copolymer styrene maleic anhydride was used as a compatibilizer while polyethylene glycol was used as an absorbent accelerator. The factors affected were water swelling ratio, water swelling rate and mechanical properties including amount of sulfur, ratio of silicon dioxide to nanocalcium carbonate, amount of PAANa and amount of compatibilizers. The results indicated that the content of absorbent water resin had direct influence to water swelling rate index and swelling ratio of WSR while the results in turn had decreased the tensile property and elongation at break of WSR. The results also found that the swelling rate index was sharply declined at sulfur content 1-2 phr and slightly decreased when increasing sulfur up to 3 phr, for swelling ratio, the results had an optimum at the content of sulfur 2 phr which is identical tensile strength. However, compatibilizer affected percentage was of weight loss due to less migration of PAANa.

Three different types of natural rubber were used to prepare WSNRs which were investigated for their properties both swelling behaviors and mechanical property (Nakason *et al.*, 2013). The first type of WSNR vulcanizates was formulated from latex mechanical blending of high-ammonia natural rubber latex with superabsorbent polymer composite (SAPC), poly (ethylene oxide) (PEO) and trimethylolpropane

trimethacrylate (TMPTMA) and another two types were formulated from solid blending of epoxidized natural rubber and maleated natural rubber with super absorbent polymer composite (SAPC), poly (ethylene oxide) (PEO) and trimethylolpropane trimethacrylate (TMPTMA). The mechanical properties and water absorbency of all WSNRs were investigated. The result showed that WSNRs containing 10 phr of PEO and 2 phr of TMPTMA had higher mechanical strength and water absorbency than those without both PEO and TMPTMA. The results also found that the increasing PEO loadings in the range of 20–40 phr showed the higher water absorbency but lower mechanical strength. However, the results exhibited the higher scorch and cure times with the lower crosslinking density and cure rate index in the MNR-modified WSNRs sample, than those unmodified WSNR and ENR-modified WSNR. Furthermore, both the ENR- and MNR-modified WSNRs exhibited the highest water absorbency but had lower mechanical strength when comparison was made to the unmodified WSNR. TGA curve result of the SAP and vulcanized rubber were thermally degraded under oxygen atmosphere, whereas 11% of the residues were bentonite and ZnO. The attempts to prepare WSR with desirable properties have been made by many of researchers, it's well known that WSR was possibly prepared through two different ways including grafting loving water monomer onto rubber and mechanical blending rubber with superabsorbent polymer/composite and other fillers. The latter was more effective due to ease in production processability and yielding under controlled properties at lowest cost. Rubbers such as natural rubber, modified natural rubber and synthetic rubber, have been formulated with superabsorbent polymer/composite and fillers to form various WSR with variety properties. WSR was formulated through mechanical blending of nitrile rubber (NBR), carbon black and other additive fillers with crosslinked sodium polyacrylated (CSP) (Jiang *et al.*, 2013). The CSP was later modified by means of interpenetrating polymer network technology with crosslinked poly (AA-co-BA). The scanning electron microscope was utilized to characterize the morphology of WSR. The obtained WSR was investigated for mechanical properties, water swelling ratio by mass and the percentage loss of CSP. The results indicated that modified CSP particle had great dispersion in the rubber matrix, leading enhancement of mechanical property while the reduction of percentage loss of CSP. The results also found that at the content of crosslinked poly (AA-co-BA) nearly 30% was used to

modify CSP, the obtained WSR exhibited the maximum of tensile strength, elongation at break and water swelling ratio. At that time the minimum value of percentage loss of CSP in WSR was disclosed. The excellence of the tensile strength, elongation at break, water swelling ratio and percentage loss of loving water resin was achieved at the content of CSP introduction in WSR about 30 phr.

A water swellable elastomer formed by dynamic vulcanized ethylene–vinyl acetate copolymer (EVA)/chlorinated polyethylene (CPE)/nitrile butadiene rubber (NBR) blends with the cross-linked poly (sodium acrylate) (CPNaAA) as a loving water resin which was firstly dispersed in the NBR rubber. In this study, the mechanical properties, water-swelling behavior, weight loss and crystallization behavior of the obtained WSRs were systemically investigated. The results found that the mechanical properties of WSRs decreased with the increasing of the loving water resin contents, especially when the CPNaAA content is above 20 phr. However, the strong water swelling behaviors and the water swelling ratio of the WSRs were observed when introducing the content of CPNaAA at 50 phr. The results also disclosed that the swelling ratio of WSRs was 669.3% at the immersion time of 120 h. The introduction of CPNaAA contents at 60 phr has led WSRs to gain the highest water swelling rate and accomplished the swelling equilibrium at about 566.3% in 23 h. For the secondary and third water-swelling behaviors experiment, the results showed that the WSRs had significantly rapid swelling equilibrium and decreasing in weight loss. The X-ray diffraction results indicated that the increasing of CPNaAA content would be increased in the crystalline structure content in EVA. The SEM micrograph study of the etched surface resulted that the CPNaAA particles dispersed finely in the WSRs and coated with cross-linked NBR rubber. Furthermore, field-emission scanning electron microscopic graphs illustrated the crystalline structure of EVA and clusters of flakes had fine dispersion on the etched surface of WSRs (Li *et al.*, 2014).

Dehbari *et al.*, (2015) studied the preparation of WSR by mechanical blending of poly (dimethylsiloxane) rubber (PDMS) as a matrix with superabsorbent polymer which was synthesized from polymerization of acrylic acid with partially neutralizing by NaOH. The Results indicated that the introduction of PAA into PDMS rubber had proved water swelling ability while the durability of WSR was decreased. They explained clearly due to poor interfaces between rubber and superabsorbent polymer.

The results also found that the tensile properties of SWR decreased after it had water immersion. However, the introduction of NaOH for PAA neutralization or aminopropyltriethoxysilane for compatibilization of PDMS and PAA increased in water swelling ability and/or durability. The results also indicated that when the compatibiliser and the neutraliser were added together both the water swelling ability and durability further increased due to the increase of interfacial cohesion amongst them (Dehbari *et al.*, 2015).

CHAPTER 3

MATERIALS AND METHODOLOGY

3.1 Materials

3.1.1 Hydroxyethyl cellulose

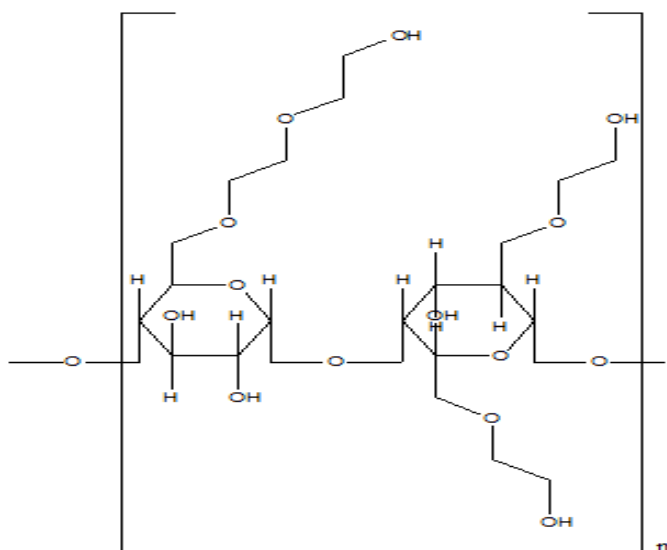


Figure 3.1 Molecular structure of HEC

Hydroxyethyl cellulose analytical reagent grade is manufactured by Merck KGaA corporate, Frankfurter Strasse, Germany. It is the most wellknown modified cellulose with gelling and thickening agent derived from the reaction of cellulose with ethylene oxide. HEC is used as the polymer backbone for polymerization of acrylamide monomer.

3.1.2 Acrylamide (AM)

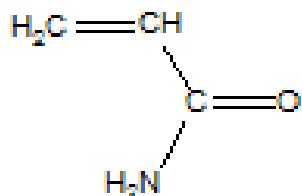


Figure 3.2 Molecular structure of acrylamide

Acrylamide (AM) with the chemical formula C_3H_5NO of 99% purity used for synthesis is supplied by Merck KGaA corporate, Frankfurter Strasse, Germany. AM is absolutely used as a chosen monomer for polymerizing on HEC backbone.

3.1.3 Potassium persulfate (KPS)

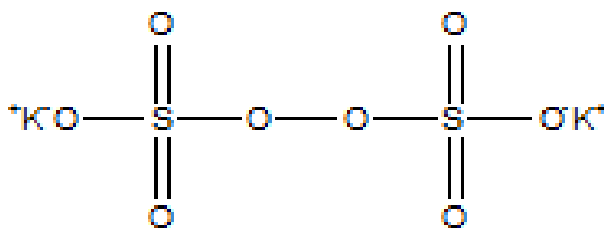


Figure 3.3 Molecular structure of KPS

Potassium persulfate (KPS) with 99% purity is manufactured by Ajax Finechem and is used as initiator in the radical polymerization.

3.1.4 *N,N'*-methylenebisacrylamide (MBA)

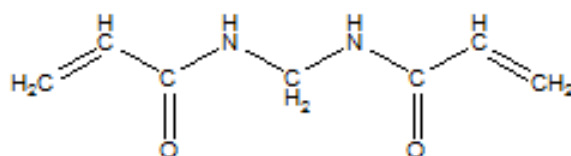


Figure 3.4 Molecular structure of MBA

N,N'-Methylenebisacrylamide (MBA) analytical reagent grade can be purchased from Fluka Buch SG, Switzerland and can be used as a cross-linking agent to construct the network of polymer.

3.1.5 Acetone

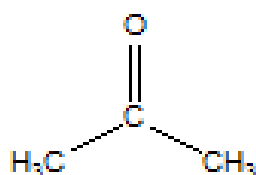


Figure 3.5 Molecular structure of acetone

Acetone analytical reagent grade with 99.5% purity is manufactured by Merck KGaA corporate, Frankfurt Strasse, Germany and was used in this study as a solvent for removing the unreacted HEC and AM.

3.1.6 Toluene

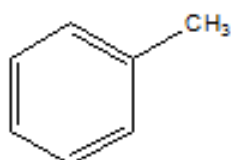
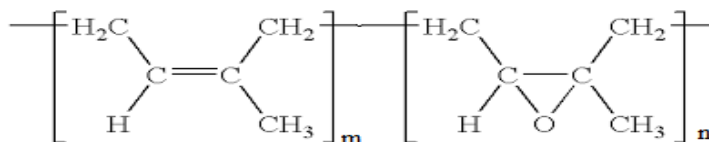


Figure 3.6 Molecular structure of toluene

Toluene analytical reagent grade with 99.5% purity is manufactured by RCI Labscan Ireland. In the process of crosslink density measurement, a solvent with good swelling of rubber can be used to define crosslink density and toluene was better choices for our works.

3.1.7 Epoxidized natural rubber (ENR-25) and (ENR-50)



Where $m = 0.75$ and $n = 0.25$ for ENR-25

$m = 0.50$ and $n = 0.50$ for ENR-50

Figure 3.7 Molecular structure of ENR-25 and ENR-50

Epoxidized natural rubber (ENR) with oxirane group randomly with 25% epoxide mole or 50% epoxide mole is manufactured by Muang Mai Guthrie Public Co., Ltd, Surathani, Thailand. ENR both 25 and 50 mole % epoxidizing were used in this study as a rubber matrix for preparation of water swellable rubber.

3.1.8 Zinc oxide

For this study, Zinc oxide (ZnO), white seal activator, laboratory grade was purchased from Metoxide Thailand Industry Chemical Co., Ltd Pathumthani Thailand. Zinc oxide works as co-activator with stearic acid in the system of sulfur vulcanization.

3.1.9 Stearic acid

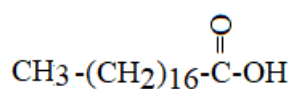


Figure 3.8 Molecular structure of stearic acid

Stearic acid Laboratory grade activator was purchased from Imperial Industry Chemical Co., Ltd Pathumthani Thailand. Stearic acid works as an accelerator couple with TBBS in sulfur vulcanization system.

3.1.10 N-tert-butyl-2-benzothiazyl sulfonamide (TBBS)

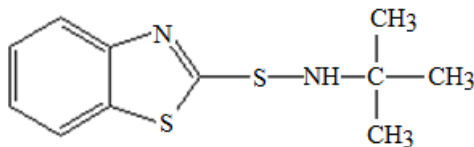


Figure 3.9 Molecular structure of TBBS

For the study, N-tert-butyl-2-benzothiazyl sulfonamide (TBBS) accelerator as a chemical grade was purchased from Flexsys America L.P. Reliance Technochem Co., Ltd Bangkok Thailand.

3.1.11 Sulfur

Sulfur (S₈) vulcanizing agent for natural rubber, laboratory grade was purchased for Ajax Chemical Co., Ltd Auckland New Zealand to be used in the current study.

3.1.12 Polyvinyl alcohol (PVA)

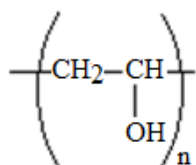


Figure 3.10 Molecular structure of PVA

As a material for the study, poly(vinyl alcohol) was purchased from Kijpaiboon Chemical Ltd., Part, Bangkok Thailand.

3.1.14 Methanol

Methanol (MeOH) analytical grade with 99.9% purity is manufactured by Merck KGaA Corporate, Frankfurter Strasse, Germany.

3.1.15 Ethanol

Ethanol ($\text{CH}_3\text{CH}_2\text{OH}$) analytical grade with 99.9% purity is manufactured by Merck KGaA corporate, Frankfurt Strasse, Germany and was purchased for the current study.

3.1.16 Sodium hydroxide

Sodium hydroxide (NaOH) with 89.5% analytical grade was purchased from Fluka Buch SG, Switzerland.

3.2 Instruments

3.2.1 Internal mixer

Internal mixer used in this study was Brabender Plasticorder, model PLE 331 (Brabender OHG Duisburg, Germany) with a mixing chamber of 80 cm^3 . The mixer consists of an enclosed mixing chamber with two rotors to perform high-speed mixing. The rotor speed and mixing temperature can be adjusted in a range of 0 to 500 rpm and 25 to 300 C, respectively.



Figure 3.11 Internal mixer Brabender plasticorder

3.2.2 Mooney Viscometer

A Mooney viscometer, model VISCAL (Tech Pro Co., LTD., USA) was used to measure Mooney viscosities of natural rubber and graft copolymers. A flat cerate disk rotates in the rubber with a fixed rotor speed of 2 rpm. Test temperature is preheated at 100 C for 1 min and testing for 4 min according to ASTM D1646-04.



Figure 3.12 Mooney viscometer

3.2.3 Fourier Transform Infrared Spectrometer (FTIR)

Infrared transmission spectra were recorded using a Fourier transform infrared (FTIR) spectrometer, model Bruker Tensor 27 from Bruker Corporation. The scan range was from 4400 to 400 cm^{-1} with the resolution better than 1 cm^{-1} (apodized), optionally better than 0.5 cm^{-1} . A sample of SAP was prepared by directly powdering with KBr and pelletizing.



Figure 3.13 Fourier transform Infrared spectrophotometer

3.2.4 X-ray diffraction

XRD patterns of bentonite clay, SAP and SAPC were determined using X-ray diffractometer (X' pert MPD, PHILIPS, Netherlands) with $\text{CuK}\alpha$ radiation source. The X-ray emitting tube was set at 40 kV operating voltage and 30 mA electric current. The sample was tested at room temperature with an angular range from 5° to 90° (2θ) and scan speed of $3^\circ/\text{min}$.



Figure 3.14 X-ray diffractometer

3.2.5 Thermogravimetry (TGA)

Thermogravimetric analyses (TGA) were determined using the Simultaneous Thermal Analyzer (model STA8000, Perkin Elmer, United States of America) with a scanning rate of $10^\circ\text{C}/\text{min}$ under gas N_2 flowing at $20\text{ mL}/\text{min}$ in the temperature range from 30 to 800°C .



Figure 3.15 Thermogravimeter analysis

3.2.6 Scanning electron microscope

Morphological properties of SAP, SAPC and the dispersion of bentonite clay particles in composites were characterized by scanning electron microscopy with energy dispersive X-ray spectroscopy (SEM, Quanta, FEI, the Netherlands).



Figure 3.16 Scanning electron microscope

3.2.7 Moving Die Rheometer (MDR)

A rotorless rheometer (Rheo Tech MD+, Tech Pro, Inc., from Cuyahoya Falls, USA) was used to determine the curing characteristics of the rubber composites at 160 °C with 1° arc and 60 min. The optimum cure time (t_{C90}) and scorch time (t_{S1}), the minimum and maximum torques (M_L and M_H , respectively), and delta torque ($M_H - M_L$) were determined from the curing curves. Cure rate index (CRI) was measured based on ASTM D52893.



Figure 3.17 Moving Die Rheometer

3.2.8 Testing Machine

Tensile properties in terms of tensile strength, elongation at break, and modulus were tested at room temperature, according to ASTM D412 using a universal tensile testing machine (Hounsfield Tensometer, model H 10KS, Hounsfield Test Equipment Co., Surrey, UK). The dumbbell-shaped specimens were first dying cut from the vulcanized rubber sheets with ASTM die type C. Then, the hardness was tested by using a durometer Shore A (Frank GmbH, Hamburg, Germany) according to ASTM D2240.

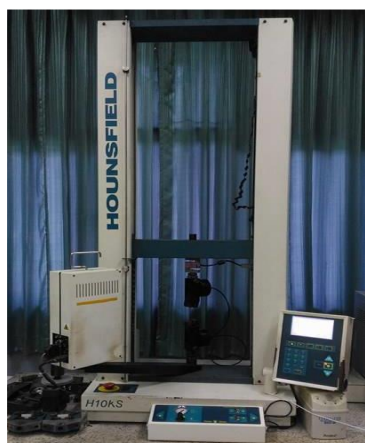


Figure 3.18 Testing machine

3.2.10 Thermogravimetric Analyzer (TGA)

Thermogravimetric Analysis (TGA) was performed using a TGA Q100 TA Instrument-Walters equipped with an EGA oven furnace. A 10-20 mg sample was placed in a platinum pan. Analyses were carried out under nitrogen or oxygen atmospheres of gas flow = $100 \text{ ml}\cdot\text{min}^{-1}$, at a heating rate of $10 \text{ }^\circ\text{C}\cdot\text{min}^{-1}$ with a temperature range of 30 to $575 \text{ }^\circ\text{C}$



Figure 3.19 Thermogravimetric analyzer

3.2.11 Hardness Tester

Indentation typed shore durometer (Afri, Italy) was used for hardness testing of specimens according to ASTM D 2240.



Figure 3.20 Hardness tester

3.3 Methodology

3.3.1 Preparation and characterization of SAP and SAPC

3.3.1.1 The effect of HEC/AM ratios on graft copolymerization of Superabsorbent polymer (SAP)

This study was firstly experimented by investigating the appropriate ratios of hydroxyethyl cellulose to acrylamide monomer by using a constant amount of potassium persulfate (KPS) initiator, a crosslink under *N', N'*-methylenebisacrylamide (MBA) and the overall reaction time for 120 minutes at a constant rate of agitation. An experiment was carried out by weighing accurately dried HEC 1.20 g which was then

dissolved in 40 mL of distilled water in next the four round bottom reaction kettle equipped with a mechanical stirrer, condenser, nitrogen line and dropping funnel. Nitrogen gas was purged thoroughly into the reactor for 10 minutes to remove oxygen gas, which can disturb the copolyrization reaction when it formed oxygen radical. The solution was then heated up to 60 °C with nitrogen gas purged continuously for 30 minutes. Subsequently, 1.0 g of KPS as initiator (0.3mol/100 g HEC) was added and stirred at the speed of 100 rpm for 10 minutes to generate radicals. To prevent immediately copolymerized reaction and avoid unwanted products, the chemical reactant (HEC + H₂O + KPS) was cooled down to 50 °C. The various amount of AM monomer (1.2, 2.4, 6.0, 12.0 and 18.0 g) with 0.3 mmol/100 g HEC of crosslinker (MBA) were incorporated carefully through dropping funnel. Reaction temperature was slowly increased up to 70 °C and kept constant until graft copolymerization was completed. The reaction parameters are indicated in Table 3.1.

Table 3.1 Various parameters on graft copolymerization

Parameters	Set of experiments				
	1	2	3	4	5
HEC/AM ratios (g/g)	Variables ^a	To be fixed	To be fixed	To be fixed	To be fixed
KPS initiator (mol/100 g HEC)	To be fixed	Variables ^b	To be fixed	To be fixed	To be fixed
Reaction temperature. (°C)	70	70	Variables ^c	To be fixed	To be fixed
Reaction time (minute)	120	120	120	Variables ^d	To be fixed
MBA crosslinker (mmol/100gHEC)	0.3	0.3	0.3	0.3	Variables ^e

Remarks:

^aHEC/AM ratios (g/g) will be varied at 1/0.5, 1/1, 1/5, 1/10 and 1/15

^bKPS contents (mol/100 g HEC) will be varied at 0.15, 0.30, 0.45, 0.60 and 0.75

^cReaction temperature (°C) will be varied at 50, 60, 70, 80 and 90

^dReaction time (minute) will be varied at 60, 90, 120 and 150

^e MBACrosslinker (mmol/100gHEC) will be varied at 0.05, 0.1, 0.2 and 0.3

Table 3.2 HEC/ AM ratios of graft copolymerization

HEC (1.2 g)	Set of experiments				
	1	2	3	4	5
AM g	1.2	2.4	6.0	12.0	18.0
KPS initiator (g / g HEC)	1	1	1	1	1
Reaction temperature. (° C)	70	70	70	70	70
Reaction time (minute)	120	120	120	120	120
MBA (mmol/100 gHEC)	0.3	0.3	0.3	0.3	0.3

The flow chart of sequential an experiment is briefly indicated in Figure 3.21. Crude products containing unreacted acrylamide, homopolymer of acrylamide and grafted copolymers were then purified by Soxhlet extraction for 24 hours using acetone and 60%EtOH/H₂O as a solvent to eliminate unreacted acrylamide and polyacrylamide, respectively.

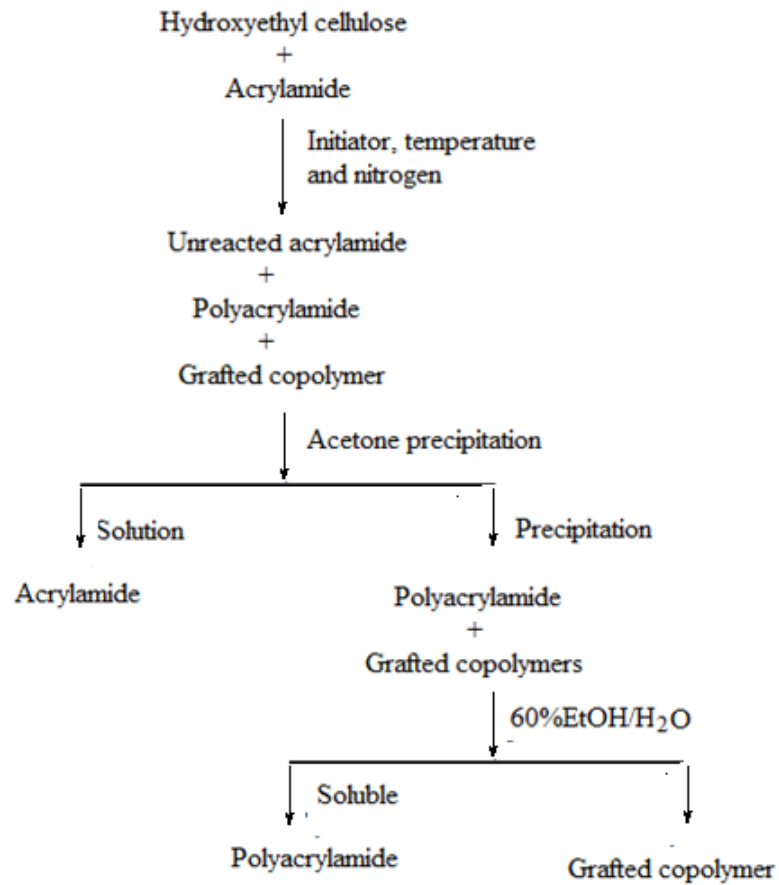


Figure 3.21 Grafted copolymerization and separation steps

The extent of grafted copolymer in terms of the grafting (G) and grafting efficiency (GE) were calculated by the following equations (Ghosh *et al.*, 1998):

$$\% \text{Grafting yield} = \frac{M_2 - M_0}{M_0} \times 100 \quad (3.1)$$

$$\% \text{Grafting efficiency} = \frac{M_2 - M_0}{M_1 - M_0} \times 100 \quad (3.2)$$

Where M_0 , M_1 and M_2 denote mass (in grams) of (HEC+AM), the weight of the dried sample before extraction and the weight of the sample after extraction, respectively.

Swelling measurement of the SAPs obtained will be performed as follows:

The resultant SAPs were dried in hot air oven at 50° C until the sample weight unchanged. The sample was then grounded into powder and filtered through 60 mesh sieve and a sample of approximately 0.2g in accurately weighed tea bags were immersed in 500 mL of distilled water at ambient temperature to reach swelling equilibrium. The sample was withdrawn at specified intervals and the tea bag was hung to remove the excess water on the surface. The weight of each swollen sample was recorded. The sample was then dried again at 50° C to a reach constant weight. The degree of water absorption (S_w) and degree of weight loss (L_w) were determined using the following equations (Zhang *et al.*, 2001; Wang *et al.*, 2002; Liu *et al.*, 2006; Saijun *et al.*, 2008).

$$S_w = \frac{W_2 - W_1}{W_1} \quad (3.3)$$

$$L_w = \frac{W_1 - W_3}{W_1} \times 100 \quad (3.4)$$

Where W_1 and W_2 denote the weights of the sample before and after the water absorption respectively, and W_3 denotes the dried weight of a sample after water absorption

The HEC/AM initial parameter ratios were investigated, and based on the water swelling properties of SAPs obtained, the ratio that gave the highest water swelling capacity was chosen for further study with another parameter. Other factors affecting water swelling capacity were obtained SAPs including KPS amount and MBA concentration. The SAPs obtained from each of sets of experiments were characterized for FTIR spectroscopic techniques.

3.3.1.2 Effect of alkaline hydrolysis, temperature and time on swelling capacity

The obtained SAPs in amide form had low water swelling capacity, an approximation of up to 30 g/g of initial weight. To improve the water swelling capacity of SAPs obtained from the various condition of copolymerization, an approximated weight 5 g of the graft copolymer was transferred to four neck round bottle flask equipped with mechanical stirring, reflux condenser and thermometer. The 100 mL solution of 2 mol/L sodium hydroxide was then added and saponified at temperature of 50, 60, 70, 80 and 90 °C for various reaction times (30, 60, 90 and 120 mins) and stirred at 100 rpm. The important condition for saponification of SAPs is shown in Table 3.3.

Table 3.3 Conditions for the saponification of SAP and SAPC

Parameters	Set of experiments	
	1	2
NaOH concentration (mol/l)	2	2
Reaction temperature (°C)	Variables ^a	To be fixed
Reaction time (minute)	60	Variables ^b
Agitation speed (rpm)	100	100

Remarks:

^a Reaction temperature will be varied at 50, 60, 70, 80 and 90 °C

^b Reaction times will be varied at 30, 60, 90, 120 and 150 mins.

Table 3.4 Parameters of saponified of SAPs

Parameters	Variable				
Concentration of NaOH (Molar)	2				
Reaction temperature (°C)	50	60	70	80	90
Reaction time (minute)	30	60	90	120	
Agitation speed (rpm)	100				

The final concentration of the graft copolymer in NaOH solution was calculated in term of percentages (w/w) of the total mass. The pH of the saponified products was then adjusted to nearly under 7 by dividing into two different methods; firstly, the sample was neutralized by the addition of a 1M HCl solution, stirred for several minutes and tested for pH liquor until it has reached to 7, and the second was washed several times with distilled water. In the final steps, the reaction contaminated by-products including ammonia, unused sodium hydroxide and sulfate ion were then removed by washing with distilled water. The final saponified products were solidified by the rapid addition of an excess amount of acetone. The solidified copolymers were then filtered through the simple filter and dried in a hot air oven at 50-60 °C until constant weight. They were then ground into powder and filtered through 60 mesh sieves to leave the powdery SAP and were tested for water swelling capacity (S_w) and weight loss (L_w) by using equation (3 and 4).

3.3.1.3 Effect of KPS amount on water swelling capacity

The SAPs produced from various HEC/ AM ratios that gave highest water swelling capacity were chosen for investigating the next parameter with influencing the graft copolymerization and water swelling capacity. The second investigation parameter was KPS amount which was used for radical initiator polymerization. Studies have indicated that KPS influence both graft copolymerization reaction and water swelling capacity of SAPs. From the HEC/AM ratios experiments, the results shown the highest water swelling capacity was archived at the HEC/AM ratios at 1 : 10, therefore an experiment further took place by weighing accurately of dried HEC 1.20 g then by dissolving in 40 mL of distilled water in the four next round bottom reaction kettle equipped with a mechanical stirrer, condenser, nitrogen line and dropping funnel. Nitrogen gas was purged thoroughly into the reactor for 10 minutes to remove oxygen gas, which can interrupt the copolymerization reaction when it formed oxygen radical. The solution was then heated up to 60 °C with nitrogen gas purged continuously for 30 minutes. Subsequently, various amount of KPS initiator (0.5, 1.0, 1.5, 2.0 and 2.5 g/1.2 g HEC) was added and stirred at speed of 100 rpm for 10 minutes to generate radicals. To prevent the immediately copolymerized reaction and avoid unwanted products, the

chemical reactant (HEC + H₂O + KPS) was cooled down to 50 °C. The exactly 12.0 g amount of AM monomer with 0.3 mmol/100 g HEC of crosslinker (MBA) were incorporated carefully through dropping funnel. Reaction temperature was slowly increased up to 70 °C and kept constant until graft copolymerization was completed. The reaction parameters are indicated in Table 3.5

Table 3.5 Various contents of KPS incorporate on graft copolymerization

HEC (1.2 g)	Set of experiments				
	1	2	3	4	5
AM (g)	12.0	12.0	12.0	12.0	12.0
KPS initiator (g/g HEC)	0.5	1.0	1.5	2.0	2.5
Reaction temperature. (°C)	70	70	70	70	70
Reaction time (minutes)	120	120	120	120	120
MBA (mmol/100gHEC)	0.3	0.3	0.3	0.3	0.3

The final SAPs obtained from various contents of KPS was tested for water swelling capacity and the highest water swelling capacity was chosen for further investigation of MBA concentration.

3.3.1.4 Effect of MBA concentration on water swelling capacity

Studies indicated that higher crosslink density in SAPs affect water swelling capacity due to producing the small pore size in the SAPs and usually increases in gel strength causing an obstacle when water attempted drawing into the network through diffusion forces. The SAPs produced at appropriate HEC/AM ratios and KPS amount with having highest water swelling capacities was then used as a pendent parameter for investigating the influence of crosslinker concentration on water swelling properties of SAPs. The experiments started by weighing accurately of dried HEC 1.20 g then dissolved in 40 mL of distilled water in the four next round bottom reaction kettles equipped with a mechanical stirrer, condenser, nitrogen line and dropping funnel. The reaction mixtures were stirred at 100 rpm while nitrogen gas was purged thoroughly

into the reactor for 10 minutes to remove oxygen gas, which can be interrupted the reaction process when oxygen free radical was formed. The solution was then heated up to 60° C with nitrogen gas purged continuously for 30 minutes. Subsequently, 0.3 mol/100 g HEC of KPS initiator was added and stirred at the speed of 100 rpm for 10 minutes to completely generate macro radicals. To prevent the immediate copolymerization reaction and avoid unwanted products, the chemical reactant (HEC + H₂O + KPS) was cooled down to 50° C. The exactly 12.0 g amount of AM monomer with various concentration of MBA (0.05, 0.1, 0.2, 0.3 and 0.4 mmol/100 g HEC of crosslinker (MBA)) were minutely incorporated through a dropping funnel. Reaction temperature was slowly increased up to 70° C and kept constant until graft copolymerization was completed. The reaction parameters are indicated in Table 3.6.

Table 3.6 Various concentration of MBA parameter on graft copolymerization of SAPs

HEC (1.2 g)	Set of experiments				
	1	2	3	4	5
AM (g)	12.0	12.0	12.0	12.0	12.0
KPS initiator (g/g HEC)	1.0	1.0	1.0	1.0	1.0
Reaction temperature. (° C)	70	70	70	70	70
Reaction time (minute)	120	120	120	120	120
MBA (mmol/100gHEC)	0.05	0.1	0.2	0.3	0.4

3.3.2 Effect of bentonite clay for preparation of superabsorbent polymer composite (SAPC)

The optimal conditions justified from the preparation of superabsorbent polymer were applied for preparation of super absorbent polymer composite (SAPC) with varying quantities of bentonite clay at 20, 30, 40, 50 and 60 wt % of HEC. Before dissolving dried HEC in distilled water, the exact amount of bentonite clay was

dispersed in 40 mL distilled water and stirred at speed of 100 rpm. After that the copolymerization reaction was performed following the same procedures as described for SAPs preparation. The condition for SAPC preparation is detailed in Table 3.7

Table 3.7 Bentonite loading on graft copolymerization of SAPC

HEC (1.2 g)	Set of experiments				
	1	2	3	4	5
AM (g)	12.0	12.0	12.0	12.0	12.0
KPS initiator (g/g HEC)	1.0	1.0	1.0	1.0	1.0
Reaction temperature. ($^{\circ}$ C)	70	70	70	70	70
Reaction time (minute)	120	120	120	120	120
MBA (mmol/100gHEC)	0.1	0.1	0.1	0.1	0.1
Bentonite clay (wt %)	20	30	40	50	60

Unreacted AM and ungrafted PAM were removed and the grafting (G) and grafting efficiency (GE) were expressed for determined using the identical equations as described previously. The effect of bentonite clay loadings on water swelling properties of SAPC was investigated following the procedures described for water swelling measurement. Degrees of water absorption (S_w) and weight loss (L_w) were calculated using the equations (3.3) and (3.4), respectively. The SAPC with the highest water swelling capacity was chosen to blend with epoxidized natural rubber for a preparation of WSR.

3.3.2.1 Effect of alkaline hydrolysis of SAPC

To improve the water swelling capability of the resultant SAPCs obtained, approximately 5 grams of the purified graft copolymer were added into four-neck round bottom flask equipped with mechanical stirrer, reflux condenser and thermometer. The exact amount in mL of 2 mol/L of sodium hydroxide solution was added and saponificated at reaction temperatures and reaction periods as detailed in Table 3.8.

Table 3.8 Conditions for alkaline hydrolysis of SAPC

Parameters	Experiments
NaOH concentration (mol/l)	2
Reaction temperature (° C)	60
Reaction time (minute)	60
Agitation speed (rpm)	100

The final concentration of the purified graft copolymer in NaOH solution was calculated in term of percentages (w/w) of the total mass. The pH of the saponified SAPCs was then adapted to nearly 7 by washing several times with distilled water and testing for liquor pH.

3.4 Preparation of water-swallowable rubber (WSR)

3.4.1 Effect of ENR and ENR/SAPC blends

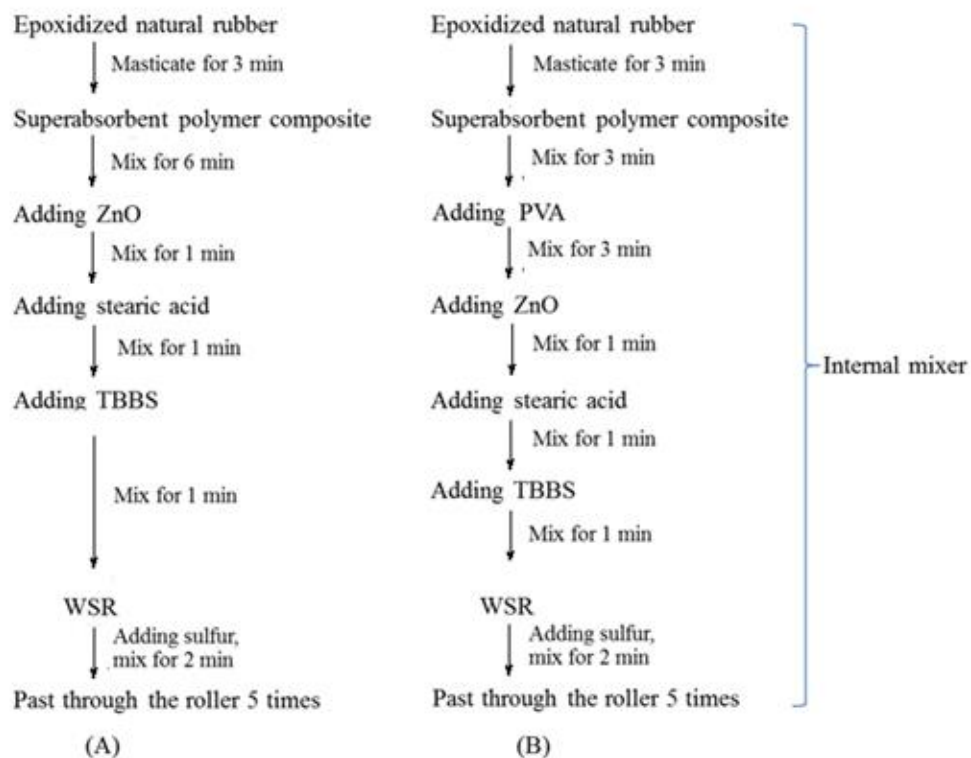
Two grades of ENRs including ENR-25 and ENR-50, with 25 and 50 mol% of epoxide groups were used to produce WSR by mechanical blending with superabsorbent polymer composite derived from filled bentonite HEC-g-PAM. The slight changes in chemical structure through the introduction of oxygen atom led ENRs changes in both chemical and physical properties. The presence of the oxirane group in ENRs was expected to have some potential interaction with hydrophilic superabsorbent polymer composite. To prepare WSR, the ENR was mixed with super absorbent polymer composite (SAPC) obtained from Part I in dried solid blending process using the internal mixer (Brabender Plastic Corder) at 40°C, a rotor speed of 60 rpm and fill factor 0.8 following the method described by Nakason *et al.* (2013). The compounding formulation and mixing procedures are shown in Table 3.9 and Figure 3.23. The mixing was done in one step; by epoxidized natural rubber mixed with other ingredients as a consequent addition of each ingredient into the internal mixer at the specified time as detailed in Figure 3.22; then sulfur as curing agent was added properly into the internal

mixer to make the final compound. The water swelling property of WSR prepared from different types of ENR was intensively investigated.

Table 3.9 Formulation of water-swellaable rubber with different types of epoxidized natural rubber

Ingredients	Quantity (phr)		Adding (mins)
ENR-25	100	-	0
ENR-50	-	100	0
SAPC	10	10	3
ZnO	6	6	9
Stearic acid	0.5	0.5	10
TBBS	1	1	11
Sulfur	2	2	12

Dumping 14 mins



Total mixing time = 14 min.

Figure 3.22 Compounding procedures for WSR preparation without compatibilizer (A) and with compatibilizer (B)

The compounds were tested for various properties as follows:

- 1). Mooney viscosity according to ASTM D1646
- 2). Cure characteristics according to ASTM D 2084

Then WSR obtained from each parameter were press-cured at 150 °C to obtain the vulcanizates for investigation of the following properties.

- 3). Tensile properties according to ASTM D 412
- 4). Hardness according to ASTM D 2240
- 5). Morphology by scanning electron microscopy (SEM).
- 6). Thermal property by differential scanning calorimetry (DSC) and thermogravimetric analysis (TGA).

7). Water swelling property following the swelling measurement method as described in Part I.

WSR from the ENR type that gave the highest water swelling absorbency and low degree percentage of weight loss was chosen for further study on the influences of ENR/SAPC ratios, and loading of compatibilizers (PVA).

3.4.2 Effect of ENR and SAPC blend ratios on swelling capacity of WSR

After investigation of ENR type with the earlier condition, it was found that ENR has the highest water absorbency and low in weight loss and thus was chosen for further investigation of various amount of SAPC (i.e. 0, 5, 10, 15 and 20 phr) by blending as the compounded formulation as given in Table 3.10. The mixing procedures with a total mixing time of 14 minutes are as shown in Figure 3.23(A).

Table 3.10 Formulation of WSR with varying SAPC loadings

Ingredients	Quantity (phr)	Adding (mins)
ENR-50	100	0
SAPC	0, 5, 10, 15, 20	3
ZnO	6	9
Stearic acid	0.5	10
TBBS	1	11
Sulfur	2	12

The compounds and vulcanizate were tested for 3.5 to 3.10

3.4.3 Effect of PVA as compatibilizer on swelling capacity of WSR

The difference in polarity of ENR and SAPC might cause a poor interaction between them, and the compatibilizer was incorporated to improve the interfacial

interaction of these two phases. In this part, the effect of compatibilizers on the preparation process and properties of WSR was further investigated. The compatibilizers; poly (vinyl alcohol) (PVA) was used to fulfill expectation in improving both water absorbency and mechanical properties. The compounding formulation is given in Table 3.11 and the mixing procedures is shown in Figure 3.23 (B). In these experiments the amounts of SAPC were fixed at 15 phr due to it giving the highest percentage of water absorbency as well as the lowest percentage of weight loss.

Table 3.11 Compounding formulation of WSR with varying amounts of PVA

Ingredients	Quantity (phr)
ENR-50	100
SAPC	15
PVA	0, 0.5, 1.0, 5.0, 10.0
ZnO	6
Stearic acid	0.5
TBBS	1
Sulfur	2

3.5 Swelling measurements

The dried samples in sheet form were cut of about 300 mg, weighted accurately, and immersed in distilled water at a temperature around 28-30° C. At regular intervals, the swollen sample was elevated from the distilled water, superficial moisture was perfectly removed using blotting paper, the weight of the sample was measured immediately and the sample was placed in the same bath for the second swelling test. After the swelling test, the samples were dried at 50°C until its weight was unchanged. The first and second water-swelling ratio by mass (S_w) and the first percentage weight loss (L_w) were calculated using equations (3.5) and (3.6).

$$S_w = \frac{W_2 - W_1}{W_1} \times 100 \quad (3.5)$$

$$L_w = \frac{W_1 - W_3}{W_1} \times 100 \quad (3.6)$$

where W_1 and W_2 are the weights of the sample before and after the water absorption respectively, and W_3 is the dried weight of a sample after water absorption.

3.6 Tensile properties

Tensile properties in terms of tensile strength, elongation at break, and modulus were tested at room temperature, according to ASTM D412 using a universal tensile testing machine (Hounsfield Tensometer, model H 10KS, Hounsfield Test Equipment Co., Surrey, UK). The dumbbell-shaped specimens were first dying cut from the vulcanized rubber sheets with ASTM die type C. Furthermore, the hardness was tested by using a durometer, Shore A (Frank GmbH, Hamburg, Germany), according to ASTM D2240.

3.7 Determination of the crosslink density

For crosslink density estimate, the equilibrium swelling was first determined by immersion of WSR sample in toluene for 7 days in the dark. The swollen WSR was then removed and weighed immediately. The weights of absorbed toluene and remaining rubber were determined by evaporating the toluene off in a hot air oven at 70°C. The crosslink density of WSR was calculated using the Flory-Rehner equation (3.7).

$$\frac{-\left[\ln(1-v_p) + v_p + \chi v_p^2\right]}{n v_0 \left[v_p^{1/2} - \frac{v_p}{2} \right]} \quad (3.7)$$

$$v_p = \frac{1}{1+Q}$$

$$Q = \frac{\text{Weight of solvent in swollen rubber} \times D_p}{\text{weight of rubber} \times D_o}$$

where n = Crosslink density

V_p = Volume fraction of rubber in the swollen polymer

χ = Huggins rubber-solvent interaction constant (0.41 for ENR)

D_p = Density of rubber (1.09 g/cm³)

V_o = Molar volume of toluene (1.069x10⁻⁴ m³/mol at 25 °C)

D_o = Density of toluene (0.8623 g/cm³ at 25°C)

3.8 Cure characterization

A rotorless rheometer (Rheo Tech MD+, Tech Pro, Inc., Cuyahoya Falls, USA) was used to determine the curing characteristics of the rubber composites at 160 °C with 1° arc amplitude over 60 min testing. The optimum cure time (t_{c90}) and scorch time (t_{s1}), the minimum and maximum torques (M_L and M_H , respectively), and delta torque ($M_H - M_L$) were determined from the curing curves. Cure rate index (CRI) was measured based on ASTM D5289 and calculated as shown in (3.8).

$$CRI = \frac{100}{t_{c90} - t_{s1}} \quad (3.8)$$

where t_{s1} is the time a unit increase in torque takes from the M_L , and t_{c90} is the time at which 90% cure is achieved.

3.9 Morphological properties

Morphological properties of the WSRs were characterized by using a scanning electron microscope equipped with energy dispersive X-ray spectroscopy (SEM, Quanta, FEI, the Netherlands).

3.10 Thermal properties

Thermogravimetric analysis (TGA) was determined using the Simultaneous Thermal Analyzer (model STA 8000, Perkin Elmer, United State of America) with a scanning rate of 10° C/min under N2 flowing at 20 mL/min in the temperature range of 30 to 800° C.

CHAPTER 4

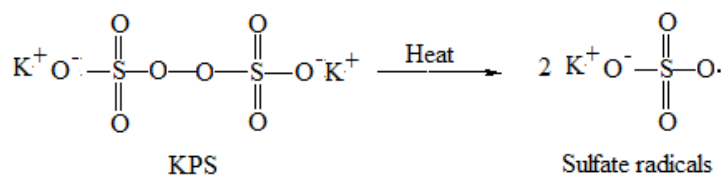
RESULTS AND DISCUSSION

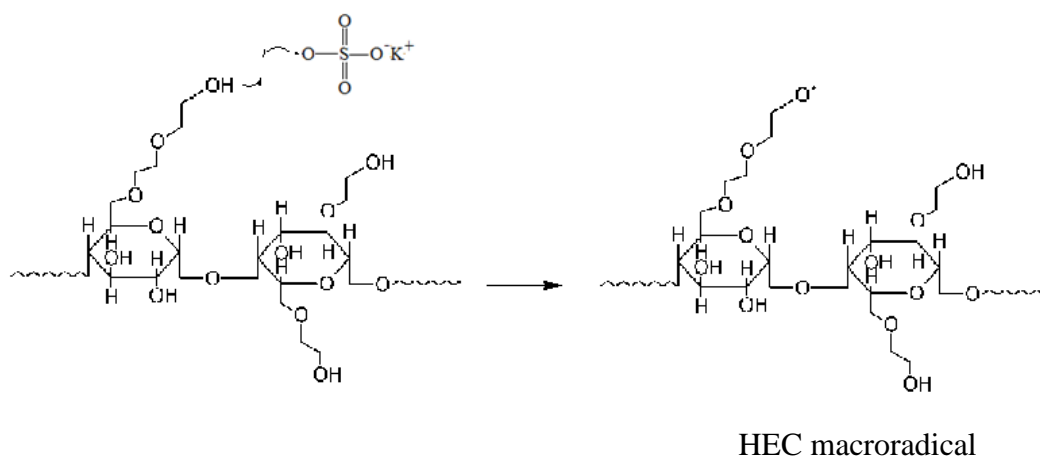
4.1 Preparation of superabsorbent polymer

Polymerization is a process in which monomers are combined chemically to produce a large molecule, namely a polymer. The monomers might be all alike, or they might represent more different compounds. Usually at least 100 monomer molecules must be combined to make a product that has certain unique physical properties. General polymerization consists basically 3 steps, including 1) thermally initiated radical of initiation system which is where the reaction starts, 2) propagation and 3) termination in which the process entirely completes polymerization. In this study, hydroxyethyl cellulose radical is where polymerizing of acrylamide starts by growing a polymer on side chain to form HEC-g-PAM. The reaction mechanism is proposed briefly by the following steps:

1. Initiation steps

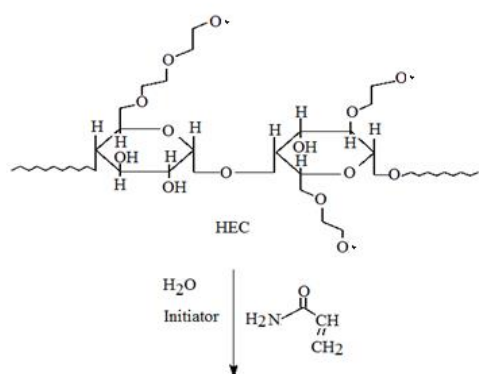
At the beginning KPS was thermally initiated into two moles of sulfate radical which then abstracted hydrogen from HEC backbone to form HEC reactive macroradical.

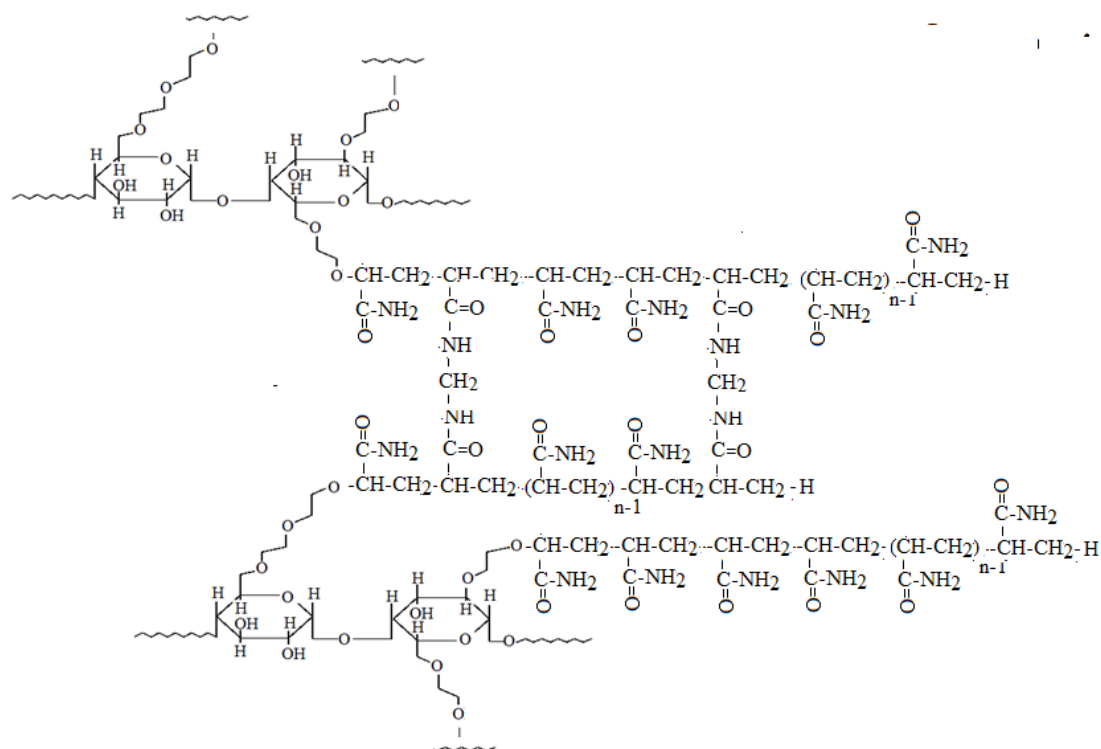




2. Propagation steps

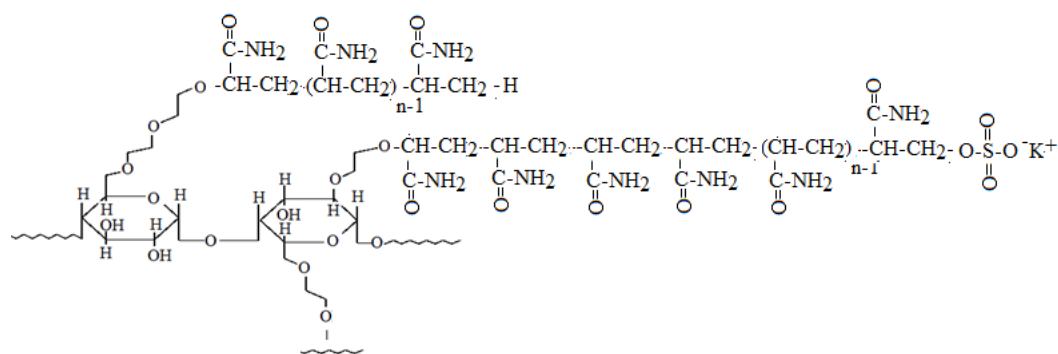
This reaction is able to occur continuously because the energy in the chemical system is lowered as the chain grows. Thermodynamically means, the sum of the energies of the polymer is less than the sum of the energies of the individual monomers. Simply put, the single bonds in the polymeric chain are more stable than the double bonds of the monomer.





3. Termination steps

This is the step that ends polymerization reaction in which usually due to cease the formation of intermediate in chain propagation, where it can be terminated with various possible processes depending on what moieties remains in the reaction system. It might be terminated by radical transfers hydrogen atom to the other to form two or more stable polymers also called disproportionation type or, in contrast it might be terminated by coupling of two macroradicals to form covalently a stable single molecule which is also called recombination type.



Termination occurs when another free radical (R-O \cdot), left over from the original splitting of the organic peroxide, meets the end of the growing chain. This free-radical terminates the chain by linking with the last macroradical of the polymer chain.

Possibly image grafted copolymers of PAM onto HEC without/with crosslinkers are shown in Figure 4.1 and Figure 4.2.

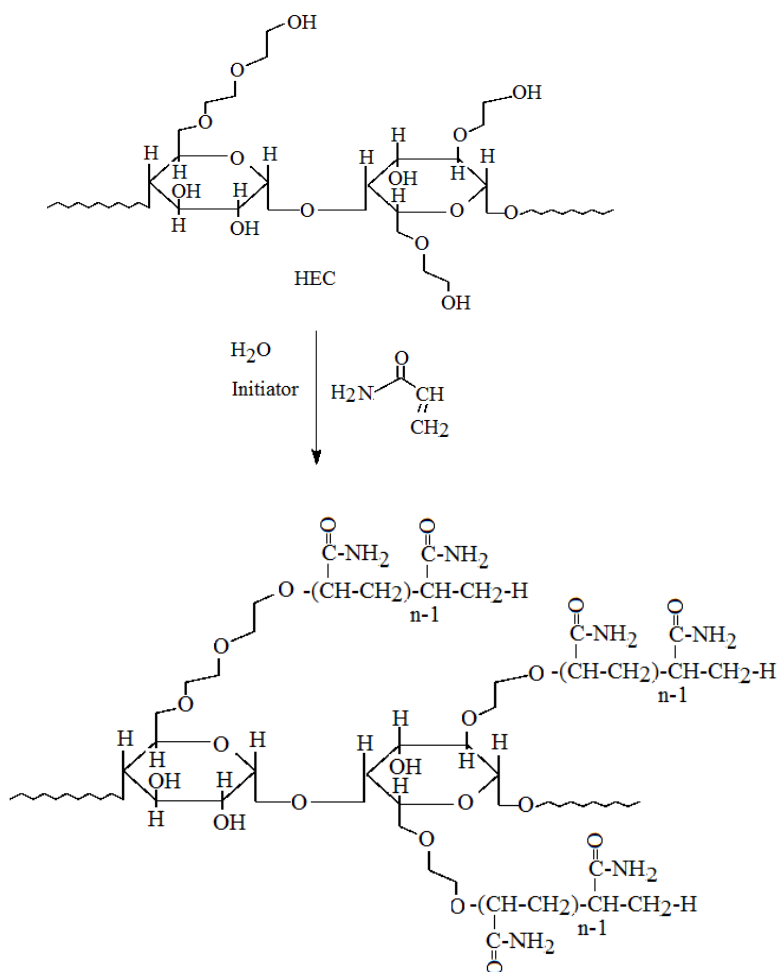
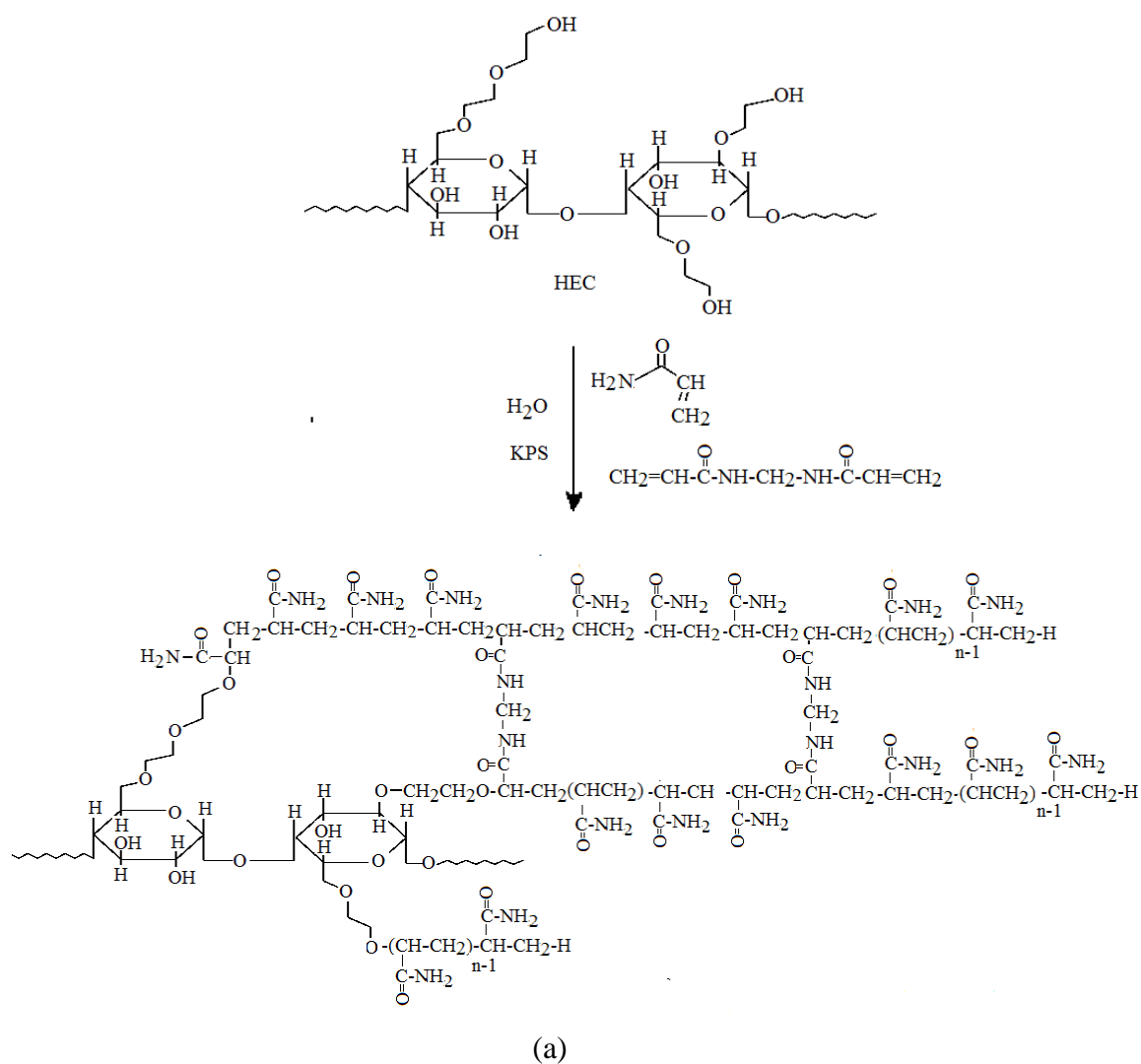


Figure 4.1 Graft copolymerization of PAM onto HEC without crosslinker

The intensive different reaction products amongst with/without crosslinker could mainly productively forecast through the formation of the polymer networks. There was no crosslinking copolymer that occurred in the reaction without crosslinker

as indicated in Figure 4.1. On the other hand, the grafted copolymer with the network formation was observed when introducing the crosslinking agent into the batch throughout the duration process of graft copolymerization. This is an important point of views because the networks formation intensively defined the influence to water swelling abilities and its mechanical properties. The reaction scheme and structural image are shown in Figure 4.2



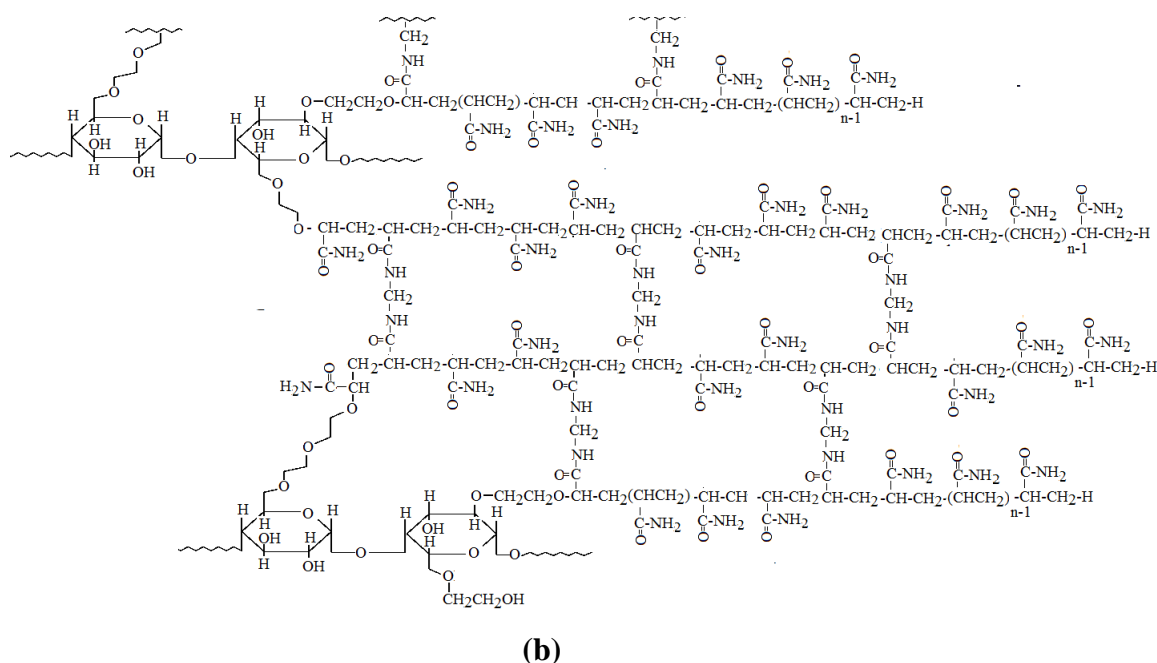


Figure 4.2 Graft copolymerization of PAM onto HEC in the presence of crosslinker (a) inter-cellulose chains crosslinking and (b) intra-cellulose chains crosslinking

Figure 4.2 presents the crosslinking amongst chains of copolymer, the crosslinking agent acted as a right hand to combine with polyacrylamide chains which was grafted onto HEC backbone while the other left bonded covalently to individual polyacrylamide producing entirely a network of polymer chains. The networks are able to form of both inter-cellulose chains and intra-cellulose chains. The existence of various hydrophilic functional groups in the polymer chains had led a water molecule that places surroundings to migrate efficiently into polymer networks.

4.1.1 Effect of HEC/AM ratio on grafting and water swelling capacity

The HEC/AM ratios were investigated for their effects on grafting parameter and water swelling capability as the result presented in Table 4.1 and Figure 4.3, respectively. The choices for fitting HEC weight was prior to the investigation by varying from 0.5, 0.75, 1.0 and 1.25 g, while AM was fixed at 5 grams of weight. The obtained copolymer under condition with tendency to produce a high yield and indicate the highest swelling capacity have led to choose for further investigation of the parameters. The results found that the best condition for the right content of HEC was

approximately at 1.2 g which was also found in the same works reported by Abdul Halim *et al.*, (2011). The AM content at 1/10 provided the percentage of grafting yield and grafting efficiency (73.77 and 67.41%), while the highest swelling capacity was observed (426 g/g). Further increases in AM contents were found to increase both percentages of grafting yield and grafting efficiency, while the water swelling capacity decreased.

Table 4.1 Effect of HEC/AM ratios on the grafting form of SAP

HEC:AM (g/g)	M _{HEC} (g)	M _{AM} (g)	M ₁ (g)	M ₂ (g)	M ₃ (g)	Grafting yield (%)	Grafting efficiency (%)
1:1	1.2	1.2	2.28	1.75	1.53	57.10	18.85
1:2	1.2	2.4	4.89	4.36	2.79	67.05	36.46
1:5	1.2	6.0	8.79	8.37	5.68	64.61	53.52
1:10	1.2	12.0	15.14	14.79	11.17	73.77	67.41
1:15	1.2	18.0	21.85	21.53	17.31	79.22	74.82

The effect of HEC/AM ratio on swelling capacity before and after alkaline hydrolysis is shown in Figure 4.3. The swelling capacity of SAP before alkaline hydrolysis did not change significantly with altering HEC/AM ratio. When the SAP was treated with alkaline base, the swelling capacity was found to increase dramatically. The highest swelling capacity was observed at 1/10 HEC/AM ratio by elevating from 23 g/g to 426 g/g. However, further increases in AM contents decreased in water swelling capacity.

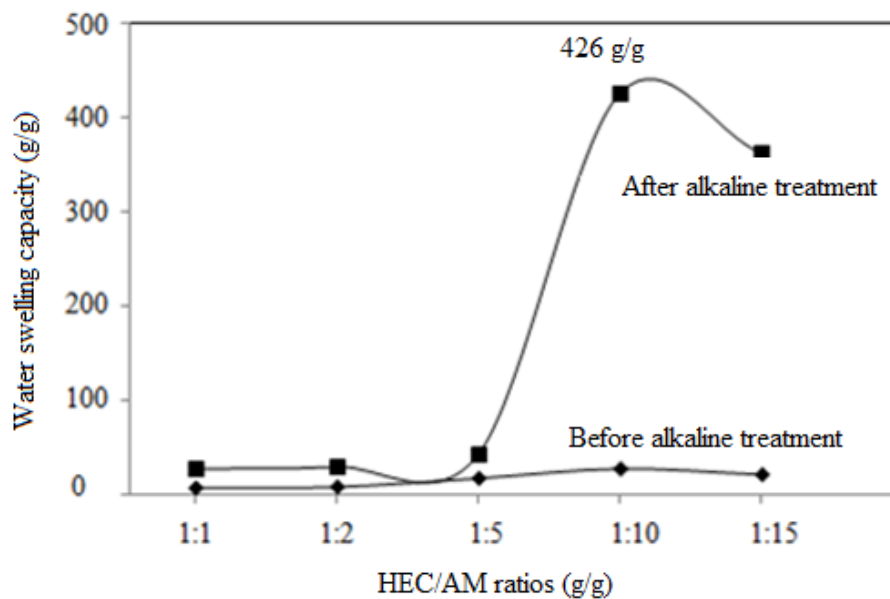


Figure 4.3. Effects of HEC/AM ratio on swelling capacity before and after hydrolysis by 2 M NaOH, [KPS] = 1 g/1.2 g HEC, [MBA] = 0.1 mmol/100 g HEC, temperature = 70° C, time 2 h, agitation speed 100 rpm, and washing 3 times with distilled water

The result clearly suggested that the hydrolysis process is considerable for SAP. The reason why the treated SAP has higher swelling capacity than those of untreated SAP could be explained by the following reasons. Before treating, the most functional group in the SAP are being in amide form as illustrated in Figure 4.4.

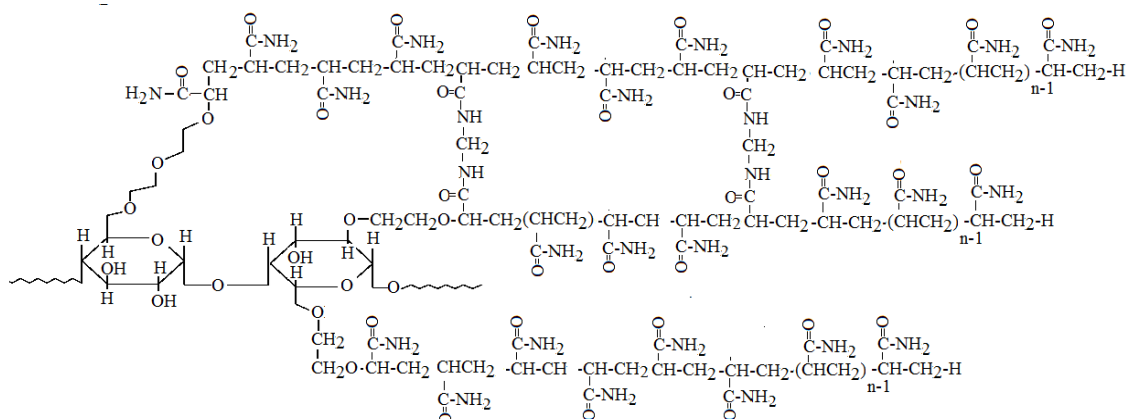


Figure 4.4. Hydrogel in amide form prepared from 1/10 HEC/AM ratio, [KPS] = 1 g/1.2 g HEC, [MBA] = 0.1 mmol/100 g HEC, temperature = 70° C, time 120 minutes, agitation speed 100 rpm

After having alkaline hydrolysis, amides were possibly predominantly converted into carboxylate salt which then partly transformed into carboxylic acid after washing several times with distilled water or through neutralization process with dilute HCl. The images of all carboxylate functional forms are displayed in Figure 4.5 and Figure 4.6. These phenomena have led to enhance the hydrophilicity, increases the interaction forces and thus enhances the swelling capacity.

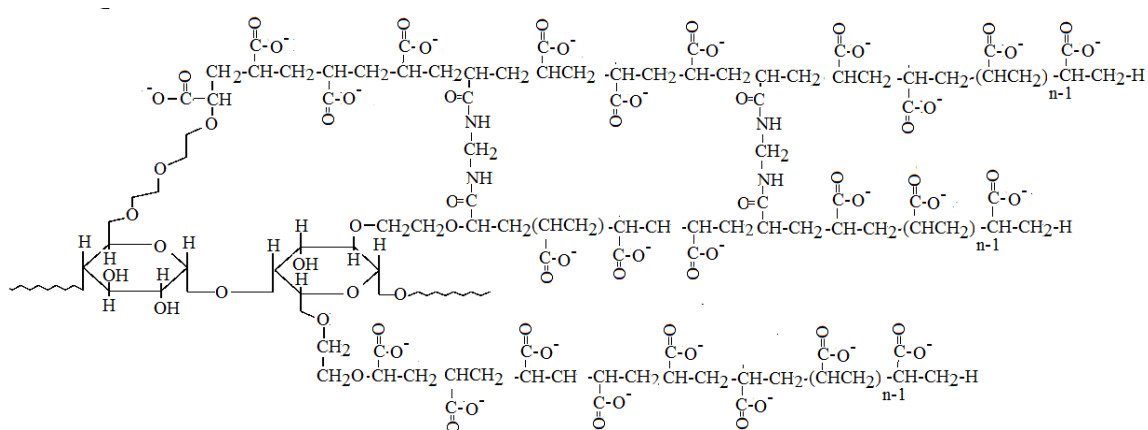


Figure 4.5 HEC-g-PAM in carboxylate form after hydrolysis with 2M NaOH at 70° C for 60 minutes

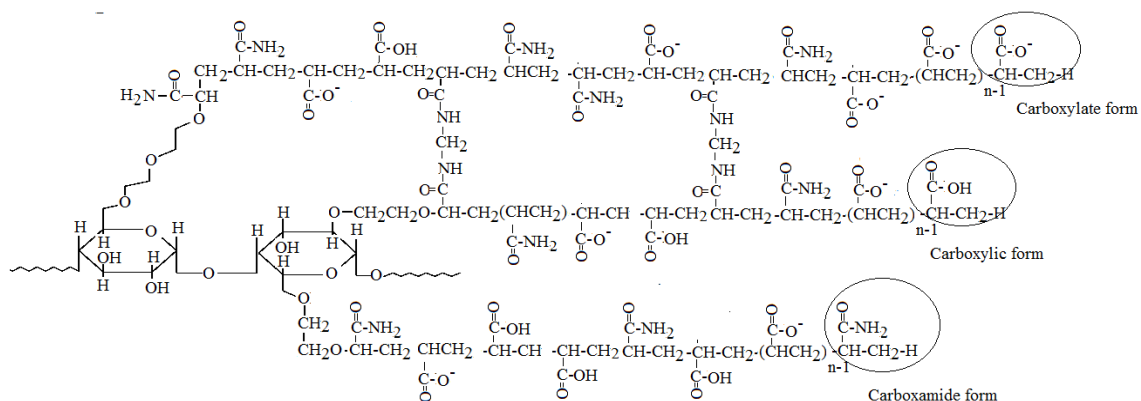


Figure 4.6 HEC-g-PAM in assortment of functional forms after hydrolysis with 2M NaOH at 70° C for 60 minutes and washing several times with distilled water

4.1.2 Infrared spectroscopy

FTIR determination confirmed the grafting reaction of PAM onto HEC. Figure 4.7 shows FTIR spectra of pure HEC and HEC-g-PAM (SAP). It was found that the FTIR spectrum of HEC showed broad band at around $3560\text{--}3320\text{ cm}^{-1}$, assigning to the stretching vibrations of $-\text{OH}$ groups in HEC with the presence of hydrogen bonding. The strong absorption peak at 2883 cm^{-1} was attributed to primary $-\text{OH}$ bending vibrations in HEC (Ethyl hydroxyl) (Pathania and Sharma 2012), while the peaks at around 1020 cm^{-1} and 1059 cm^{-1} were assigned to $-\text{C}-\text{OH}$ stretching vibrations in HEC (Jagadish and Vishalakshi 2012; Wu *et al.* 2012; Heridia-Guerero *et al.* 2016; Olivera *et al.* 2015). After grafting with PAM (HEC-g-PAM), a shoulder peak at 3195 cm^{-1} was observed due to N-H stretching vibrations of PAM, in addition to the broad band around $3560\text{--}3320\text{ cm}^{-1}$. The absorption bands around 1020 cm^{-1} , 1059 cm^{-1} and 2883 cm^{-1} were disappeared, and new absorption bands that emerged at 1668 , 1438 and 1116 cm^{-1} were assigned to $-\text{C}=\text{O}$ stretching vibrations of carboxamide functional group, CH_2 bending vibrations in the added PAM moieties, and asymmetric stretching vibrations of C-O-C, respectively.

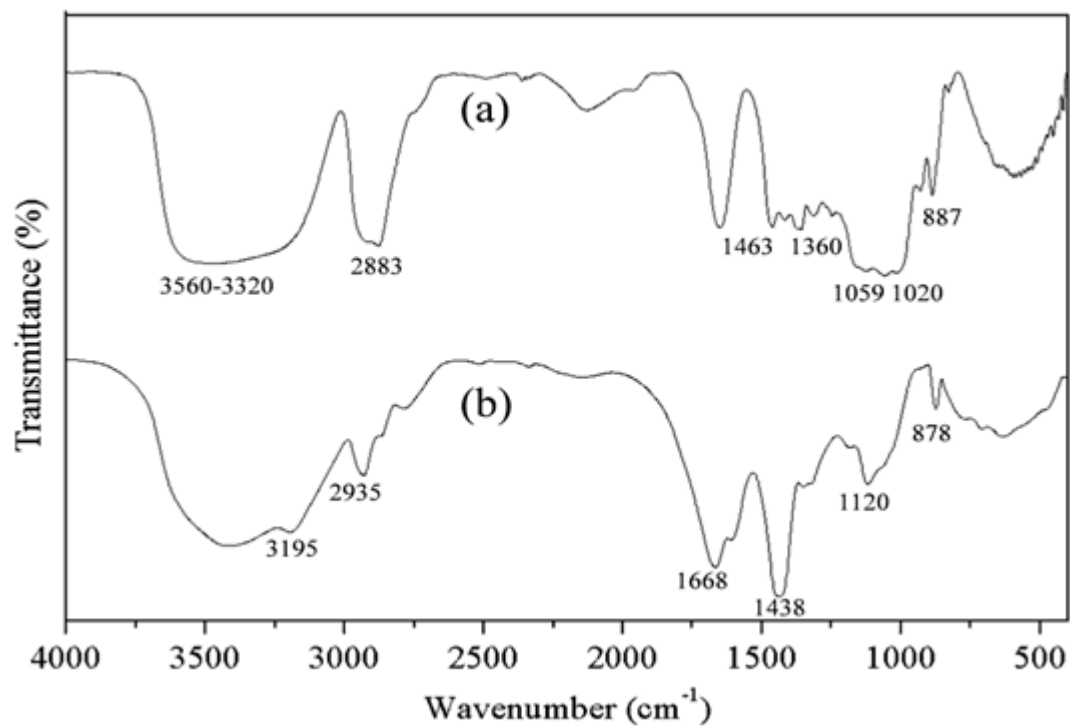


Figure 4.7 FTIR spectra of (a) HEC and (b) HEC-g-PAM before alkaline hydrolysis

The FTIR result as the details in Figure 4.7 clearly evidenced that the graft copolymerization of PAM onto HEC backbone was successfully accomplished. The proposed grafting copolymerization reaction between HEC and PAM is shown in Figure 4.8.

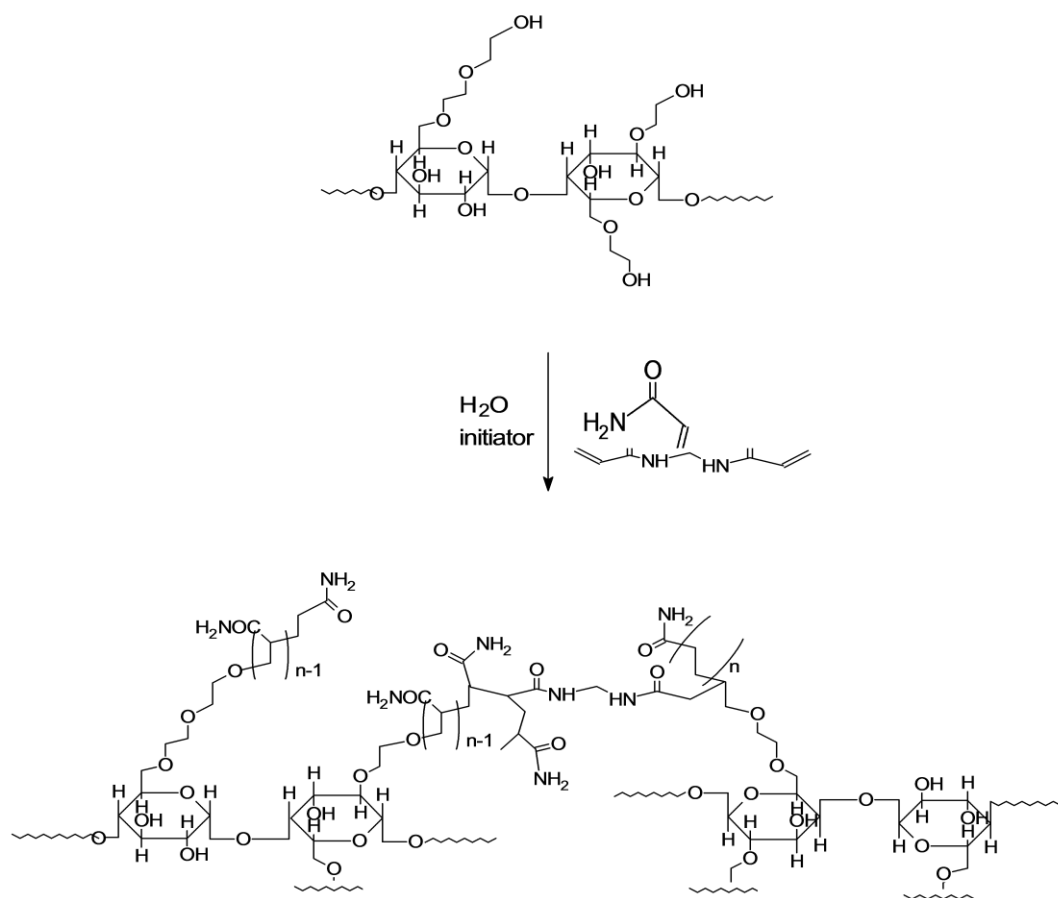


Figure 4.8 Propose grafting copolymerization reaction between HEC and PAM

This reaction occurred continuously because the energy in the chemical system is lowered as the chain grows. Thermodynamically speaking, the sum of the energies of the polymer is less than the sum of the energies of the individual monomers. Simply put, the single bonds in the polymeric chain are more stable than the double bonds of the monomer.

Figure 4.9 shows comparative FTIR spectra of HEC-g-PAM before and after hydrolysis and washing several times with distilled water. For HEC-g-PAM free from alkaline hydrolysis (Figure 4.9(a)), broad peak centered at 3450 cm^{-1} was assigned to –OH stretching vibration of HEC. The shoulder peak at 3195 cm^{-1} was assigned to the –NH stretching vibration of amide (PAM) and the peak at 1668 cm^{-1} was assigned to –C=O stretching vibrations of carboxamide functional group. After alkaline hydrolysis, the peak at 3450 cm^{-1} was found to broaden, suggesting that hydrogen bonding and –

C–OH of carboxylic may be formed and the shoulder peak at 3195 cm^{-1} almost disappeared. These phenomena suggested that the number of –OH group increased while the number of –NH decreased. It was also found that the peak at 1668 cm^{-1} was split into double peaks, *i.e.*, the peaks at 1670 cm^{-1} and 1566 cm^{-1} (Figure 4.9 b, c and d). These two peaks were the characteristic peak of –C=O asymmetric and symmetric stretching vibrations of carboxylate group which are generally observed in carboxylate form (Solumons *et al.* 2014). It is very interesting to note that the peak corresponding to the vibration of –OH (3450 cm^{-1}) and carboxylate groups (1670 and 1556 cm^{-1}) were enhanced by increasing number of washing cycles.

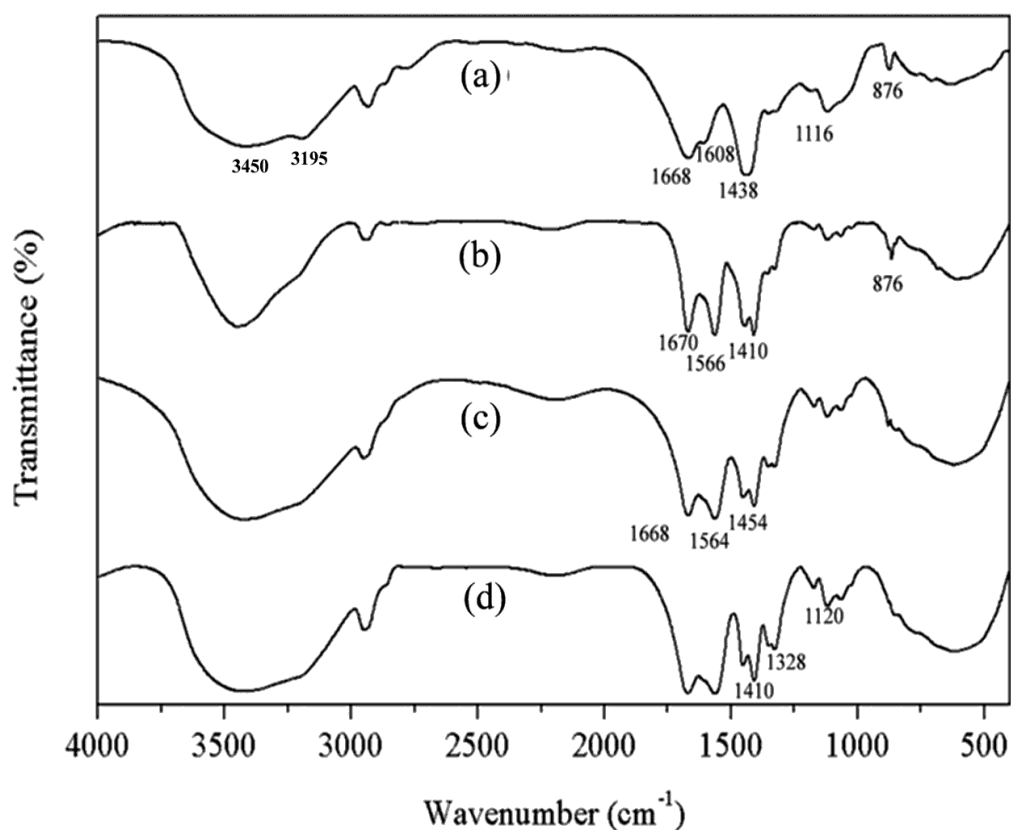


Figure 4.9 FTIR spectra of (a) HEC-g-PAM and HEC-g-PAM after alkaline hydrolysis were affected by wash cycles with distilled water: (b) washing 1, (c) washing 2, and (d) washing 3

Based on FTIR determination, it suggested that a part of amide form was altered into carboxylic acid and carboxylate forms, and the number of carboxylic acid and

carboxylate forms were increased with increasing washing cycles. The structure of HEC-g-PAM after alkaline hydrolysis have been previously proposed in Figure 4.5.

4.1.3 Effect of initiator amount on swelling capacity

Graft copolymerization of PAM onto HEC was carried out in aqueous solution using KPS as initiator. Effects of KPS amount were investigated in the range 0.5-2.5 g/(1.2 g HEC) and the result is shown in Figure 4.10. The highest water swelling capacity (about 426 g/g) was observed with 1 g of KPS, and its swelling capacity decreased to 69.37 g/g with KPS amount at 2.5 g/1.2 g HEC. The result suggested that a proper amount of initiator for inducing the graft copolymer was 1 g of KPS. The decrease of water swelling capacity at higher content of initiator was attributed to the formation of chain transfer to initiator resulting in decrement of grafting efficiency (Su 2013). The grafting efficiency found to shift down from 67.41 to 44.84, 43.35 and 35.46 at KPS contents 1.0, 1.5, 2.0 and 2.5 g, respectively.

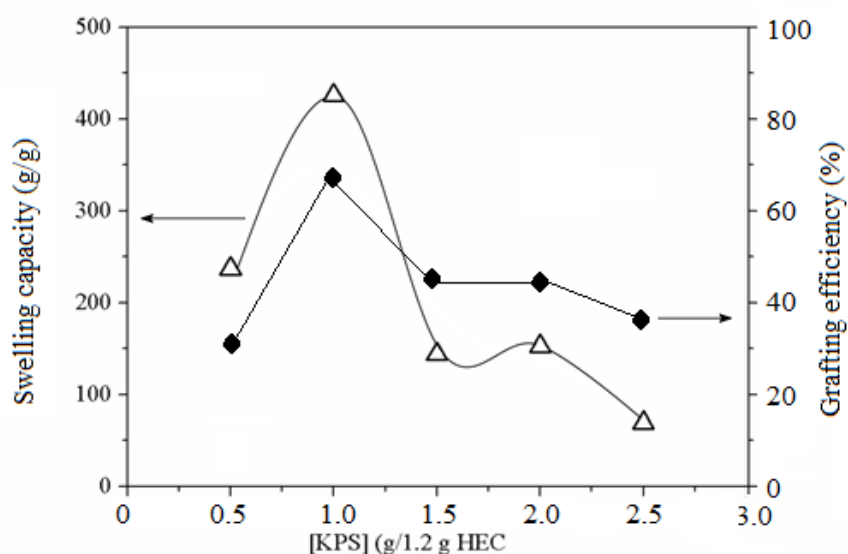


Figure 4.10 Effects of KPS on S_w and %GF of SAP at HEC/AM = 1/10, MBA = 0.1 mmol/100 g HEC, reaction temperature 60 °C and reaction time 2 h

4.1.4 Effect of crosslinking agent concentration on swelling capacity

Crosslink density was an important factor to define the property of hydrogel both water swelling capacity and mechanical property. The three-dimensional network graft copolymer of PAM and HEC was constructed by using MBA as a crosslinking agent. Influences of MBA concentration on water swelling capacity were experimented in the range 0.05, 0.1, 0.2 and 0.3 mmol/ (100 g HEC) and the result is shown in Figure 4.11.

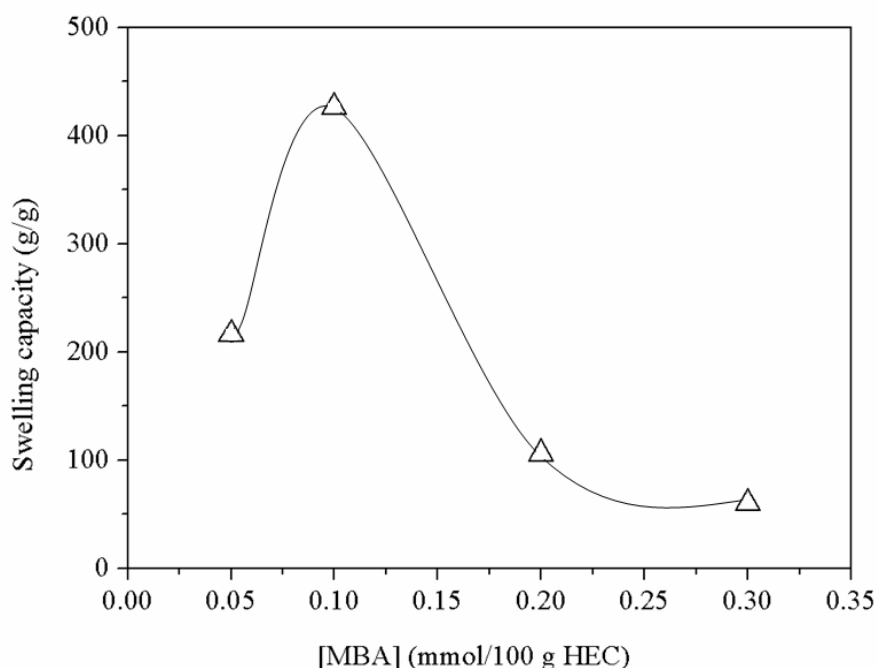


Figure 4.11 Effects of MBA concentration on swelling capacity at 24 hours of an immersion time

Figure 4.11 illustrates effects of MBA concentration on water swelling capacity of graft copolymer at HEC/AM = 1/10, KPS = 1 g /1.2 g HEC, reaction temperature 60 °C and reaction time 2 hours. It is clearly displayed that at concentration 0.1 mmol/ (100 g HEC) of [MBA] provided the highest swelling capacity (426 g/g), with an overdose giving much poorer swelling. Since the MBA served as crosslinker, increase addition of MBA increased amount of crosslinking site, which later on decrease the network size. Thus, ability of water swelling capacity decreased.

4.1.5 Influences of alkaline hydrolysis temperature and time on swelling capacity

The resultant HEC-g-PAM copolymer mostly in carboxamide form usually have low water swelling capacity of approximately up to 30 g/g. To improve the swelling capacity of the SAP, approximately 5 g of grafted copolymer was hydrolyzed with 100 mL of 2 M NaOH solution. The swelling capacity of treated SAP obtained from the various hydrolysis temperature is displayed in Figure 4.12. The highest water swelling capacity (426 g/g) was observed at 70°C of hydrolyzed temperature at the reaction time 60 minutes.

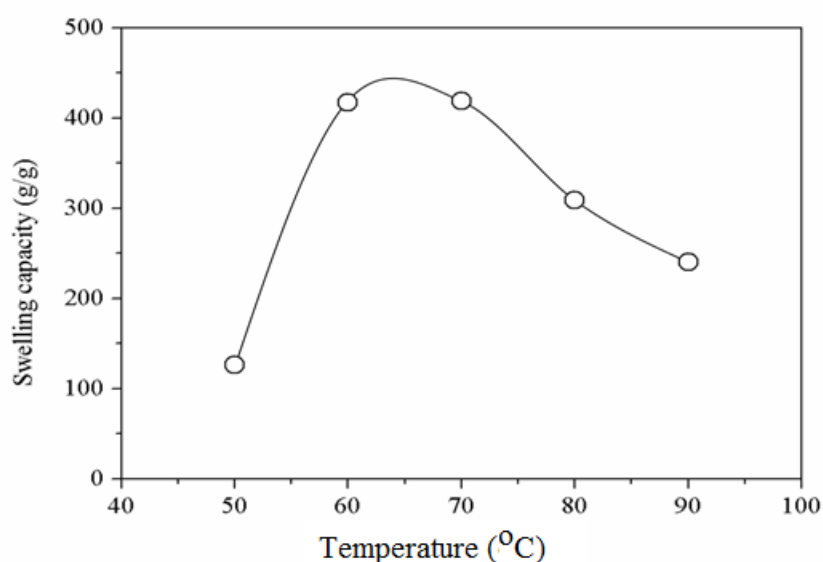


Figure 4.12 The influence of hydrolysis temperature on swelling capacity of SAP prepared at HEC/AM = 1/10, KPS = 1 g /1.2 g HEC, MBA = 0.1 mmol/100 HEC, and reaction time 120 mins

Besides the temperature, the reaction time is therefore an important parameter that influence swelling capacity of HEC-g-PAM hydrogel. Reaction time for alkaline hydrolysis varied by 30, 60, 90 and 120 minutes while the reaction temperature fixed at 70 °C. Results found that the optimal reaction time for obtaining the highest swelling capacity was at 60 minutes. The detail is demonstrated in Figure 4.13.

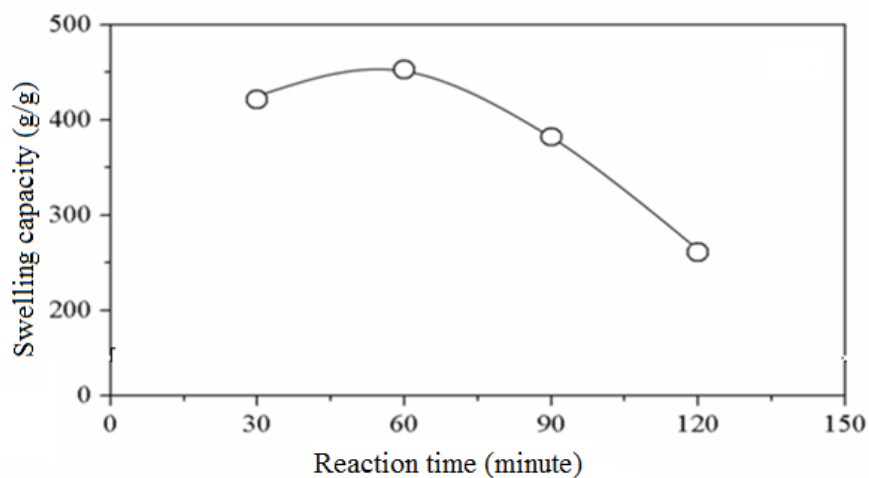


Figure 4.13 Influence of reaction time for alkaline hydrolysis on water swelling capacity of SAP prepared through HEC/AM =1/10, KPS = 1 g /1.2 g HEC, MBA = 0.1 mmol/100 HEC, and reaction time 120 mins.

4.1.6 Effect of bentonite clay loading on swelling capacity

The effects of bentonite clay loading (10, 20, 30, 40, 50 and 60% wt) on water swelling properties of the SAP composites were investigated and the result is shown in Figure 4.14. The degree of water absorption (S_w) was calculated using equation (2). The SAP with 426 g/g water swelling capacity was used to prepare the super absorbent polymer composites (SAPCs). The highest swelling capacity was observed at 40% clay loading that about 538 g/g then the swelling capacity decreased after 40% clay loading was introduced. Several studies have shown that the introduction of bentonite clay in a suitable amount in in-situ graft copolymerization of a monomer improves the water swelling capacity. Because the filler dispersion in a composite facilitates particle size expansion (Xie *et al.* 2011; Zhang and Wang 2007; Kaleleh *et al.* 2013). In addition, the incorporation of bentonite increases the strength of a superabsorbent polymer by formation of new ester bonds (Hosseinzadeh *et al.* 2011). The sodium bentonite salt was formed when treated with alkaline leading to enhance the water swelling capacity (Nakason *et al.* 2010).

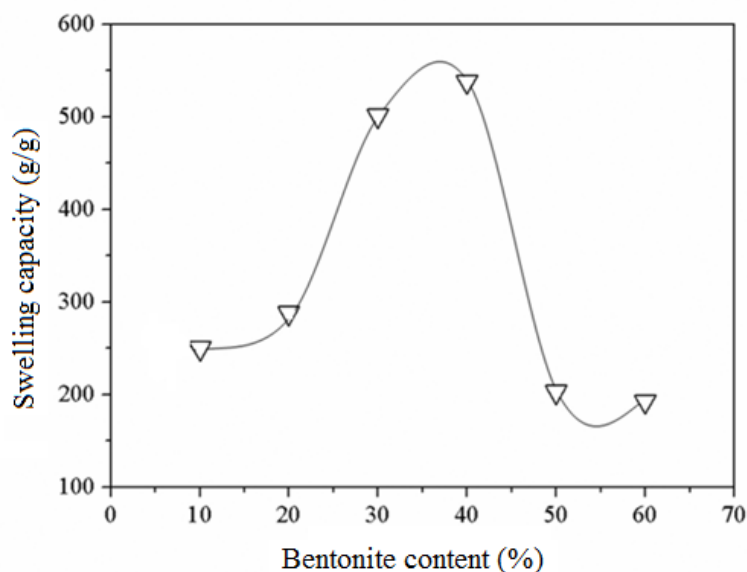


Figure 4.14 Effects of bentonite clay loading on water swelling capacity. HEC/AM (g/g) = 1/10, KPS = 1 g/ (1.2 g HEC), [MBA] = 0.1 mmol/ (100 g HEC), temperature = 70° C

At higher contents bentonite favors to form a coarser due to self's agglomerate leading to decrement in dispersion which finally reduced the water swelling capacity (Zhang and Wang 2007).

4.2 Preparation of WSR

4.2.1 Types of Rubber and SAPC contents of various WSR

In this step, SAPC with 538 (g/g) water swelling capacity was applied to compound WSR. The experiments were executed at ambient temperature using internal mixer (Brabender plasticorder) with controlling temperature of mixing chamber at 40° C. The initial mixing temperature was set at 40° C to prevent a degradation in rubber phase according to Nakason *et al.*, (2013). Two grades of epoxidized natural rubber with 25 mole % of epoxide group (ENR-25) and 50 mole % of epoxide group (ENR-50) were separately compounded as a rubber matrix and dispersed 10 phr superabsorbent polymer composite (SAPC) with ZnO 6 phr, stearic acid 0.5 phr, TBBS 1 phr and sulfur 2 phr. The mixing procedures with a total mixing time of 14 minutes were done as

follows procedure described by Nakason *et al.*, (2013) and following the formulation procedure as shown in Table 3.9 and Figure 3.22 (A)

The obtained WSRs were tested for water swelling behaviors, including water absorbency and weight loss. The WSR from such ENRs that gave a high of water absorbency and lowest weight loss were chosen as a rubber matrix for further investigation on the influence of SAPC content on water swelling behaviors and mechanical properties. The experiments found that the ENR-50 formulation promised the greatest swelling behaviors (Figure 4.15) thus providing to compound with various loadings of SAPC (i.e. 0, 5, 10, 15 and 20 phr) and were tested for swelling behaviors as well as mechanical properties. The formulation is given in Table 4.2.

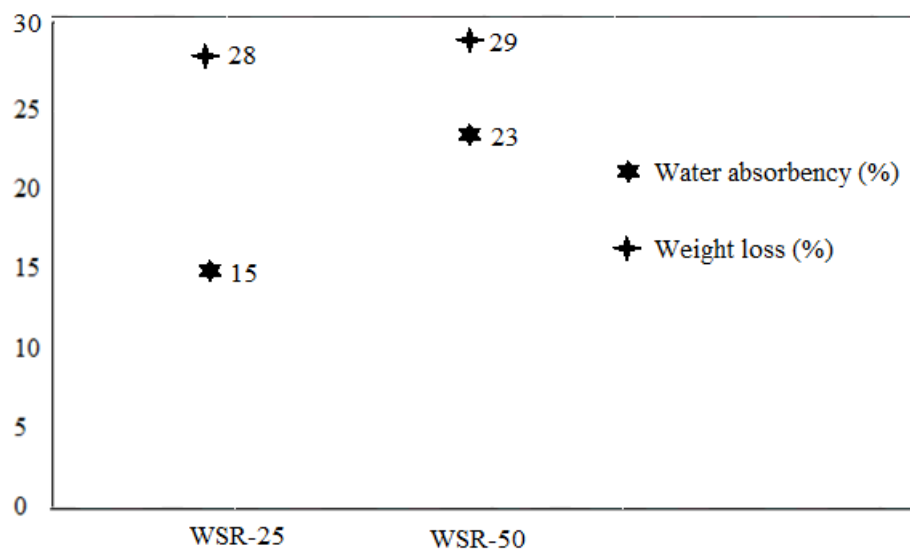


Figure 4.15 Swelling behaviors of WSR-25 and WSR-50 at 30 days of soaking time (Results have been done in triplicate and appeared in an average values)

Table 4.2 Formulation of WSR with varying SAPC loadings

Ingredients	Quantity (phr)
ENR -50	100
SAPC	0, 5, 10, 15, 20
ZnO	6
Stearic acid	0.5
TBBS	1
Sulfur	2

4.2.1.1 Swelling properties of WSR

Figure 4.16 shows the water swelling capacity of WSR containing different SAPC contents at various soaking times. It is generally seen that the water swelling capacity of WSR increased with increasing soaking time up to 30 days, after that the swelling capacity tended to level off. This result suggests that the ability of water absorbent in WSR is optimized at 30 days, thus no more changes in water swelling absorbency after 30 days of soaking. It is also seen that the water absorbency of WSR increases with increasing amounts of water absorbent polymer composite (SAPC) contents. This surely attributes to the decrease of cross-linked density and the increase of active site for water absorption as the number of water absorbent materials in the WSR increased. The dependence of water absorbency of the water swellable rubbers with the superabsorbent polymer/composite (SAP/SAPC) contents was also found by others (Wang *et al.*, 1998; Wang *et al.*, 1999; Wang *et al.*, 2002; Wei *et al.*, 2014). Thus, the amount of SAPC contents has played an important role in the water absorbency of the WSR.

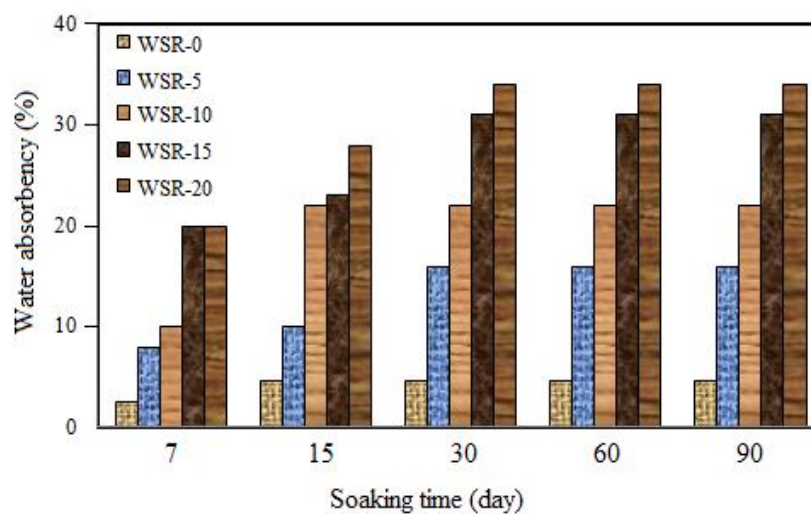


Figure 4.16 Plot of first water absorbency of WSR containing various SAPC loading with soaking time

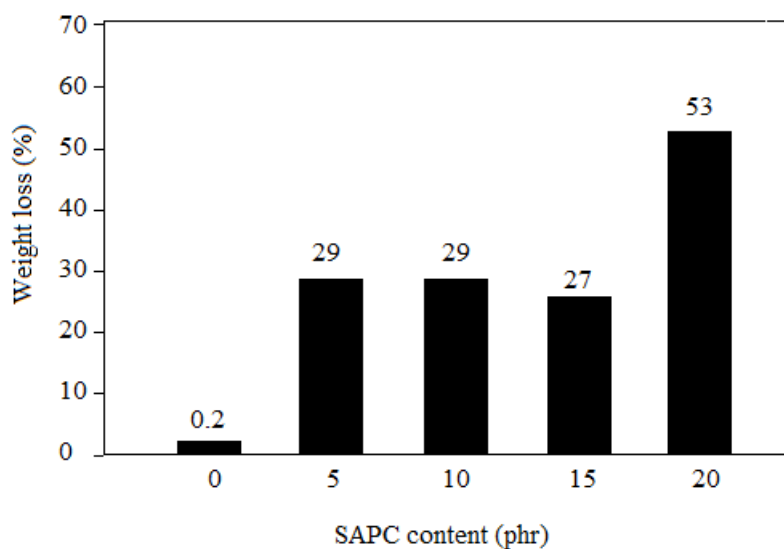


Figure 4.17 Graphical difference of SAPC loading affecting (%) weight loss of WSR prepared by blending of ENR-50 with various loadings of SAPC after having first water immersion (the results were done in triplicate and reported in an average values)

Figure 4.17 shows percentage weight loss of WSR containing various SAPC loadings at 30 days of soaking time. The percentage weight loss of WSR samples tends

to increase with increasing SAPC loading. The highest weight loss is found at 20 phr of SAPC loadings in WSR around 53% average. The result supports well with the second water absorbency of WSR samples.

4.2.1.2 Second swelling test

Figure 4.18 indicates the second water absorbency of WSR at various contents of SAPC with different soaking time. The results found that the second water absorbency of WSR with various contents of SAPC was decreased nearly more than 1-fold, especially for WSR at 20 phr SAPC contents, the second water absorbency was changed from 34% to 16% (2.13-folds). This was due to the large amounts of SAPC left out from WSR samples which was consistent with SEM micrographs and weight loss.

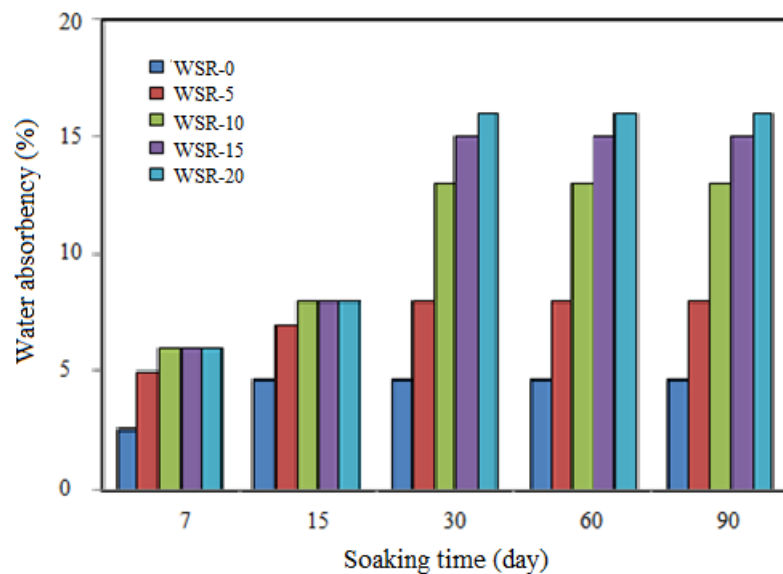


Figure. 4.18 Second water absorbency of WSR at various SAPC loading with soaking time

4.2.1.3 FTIR determination

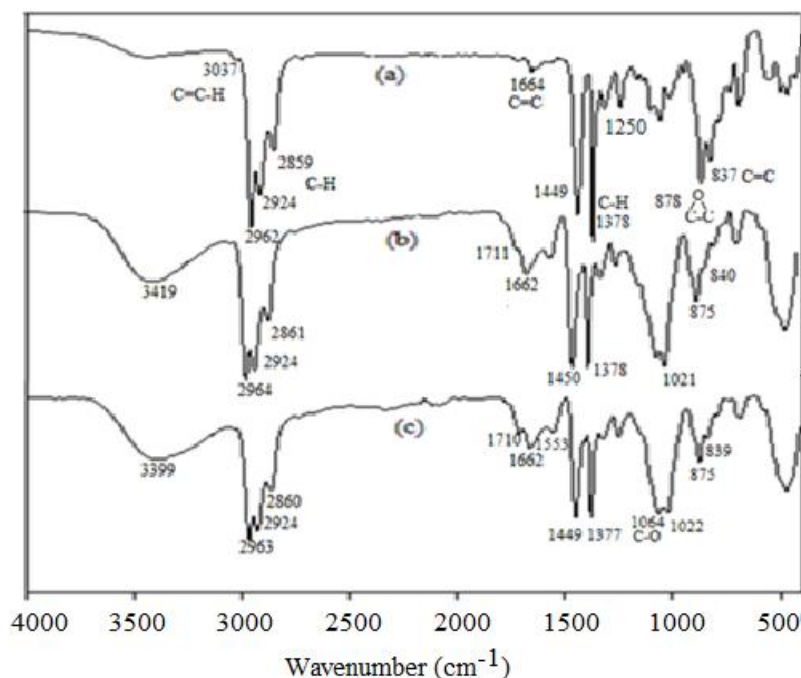


Figure 4.19 FTIR spectra of (a) ENR-50, (b) WSR before water absorption and (c) WSR after water absorption, WSR prepared by SAPC loading 15 phr

Fourier-Transform Infrared (FTIR) determination was basically used to characterize the compatibility of the blends. Figure 4.19 shows the FTIR spectra of (a) ENR-50 which indicates the predominant absorption peak at 3037 cm^{-1} (weak) was assigned to stretching vibration of $\text{Csp}^2\text{-H}$, the strong to medium peaks at 2962 , 2924 and 2859 cm^{-1} were attributed to $\text{Csp}^3\text{-H}$ stretching vibration, the weak peak at 1664 cm^{-1} ($\text{C}=\text{C}$ stretching), 1449 cm^{-1} ($-\text{CH}_2-$ deformation), and 1378 cm^{-1} (methyl C-H deformation). The evidence that contained of epoxide in molecule is confirmed by the medium intensity of peak at 878 cm^{-1} while also the peak with weak intensity at 837 cm^{-1} is due to $=\text{C-H}$ bending vibration of natural rubber; and (b) represents FTIR of WSR before having water absorption and (d) represents absorption peaks WSR after 30 days of water immersion. It clearly shows FTIR peak around $1700\text{-}1550\text{ cm}^{-1}$ assigning to carbonyl groups containing in SAPC, probably appearing in assortments of amide, acid and carboxylate salt. After submerging in distilled water, the strong intensity peak of FTIR at 1064 cm^{-1} which corresponds to C-O stretching vibration of ether slightly

increased probably due to ring opening in epoxidized natural rubber and transformed into C-O-C. This phenomenon supports well with the altering peak of epoxide at 875 cm^{-1} from low to high intensity.

4.2.1.4 Tensile properties

Figure 4.20 shows modulus at 100% and 300% strain for the WSR filled with different SAPC contents. Both modulus at 100% and 300% strain of the WSR slightly increase with increasing SAPC content due to the increase of WSR stiffness with the addition of SAPC. Generally, the modulus at low strain of composites depends on various factors. Among them, interatomic bonding strength or in turn nature of bonds and binding energy, the materials with greater of bonding strength usually exhibits the high stiffness.

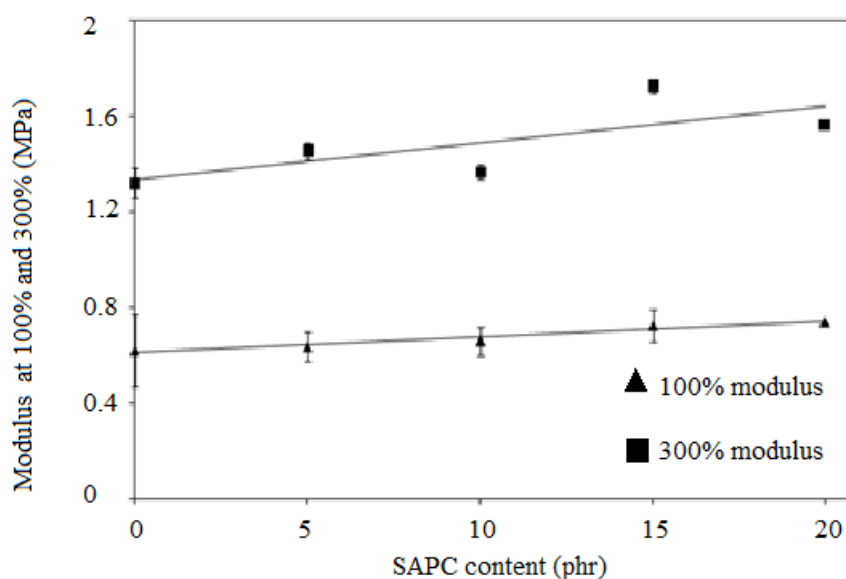


Figure 4.20 Relationship of modulus at 100% and 300% strain for the WSR filled with different SAPC contents

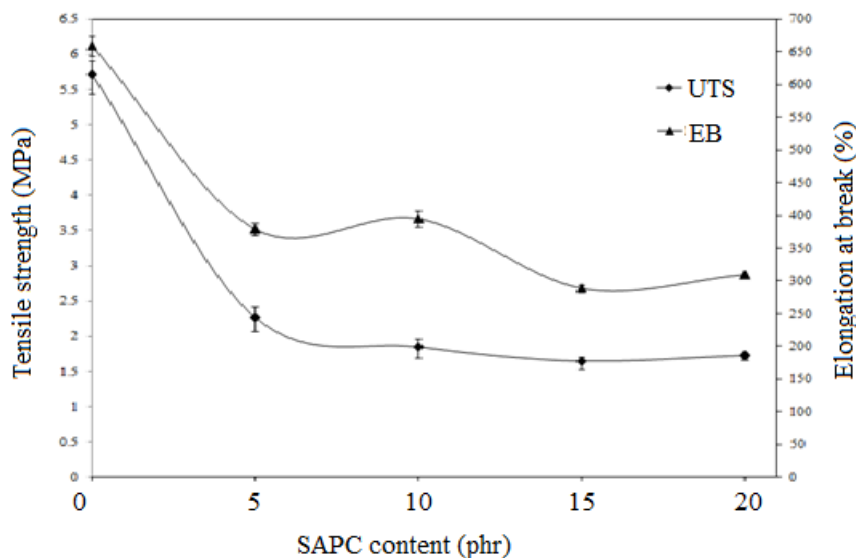


Figure 4.21 Tensile strength and elongation at break for the WSR filled with different SAPC contents

Figure 4.21 shows the effect of SAPC addition on tensile strength and elongation at break of WRS. The results found the addition of SAPC decreases both the tensile strength and elongation at break. The reduction of both properties could be explained by 2 reasons. They are, the reduction of cross-linked density (Figure 4.22) and the presence of SAPC in the WRS matrix acts as stress concentration point. Therefore, the sample breaks easier when the SAPC was added.

4.2.1.5 Determination of the crosslink density

The Floryl-Rehner equations was calculated for crosslink density, an experiment was firstly measured the equilibrium swelling by immersion WSR sample in toluene, and was allowed to swell for 7 days in the dark to certain reach equilibrium. The swollen WSR was then eliminated and weighed immediately. The weights of swelling toluene and rubber were determined after removing toluene by hot air oven at temperature of 70°C. (Lopez-Manchado, 2003; Du, 2003). The cross-linked density of WSR drastically decreases when 5 phr SAPC was introduced by shifting down from $2.24 \times 10^{-5} \text{ mol/dm}^3$ to $2.30 \times 10^{-6} \text{ mol/dm}^3$. It is very interesting that the cross-linked density of WRS decreases with increasing of SAPC loading as can be seen in Figure

4.22, However, further increased addition of SAPC does not significantly affect the formation of cross-linked density. This suggests that the presence of SAPC in the WRS hindered the formation of cross-linked density.

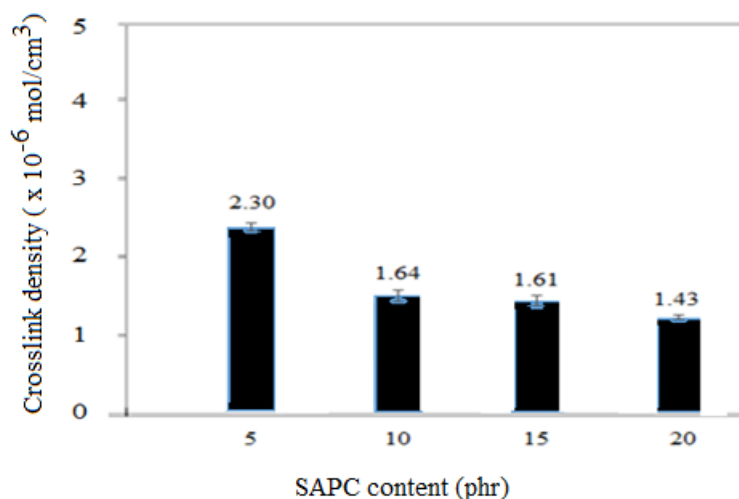


Figure 4.22 Crosslink density of WSR at different SAPC contents

The process how SAPC hinders the formation of crosslink could probably explain the mechanism of the sulfur vulcanization systems. It is well known that in the system of sulfur curing, there are at least five steps of mechanism including the first steps, this is the process of accelerator reacting to ZnO forming Zn²⁺-accelerator complex, while the second steps that is the process of entire sulfur combined to Zn²⁺-accelerator complex forming intermediate sulfur-Zn²⁺-accelerator or polysulfidic accelerator (Heideman, 2005). This is an important point of view due to the complexity that containing Zn²⁺ could sometime form a ligand, especially in the presence of amine or carboxylate ions. In fact, the SAPC used as a dispersing hydrophilic polymer in this blend is based on the graft copolymer of HEC and PAM. The final structure of grafted copolymer probably encloses the multifunctional groups such as carboxylic acid, carboxylate and amide forms as shown in Figure 4.23.

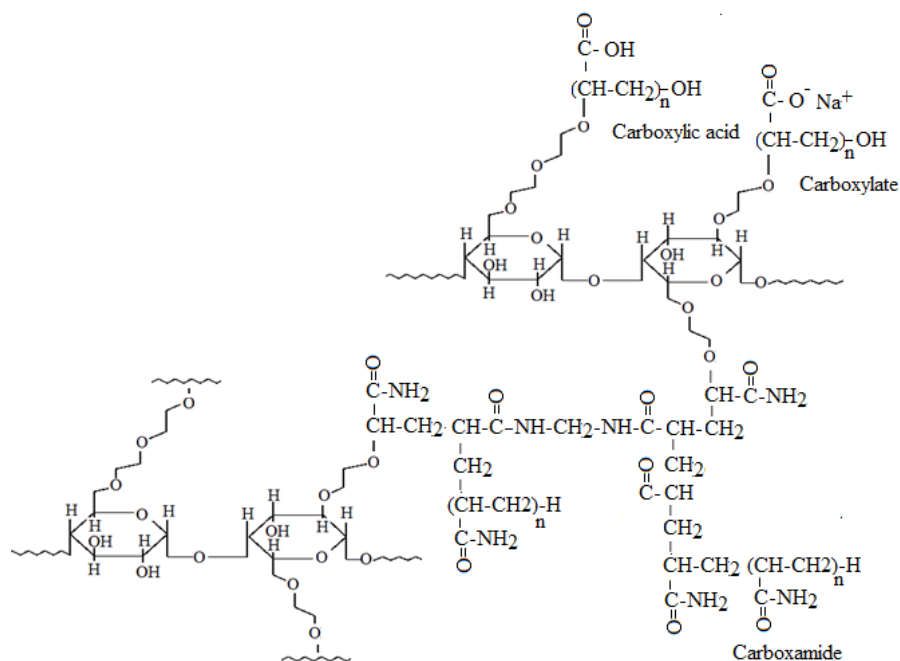


Figure 4.23 Tentative multifunctional groups structure appearing in SAPC

The occurring ligand between Zn^{2+} complex and SAPC allows them to intrinsically increase in molecular sizes of complex. The third to five steps, these are the process of intermediate sulfur- Zn^{2+} -accelerator or polysulfidic accelerator initially reacted to rubber forming rubber-sulfur-accelerator, then formed rubber-sulfur-rubber and the final stage entirely forms a network amongst rubber chain. In this process, it is probably a steric effect due to increase of the size of complexity when the Zn^{2+} forms a ligand with specific functional group of SAPC. This leads to obstruct the diffusion of complex into rubber and hinder the construction of the network, thus decreasing the cross-linked density of rubber. These results are also found when natural rubber is blended with epoxidized natural rubber and montmorillonite modified with quaternary ammonium (Arroyo, 2007) and the cross-linked density of rubber compounded based on natural rubber reinforce with octadecylamine-modified bentonite is decreased when compared to natural rubber reinforced with organoclay (Lopez-Manchado, 2003).

4.2.1.6 Cure characteristic

Figure 4.24 shows the plot of torque versus time obtained from MDR test WSR with and without SAPC. It can be seen that the torque at different time of samples with SAPC increased with increasing SAPC contents due to the increase of sample stiffness. The cure characteristics, in term of scorch time (t_{s1}), cure time (t_{c90}), cure rate index (CRI), minimum torque (M_L), maximum torque (M_H) and torque different ($M_H - M_L$) are summarized in Table 4.3.

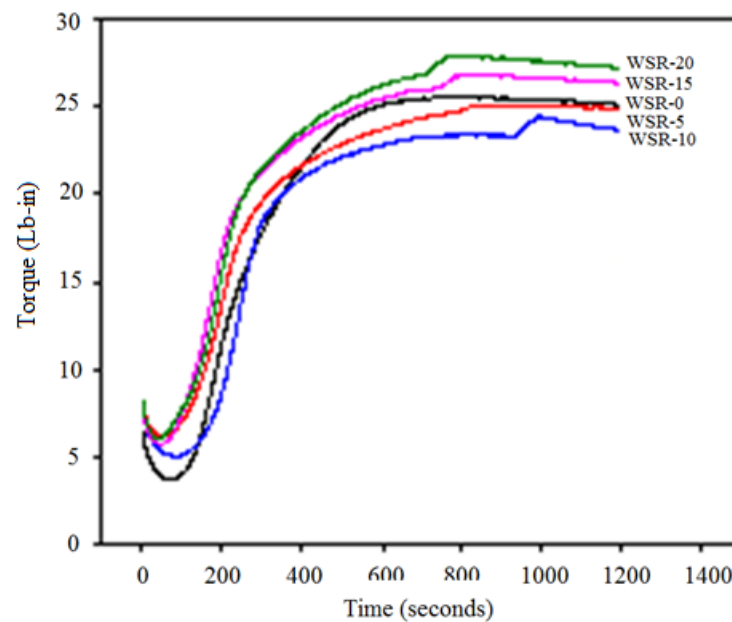


Figure 4.24 Cure-curves of WSR at different contents of SAPC

Table 4.3 Cure characteristics (t_{s1} , t_{c90} , CRI, M_L , M_H and M_H-M_L) of WSR with and without SAPC

Sample name	t_{s1}	t_{c90}	CRI	M_L	M_H	M_H-M_L
WSR-0	2.03	7.46	18.41	3.64	25.39	21.75
WSR-5	1.47	8.54	14.14	6.21	25.12	18.91
WSR-10	1.55	8.41	14.57	5.01	23.81	18.80
WSR-15	1.29	8.37	14.12	5.73	26.91	21.18
WSR-20	1.22	9.04	12.78	5.98	27.92	21.94

In the scorch region, it was found that all WSR filled with SAPC exhibits higher minimum torque than that of WSR without SAPC. This is due to the inter-atomic bonding forms between rubber and SAPC phases leading to the increase of uncured WSR viscosity. In the curing regions, the CRI was found to be retarded when the SAPC was added to WRS. This was attributed to the SAPC performed acid characteristic since the SAPC contains various hydroxyl groups (-OH) from indigenous hydroxyethyl cellulose and amides when treated with alkaline base transformed into acid functional groups in the molecules. Thus, the rate of vulcanization was retarded (Wang *et al.*, 1998). After curing region, the MDR curve of WSR with 15 and 20 phr SAPC shows a higher modulus than that of unfilled WSR. On the other hand, the torque of WSR-5 and WSR-10 shows lower value of modulus than that without SAPC. With increase addition of SAPC, it is found that the t_{s1} , t_{c90} , M_L and M_H are independent with addition of SAPC. It is interesting to note that the cure characteristics obtained from MDR test is independent with the amount of cross-linked density obtained from swelling test due to different testing procedures.

4.2.1.7 Morphological properties

Morphological properties of WSRs were characterized by using scanning electron microscopy with energy dispersive X-ray spectroscopy (SEM, Quanta, FEI, the Netherlands). Figure 4.25 shows SEM micrographs of the WRS containing 15 phr SAPC. Poor dispersion and the detachment of SAPC were noticed in the sample containing 15 phr SAPC before and after immersion in water, respectively. The left out of SAPC after immersion in water suggests that the interaction between SAPC and matrix was very poor. The poor dispersion of SAPC and the weak interaction between SAPC and matrix were also the reason for the reduction of tensile strength and elongation at break.

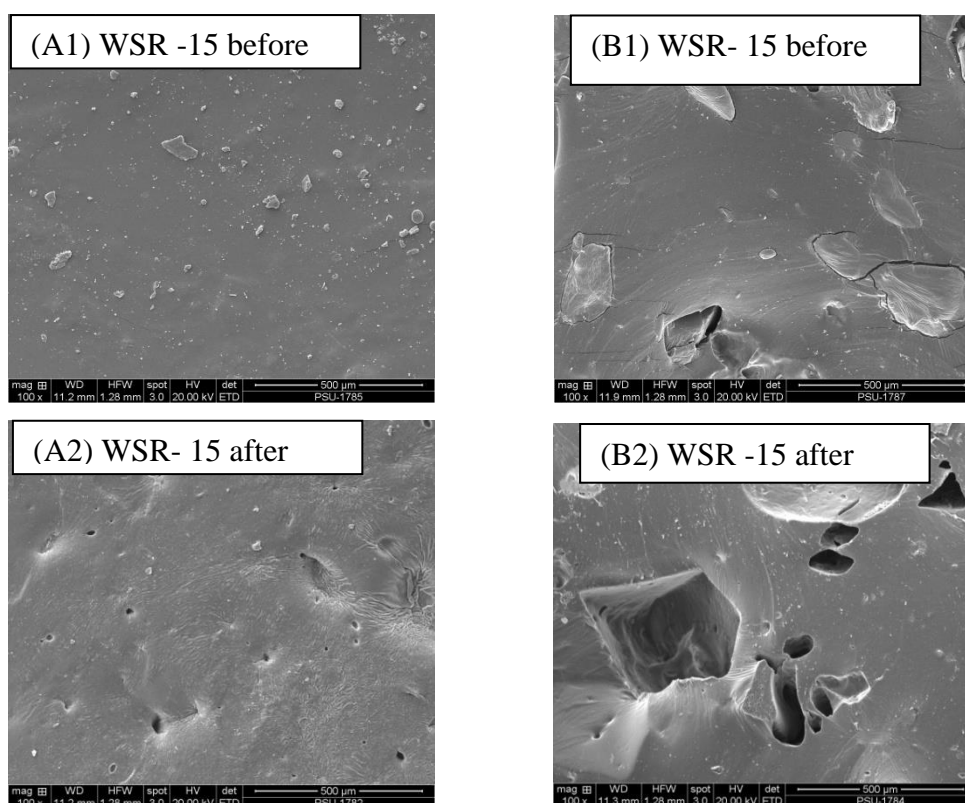


Figure. 4.25 SEM micrographs of WSR with 15 phr SAPC (A) surface and (B) cross section before and after immersion in water

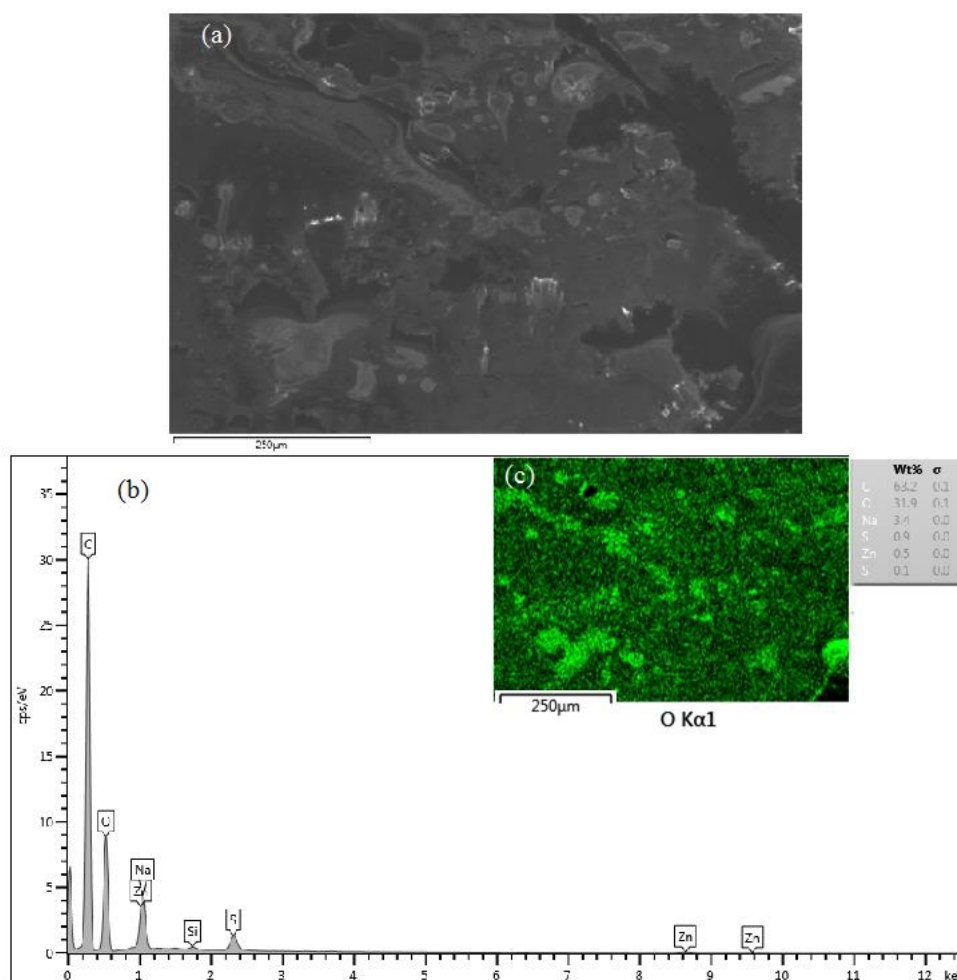


Figure 4.26 SEM micrographs of WSR with 15 phr SAPC: (a) surface (fracture images; magnification x250; scale bar 250 μm), and (b and c) SEM/EDX of WSR with X-ray mapping of O

In Figure 4.26, the SEM micrographs of WSR with 15%SAPC (a) presents that the fracture surfaces of WSR shows fine dispersion with irregular shapes and sizes of particles in the rubber. The EDX analysis was also executed to establish the dispersion of SAPC in WSR (b) and (c). As well as, the X-ray mapping of O the bright green bars over the darker green background shows the distribution of O in the rubber matrix.

4.2.1.8 Hardness

The durometer is a worldwide machine that measures the penetration of a stress-loaded metal sphere into the rubber and is defined as the resistance to

indentation which usually informed Hardness. Hardness broadband measurements in rubber are expressed in Shore A units according to ASTM D2240 test procedures. The Hardness shore A of WSR recipes with different loading of SAPC are indicated in Table 4.4

Table 4.4 Shore A hardness of WSR recipes at different loading of SAPC

Sample	Hardness (shore A)
WSR-0	30 ±0.5
WSR-5	31 ±0.5
WSR-10	31 ±0.5
WSR-15	32 ±0.5
WSR-20	32 ±0.5

Table 4.4 shows the Shore A hardness of the WSR compound formulated with different contents of SAPC as compared to that of WSR recipes without SAPC compound. The results found that the hardness for all WSR compounds formulated are higher than that of the reference compound (WSR-0). The hardness shore A is slightly increased at the initial SAPC introduction by shifting from 30 to 31 and, finally reaches to 32 at 20 phr SAPC contents. However, the overall results found the hardness shore are stable and unchangeable, that means the SAPC introduction does not affect hardness Shore A values.

4.2.2 Effect of compatibilizer on swelling behaviors and mechanical properties

Phase separation is the biggest problems which is always encountered in rubber blends during formulation that causes escalation to the obtained product which are inferior to swelling property and/or mechanical property. Compatibilizer is worldwide recommended to introducing for improving the property of the blends. In this study, polyvinyl alcohol (PVA) is associated into the blends and tested for the ends WSR properties.

4.2.2.1 Swelling measurements

Figure 4.27 plots the the % of water absorbency versus soaking time of WSR fabricated from blending of 100 phr ENR-50, 15 phr SAPC, 6 phr ZnO, 0.5 phr stearic acid, 1 phr TBBS and 2 phr sulfur with different PVA contents. The results found that the water absorbency is increased with increasing levels of PVA and eventually reaches an equilibrium at 60 days of time immersion. However, there is no change in swelling capacity even further increasing PVA levels as much as the soaking time increased. The additional results found that the highest swelling capacities of WSR around 68% are found at PVA contents 10 phr and 60 days of time immersion.

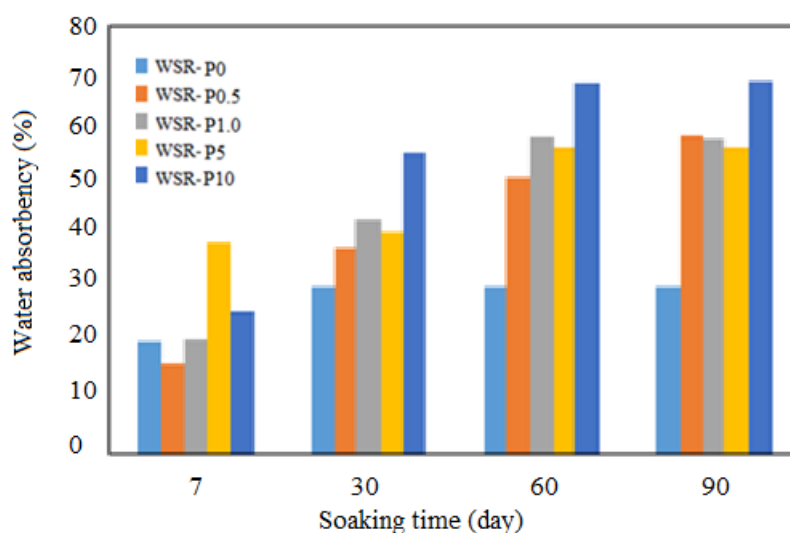


Figure. 4.27 Plot of water absorbency of WSR containing various PVA loading with soaking time, prepared from mechanical blending of 100 phr ENR-50, 15 phr SAPC, 6 phr ZnO, 0.5 phr stearic acid, 1 phr TBBS and 2 phr sulfur

The end properties of WSR is judged not only water absorbency but also weight loss therefore the need properties should be considered of both. The properties that meets the greatest absorbency and mere in weight loss are defined as the end product of WSR formulation.

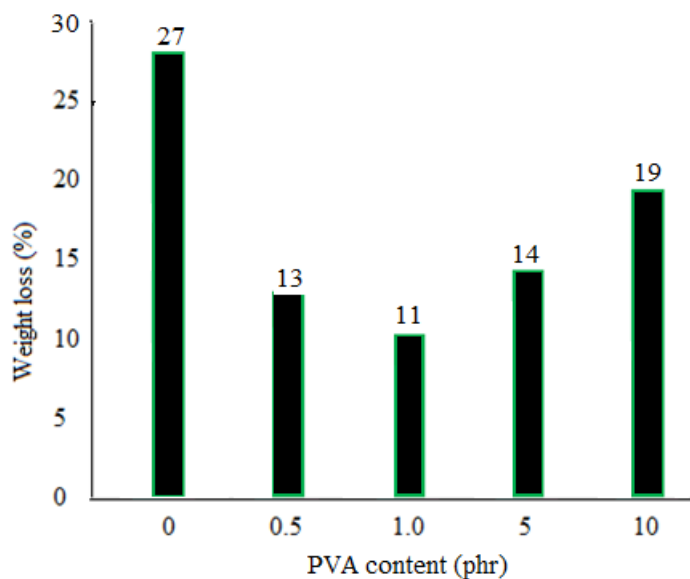


Figure 4.28 Weight loss (%) at PVA contents of WSR after first water swelling capacity (Results done in triplicate and reported in an average values)

Figure 4.28 indicates percentage weight loss of WSR loading different contents of PVA at 30 days of soaking time. The results found that the introduction of PVA into WSR affects the overall weight loss positively. The percentages weight loss is found to decrease drastically when the 0.5 phr of PVA is introduced by shifting down from 27% at without PVA to 11% with PVA content at 1.0 phr. However, the results additionally disclose that the weight loss of WSR with PVA after 1.0 phr loading are found to increase with further increase of PVA contents. The reason is because the native $-OH$ containing in PVA can better form hydrogen bond with surrounding water which leads to dissolve well in water. As the PVA migrates out from WSR recipes thus affecting the increment of weight loss.

4.2.2.2 FTIR determination

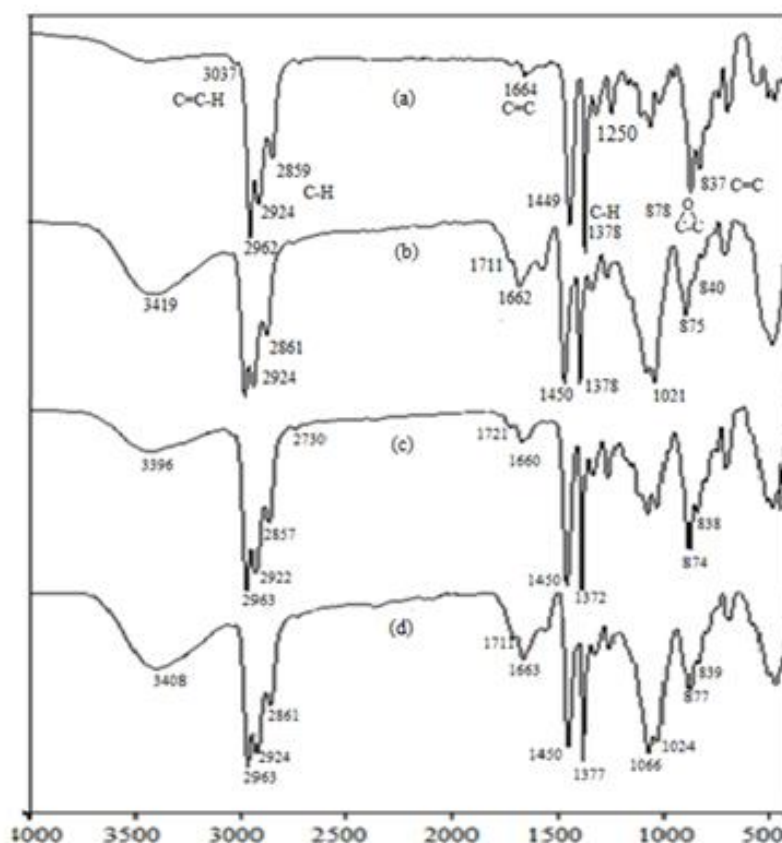


Figure 4.29 FTIR spectra of (a) ENR-50, (b) WSR with SAPC, (c and d) WSR with PVA loading 5 phr before and after water absorption, WSR prepared by blending ENR-50 and SAPC loading 15 phr, ZnO 6 phr, Stearic acid 0.5 phr, TBBS 1 phr and Sulfur 2 phr

Figure 4.29 presents FTIR data scan from 4000-500 cm^{-1} . The weak absorption band (a) at 878 cm^{-1} and medium absorption peak at 1250 cm^{-1} is assigned to the stretching vibration and deformation vibration of oxirane group in ENR. Figure 4.29(b) shows the absorption band at 1711 and 1662 cm^{-1} assigned to stretching vibration of ester carbonyl and carboxylate of SAPC, respectively. Strong absorption peaks at 1450 and 1378 cm^{-1} are assigned to $-\text{CH}_2-$ and $-\text{CH}_3$ bending vibration of ENR and methylene moieties in SAPC, respectively. Additional absorption peaks found at 1021 cm^{-1} is assigned to stretching vibration of $-\text{C}-\text{O}-\text{C}-$ that forms instead of cellulose $-\text{C}-\text{OH}$ in SAPC due to form of grafted copolymers. Figure 4.29(c) shows the new

absorption band at 1721 cm^{-1} is assigned to stretching vibration of ester carbonyl from SAPC. The slight change of -C-H stretching vibration band at 2922 cm^{-1} indicates methylene moieties in WSR are involved. Moreover, the strong peak at 1450 cm^{-1} designates as -C-H bending vibration of methylene is forcefully evidenced PVA embedding in WSR. Figure 4.28(d) indicates the absorption peak of WSR with PVA content after first water swelling capacity test. The results found that the most predominant peaks appear and are comparable to absorption peak of before swelling in water. However, there are slight differences of absorption peak at around $1060\text{-}1022\text{ cm}^{-1}$ that the strong signal due to formation of new -C-O-C- instead of -C-OH- in WSR that emerges.

4.2.2.3 Cure characteristic

Figure 4.30 shows the plot of torque versus time obtained from MDR test of WSRs with different contents of PVA. It is found that the torque at different times of WSR samples with PVA increases with increasing PVA contents due mainly to the viscosity of WSR samples decrease. The cure characteristics, in term of scorch time (t_{s1}), cure time (t_{c90}), cure rate index (CRI), minimum torque (M_L), maximum torque (M_H) and torque different ($M_H - M_L$) are summarized in Table 4.5.

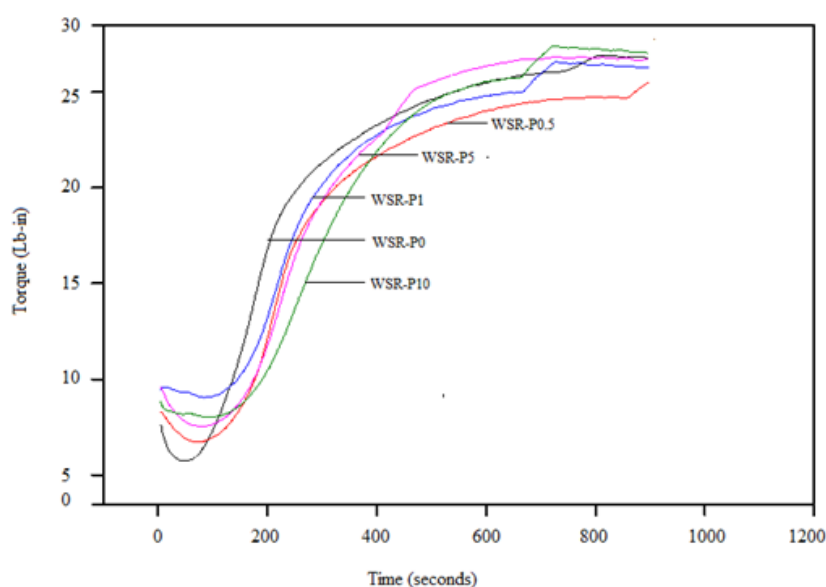


Figure 4.30 Cure-curves of WSR at different contents of PVA

Table 4.5 t_{s1} , t_{c90} , CRI, M_L , M_H and M_H-M_L from WSR at different contents of PVA, SAPC 15 phr, ZnO 6 phr, Stearic acid 0.5 phr, TBBS 1 phr and Sulfur 2 phr

Sample name	t_{s1}	t_{c90}	CRI	M_L	M_H	M_H-M_L
WSR-P0	1.29	8.37	14.12	5.73	26.91	21.18
WSR-P0.5	2.12	9.21	14.10	6.75	24.76	18.01
WSR-P1	2.26	10.07	12.81	8.67	26.51	17.84
WSR-P5	2.22	7.42	19.23	7.53	26.82	19.29
WSR-P10	2.43	9.50	14.14	8.01	27.41	19.40

In the scorch region, the torque of all WSR filled with PVA are higher than that WSR samples without PVA. The highest torque is found at 10 phr of PVA contents and the torque trend is found to increase with increase of the PVA contents. The reasons how the PVA affects the torque it because it hinders such inter-atomic bonding forms amongst rubber, PVA and SAPC phases, leading to retard the cured WSR properties. In the curing regions, the t_{c90} mostly increases when PVA are introduced except for PVA content at 5 phr, the T_{c90} drastically decreases and at this level the CRI results also found to be retarded. However, the overall CRI results of all WSR articles with PVA contents found to be accelerated. After curing region, the MDR curve of WSR with PVA contents shows a lower modulus than that of WSR without PVA. On the other hand, the torque of WSR-5 and WSR-10 showed lower value of modulus than that without SAPC. With increase addition of SAPC, it is found that the t_{s1} , t_{c90} , M_L and M_H are independent with addition of SAPC. It is interesting to note that the cure characteristics obtained from MDR test is independent with the amount of cross-linked density obtained from swelling test due to different testing procedures.

4.2.2.4 Tensile properties

The tensile strength and elongation at break of WSR filled with different contents of PVA are indicated in Table 4.6. At the earlier stages, the addition of PVA affected the tensile strength by drastically decreasing from 1.64 to 0.97 and the elongation at break shifted down from 288 to 262. After the 1 phr of PVA contents is introduced, both the tensile strength and elongation at break found to decrease while the tensile strength found to decrease at PVA contents higher than 1 phr. However, the lowest tensile strength and elongation at break are recorded. At the latter stages the further addition of PVA contents the tensile strength are found to decrease with increasing EVA contents. But there are not significant changes in elongation at break that means the introduction of PVA have no effect to WSR samples.

Table 4.6 Tensile properties of WSR filled with different PVA contents

PVA contents (phr)	Tensile strength (MPa)	Elongation at break (%)
0	1.64	288
0.5	0.97	262
1	1.49	288
5	1.39	263
10	1.17	266

4.2.2.5 Hardness

The depth of an indentation in the material is usually proportional to the material hardness. The introduction of compatibilizer into rubber recipes is always done to enhance the compatibility of rubber compound. The final product's properties are prospective improvement and meets worldwide properties with various applications. The sealing property is an important need to functionally achieve. The Hardness shore A of WSR recipes with different contents of PVA is indicated in Table 4.7.

Table 4.7 Shore A hardness of WSR with PVA formulation, WSR prepared by blending ENR-50 and SAPC 15 phr, ZnO 6 phr, Stearic acid 0.5 phr, TBBS 1 phr and Sulfur 2 phr

Sample	Hardness (shore A)
WSR-P0	32 \pm 0.5
WSR-P0.5	32 \pm 0.5
WSR-P1	33 \pm 0.5
WSR-P5	33 \pm 0.5
WSR-P10	34 \pm 0.5

Table 4.7 shows the Shore A hardness of the WSR formulated with different contents of PVA compared to that without PVA formulation. The results found that the hardness for all WSRs is higher than that of the reference (WSR-P0). The hardness shore A unchanges at the initial of PVA introduction (0.5 phr) and slightly increases with further increasing PVA contents. There is however the PVA contents are not affected to hardness values as well, demonstrating that the PVA introduction into rubber formulation is independent to shore A hardness.

4.2.2.6 Determination of the crosslink density

Table 4.8 presents the influence of PVA contents on the cross-linked density formation in WRS. The results found that the cross-linked density of WSRs increases with increasing PVA contents. This concludes that the presence of PVA in the WRS have a little hindered the formation of cross-linked density.

Table 4.8 Shows cross-linked density of WSR at different PVA contents

Sample	Crosslink density (mol/cm ³)
WSR-P0	1.61 x 10 ⁻⁶
WSR-P0.5	1.29 x 10 ⁻⁶
WSR-P1.0	1.26 x 10 ⁻⁶
WSR-P5.0	1.53 x 10 ⁻⁷
WSR-P10.0	1.28 x 10 ⁻⁷

4.2.2.7 Morphological properties

Figure 4.31 shows SEM micrographs of the WRS containing 10 phr PVA before and after having water immersion. The detachment of SAPC is a strong evidence of the weakest interaction amongst phase in rubber formulation. Noticed in the sample containing 15 phr SAPC before and after immersion in water, respectively. The left out of SAPC after immersion in water suggests that the interaction between SAPC and matrix is very poor. The poor dispersion of SAPC and the weak interaction between SAPC and matrix are also the reason for the reduction of tensile strength and elongation at break.

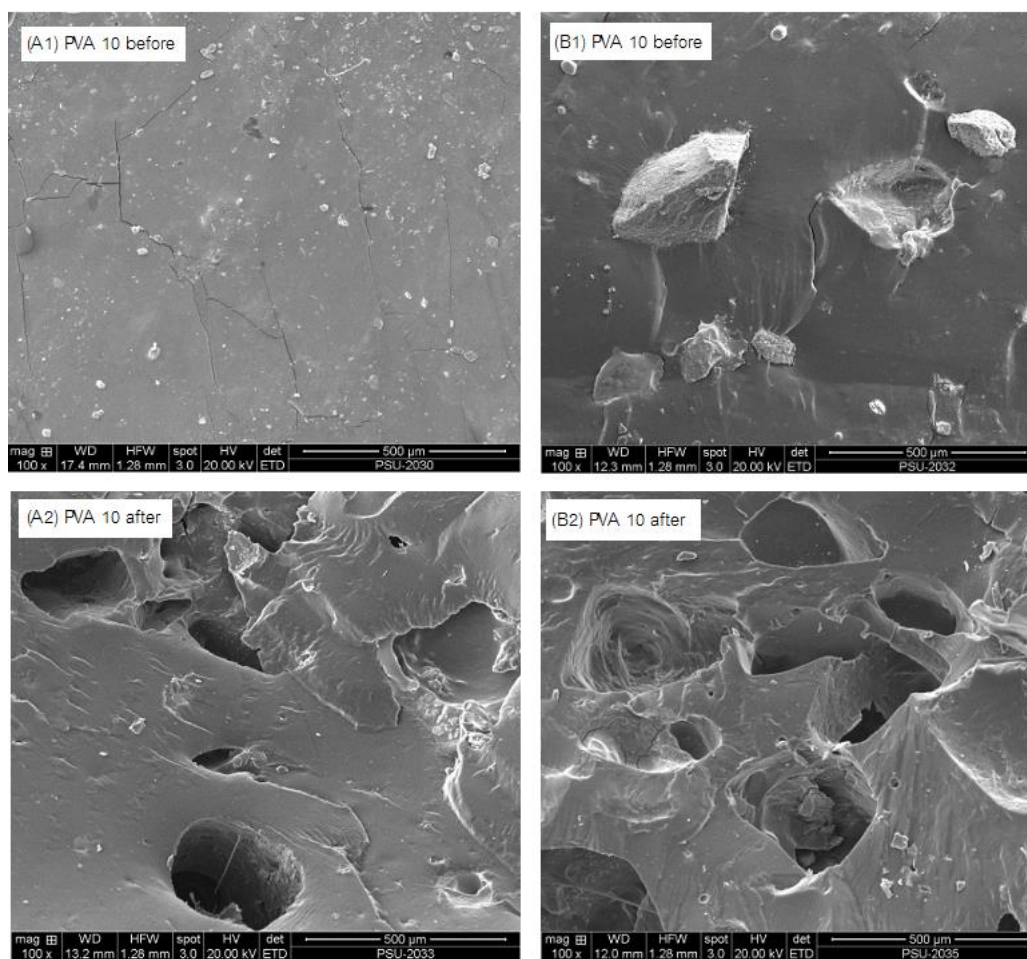


Figure. 4.31 SEM micrographs of WSR with 10 phr PVA (A) surface and (B) cross section before and after immersion in water

4.2.2.8 Thermogravimetric (TG) and Derivative Thermogravimetric (DTG)

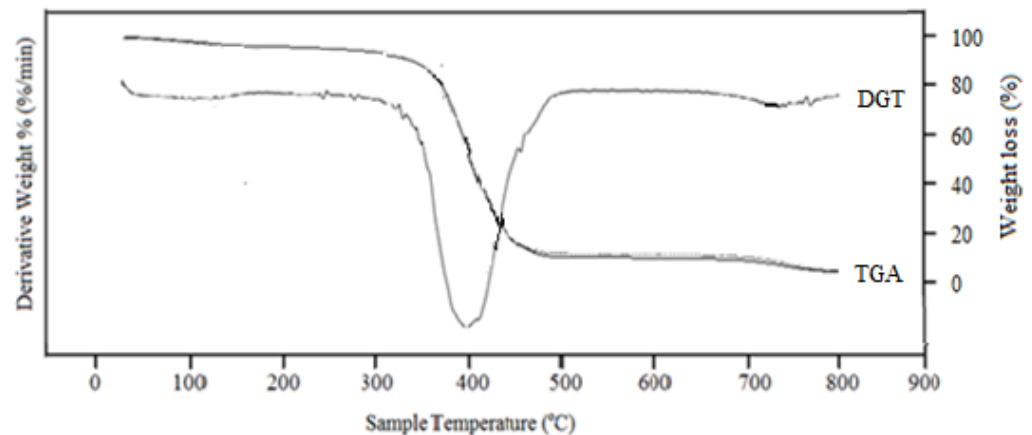


Figure 4.32 TGA and DGT curves water swellable rubber with 5 phr of PVA

Figure 4.32 indicates WSR samples of its weight due to decomposition and gasification. The weight loss at temperature of around 25-150° C is probably determined due to moisture containing in rubber recipes lost out. The next stage is at the temperature of around 150-350° C where the curve was due to weight loss of PVA lost from WSR articles. The important stages have been found above the temperature of 380° C the weight loss found to drastically decreases because of rubber decomposition (Reguieg *et al.*, 2020). After temperature of 470° C WSR with PVA, TGA curves show slight decreases of thermal decomposition due to others ingredients, while at temperatures around 690-800° C TGA curves have slight weight loss probably from the breakage of copolymer composite chains. The percentages remain of about 4% at the end of the temperature due to the composite reinforcing filler, bentonite clay that assists superabsorbent polymer composite. Moreover, DGT curves of WSR filled with PVA found that WSR samples are thermally decomposed at around temperature of 350 to 420° C, where the highest percentage derivatives of samples have reached, the results have conformed well with the TGA curve.

CHAPTER 5

CONCLUSIONS

5.1. Generals

The aim of this research is to produce a water swellable rubber by means of mechanical blending of epoxidized natural rubber matrix with dispersed superabsorbent polymer composite. The experiments consist of two main procedures including 1) preparation of superabsorbent polymer and composite, and 2) formulation of water swellable rubber. The former was conducted from grafting copolymerization reaction of hydroxyethyl cellulose with polyacrylamide and association bentonite clay composite. The full sets of reaction parameter affect the swelling properties of grafted copolymers including HEC/AM ratios, amount of initiator, concentration of crosslinker and reaction conditions. Moreover, the process in which altering amide form into carboxylate/carboxylic forms were actually conducted by alkaline hydrolysis with 2M NaOH and washing several times with distilled water for enhancement of the swelling property. The obtained hydrolyzed grafted copolymers with highest water swelling properties were further associated bentonite clay composite (SAPC) and were tested for swelling properties. The latter is the procedure to prepare a water swellable rubber from mechanical blending of epoxidized natural rubber with super absorbent polymer composite using internal mixer (Brabender Plasticorder). The full sets of reaction parameters were also investigated and individually tested for swelling behaviors and mechanical properties.

5.2 Preparation of SAP and SAPC

The SAPs were successfully prepared from grafting copolymerization of polyacrylamide onto HEC backbone. The networks conformation was constructed using *N, N'*-methylenebisacrylamide and, its concentration also has practically controlled the networks sizes of grafted copolymers. The evidence of grafting reaction confirms comprehensively from FTIR determination of pure HEC and HEC-g-PAM

(SAP) by showing predominant absorption band of both HEC and PAM. Increasing ability of water swelling could be done by treating the obtained HEC-g-PAM with 2M NaOH under temperature and time, and practical amide have been altered into carboxylate, and further interchanged to carboxylic acid when neutralizing with acid and/or distilled water. The overall conclusions could be expressed as follows.

1. Superabsorbent polymer and its filled composites are synthesized through graft copolymerization of polyacrylamide onto hydroxyethyl cellulose in solution polymerization condition under the nitrogen atmosphere.

2. The optimum conditions that give the highest water swelling capacities are archived at the HEC/AM ratios of 1/10, by using 1 g/ (1.2 g HEC) of KPS initiator, 0.1 mmole/ (100 g HEC) of MBA crosslinker at the temperature of 70° C and reaction time for 120 minutes.

3. Alkaline hydrolysis can further be treated to convert amide form into carboxylic salt by using 2M NaOH at mechanical stirrer of 100 rpm, after washing it with distilled water, the water swelling capacity up to 426 g/g discloses at the temperature of 70° C and 60 minutes.

4. The successful synthesis of HEC-g-PAM is confirmed from FTIR spectra by comparing the adsorption peak of HEC and its grafted copolymer.

5. The Bentonite clay filler in the SAPC composites gives the highest 538 g/g water swelling capacity at 40% loading level.

5.3 Formulation of Water Swellable Rubber (WSR)

The grafted copolymer composite with the highest water swellable capacity that was obtained previously from graft copolymerization of HEC, PAM and associated bentonite clay further formulates WSR. SAPC fundamentally works as a water absorbent material that is embedded in rubber matrix. When WSR is attached to surrounding water

1. Water swellable rubber (WSR) was prepared by mechanical blending from ENR-50 as the rubber matrix and SAPC as the dispersed water absorbing filler, together with an activator, accelerator and crosslinking agent. The SAPC was first synthesized by grafting copolymerization of PAM onto HEC backbones with added bentonite clay.

The compounding was carried out in an internal mixer (Brabender Plasticorder) at 40° C, 60 rpm rotor speed and 80% fill factor.

2. The first and second water absorbencies of WSR increases with SAPC content, but the second water absorbency is much lower than the first due to loss of SAPC from WSR during first immersion. The weight loss is also found to increase with increasing SAPC content.

3. The mechanical properties such as tensile strength and elongation at break decreases with increase of SAPC content, while modulus increases. The morphology of the blends after water immersion shows the loss of dispersed SAPC phases from WSR, which negatively affects the second water absorbency, tensile strength, and also elongation at break.

4. The addition of PVA into formulated WSR could increase both swelling capacity and mechanical property.

REFERENCES

- Abdullahi, R., Taghizadeh, M. T. and Savani S. 2018. Thermal and mechanical properties of graphene oxide nanocomposite hydrogel based on poly (acrylic acid) grafted onto amylose. *Polymer Degradation and Stability*. 147, 151-158.
- Abidin, A. and Puspasari, T. 2013. Utilization of cassava starch in manufacturing of superabsorbent polymer composite to reduce cost and time of production Available from: <https://www.researchgate.net/publication/309740819> Utilization of cassava starch in manufacturing of superabsorbent polymer composite to reduce cost and time of production [accessed May 02 2018].
- Abu-Abdeen, M., Elamer, I. 2010. Mechanical and swelling properties of thermoplastic elastomer blends. *Materials and Design*. 31, 808-815.
- Ahmed, S. and Ikram, S. 2016. Chitosan based scaffolds and their applications in wound healing. *Achievements in the Life Sciences*. 10(1), 27-37.
- Anitha, A., Sowmya, A., Sudheesh Kumar, P. T., Deepthi, S., Chennazhi, K. P., Ehrlich, M., Tsurkan, M. and Jayakumar, C. 2014. Chitin and chitosan in selected biomedical applications. *Progress in Polymer Science*. 39(9), 1644-1667.
- Arayaprane, W. and Rempel, G. L. (2013). Effects of polarity on the filler-rubber Interaction and properties of silica filled grafted natural rubber composites. *Journal of Polymers*. 2013, 1-9.
- Ariyawiriyanan, W., Nuinu, J., Sae-heng, K. and Kawahara, S. 2013. The Mechanical properties of vulcanized deproteinized natural rubber. *Energy Procedia*. 34, 728 – 733.
- Bo-Ziang, W., Shua-quan, L. and Chao-qun, Li. 2015. Preparation and characterization of water swelling rubber by bentonite/acrylamide grafted and modified natural rubber. *Journal of Material Science and Engineering*. 3, 415-419.
- Calo, E., Khutoryanskiy, V. V. 2015. Biomedical applications of hydrogels: A review of patents and commercial products. *European Polymer Journal*. 65, 252–267.

- Caner, H., Hasipoglu, H., Yilmaaz, O. and Yilmaaz, E. 1998. Graft copolymerization of 4-vinylpyridine onto chitosan I. by ceric ion initiation. *European Polymer Journal*. (34), 493-497.
- Carone Jr, E., Kopcaka, U., Goncalves, M.C. and Nunes, S.P. 2000. In situ compatibilization of polyamide 6/natural rubber blends with maleic anhydride. *Polymer*. 41, 5929–5935.
- Chen, J., Park, H. and Park, K. 1999. Synthesis of superporous hydrogels: hydrogels with fast swelling and superabsorbent properties. *Journal of Biochemical Material Researchs Part A*. 44(1), 53–62.
- Cook, J. P., Goodall, G. W., Khutoryanskaya, V. V. 2012. Microwave-assisted hydrogel synthesis: a new method for crosslinking polymers in aqueous solutions. *Macromolecular Rapid Communications*. 33, 332–336.
- Dechnarong, N., Nimpaiboon, A. and sakdapipanich, J. 2015. Improvement of filler-rubber interaction by grafting of acrylamide onto saponified natural rubber under ultraviolet radiation as a continuous process. *Key Engineering Materials*. 659, 414-417.
- Dehbari, N. and Tang, Y. 2015. Water swellable rubber composites: an update review from preparation to properties. *Journal. Applied Polymers Science*. 42786,
- Demitri, C., Scalera, F., Madaghiele, M., Sannino, A. and Maffezzoli, A. 2013. Potential of cellulose-based superabsorbent hydrogels as water reservoir in agriculture. *International Journal of Polymer Science*. 2013 Article ID 435073, 6 pages.
- Dong, Z., Liu, M., Jia, D. and Zhou, Y. 2013. Synthesis of natural rubber-g-maleic anhydride and its use as a compatibilizer in natural rubber/short nylon fiber composites. *Chinese Journal of Polymer Science*. 31(8), 1127–1138.
- El Sayed, A., Abdel-Razik, D. S., Badawy, E. A. and El, Nahas. 2015. Graft copolymerization of acrylamide onto corn starch using Mohr's Salt/hydrogen peroxide redox system in aqueous media under visible light. *International Journal of Modern Organic Chemistry*. 4(1), 1-17.
- El-Sherbiny, I. M. and Yacoub, M. H. 2013. Hydrogel scaffolds for tissue engineering: progress and challenges. *Global Cardiology Science and Practice*. 38, 317-342.

- El-Wakil, A. A. 2006. Synthesis, characterization, and evaluation of natural rubber-graft-*N*-(4-aminodiphenyl methane) acrylamide as an antioxidant. *Journal of Applied Polymer Science*. 101, 843–849.
- Eng, A. H. and Ong, E. L. 2000. *Plastics Engineering: Handbook of Elastomers*, Books.google.com.
- Fakhrul-Razi, A., Isam, Y. M., Qudsieh, H., Wan Yunus, W. M. D. Z., Mansor, B. A. And Mohamad Zaki, A. B. R. 2000. Graft copolymerization of methyl methacrylate onto sago starch using ceric ammonium nitrate and potassium persulfate as redox initiator systems. *Journal of Applied Polymer Science*. 82, 1375–1381.
- Faullimmel, J. G., Kiatkamjornwong, S. and Rungsriwong, N. 1988. Graft copolymerization of acrylonitrile onto cassava starch. I. synthesis of saponified starch-g-polyacrylonitrile by manganic pyrophosphate initiation. *Journal of Science Research Chulalongkorn University*. 13: 42 – 49.
- Gelling, I. R. 1985. Modification of natural rubber latex with peracetic acid. *Rubber Chemistry and Technology*. 58(1), 86-96.
- Gelling, I. R., Tinker, A. J. and Haidzir, A. R. 1991. Solubility parameters of epoxidised Natural rubbers. *Journal of Natural Rubber Research*. 6(1), 271-291.
- Ghosh, P., Chattopadhyay, B. and Sen, A. 1998. Modification of low density polyethylene (LDPE) by graft copolymerization with some acrylic monomers. *Polymer*. 39, 193-201.
- Hamzah, R., Abu Bakar, M., Khairuddean, M., Ahmed Muhammed, I. and Adnan, R. 2012. A structural study of epoxidized natural rubber (ENR-50) and its cyclic-dithiocarbonate derivatives using NMR spectroscopy techniques. *Journal of Molecules*. 17, 10974-993.
- Heideman G, Datta R. N., Noordermeer, J. W. M., and Van Baarle, B. 2005. Influence of zinc oxide during different stages of sulfur vulcanization elucidated by model compound studies. *Journal of Applied Polymer Science*. 95, 1388–1404.
- Heping, Y., Sidong, L., and Zheng, P. 1999. Prerparation and study of epoxidized natural rubber. *Journal of Thermal Analysis and Calorimetry*. 58, 293-299.

- Héroid, R. and Fouassier, J. P. 1981. Photochemical grafting of vinyl monomers onto starch. *Starch*. 33(3), 90–97.
- Hu, Z. H. and Zhang, L. M. 2002. Water-soluble ampholytic grafted polysaccharides II synthesis and characterization of graft terpolymer of starch with acrylamide and [2-(methylacryloylox)] ethyl dimethyl (3-sulfopropyl) ammonium. *Journal of Macromolecular Science Part A*. 39(5), 419–430.
- Huang, K. C., Couttenye, R. A. and Hoag, G. E. 2002. Kinetic of heat-assisted persulfate oxidation of methyl tert butyl ether (MTBE). *Chemosphere*. 49(4), 413-420.
- Jiang, X. L., Hu, K., Yang, P. and Ren, J. 2013. Study on preparation and properties of water swellable rubber modified by interpenetrating polymer networks. *Plastics, Rubber and Composites*. 42(8), 327-333.
- Joubert, F., Yeo, R. P., Sharples, G. J., Musa, O. M., David, R.W., Hodgson, D. R. W., and Cameron, N. R. 2015. Preparation of an antibacterial poly (ionic liquid) graft copolymer of hydroxyethyl cellulose. *Biomacromolecules*. 06 November. 1-39.
- Jyothi, A. N. 2010. Starch graft copolymers: novel applications in industry. *Composite Interfaces*. 17, 165–174.
- Kiatkamjornwong, S. and Faullimmel, J. G. 1991. Synthesis of cassava starch-based water absorbing polymer for agriculture application. *Journal Natural Research Council Thailand*. 23, 15- 23.
- Kiatkamjornwong, S. and Meechai, N. 1997. Enhancement of the grafting performance and of the water absorbing of cassava starch graft copolymer by gamma radiation. *Radiation Physic Chemistry*. 49, 689–696.
- Kohjiya, S. and Ikeda, Y. 2014. Chemistry, manufacture and applications of natural rubber. Woodhead Publishing 225 Wyman street Waltham MA 02451 USA, 31-35 pp 493.
- Kuang, J., Yuk, K. Y. and Huh, K. M. 2011. Polysaccharide-based superporous hydrogels with fast swelling and superabsorbent properties. *Carbohydrate Polymers*. 83, 284–290.
- Kuczkowski, J. A. and Gillick, J. G. 1984. Polymer-bound antioxidants. *Rubber Chemistry and Technology*. 57(3), 621-651.

- Li, P., Siddaramaiah, N. H., Kim, H. S. and Lee, J. 2008. Novel PAAm/laponite clay nanocomposite hydrogels with improved cationic dye adsorption behavior. *Composites B*. 39, 756–763.
- Li, S., Lang, F., Du, F. and Wang Z. 2014. Water-swellaable thermoplastic vulcanizates Based on ethylene–vinyl acetate copolymer/chlorinated polyethylene/cross-linked sodium polyacrylate/nitrile butadiene rubber blends. *Journal of Thermoplastic Composite Materials*. 27(8), 1112–1126.
- Li, S., Lang, F., Du, F., and Wang, Z. 2013. Water-swellaable thermoplastic vulcanizates based on ethylene–vinyl acetate copolymer/chlorinated polyethylene/crosslinked sodium polyacrylate/nitrile butadiene rubber blends. *Journal of Thermoplastic Composite Materials*. 1–15.
- Liu, C., Ding, J., Zhou, L. and Chen, S. 2006. Mechanical properties, water-swelling behavior, and morphology of water-wellaable rubber prepared using crosslinked sodium polyacrylate. *Journal of Applied Polymer Science*. 102, 1489–1496.
- Liu, P. and Wang, T. 2007. Adsorption properties of hyperbranched aliphatic polyester grafted attapulgite towards heavy metal ions. *Journal of Hazardous Materials*. 149, 75–79.
- Liu, P., Jiang, L., Zhu, L., Guo, J. and Wang, A. 2015. Synthesis of covalently crosslinked attapulgite/poly (acrylic acid-co-acrylamide) nanocomposite hydrogels and their evaluation as adsorbent for heavy metal ions. *Journal of Industrial and Engineering Chemistry*. 23, 188-193.
- Liu, Y., Liu, Z., Zhang, Y. and Deng, K. 2003. Graft copolymerization of methyl acrylate onto chitosan initiated by potassium doperiodatocuprate (III). *Journal of Applied Polymer Science*. 89, 2283–2289.
- Liu, Y., Wang, W. and Wang, A. 2010. Adsorption of lead ions from aqueous solution by using carboxymethyl cellulose-g-poly (acrylic acid)/attapulgite hydrogel composites. *Desalination*. 259, 258–264.
- Mahittikul, A., Prasassarakicha, P. and Rempel, G. L. 2009. Hydrogenation of natural rubber latex in the presence of [Ir(cod)(PCy₃)(py)]PF₆. *Journal of Molecular Catalysis A: Chemical*. 297, 135–141.

- Mascia, L., Russo, P., Verdolotti, L., Clarke, J., Lavorgna, M. and Acierno, D. 2015. Probing the postgelation reactions of epoxidized natural rubber cross-linked with dodecenyl succinic anhydride. *Rubber Chemistry and Technology*. 88(4), 560–573.
- Matador Rubber. SRO. 2007. *Rubber Chemistry. Education and Culture. Leonardo Da vinci*. pp. 94.
- Moccasin, C., Kaesaman, A., Homsin, S. and Kiatkamjornwong, S. 2001. Rheological and curing behavior of reactive blending. I maleated natural rubber–cassava starch. *Journal of Applied Polymer Science*. 81, 2803–2813.
- Mohamad, N., Yaakub, J., Abd Razak, J., Yaakob, M. Y., Shueb, M. I. and Muchtar, A. 2014. Effects of epoxidized natural rubber (enr-50) and processing parameters on the properties of NR/EPDM blends using response surface methodology. *Journal of Applied Polymer Science*. 131(40713), 1-8.
- Mostafa, K. H. M. 1995. Graft polymerization of acrylic acid onto starch using potassium permanganate acid (redox system). *Journal of Applied Polymer Science*. 56, 263-269.
- Muhamad, Z., Ismail, S. and Chantara Thevy, R. 2006. Characterization of epoxidized Natural rubber/ethylene vinyl acetate (enr-50/eva) blend: effect of blend ratio. *Journal of Applied Polymer Science*. 99, 1504–1515.
- Nakason, C., Kaesaman, A. and Supasanthitkul, P. 2004. The grafting of maleic anhydride onto natural rubber. *Polymer Testing*. 23, 35–41.
- Nakason, C., Nakaramontri, Y., Kaesaman, A., Kangwansukpamonkon, W. and Kiatkamjornwong, S. 2013. Synthesis and characterization of water swellaable natural rubber vulcanizates. *European Journal Polymer*. 49, 1098-1110.
- Nakason, C., Tobprakhon, A. and Kaesaman, A. 2005. Thermoplastic vulcanizates based on poly (methyl methacrylate)/epoxidized natural rubber blends: mechanical, thermal, and morphological properties. *Journal of Applied Polymer Science*. 98, 1251-1261.
- Nakason, C., Wohmang, T., Kaesaman, A. and Kiatkamjornwong, S. 2010. Preparation of cassava starch graft polyacrylamide superabsorbents and associated composites by reactive blending. *Carbohydrate Polymers*. 81(2), 348-357.

- Okieimen, F. E. and Urhoghide, I. N. 2002. Graft copolymerization of acrylonitrile and methyl methacrylate monomer mixtures on crumb natural rubber. *Journal of Applied Polymer Science*. 84, 1872–1877.
- Peng, S., Shi, R., Yang, R., Zhou, D. and Wang, Y. 2008. Hydroxyethylcellulose-graft-poly (*N, N*-dimethylacrylamide) copolymer as a multifunctional separation medium for CE. *Electrophoresis*. 29(21), 4351–4354.
- Peng, Z. and Chen, F. 2010. Synthesis and properties of temperature-sensitive hydrogel based on hydroxyethyl cellulose. *International Journal of Polymeric Materials*. 59(6), 450–461.
- Piorkowska, E. and Rutledge, G. C. 2013. *Handbooks of polymer crystallization. Technology and Engineering*. John Wiley & Sons, May 30, 2556 BE. pp. 498.
- Pledger, J. R. H., Young, T. S., Wu, G. S., Butler, G. B. and T. E. Hogen-esch, T. E. 1985. Synthesis and characterization of water-soluble starch-acrylamide graft copolymers. *Journal Macromolecular Science Chemistry*. A22(4), 415-436.
- Polgar, L. M., Fallani, F., Cuijpers, J., Raffa, P., Broekhuis, A. A., Duin, M. V. and Picchioni, F. 2017. Water-swallowable elastomers: synthesis, properties and applications. *Reviews in Chemical Engineering*. 1-28.
- Pradhan, A. K., Rana, P. K., Sahoo., P. K. 2015. Biodegradability and swelling capacity of kaolin based chitosan-g-PHEMA nanocomposite hydrogel. *International Journal of Biological Macromolecules*. 74, 620–626.
- Pukkate, N., Kitai, T., Yamamoto, Y., Kawazura, T., Sakdapipanich, J. and Kawahara, S. 2007. Nano-matrix structure formed by graft-copolymerization of styrene onto natural rubber. *European Polymer Journal*. 43, 3208-3214.
- Reguieg, F., Ricci, L., Bouvacoub, N., Belbachir, M. and Monica Bertoldo, M. 2020. Thermal characterization by DSC and TGA analyses of PVA hydrogels with organic and sodium MMT. *Polymer Bulletin*. 77, 929–948.
- Ren, W., Peng, Z., Zhang, Y. and Zhang, Y. 2004. Water-swelling elastomer prepared by in situ formed lithium acrylate in chlorinated polyethylene. *Journal Applied Polymer Science*. 92, 1804–1812.
- Ren, W., Peng, Z., Zhang, Y. and Zhang, Y. 2005. Preparation and properties of a water swelling rubber by in situ formed lithium acrylate in nitrile rubber. *Polymers and Polymer Composites*. 13(2), 181-190.

- Rodger, E. R. 1979. Vulcanization systems. In: developments in rubber technology. (Eds. I A. Whelaw and S. K. Lee). Applied Science Publishers Ltd. London, pp.105-150.
- Rzayev, Z. M. O. 2011. Graft copolymers of maleic anhydride and its isostructural analogues: high performance engineering materials. *International Review of Chemical Engineering*. 3(2), 153-215.
- Rzayev, Z.M.O. 2011. Graft copolymers of maleic anhydride and its isostructural analogues: high performance engineering materials. *International Reviews of Chemical Engineering*. 3(2), 153-215.
- Sadeghi, H., Mirdarikhvande, S., Godarzi, A., Alahtari, M., Shasavari, H. and Mansouri, L. 2015. Rate evaluation of graft copolymerization of hydrophilic monomers on to natural polymer. *Oriental Journal of Chemistry*. 30(1), 325-328.
- Sadeghi, M. and Hosseinzadeh, H. 2010. Studies on graft copolymerization of 2-hydroxyethylmethacrylate onto kappacarrageenan initiated by ceric ammonium nitrate. *Journal of the Chilean Chemical Society*. 55(4), 497-502.
- Sahama, S. H., Essa, D. M., Osman, E. M. and Ibrahim, S. F. 2015. Synthesis and characterization of hydroxyethyl cellulose grafted copolymers and its application for removal of nickel ions from aqueous solutions. *International Journal of Engineering Innovation and Research*. 4(4), 645-653.
- Sahoo, S., Maiti, M., Ganguly, A., George, J. J. and Bhowmick, A. K. 2007. Effect of zinc oxide nanoparticles as cure activator on the properties of natural rubber and nitrile rubber. *Journal of Applied Polymer Science*. 105, 2407–2415.
- Sahraei, R. and Ghaemy, M. 2017. Synthesis of modified gum tragacanth/graphene oxide composite hydrogel for heavy metal ions removal and preparation of silver nanocomposite for antibacterial activity. *Carbohydrate Polymers*. 157, 823-833.
- Samaha, S.H., Essa, D.M., Osman, E.M. and Ibrahim, S.F. 2015. Synthesis and characterization of hydroxyethyl cellulose grafted copolymers and its application for removal of Nickel Ions from aqueous solutions. *International Journal of Engineering Innovation and Research*. 4(4)., 645-653.

- Sangsirimongkolying, R., Damronglerd, S. and Kiatkamjornwong, S. 1999. Pilot-scale production of highly water absorbing polymer from native cassava starch by hydrogen peroxide-ascorbic acid initiation. *Journal of Science Research Chulalongkorn University*. 24, 1 –12.
- Shanmugapriya, A., Ramammurthy, R., Munusamy, V. and Parapurath, S. N. 2011. Optimization of ceric ammonium nitrate initiated graft copolymerization of acrylonitrile onto chitosan. *Journal of Water Resource and Protection*. 3, 380-386.
- Sharma, B. R., Kumar, V. and Soni, P. L. 2002. Ceric ammonium nitrate-initiated graft copolymerization of acrylamide onto cassia taro gum. *Journal of Applied Polymer Science*. 86(13), 3250-3255.
- Sharma, R., Balbir, R., Kaith, S., Kalia, S., Pathania, D., Kumar, A., Sharma, N., Reva, M. S. and Schauer, C. 2015. Biodegradable and conducting hydrogels based on guar gum polysaccharide for antibacterial and dye removal applications. *Journal of Environmental Management*. 162, 37-45.
- Shirsath, S.R., Patil, A. P., Bhanvase, B. A. and Sonawane, S.H. 2015. Ultrasonically prepared poly(acrylamide)-kaolin composite hydrogel for removal of crystal violet dye from wastewater. *Journal of Environmental Chemical Engineering*. 3(20), 1152-1162.
- Soleimani, K., Tehrani, A. D. and Adeli, M. 2018. Bioconjugated graphene oxide hydrogel as an effective adsorbent for cationic dyes removal. *Ecotoxicology and Environmental Safety*. 147, 34–42.
- Sonawane, S. H., Chaudhari, P. L., Ghodke, S. A., Ambade, S., Gulig, A., Mirikar, A., and Bane, A. 2008. Combined effect of ultrasound and nanoclay on adsorption of phenol. *Ultrasonics Sonochemistry*. 15(6), 1033–1037.
- Sonawane, S.H., Chaudhari, P.L., Ghodke, S.A., Parande, M.G., Bhandari, V.M., Mishra, S. and Kulkarni, R.D. 2009. Ultrasound assisted synthesis of polyacrylic acid–nanoclay nanocomposite and its application in sonosorption studies of malachite green dye. *Ultrasonics Sonochemistry*. 16 (3), 351–355.

- Soppirnath, K. S. and Aminabhavi, T. M. 2002. Water transport and drug release study from cross-linked polyacrylamide grafted guar gum hydrogel microspheres for the controlled release application. *Europeans Journal of Pharmaceutic and Biopharmaceutics*. 53, 87–98.
- Spychaji, T., Schmidt, B., Ulfig, K. and Markowska-Szczupak, A. 2012. Starch-grafted-*N*-vinylformamide copolymers manufactured by reactive extrusion: synthesis and characterization. *Polimery*. 57(2), 95-100.
- Suksawad, P., Yamamoto, Y. and Kawahara, S. 2011. Preparation of thermoplastic elastomer from natural rubber grafted with polystyrene. *European Polymer Journal*. 47(3), 330–337.
- Taheri, S., Hassani, Y., Mohamad Sadeghi, G. M., Moztarzadez, F., Li, M. C. 2016. Graft copolymerization of acrylic acid on to styrene butadiene rubber (SBR) to improve morphology and mechanical properties of SBR/ polyurethane blend. *Journal of Applied Polymer Science*. 133, 1-11.
- Tanodekaew, S., Prasitsilp, M., Swasdison, S., Thavornytikarn, B., Pothsree, T. and Patepasen, R. 2004. Preparation of acrylic grafted chitin for wound dressing application. *Biomaterials*. 25, 1453–1460.
- Ullah, F., Othman, M. B. H., Javed, F., Ahmed, Z. and Md Akil, H. 2015. Classification, processing and application of hydrogels: A Review. *Material Science and Engineering*. 57, 414-433.
- Utracki, L. A., Walsh, D. J. and Weiss, R. A. 1989. Polymer alloys, blends, and ionomers: an overview multiphase polymers: blends and ionomers. Chapter 1, 1–35.
- Valsa George, I., John Britto, M. and Sebastian, S. 2003. Studies on radiation grafting of methyl methacrylate onto natural rubber for improving modulus of latex film. *Radiation Physics and Chemistry*. 66, 367–372.
- Wang, B., Liu, Z., Liao, S. and Li, C. 2015. Preparation and properties of water-swallowable natural rubber vulcanizates. *Materials Research Innovations*. 19(8), 198-203.

- Wang, C., Zhang, G., Dong, Y., Chen, X. and Tan, H. 2002. Study on a water-swelling rubber compatibilized by amphiphilic block polymer based on poly(ethylene oxide) and poly(butyl acrylate). *Journal of Applied Polymer Science*. 86, 3120–3125.
- Wang, G., Li, M. and Chen, X. 1998. Preparation and water-absorbent properties of a water-swelling rubber. *Journal of Applied Polymers Science*. 68(8), 1219-1225.
- Wang, X. and Wang, A. 2010. Adsorption characteristics of chitosan-g-poly (acrylic acid)/attapulgitite hydrogel composite for Hg (II) ions from aqueous solution. *Journal of Separation Science and Technology*. 45, 2086-2094.
- Wei, F., Yu, H., Zeng, Z., Liu, H., Wang, Q., Wang, J. and Li, S. 2014. Preparation and structural characterization of hydroxyethyl methacrylate grafted natural rubber latex. *Polímeros*. 24(3), 283-290.
- Xiang, Y., Peng, Z. and Chen, D. 2006. A new polymer/clay nano-composite hydrogel with improved response rate and tensile mechanical properties. *European Polymer Journal*. 42(9), 2125–2132.
- Xu, H., Liu, J., Fang, L. and Wu, C. 2007. In situ grafting onto silica surface with epoxidized natural rubber via solid state method. *Journal of Macromolecular Science Part B, Physics*. 46, 693–703.
- Yang, R., Wang, Y. and Zhou, D. 2007. Novel hydroxyethylcellulose-graft-polyacrylamide copolymer for separation of double-stranded DNA fragments by CE. *Electrophoresis*. 28, 3223–3231.
- Zhang, Y., He, P., Zou, Q. and He, B. 2004. Preparation and properties of water-swelling elastomer. *Journal of Applied Polymer Science*. 93, 1719–1723.
- Zhang, Z. T. 2012. Preparation, water absorbent and mechanical properties of water swelling rubber. *Plastics, Rubber and Composites*. 41(8), 326-331.
- Zhang, Z., Zhang, G., Li, D., Liu, Z. and Chen, X. 1999. Chlorohydrin water-swelling rubber compatibilized by an amphiphilic graft copolymer. II. effects of PVA-g-PBA and CPA on water-swelling behaviors. *Journal of Applied Polymer Science*. 74, 3145–3152.

- Zhang, Z., Zhang, G., Wang, C., Liu, D., Liu, Z. and Chen, X. 2001. Chlorohydrin water-swellaable rubber compatibilized by an amphiphilic graft copolymer. III. effects of PEG and PSA on water-swelling behavior. *Journal of Applied Polymer Science*. 79, 2509–2516.
- Zhang, Z., Zhang, G., Zhang, Y., Wang, Z., Yu, D., Hu, X., Hu, C. and Tang, X. 2004. Mechanical properties, water swelling behavior, and morphology of swellaable rubber compatibilized by PVA-g-PBA. *Polymer Engineering and Science*. 44(1), 72-78.

APPENDIX

Appendix A: Article 1

Superabsorbent materials derived from hydroxyethyl cellulose and bentonite: Preparation, characterization and swelling capacities

Polymer Testing 64 (2017) 321–329



Contents lists available at ScienceDirect

Polymer Testing

journal homepage: www.elsevier.com/locate/polymtest

POLYMER TESTING

Superabsorbent materials derived from hydroxyethyl cellulose and bentonite: Preparation, characterization and swelling capacities



Ajaman Adair^{a,*}, Azizon Kaesaman^a, Pairote Klinpituksa^b

^a Department of Rubber Technology and Polymer Science, Faculty of Science and Technology, Prince of Songkla University, Pattani 94000, Thailand

^b Department of Science, Faculty of Science and Technology, Prince of Songkla University, Pattani 94000, Thailand

ARTICLE INFO

Keywords:
Hydrogel
Superabsorbent polymer
Hydroxyethyl cellulose
Acrylamide
Graft copolymerization

ABSTRACT

Superabsorbent polymers (SAPs) and composites (SAPCs) were prepared entirely by graft copolymerization of polyacrylamide (PAM) onto hydroxyethyl cellulose (HEC), using potassium persulfate (KPS) as an initiator, and *N,N'*-methylenebisacrylamide (MBA) as a crosslinker, in an aqueous solution. The extent of grafting was evaluated from % grafting efficiency (%GE) for various HEC/AM ratios, and a near optimal ratio was determined. Influences of various preparation parameters, *i.e.*, the ratio of HEC/AM, amount of initiator and crosslinker, reaction temperature and time, and amount of filler on water swelling capacity of SAPs and SAPCs were studied. An FT-IR determination confirmed that the PAM was successfully grafted onto the HEC backbone, by showing absorption bands of the HEC backbone and new absorption bands from the grafted copolymer. The swelling capacity of SAPs and SAPCs depended strongly on different parameters, and the maximum swelling capacity was over 426 g/g and 538 g/g for the SAPs and SAPCs, respectively.

1. Introduction

Superabsorbent polymers (SAPs) are functional materials composed of a slightly crosslinked network of a super hydrophilic polymer in a loose three-dimensional network of polymer chains [1–3]. The SAPs generally contain carboxylic acid, partially neutralized carboxyl groups, carboxamide and carboxylate salt. They draw surrounding water into the polymer network by diffusion while the polymer backbone chains maintain their network structure due to crosslinking, so the network swells and expands. The covalent crosslinks forming 3-dimensional network can also prevent the polymer from dissolving in water. The SAPs possess not only high fluid absorption capacity, but can also retain the absorbed fluid for long periods even under high temperature and mechanical compression. They are able to absorb large quantities of water without dissolving, even exceeding 1500 fold their dry weight [4]. Due to such extraordinary properties, the SAPs have attracted much attention and are produced for many applications. For example, they are used in disposable baby diapers, in agriculture as soil amendments, in controlled release of drugs as carriers, in coal dewatering, in waste water treatment [5], and in cosmetics and absorbent pads [6]. The SAPs were originally synthetic crosslinked polyacrylic acid and polyacrylate salt derivatives of petroleum products. Their costs have tended to increase as petroleum based products relying on non-renewable raw materials. Based on the sources of raw materials, the

SAPs are generally classified into three types, namely natural (polysaccharide derivatives), semi-artificial (cellulosic primitive derivatives), and artificial or synthetic polymers [7]. Although the SAPs pose no direct threat to human life or health, the disposal of synthetic SAP waste is a source of various environmental pollutants [3,8,9]. This problem has become the motivation for academic studies by both polymer technologists and manufacturers to produce comparable SAPs that have reduced needs for a disposal system.

Natural SAPs are attractive due to their renewability and biodegradability. They can be degraded by natural biological processes, including actions of enzymes, micro-organisms and water, transforming into harmless and simple compounds that are environmentally safe. Amongst them, polysaccharides and proteins have been employed to prepare SAPs due to availability in large scale as feedstock, renewability and biodegradability. Polysaccharides are naturally polymeric carbohydrate molecules composed of monosaccharide units joined by glycosidic bonds. The structure varies from linear to highly branched. Examples of polysaccharides include cellulose and chitin. Cellulose is the main component of cell walls in lignocellulosic plants, and is embedded in a matrix composed of hemicellulose, lignin and other polymers [10]. Various cellulose derivatives, such as cellulose acetate, carboxymethyl cellulose, hydroxyethyl cellulose and so on, have been utilized as polymer backbones in SAPs expecting to achieve biodegradability. Hydroxyethyl cellulose (HEC) is modified cellulose

* Corresponding author. Tel.: +66 818984695.
E-mail address: nadair1969@gmail.com (A. Adair).

<http://dx.doi.org/10.1016/j.polymertesting.2017.10.018>

Received 3 July 2017; Received in revised form 27 September 2017; Accepted 21 October 2017
Available online 25 October 2017
0142-9418/© 2017 Elsevier Ltd. All rights reserved.

synthesized by reacting ethylene oxide and cellulose with an alkaline catalyst under carefully controlled conditions. Since the HEC chains have abundant reactive hydroxyl groups, they can be modified by graft polymerization with hydrophilic vinyl monomers to produce materials with desirable properties [11]. Many studies have reported on HEC based superabsorbents and composites. A series of pH- and saline-responsive composite hydrogels were prepared by a facile free radical graft copolymerization of HEC with sodium acrylate (Na^+A^-) and medicinal stone (MS). It revealed that introducing 10 wt% MS greatly enhanced the swelling capacity by 400% [5]. The water absorbency of organo-vermiculite (OVMT) HEC-g-PAA/OVMT nano-composite was increased up to 670 g/g by increasing the organification degree, and reached maximal absorption at the optimal organification degree of 2.62 wt% [12]. A novel separation medium based on HEC-g-PAM was applied in dsDNA separation by capillary electrophoresis [13].

In this work, SAP and SAPC were synthesized by grafting polyacrylamide onto a cellulose derivative via solution copolymerization, to produce SAPs and SAPC with high water swelling capacity and biodegradability. The bentonite clay was incorporated in SAPC to target water swellable rubber (WSR) by means of mechanical blending with epoxidized natural rubber. The effects of the mass ratio HEC/AM on grafting efficiency, the amount of initiator, the concentration of MBA, the alkaline treatment conditions and the bentonite clay loading on the water swelling capacity were further investigated. FTIR spectra were used to characterize and confirm successful graft copolymerization. The XRD patterns, TGA analysis, and scanning electron micrographs were also utilized to confirm the formation of SAPC.

2. Experimental studies

2.1. Materials

Hydroxyethyl cellulose (HEC) (AR grade) was purchased from Merck KGaA Corporate (Frankfurter Straße, Germany). Acrylamide (AM), having 99% purity used for synthesis was supplied by Merck KGaA Corporate (Frankfurter Straße, Germany). Potassium persulfate (KPS) with 99% purity manufactured by Ajax Finechem was used as initiator. *N,N'*-methylenebisacrylamide (MBA) and sodium hydroxide (AR grade) purchased from Fluka (Buch SG, Switzerland) were used as crosslinker and in alkaline hydrolysis, respectively. Bentonite clay was manufactured by Sigma Aldrich (St. Louis, Missouri, USA).

2.2. Preparation of SAP and SAPC

HEC was first dried in a hot air oven for a couple of days, thereafter 1.2 g was dissolved in 40 mL of distilled water in a four-neck round-bottom flask reactor, equipped with a mechanical stirrer, condenser, dropping funnel and nitrogen line. The reactant (HEC + H_2O) was stirred at 100 rpm for 30 min with nitrogen gas purging. The slurry was then heated up to 60 °C and maintained at this temperature for 30 min. Subsequently, 1.0 g of initiator (KPS) (0.3 mol/100 g HEC) was further added and stirred continuously for 10 min to completely generate free radicals. The reaction temperature was then lessened to 50 °C to prevent immediate graft copolymerization. The solution of 12 g AM with MBA crosslinker (0.1 mmol/100 g HEC) was added through the dropping funnel, and the temperature was raised to 70 °C to initiate the actual polymerization and was maintained until graft reaction has completed. On preparation of superabsorbent polymer composite (SAPC), the bentonite forms Na^+ monmorillonite ($\text{Al}_2\text{O}_3 \cdot 4\text{SiO}_2 \cdot \text{H}_2\text{O}$) with 90 meq/100 g cation exchange capacity, at 40 wt % loading was first dispersed in 40 mL distilled water and stirred continuously at 100 rpm, and then incorporated into dried HEC until slurry formation. Otherwise, the graft copolymerization was performed similarly as described above for producing SAP.

2.3. Purification of grafted copolymer

Crude product in gel form was cut into small pieces and subjected to Soxhlet extraction for 24 h using acetone, and 40% ethanol/water as the solvents, to remove the homopolymer (PAM), and unreacted AM. The percentage of grafting efficiency (GE%) was calculated using equation (1) [14–16].

$$\text{Grafting efficiency (\%)} = \frac{M_2 - M_0}{M_1 - M_0} \times 100 \quad (1)$$

where M_0 , M_1 and M_2 are the masses (in gram) of initial sample, grafted sample before extraction of homopolymer, and grafted sample after extraction of homopolymer, respectively.

2.4. Alkaline treatment

The resultant HEC-g-PAM copolymer with carboxamide form had poor water swelling capacity of approximately up to 30 g/g. To improve the swelling capacity of the SAPs, approximately 5 g of grafted copolymer was transferred into the round bottom reactor equipped with a mechanical stirrer, condenser and thermometer. Thereafter 100 mL of 2M NaOH solution was added for hydrolysis while stirring at 100 rpm, at various temperatures (50, 60, 70, 80 and 90 °C) and for an interval reaction time (30, 60, 90 and 120 min). The final concentration of purified grafted copolymer in NaOH solution was calculated as a percentage (w/w) of the total mass. All treated SAPs were then adjusted to pH near 7 by washing three times with distilled water, with the liquors tested for pH, and eventually the dried SAPs were tested for water swelling capacity.

2.5. Measurements

The tea bag was first tested for its swelling capacity and the dried powdery SAP sample of approximately 0.2–0.5 g in a tea bag was immersed in distilled water at room temperature, allowed to reach swelling equilibrium, and the final state was measured to determine the degree of water absorption (S_w) according to equation (2) [5].

$$S_w = \frac{W_2 - W_1}{W_1} \quad (2)$$

where W_1 and W_2 are the weights of the sample before and after water absorption.

All swelling capacity experiments were performed in triplicate and average values are reported.

2.6. Characterizations

Infrared transmission spectra were recorded using a Fourier transform infrared (FT-IR) spectrometer, model Bruker Tensor 27 from Bruker Corporation. The scan range was from 4400 to 400 cm^{-1} with the resolution better than 1 cm^{-1} (apodized), optionally better than 0.5 cm^{-1} . A sample of SAP was prepared by directly powdering with KBr and pelletizing.

2.7. X-ray diffraction

XRD patterns of bentonite clay, SAP and SAPC were determined using X-ray diffractometer (X' pert MPD, PHILIPS, Netherlands) with CuK α radiation source. The X-ray emitting tube was set at 40 kV operating voltage and 30 mA electric current. The sample was tested at room temperature with an angular range from 5° to 90° (2 θ) and scan speed of 3°/min.

2.8. Thermogravimetry (TGA)

Thermogravimetric analyses (TGA) were determined using the

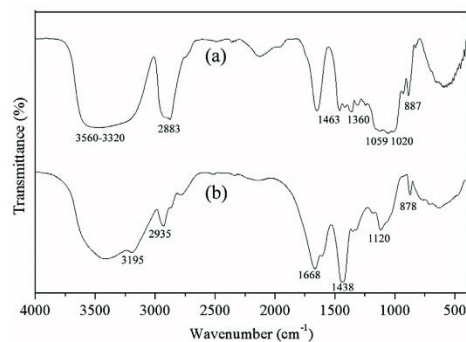


Fig. 1. FTIR spectra of (a) HEC and (b) HEC-g-PAM.

Simultaneous Thermal Analyzer (model STA8000, Perkin Elmer, United States of America) with a scanning rate of 10 °C/min under gas N_2 flowing at 20 mL/min in the temperature range from 30 to 800 °C.

2.9. Scanning electron microscope

Morphological properties of SAP, SAPC and the dispersion of bentonite clay particles in composites were characterized by scanning electron microscopy with energy dispersive X-ray spectroscopy (SEM, Quanta, FEI, the Netherlands).

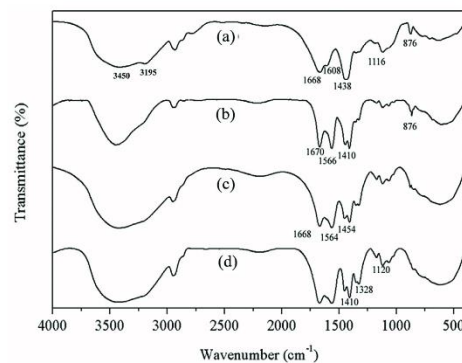


Fig. 3. FTIR spectra of (a) HEC-g-PAM and HEC-g-PAM after alkaline treatment were affected by wash cycles with distilled water: (b) washing 1, (c) washing 2, and (d) washing 3.

3. Results and discussion

3.1. Infrared spectroscopy

FT-IR analysis was used to confirm the grafting reaction of PAM onto HEC. Fig. 1 shows FT-IR spectra of pure HEC and HEC-g-PAM (SAP). It was found that the FT-IR spectrum of HEC showed a broad

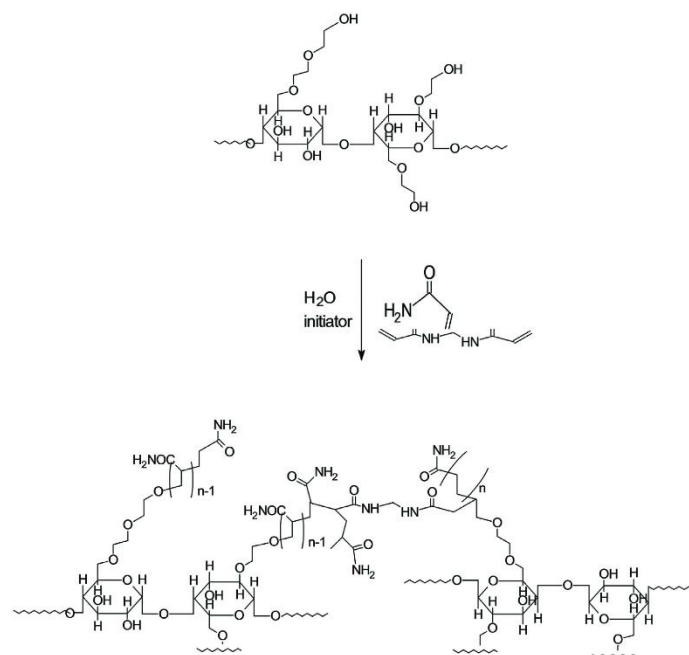


Fig. 2. Proposed grafting reaction between HEC and PAM.

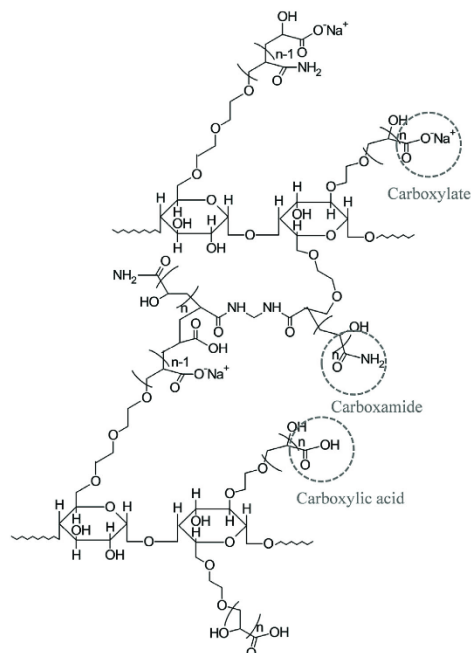


Fig. 4. HEC-g-PAM in carboxylate form after alkaline hydrolysis with 2M NaOH at 70 °C for 60 min and washing several times with distilled water.

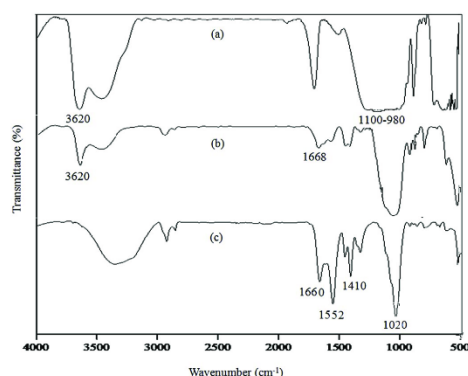


Fig. 5. FTIR spectra of (a) bentonite clay, (b) mixed SAP and bentonite clay and (c) SAPC after alkaline hydrolysis with 2M NaOH.

band at around 3560–3320 cm^{-1} , assigned to the stretching vibrations of $-\text{OH}$ groups of HEC, while the peak broadening was attributed to the presence of hydrogen bonding between them. The strong absorption peak at 2883 cm^{-1} was attributed to primary $-\text{OH}$ bending vibrations of HEC (Ethyl hydroxyl) [16], while the peaks at around 1020 cm^{-1} and 1059 cm^{-1} were assigned to $-\text{C}-\text{OH}$ stretching vibrations of HEC

[17–20]. After grafting with PAM (HEC-g-PAM), a shoulder at 3195 cm^{-1} was observed due to N-H stretching vibrations of PAM, in addition to the broad band around 3560–3320 cm^{-1} . The absorption bands around 1020 cm^{-1} , 1059 cm^{-1} and 2883 cm^{-1} had disappeared, and new absorption bands had emerged at 1668, 1438 and 1116 cm^{-1} ; these were assigned to $-\text{C}=\text{O}$ stretching vibrations of the carboxamide functional group, CH_2 bending vibrations in the added PAM moieties, and asymmetric stretching vibrations of C-O-C, respectively. The FT-IR results suggest that the graft copolymerization of PAM onto HEC backbone was successful. The proposed grafting reaction between HEC and PAM is shown in Fig. 2.

Fig. 3 shows FTIR spectra of HEC-g-PAM before and after alkaline treatment and washing with distilled water. For the HEC-g-PAM free from alkaline treatment (Fig. 3(a)), broad peak centered at 3450 cm^{-1} was assigned to $-\text{OH}$ stretching vibrations of HEC backbone. The peak shoulder at 3195 cm^{-1} was assigned to the $-\text{NH}$ stretching vibrations of amide (PAM) and the peak at 1668 cm^{-1} was assigned to $-\text{C}=\text{O}$ stretching vibrations of the carboxamide functional group. After alkaline treatment, the peak at 3450 cm^{-1} was found to be broadened, suggesting that hydrogen bonding and $-\text{C}-\text{OH}$ of carboxylic may be formed and the shoulder peak at 3195 cm^{-1} had almost disappeared. This suggests that the number of $-\text{OH}$ groups was increased while the number of $-\text{NH}$ was decreased. It is also found that the peak at 1668 cm^{-1} was split into double peaks, i.e., the peaks at 1670 cm^{-1} and 1566 cm^{-1} (Fig. 3 b, c and d). These two peaks are characteristic of $-\text{C}=\text{O}$ asymmetric and symmetric stretching vibrations of carboxylate groups, which are generally observed in the carboxylate form [21]. It is very interesting to note that the peaks corresponding to the vibrations of $-\text{OH}$ (3450 cm^{-1}) and carboxylate groups (1670 and 1556 cm^{-1}) were enhanced with increasing number of washing cycles.

Based on FT-IR analysis, it can be suggested that a partial form of amide was transformed to carboxylic acid and carboxylate forms, and the number of carboxylic acid form was relatively increased with increasing washing cycles. The form of HEC-g-PAM after alkaline treatment can be proposed as shown in Fig. 4.

Fig. 5 shows FTIR spectra of the superabsorbent polymer composite by introducing bentonite clay at 40%wt (Fig. 5(a)). The sharpened peak at around 3620 cm^{-1} was due to $-\text{OH}$ stretching vibrations in bentonite sheet together with a broad peak centered at 1020 cm^{-1} assigned to Si-O-Si stretching vibrations. There were no changes to FTIR peaks of bentonite clay after it had mechanical mixing with SAP as shown in Fig. 5(b), of the spectra of bentonite clay and SAP with different intensities. The FTIR spectrum of SAPC (Fig. 5 (c)) shows a broad peak at around 3560–3320 cm^{-1} corresponding to $-\text{OH}$ stretching vibrations in HEC, while the intense peak at 3620 cm^{-1} was changed. The stretching vibrations of Si-O-Si in bentonite sheet shows strongest and narrow peak at 1020 cm^{-1} , whereas the major peaks that evidenced C=O stretching vibrations of amide, carboxylate and carboxylic functional groups emerged around 1400–1680 cm^{-1} . It's interesting to note that the change of broad peaks at around 1100–980 cm^{-1} (Fig. 5(a)) to sharp peaks at 1020 cm^{-1} (Fig. 5(c)) was due to the exfoliation of bentonite sheets from transform of crystallinity into amorphous state [22].

3.2. X-ray diffraction

Fig. 6 Shows XRD patterns of (a) bentonite clay, (b) SAP and (c) SAPC. The characteristic bentonite XRD patterns with low intensity of the broad peak below 10° (Fig. 6(a)) indicates the semicrystalline forms of bentonite. The XRD patterns of SAP and SAP composite (Fig. 6 (b) and (c)) show identical characteristic peaks that indicate both were in amorphous state. The XRD patterns of SAP show higher relative intensity than those of SAP composite. This was due to more amorphous state formation when the bentonite clay had been introduced. It's well-known that the amorphous state increases the surface area, which in turn increases the water swelling capacity. The bentonite clay Na-MMT

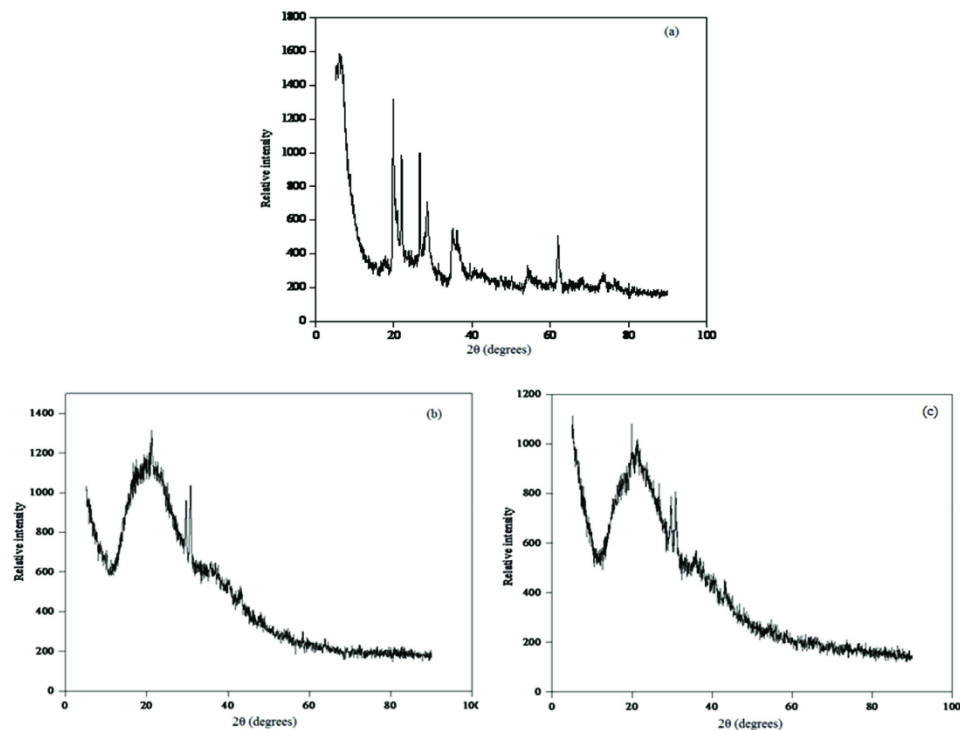


Fig. 6. XRD diffractograms of (a) bentonite clay, (b) SAP with HEC/AM (g/g) = 1/10, KPS = 1 g/(1.2 g HEC), [MBA] = 0.1 mmol/(100 g HEC), temperature = 70° C, (c) SAPC (40%wt bentonite clay).

is hydrophilic and expands the interlayer spaces readily when immersed in water, while at concentrations less than 10% it can be laminated into single layer which was exfoliated in the polymer matrix and converted to amorphous state.

3.3. Thermogravimetry (TGA)

The SAP and SAPC TGA curves show various stages of weight loss. The weight loss at temperatures around 50–300° C can be ascribed to moisture and HEC with hydroxyethyl sides moieties lost from the samples. The important stage of weight losses in temperature range of 400–450° C was ascribed to the thermal decomposition of acrylamide, acrylate and other side groups of copolymer and also MBA moieties in the polymer networks. After this stage both SAP and SAPC TGA curves show identical thermal decomposition, while at temperatures around 500–700° C SAPC TGA curves show improved thermal stability due to the presence of bentonite clay. The last stage of SAPC at temperatures around 700–800° C had slight weight loss from the breakage of copolymer chains [23].

3.4. SEM/EDX spectroscopy

Fig. 7 Shows morphological images of (a) SAP, and (b) SAPC with 40%wt of bentonite fillers. It can be seen that the fracture surfaces of SAPC show fine dispersion with regular shapes and sizes of particles in

the polymer. The EDX analysis was also executed to establish the dispersion of bentonite clay in SAPC (Fig. 7(c)). In the X-ray mapping of Si (Fig. 7(c), inset), the white spots over the darker background show the distribution of Si in the polymer matrix.

3.5. Effect of HEC/AM ratio on grafting and water swelling

Effect of HEC/AM ratio on grafting efficiency of AM onto HEC is shown in Fig. 8. It was found that the grafting efficiency increased with AM content. The highest grafting efficiency was obtained at 1/15 HEC/AM.

The effect of HEC/AM ratio on swelling capacity before and after alkaline treatment is shown in Fig. 9. The swelling capacity of SAP before alkaline treatment (hydrolysis) was not changed significantly by the HEC/AM ratio. When the SAP was treated with alkaline, the swelling capacity was found to increase significantly. The highest swelling capacity was observed at 1/10 HEC/AM ratio. Further increases in AM content decreased the water swelling capacity. The results indicate that the treatment process is important for SAP. The reason why the treated SAP has higher swelling capacity than the untreated SAP could be as follows. Before treating, the major components in the SAP were in the amide form (Fig. 3(b)). After treatment, a part of amides was changed to carboxylate salt and carboxylic acid (Fig. 3 b, c and d), and the dissociated alkaline carboxylate groups increased osmotic pressure in SAP and thus increased the swelling capacity, while the repulsive forces

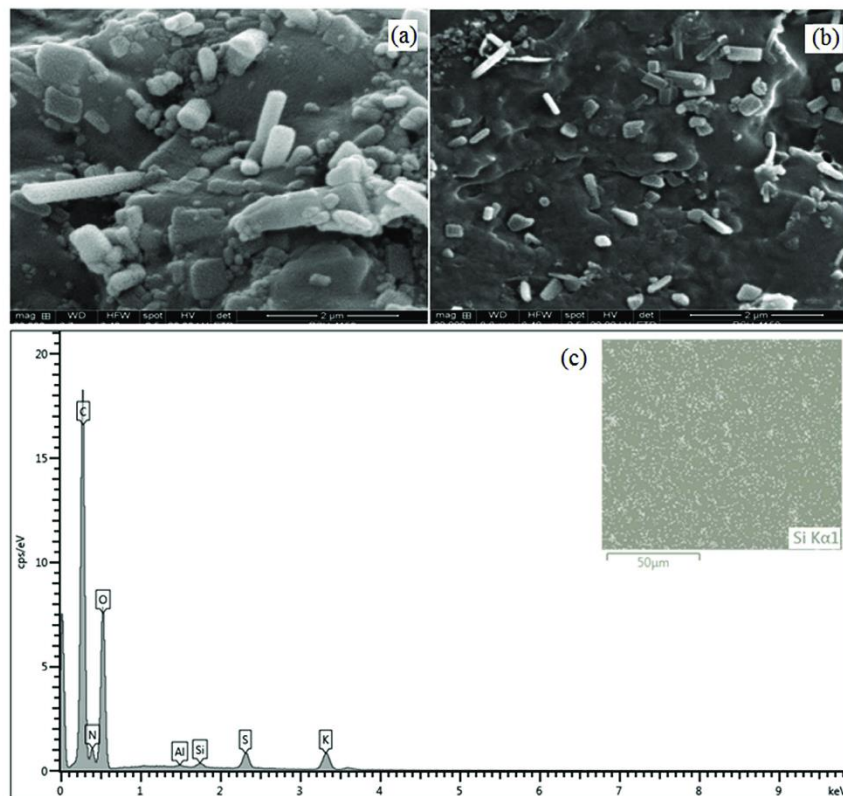


Fig. 7. SEM images of (a) SAP, (b) SACP (fracture images; magnification $\times 20000$; scale bar $2\ \mu\text{m}$) and (c) SEM/EDX of SACP with X-ray mapping of Si.

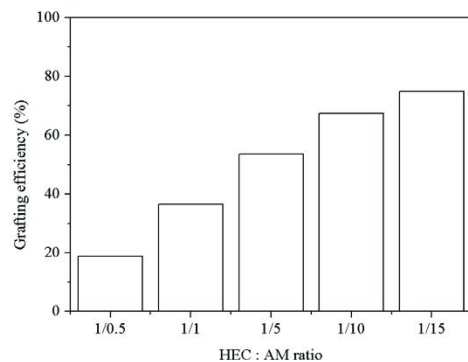


Fig. 8. Effect of HEC/AM ratios on grafting efficiency (%) of SAP, [KPS] = 1 g, [MBA] = 0.1 mmol/100 g HEC, temperature = 70°C , time 120 min, agitation speed 100 rpm.

between negative charges expanded the polymer coils.

3.6. Effect of initiator amount and crosslinker concentration on swelling capacity

Graft copolymerization of PAM onto HEC was carried out in aqueous solution using KPS as initiator. Effects of KPS amount were investigated in the range 0.5–2.5 g/(1.2 g HEC) and the results are shown in Fig. 9 (b). The highest water swelling capacity (about 426 g/g) was observed with 1 g of KPS, and it decreased to 69 g/g when KPS amount was at 2.5 g/1.2 g HEC. The results suggest that an optimal amount of the initiator for inducing the graft copolymer was 1 g of KPS. The decrease of water swelling capacity at higher levels of initiator was attributed to chain transfer decreasing grafting efficiency and chain length [24].

Fig. 9 (c) shows the effects of MBA dosage on the swelling capacity of SAP. It is seen that 0.1 mmol/(100 g HEC) of [MBA] provided the highest swelling capacity (426 g/g), with an overdose giving much poorer swelling. Since the MBA served as crosslinker, it increased the crosslinking, which later on decreased the network mesh size and ability of water swelling. The increase of network crosslink density also let to increase physical entanglements between polymer chains,

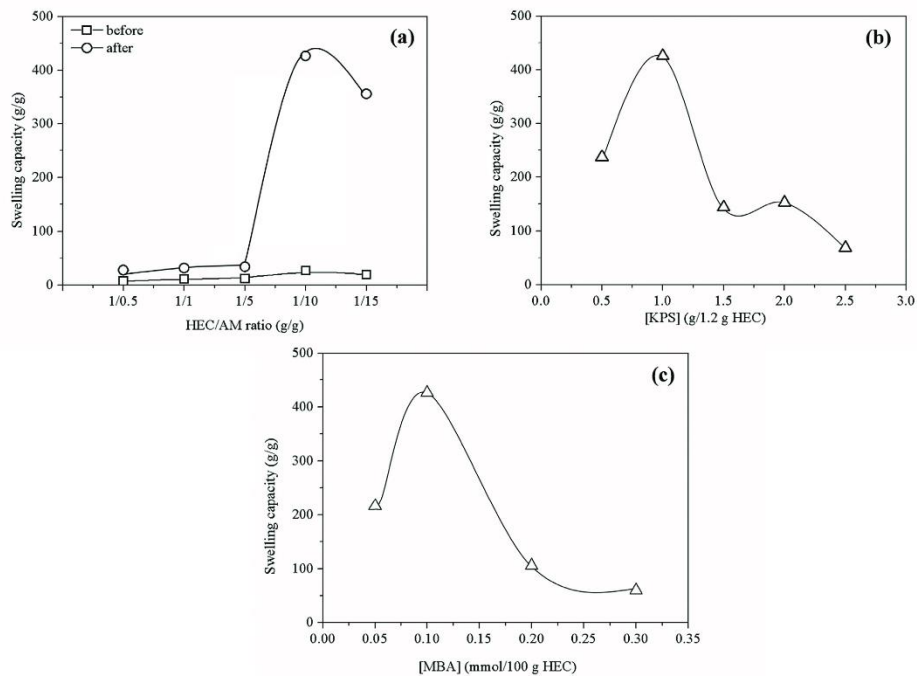


Fig. 9. Effects of (a) HEC/AM ratio on swelling capacity before and after hydrolysis by alkaline treatment. [2M NaOH], (b) KPS amount on swelling capacity and (c) MBA dose on swelling capacity of SAP.

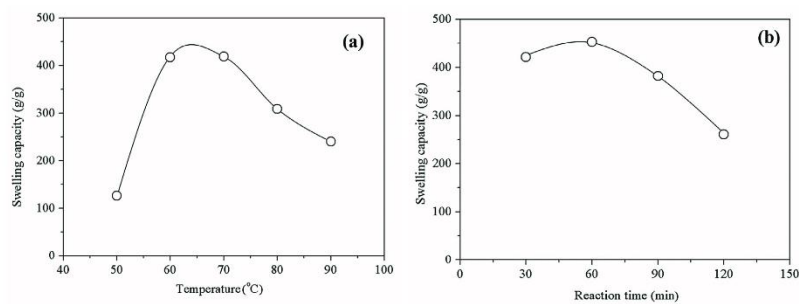


Fig. 10. The influence of (a) treatment temperature and (b) reaction time on water swelling of SAP.

decreasing the swelling property. Moreover, the higher crosslink between polymer concealed the process of ionization of carboxylate groups, leading to decrease the relaxation of polymer which was responsible for decreasing swelling property of hydrogel [25].

3.7. The influences of alkaline treatment temperature and time on swelling capacity of SAP

The resultant HEC-g-PAM copolymer with carboxamide had low water swelling capacity of approximately up to 30 g/g. To improve the swelling capacity of the SAP, approximately 5 g of grafted copolymer was treated with 100 mL of 2M NaOH solution. The swelling capacity of treated SAP obtained with the various treatment temperatures is

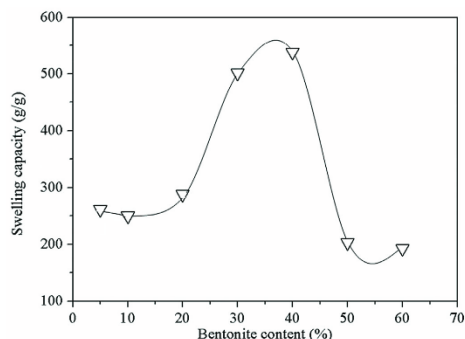


Fig. 11. The effects of bentonite clay loading on water swelling capacity. HEC/AM (g/g) = 1/10, KPS = 1 g/(1.2 g HEC), [MBA] = 0.1 mmol/(100 g HEC), temperature = 70 °C.

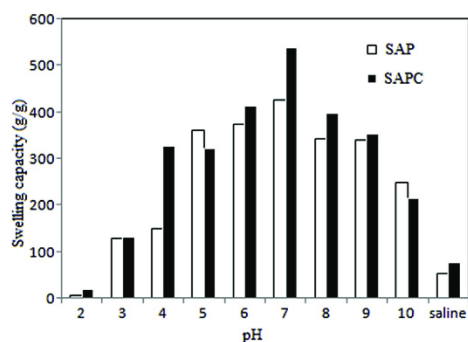


Fig. 12. Swelling capacities of SAP and SAPC after alkaline treatment and neutralization with distilled water, measured at various pH-values in saline solution.

displayed in Fig. 7. The highest water swelling capacity (426 g/g) was observed at 70 °C treatment temperature. The optimal reaction time for obtaining the highest swelling capacity was 60 min as shown in Fig. 10.

3.8. Effect of bentonite clay loading on swelling capacity

The effects of bentonite clay loading (10, 20, 30, 40, 50 and 60%) on water swelling properties of the SAP composites were investigated and the result is shown in Fig. 11. The degree of water absorption (S_w) was calculated using equation (2). The resultant SAP with highest water swelling capacity was then initiated to produce the super absorbent polymer composites (SAPCs). After it had alkaline treatment, 538 g/g water swelling capacity was observed at 40%wt clay loading, while the water swelling capacity decreased with further loading of the clay. The alkaline treatment formed sodium bentonite salt, which can enhance the water swelling capacity [9]. Several studies have disclosed that introduction of bentonite clay in a suitable amount in in-situ graft copolymerization of a monomer improves the water swelling capacity. The filler dispersion in a composite facilitates particle size expansion [26,27,28]. In addition, the incorporation of bentonite increases the strength of a superabsorbent polymer by formation of new ester bonds [29]. A dual crosslink hydrogel formed when clay nanosheets and Iron ion (Fe^{3+}) were incorporated, as first crosslinks formed by clay

acted interaction by hydrogen bonds with acrylamide and acrylic acid, while secondary crosslinks formed by ionic interactions between iron and carboxylate salt [30]. Self-healing and supertough polyacrylic hydrogel was formed when introducing dual crosslinks with graphene oxide- Fe^{3+} [31].

3.9. Influence of pH and saline solution on swelling capacity

The diffusion of water molecules into polymer matrix strongly affects the swelling behavior of SAP. The swelling capacities of SAP and SAPC at different pH values were later investigated also with saline solution (0.90% w/v of NaCl). It was found that the swelling capacities of all samples in saline solution were nearly 4 times smaller than in distilled water (Fig. 12), due to the counter ion effect of sodium ions on the polymer. With increased Na^+ concentration, these tended to condense around the fixed carboxylate ion charges. This decreased the repulsion between negative charges, and thus the swelling capacity decreased [32].

A report has revealed that water swelling capacity of SAPs is affected by environmental pH. So, the swelling capacity of the SAPs and SAPCs was investigated at various pH values ranging from 2 to 10 at ambient temperature. The results clearly show that pH influenced the swelling capacity of SAP and SAPC. Away from neutral pH 7 the swelling capacity dramatically decreased, down to nearly zero at pH below 2. This was due to the ions from HCl and NaOH decreasing the swelling capacity of SAPs. At low pH, the swelling capacity decreases as the carboxylate groups on the polymer network are protonated by HCl, leading the polymer to become hydrophobic. At high pH, the swelling capacity also decreases by “charge screening effect” of excess Na^+ in the solution, which shields the carboxylate anions and prevents effective anion-anion repulsion. At pH = 7, the electrostatic repulsion between COO^- groups enhances the swelling capacity [33,34].

4. Conclusions

This study aimed to synthesize a superabsorbent polymer and its filled composites, based on hydroxyethyl cellulose grafted with polyacrylamide and associated bentonite clay. The key observations can be summarized as follows.

1. Superabsorbent polymer and its filled composites were synthesized through graft copolymerization of polyacrylamide onto hydroxyethyl cellulose by solution polymerization under nitrogen atmosphere.
2. The highest water swelling capacities were achieved at the HEC/AM ratio 1/10, by using 1 g/(1.2 g HEC) of KPS initiator, 0.1 mmole/(100 g HEC) of MBA crosslinker, at the temperature of 70 °C and reaction time for 120 min.
3. Alkaline hydrolysis further converted the amide form into carboxylate salt by using 2M NaOH with mechanical stirring at 100 rpm. After washing with distilled water, the water swelling capacity up to 426 g/g was achieved, by treatment at 70 °C for 60 min.
4. The successful synthesis of HEC-g-PAM was confirmed by FTIR spectra on comparing absorption peaks of HEC and its grafted copolymer.
5. The bentonite clay filler in the SAPC composites gave the highest 538 g/g water swelling capacity at 40%wt loading level.
6. The XRD, TGA and SEM/EDX techniques were used to assess the composite and the dispersion of bentonite clay in it.

References

- [1] S. Kiatkamjornwong, Superabsorbent polymers and superabsorbent polymer composites, *Sci. Asia* 33 (2007) 39–43.
- [2] H. Wage, J. Bertling, Water-swellable Materials Application in Self-healing Systems, Noordwijk aan Zee, The Netherlands, The First International Conference on Self-

- healing Materials, vols 18–20, 2007, pp. 1–9. April.
- [3] F. Nnadi, C. Brave, Environmentally friendly superabsorbent polymers for water conservation in agriculture lands, *J. Soil Sci. Environ. Manage* 2 (7) (2011) 206–211.
- [4] M.R. Guillermea, et al., Synthesis of a novel superabsorbent hydrogel by copolymerization of acrylamide and cashew gum modified with glycidyl methacrylate, *Carbohydr. Polym.* 61 (2005) 464–471.
- [5] W. Wang, et al., Synthesis, swelling and responsive properties of a new composite hydrogel based on hydroxyethyl cellulose and medicinal stone, *Composites:Part B* 42 (2011) 809–818.
- [6] R.H. Todd, S.K. Daniel, Hydrogels in drug delivery, *Prog.Chall. Polym.* 49 (2008) 1993–2007.
- [7] R.L. Mikkelsen, Using hydrophilic polymers to control nutrient release, *Nutr. Cycl. Agroecosys* 38 (1) (1994) 53–59.
- [8] J. Akhter, et al., Effect of hydrogels amendment on water storage of sandy loam and loam soils and seedling growth of barley, wheat and chickpea, *Plant, Soil Environ.* 50 (10) (2004) 463–469.
- [9] C. Nakason, et al., Preparation of cassava starch-graft-polyacrylamide superabsorbents and associated composites by reactive blending, *Carbohydr. Polym.* 81 (2010) 348–357.
- [10] E.S. Abdul-Halim, Preparation and characterization of poly(acrylic acid)-hydroxyethyl cellulose graft copolymers, *Carbohydr. Polym.* 90 (2012) 930–936.
- [11] S.B. Lin, et al., Study of microstructure and properties of HEC-g-AA/SiO₂ organic-inorganic hybrid materials, *Compos. Interface* 11 (2004) 271–276.
- [12] J. Wang, et al., Effect of modified vermiculite on the synthesis and swelling behaviors of hydroxyethyl cellulose-g-Poly(acrylic acid)/vermiculite superabsorbent nanocomposites, *J. Polym. Res.* 18 (2011) 401–408.
- [13] R. Yang, Y. Wang, D. Zhou, Novel hydroxyethyl cellulose-graft-polyacrylamide copolymer for separation of double stranded DNA fragments by CE, *Electrophoresis* 28 (2007) 3223–3231.
- [14] P. Ghosh, B. Chattopadhyay, A.K. Sen, Modification of low density polyethylene (LDPE) by graft copolymerization with some acrylic monomers, *Polymers* 39 (1) (1998) 193–201.
- [15] S. Riyajan, P. Kaewittarit, A novel natural rubber-graft-cassava starch foam for oil/gasohol absorption, *Polym. Int.* 65 (2016) 491–502.
- [16] D. Pathania, R. Sharma, Synthesis and characterization of graft copolymers of methacrylic acid onto gelatinized potato starch using chronic acid initiator in the presence of air, *Adv. Mat. Lett.* 3 (2) (2012) 136–142.
- [17] N.H. Jagadish, B. Vishalakshi, Effect of crosslinking on swelling behaviour of IPN hydrogels of guar gum & polyacrylamide, *Der Pharma Chem.* 4 (3) (2012) 946–955.
- [18] F. Wu, et al., Synthesis and characterization of a novel cellulose-g-poly(acrylic acid-co-polyacrylamide) superabsorbent composite based on flax yarn waste, *Carbohydr. Polym.* 87 (4) (2012) 2519–2525.
- [19] J.A. Heredia-Guerrero, et al., Infrared spectroscopy as a tool to study plant cuticles, *Spectro. Asia* 12 (4) (2016) 8–11.
- [20] R.L. Oliveira, et al., Synthesis and characterization of methylcellulose produced from bacterial cellulose under heterogeneous condition, *J. Braz. Chem. Soc.* 26 (9) (2015) 1861–1870.
- [21] G. Solumons, C. Fryhle, S. Snyder, *Organic Chemistry*, eleventh ed., John Wiley & Sons Singapore Pte.Ltd, 2014, p. 779.
- [22] B. Tyagi, C.D. Chudasama, R.V. Jasra, Determination of structural modification in acid activated montmorillonite clay by FT-IR spectroscopy, *Spectrochim. Acta Part A* 64 (2006) 273–278.
- [23] R.C.F. Leite, et al., Novel superabsorbent hydrogel composite based on poly(acrylamide-co-polyacrylate)/montmorillonite: characterization and swelling performance, *Quim. Nova* 38 (3) (2015) 1–17.
- [24] W.F. Su, Radical Chain Polymerization, in: W.F. Su (Ed.), vol. 82, Springer-Verlag Berlin Heidelberg, Berlin, 2013, pp. 137–183.
- [25] S. Shah, N.M. Ranjha, Z. Javaid, Development and evaluation of pH-dependent interpenetrating network of acrylic acid/polyvinyl alcohol, *Iran. Polym. J.* 22 (11) (2013) 811–820.
- [26] Y. Xie, et al., Synthesis and characterization of poly(sodium acrylate)/bentonite superabsorbent composite, *J.Physic:Conference Ser.* 339 (2012008) (2011) 1–4.
- [27] J. Zhang, A. Wang, Study on superabsorbent composites. IX: synthesis, characterization and swelling behaviors of polyacrylamide/clay composites based on various clays, *React. Funct. Polym.* 67 (8) (2007) 737–745.
- [28] H.A. Kalaleh, M. Tally, Y. Atassi, Preparation of a clay based superabsorbent polymer composite of copolymer poly (acrylate-co-acrylamide) with bentonite via microwave radiation, *Res. Rev. Polym.* 4 (4) (2013) 145–150.
- [29] H. Hosseinzadeh, M. Saadeghzadeh, M. Babazadeh, Preparation and properties of carrageenan-g-poly(acrylic acid)/bentonite superabsorbent composite, *J. Biomater. Nanotechnol* 2 (2011) 311–317.
- [30] Y. Hu, Z. Du, X. Deng, T. Wang, Z. Yang, W. Zhou, C. Wang, Dual physically cross-linked hydrogels with high stretchability, toughness, and good self recoverability, *Macromolecules* 49 (15) (2016) 5660–5668.
- [31] L. Zhao, J. Huang, T. Wang, W. Sun, Z. Tong, Multiple shape memory, self-healable, and supertough PAA-GO-Fe₃O₄ hydrogel, *Macromol. Mat. Eng.* (2016) 1–9.
- [32] S. Nesrin, A. Djamel, Synthesis, characterization and rheological behavior of pH sensitive poly(acrylamide-co-acrylic acid) hydrogels, *Arab. J. Chem.* 10 (2017) 539–547.
- [33] Y. Su, et al., Synthesis and swelling behaviors of wheat straw cellulose-g-poly (potassium acrylate)/PDMDAAC amphoteric semi-IPNs superabsorbent resin, *Adv. Mat. Res.* 750–752 (2013) 1415–1419.
- [34] F. Wu, et al., Synthesis and characterization of a novel cellulose-g-poly(acrylic acid-co-acrylamide) superabsorbent composite based on flax yarn waste, *Carbohydr. Polym.* 87 (2012) 2519–2525.

Appendix B: Article 2

Water-swellaable rubber blend from epoxidized natural rubber and superabsorbent polymer composite

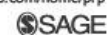


Progress in Rubber,
Plastics and Recycling
Technology

Article

Water-swellaable rubber blend from epoxidized natural rubber and superabsorbent polymer composite

Progress in Rubber Plastics and Recycling Technology
1–15
© The Author(s) 2019
Article reuse guidelines:
sagepub.com/journals-permissions
DOI: 10.1177/1477760619895025
journals.sagepub.com/home/prp



Ajaman Adair¹ , Azizon Kaesaman¹
and Pairote Klinpituksa²

Abstract

Epoxidized natural rubber (ENR) and a superabsorbent polymer composite (SAPC) along with other minor components were mechanically blended in an internal mixer (Brabender Plasticorder) at 40°C and 60 r/min rotor speed with 80% fill factor. The SAPC was synthesized by grafting polyacrylamide onto hydroxyethyl cellulose backbones and adding bentonite clay. The first water-swelling behavior was investigated with alternative epoxidation levels of the ENR. Water-swellaable rubber (WSR) performed well in terms of water absorbency, and weight loss was achieved with 50 mole% epoxidation level, so this ENR was chosen for the rubber matrix from which WSR was prepared with various contents of SAPC (0, 5, 10, 15, and 20 phr). The results indicated that SAPC loading positively affected water absorbency, which was resulted by increasing weight loss and loss of mechanical properties, such as tensile strength and elongation at break. However, the modulus increased with SAPC content. WSR formulated from ENR-50, SAPC, and other ingredients resulting in good water-swelling behaviors and modulus, while the tensile strength and elongation at break had opposition. SAPC was an important factor to control the overall WSR properties.

Keywords

Water-swellaable rubber, epoxidized natural rubber, superabsorbent polymer composite, graft copolymerization

Received 28 April 2019; accepted 20 September 2019

¹ Department of Rubber Technology and Polymer Science, Faculty of Science and Technology, Prince of Songkla University, Pattani, Thailand

² Department of Science, Faculty of Science and Technology, Prince of Songkla University, Pattani, Thailand

Corresponding author:

Ajaman Adair, Department of Rubber Technology and Polymer Science, Faculty of Science and Technology, Prince of Songkla University, Pattani 94000, Thailand.
Email: nadair1969@gmail.com

Introduction

Natural rubber is a hydrophobic material with almost no swelling in water, and its surface is not wettable with water unless functional chemical modifications are done. A new functional material named water-swallowable rubber (WSR) is composed mainly of elastomer with added hydrophilic polymer.¹ The WSRs possess not only the general rubber properties, such as high elasticity, resilience, and high toughness, but can also absorb large quantities of water. Their volumetric expansion can be up to 1.5-fold in water (or in other fluids). They have been applied in underground engineering as caulking, sealing, and leakage-stopping materials.² WSRs are generally manufactured by one of the two methods, namely by grafting hydrophilic monomers on rubber backbone or by mechanical blending of a rubber matrix with a superabsorbent polymer to form a composite. The latter is the most promising way due to ease of production, desirable product properties, and low cost.

Therefore, multicomponent polymer blends received attention from both academic technologists and manufacturers producing WSR, and excellent water absorption and mechanical properties have been achieved. Various rubbers have been used as the elastomeric material on producing WSR by mechanical blending with various types of superabsorbent polymers/composites (SAPs/SAPCs), such as natural rubber,^{3–6} epoxidized natural rubber (ENR), maleated natural rubber,⁷ chloroprene rubber,^{8,9} epichlorohydrin rubber,^{10–12} and synthetic chlorinated polyethylene rubber.¹³ Further components have been incorporated to modify the final properties of WSR composites. The typical SAP in WSR composites used to be synthetic polyacrylate, the cost of which depends strongly on petroleum products. Despite no definitely known threat to human health, the waste disposal of these composites is problematic due to a wide range of environmental pollutants.^{14,15} Biodegradable SAPCs derived from natural polymers have been used in several research studies to produce WSR, for example, cassava starch grafted with polyacrylamide (PAM) and combined with bentonite clay.⁷ Sodium salt of polyethylene glycol was blended with chlorinated polyethylene to form a water-swallowable elastomer (WSE) that gave higher swelling capacities and faster swelling rates than WSE prepared by grafting polyethylene glycol onto chlorinated polyethylene.¹⁶ However, there are no prior reports about WSR prepared with the SAPC from hydroxyethyl cellulose grafted PAM (HEC-g-PAM)/bentonite dispersed in a rubber matrix. Thus, the current study focused on using this SAPC dispersed as the water-absorbing polymer in ENR, with an expectation of good water swelling behavior and mechanical properties.

In this work, the WSRs were prepared by mechanical blending of ENR with an SAPC using an internal mixer (Brabender Plasticorder). The SAPC was synthesized by graft copolymerization of PAM onto HEC backbones, with also bentonite clay in the composite. First, producing the WSR was tested using ENR-25 and ENR-50 as alternatives for the matrix, with fixed contents of SAPC and other ingredients, and the first water absorbency and weight loss were assessed. High water absorbency and low weight loss were targeted, so ENR-50 was selected to make WSR with various contents of SAPC. The influences of SAPC content on swelling behavior, such as first water absorbency, weight loss, and second water absorbency, on mechanical properties, and on morphology of the blends were further investigated.

Experimental methods

Materials

ENR (ENR-25 and ENR-50, with 25% and 50% mole epoxide contents) was manufactured by Muang Mai Guthrie Public Co., Ltd (Surathani, Thailand); HEC (analytical reagent (AR) grade)

was purchased from Merck KGaA Corporate (Frankfurter Strasse, Germany); bentonite clay was manufactured by Sigma-Aldrich (St Louis, Missouri, USA); acrylamide (AM) of 99% purity used for synthesis was supplied by Merck K GaA Corporate (Frankfurter Strasse, Germany); potassium persulfate (KPS) with 99% purity manufactured by Ajax FineChem was used as initiator; *N, N'*-methylenebisacrylamide (MBA) and sodium hydroxide (NaOH, AR grade) purchased from Fluka (Buch SG, Switzerland) were used as a cross-linker and in alkaline hydrolysis treatment, respectively; zinc oxide (ZnO), white seal activator, lab grade, was purchased from Metoxide Thailand Co., Ltd (Pathumthani, Thailand); stearic acid activator, lab grade, was purchased from Imperial Industry Chemical Co., Ltd (Pathumthani, Thailand); *N*-tert-butyl-2-benzothiazyl sulfenamide (TBBS) accelerator, chemical grade, was purchased from Flexsys America L.P. (Reliance Technochem Co., Ltd, Bangkok, Thailand); and sulfur, vulcanizing agent for NR, lab grade, was obtained from Ajax Chemical Co., Ltd (Auckland, New Zealand).

Preparation of SAPC

The SAPC was prepared first by dispersing 40%wt% bentonite clay in distilled water and then by mixing with 1.2 g HEC until gel formation; 0.3 mol/100 g HEC of KPS and 12 g AM with MBA 0.1 mmol/100 g HEC solution were reacted in a four-necked reactor under nitrogen atmosphere at a rotor speed of 100 r/min, 70°C, and 120 min. The crude SAPC in gel form was purified by multistep Soxhlet extraction to finally obtain SAPC, which was further treated with 2 M NaOH solution while stirring at 100 r/min and 60°C for an hour. The procedure was as described by Adair et al.¹⁷ The SAPC with 538 g/g water absorbency was used to prepare WSR by means of mechanical blending with the ENR matrix.

Preparation of WSR

The experiments were performed at ambient temperature using an internal mixer (Brabender Plasticorder) with chamber temperature controlled to 40°C. Two grades of ENR, namely with 25 mole% epoxide groups (ENR-25) and with 50 mole% of epoxide groups (ENR-50), were tested as the rubber matrix by dispersing 10 phr SAPC with ZnO 6 phr, stearic acid 0.5 phr, TBBS 1 phr, and sulfur 2 phr. The obtained WSRs were investigated for water-swelling behavior, specifically water absorbency and weight loss. High water absorbency and low weight loss are desirable, so these were the criteria to select the better ENR matrix. With this matrix, the influence of SAPC content on water-swelling behavior and mechanical properties was tested. The total mixing time was 14 min with the procedure described in Nakason et al.,⁷ and the blend proportions are given in Table 1.

Swelling measurements

Swelling measurements including water absorbency and weight loss were performed in triplicate, and average values are reported. About 300 mg samples of the dried sheets were cut, weighed accurately, and soaked in distilled water at ambient temperature (around 28–30°C). At regular intervals, the swollen sample was taken out from the distilled water, superficial moisture was carefully removed using blotting paper, and the weight of the sample was measured immediately and the sample was placed back in the same bath. After the swelling test completed, the samples

Table I. Formulations of WSR with varying SAPC loadings.

Ingredients	Quantity (phr)
ENR-50	100
SAPC	0, 5, 10, 15, 20
ZnO	6
Stearic acid	0.5
TBBS	1
Sulfur	2

WSR: water-swellaible rubber; SAPC: superabsorbent polymer composite; ENR: epoxidized natural rubber; TBBS: *N*-tert-butyl-2-benzothiazyl sulfenamide; ZnO: zinc oxide.

were dried at 50°C until constant weight. The first and second water-swelling ratio by mass (S_w) and the first percentage of weight loss (L_w) were calculated using equations (1) and (2)^{9,12}:

$$S_w = \frac{w_2 - w_1}{w_1} \times 100 \quad (1)$$

$$L_w = \frac{w_1 - w_3}{w_1} \times 100 \quad (2)$$

where w_1 and w_2 are the weights of the sample before and after the water absorption, respectively, and w_3 is the dried weight of a sample after water absorption.

Tensile properties

Tensile properties in terms of tensile strength, elongation at break, and modulus were tested at room temperature, according to ASTM D412 using a universal tensile testing machine (Hounsfield Tensometer, model H 10KS, Hounsfield Test Equipment Co., Surrey, UK). The dumbbell-shaped specimens were first die cut from the vulcanized rubber sheets with ASTM die type C. Furthermore, the hardness was tested using a durometer, Shore A (Frank GmbH, Hamburg, Germany), according to ASTM D2240.

Determination of the cross-link density

For cross-link density estimation, the equilibrium swelling was first determined by immersion of WSR sample in toluene for 7 days in the dark. The swollen WSR was then removed and weighed immediately. The weights of absorbed toluene and remaining rubber were determined by evaporating the toluene off in a hot air oven at 70°C. The cross-link density of WSR was calculated using the Flory–Rehner equation (3)^{18,19}:

$$\frac{-[\ln(1 - v_p) + v_p + \chi v_p^2]}{n v_0 \left[v_p^{1/2} - \frac{v_p}{2} \right]} \quad (3)$$

$$v_p = \frac{1}{1 + Q}$$

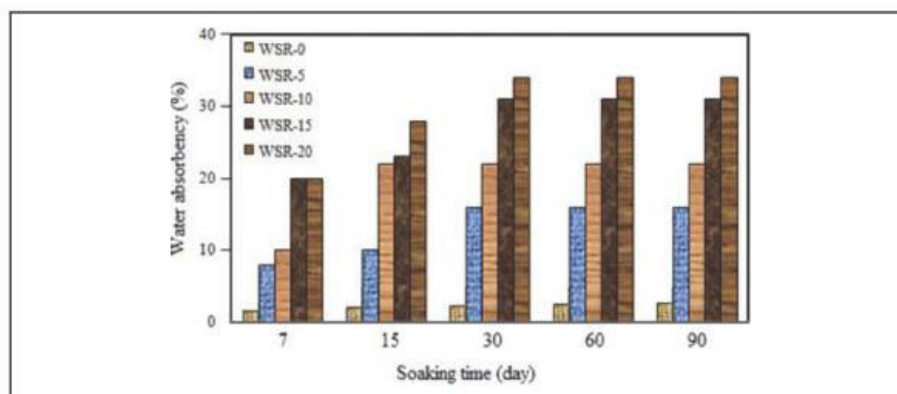


Figure 1. Time profiles of first water absorbency for WSRs with various SAPC loadings. WSR: water-swollable rubber; SAPC: superabsorbent polymer composite.

where n is cross-link density, v_p is volume fraction of rubber in the swollen polymer, χ is Huggins rubber–solvent interaction constant (0.41 for ENR), D_p is density of rubber (1.09 g/cm^3), V_0 is molar volume of toluene ($1.069 \times 10^{-4} \text{ m}^3/\text{mol}$ at 25°C), and D_0 is density of toluene (0.8623 g/cm^3 at 25°C).

Cure characterization

A rotorless rheometer (Rheo Tech MD+, Tech Pro, Inc., Cuyahoya Falls, Ohio, USA) was used to determine the curing characteristics of the rubber composites at 160°C with 1° arc amplitude over 60 min testing. The optimum cure time (t_{c90}) and scorch time (t_{s1}), the minimum and maximum torques (M_L and M_H , respectively), and δ torque ($M_H - M_L$) were determined from the curing curves. Cure rate index (CRI) was measured based on ASTM D5289 and calculated as shown in equation (4)^{20,21}:

$$\text{CRI} = \frac{100}{t_{c90} - t_{s1}} \quad (4)$$

where t_{s1} is the time a unit increase in torque takes from the M_L , and t_{c90} is the time at which 90% cure is achieved.

Morphological properties

Morphological properties of the WSRs were characterized using a scanning electron microscope (SEM) equipped with energy-dispersive X-ray (EDX) spectroscopy (Quanta, FEI, the Netherlands).

Results and discussion

Swelling properties of WSR

Figure 1 shows the water-swelling capacity of WSR with tested SAPC contents at various soaking times. It is generally seen that the water swelling of WSR increased with soaking time of up to 30

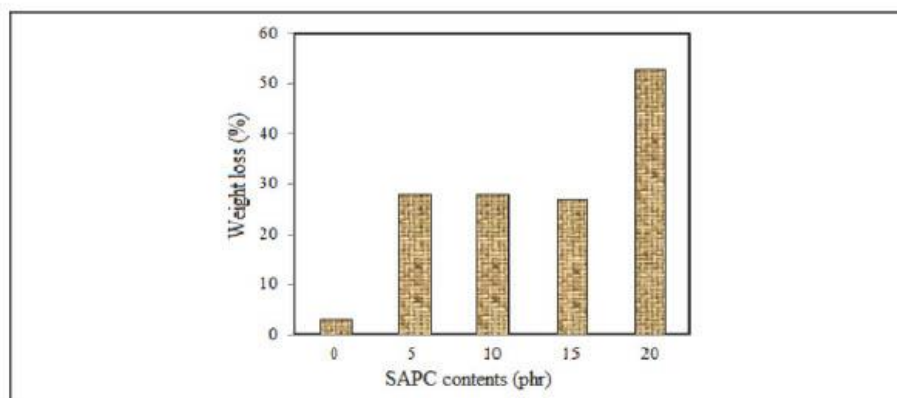


Figure 2. The weight loss (%) during first water immersion of WSR prepared from ENR-50 with various loadings of SAPC.

WSR: water-swellable rubber; SAPC: superabsorbent polymer composite; ENR: epoxidized natural rubber.

days and then tended to level off. It is also seen that the water absorbency of WSR increased with the content of water-absorbent polymer composite (SAPC) in the composites. This was attributed both to the decrease of cross-linked density and to the increase of active sites for water absorption. Similar dependence of water absorbency on SAP/SAPC content has been reported earlier.^{2,8,22} Thus, the SAPC content plays an important role in the water absorbency of the WSR, as expected.

Figure 2 shows the weight loss of WSR with various SAPC loadings at 30 days of soaking. The weight loss prone to increase with SAPC loading, being highest for the case with maximal 20 phr SAPC in WSR. The results match well with the water absorbencies of the WSR samples.

Tensile properties

The moduli at 100% and 300% strains for the WSR filled with various SAPC contents were shown in Figure 3. Both moduli slightly increased with SAPC content, indicating stiffness increase with the addition of SAPC. Generally, for a composite, the modulus at low strains depends on various factors, such as interatomic bonding strength or the nature of bonds and the binding energy. Usually, materials with greater bonding strength exhibit higher stiffness.

Figure 4 shows the effects of SAPC addition on tensile strength and elongation at break of the WSR. SAPC decreased both tensile strength and elongation at break, which could be explained as follows. SAPC reduced cross-linked density (Figure 5) and the SAPC phases in WSR matrix acted as stress concentration points that caused easier/earlier failure with SAPC added.

Cross-link density

Effects of SAPC addition on the cross-link density in WSR are based on estimates from the Flory–Rehner equation. Figure 5 shows the effects of SAPC content on the cross-link density of WSR. It is very interesting that the cross-link density of WSR decreased with the addition of SAPC. As can be seen in Figure 5, the cross-link density decreased sharply when 5 phr SAPC was added, while

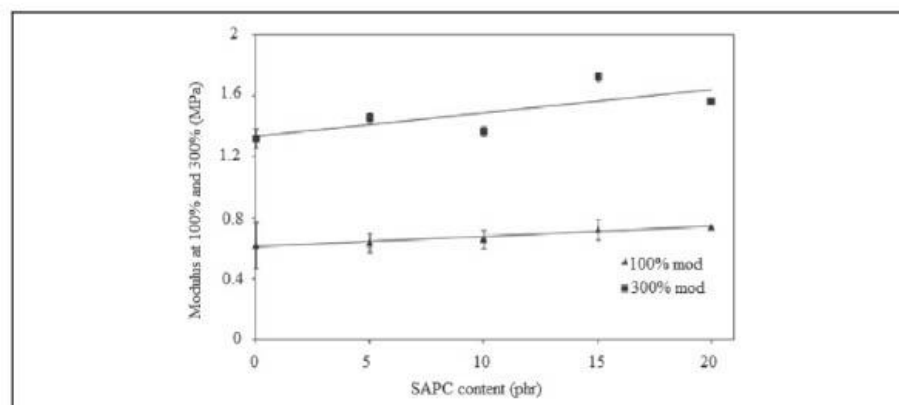


Figure 3. The moduli at 100% and 300% strains for the WSR with various SAPC contents. WSR: water-swellaable rubber; SAPC: superabsorbent polymer composite.

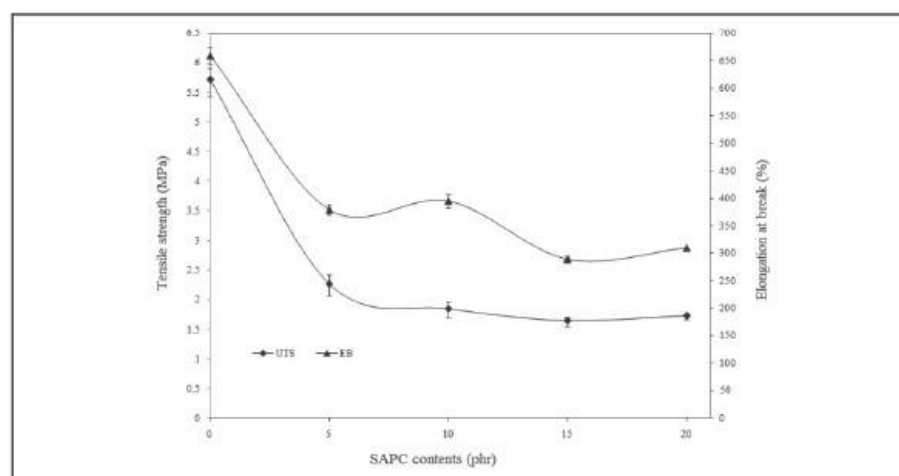


Figure 4. Tensile strength and elongation at break for the WSR with various SAPC contents. WSR: water-swellaable rubber; SAPC: superabsorbent polymer composite.

further addition had no significant effect. In other words, SAPC hindered cross-linking, but this effect saturated quickly.

The mechanism by which SAPC hindered cross-linking may relate to the sulfur vulcanization system. It is well known that in sulfur curing, there are at least five steps involved, and in the first step, the accelerator reacted with ZnO forming Zn^{2+} -accelerator complex, while in the second step, sulfur reacted with the Zn^{2+} -accelerator complex forming an intermediate sulfur- Zn^{2+} -accelerator or

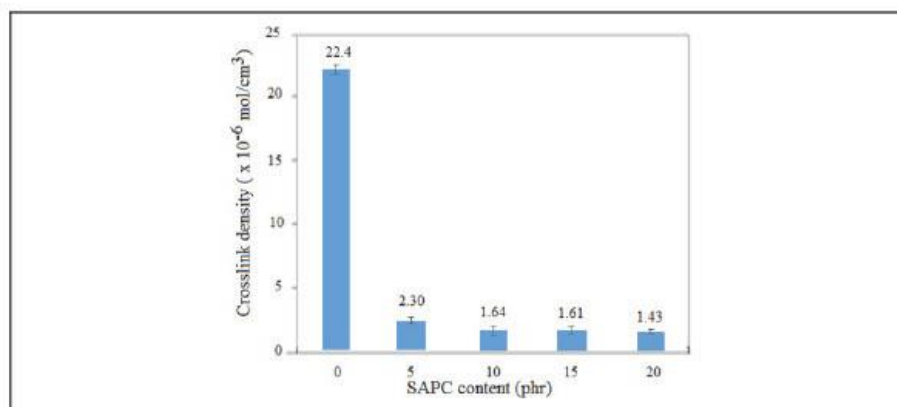


Figure 5. Cross-link density of WSR with various SAPC contents. WSR: water-swellable rubber; SAPC: superabsorbent polymer composite.

polysulfidic accelerator.²³ This is important because the complex containing Zn^{2+} could have ligands, especially in the presence of amine or carboxylate ions. In fact, the SAPC, used as a dispersed hydrophilic polymer phase in the blend, was based on copolymers HEC and PAM. The final structure of the grafted copolymer was probably enclosed by multifunctional groups, such as carboxylic acid, carboxylate, and amide forms, as shown in Figure 6.

The complexation of Zn^{2+} complex and SAPC forms comparatively large-sized complexes. In the third to fifth steps of vulcanization, the intermediate sulfur- Zn^{2+} -accelerator or polysulfidic accelerator that formed rubber-sulfur-accelerator groups then further formed rubber-sulfur-rubber groups, and in the final stage, these formed a network of rubber chains. This process probably had steric effects from increase in size of the complexes, when the Zn^{2+} as a ligand bonded with specific functional groups of SAPC. This obstructed diffusion of the complex into rubber and hindered network formation, thus decreasing the cross-link density. Similar behavior has been found when natural rubber was blended with ENR and montmorillonite modified with quaternary ammonium,²⁴ and the cross-link density of rubber compound based on natural rubber reinforced with octadecylamine-modified bentonite also decreased relative to natural rubber reinforced with organoclay.¹⁸

FTIR determination

The characterization of the blends' compatibility was using Fourier transform infrared (FTIR) determination. In Figure 7, the FTIR spectra of ENR-50 (Figure 7(a)) indicated that the predominant absorption peak at 3037 cm^{-1} (weak) was assigned to stretching vibration of Csp^2-H , the strong to medium peaks at 2962 , 2924 , and 2859 cm^{-1} were attributed to Csp^3-H stretching vibration, and the weak peak at 1664 cm^{-1} ($C=C$ stretching), 1449 cm^{-1} ($-CH_2-$ deformation), and 1378 cm^{-1} (methyl $C-H$ deformation). In addition, the epoxide in molecule was confirmed by the medium intensity of peak at 878 cm^{-1} , while the peak with weak intensity at 837 cm^{-1} was due to $C=C-H$ bending vibration of natural rubber.²⁵ The FTIR spectra (Figure 7(b)) represented

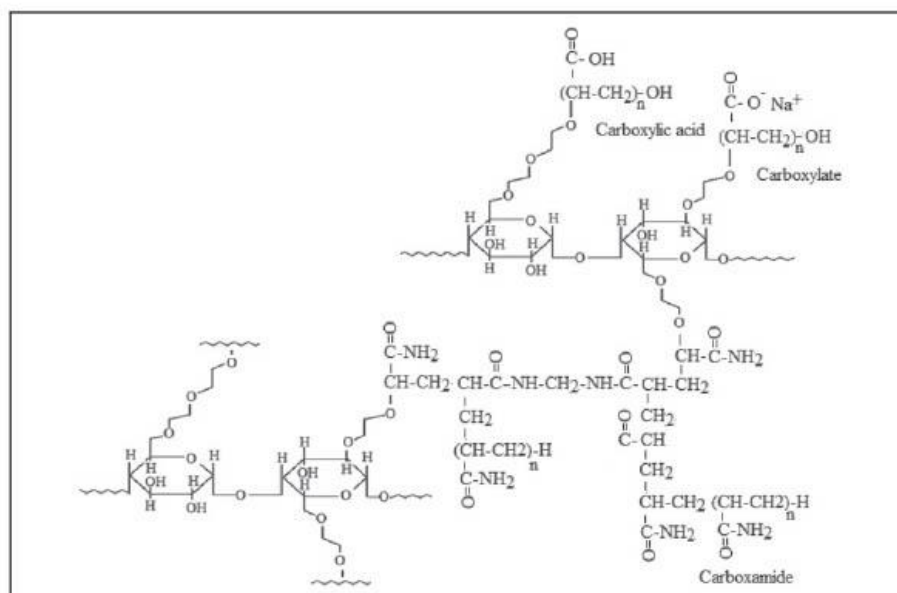


Figure 6. Proposed structure of SAPC that includes multifunctional groups (modified from Adair et al.).¹⁷ SAPC: superabsorbent polymer composite.

before water absorption of WSR and (Figure 7(c)) represented absorption band of WSR after water absorption of 30 days. Moreover, the FTIR peak around $1700\text{--}1550\text{ cm}^{-1}$ clearly indicated that SAPC contained carbonyl groups containing, probably assortments of amide, carboxylic acid, and carboxylate salt. After having water immersion, there was slightly increased intensity of FTIR peak at 1064 cm^{-1} , which was assigned to C–O stretching vibration of ether. This exactly means epoxide ring has been broken and has altered into C–O–C. This phenomenon was supported well with the altering peak of epoxide at 875 cm^{-1} .

Cure characteristics

Figure 8 showed the time profile of torque of WSR with and without SAPC using oscillating disk rheometer (ODR). It demonstrated that the SAPC content was affected by the increasing torque due to the increased stiffness by the formation of cross-links. The incremental torque values clearly evidenced that the processing of rubber compounds characterized by higher contents of SAPC filler became harder and the cross-link structures between ENR-50 and SAPC hindered its blending. The cure characteristics, such as t_{s1} , t_{c90} , CRI, M_L , M_H , and torque difference ($M_H - M_L$), are summarized in Table 2.

In the scorch region, it was found that all WSRs filled with SAPC exhibited higher minimum torque than the WSR without SAPC. This is due to the interatomic bonding of rubber and SAPC phases that increased viscosity of uncured WSR. In the curing region, the CRI was retarded by the added SAPC. This is attributed to the acid characteristics of SAPC as it contains various hydroxyl

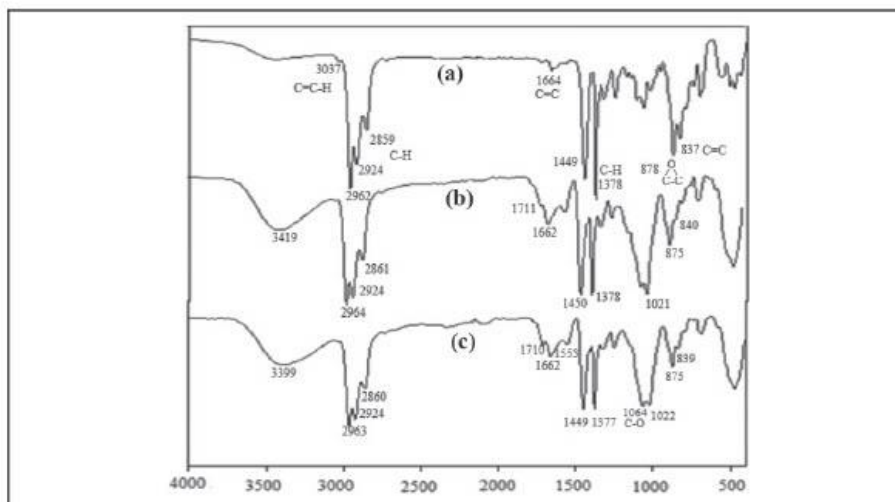


Figure 7. Indicates FTIR spectra of (a) ENR-50, (b) WSR before water absorption, and (c) WSR after water absorption, WSR prepared by blending ENR-50 and SAPC loading 15 phr, ZnO 6 phr, stearic acid 0.5 phr, TBBS 1 phr, and sulfur 2 phr.

WSR: water-swellable rubber; SAPC: superabsorbent polymer composite; ENR: epoxidized natural rubber; TBBS: *N*-tert-butyl-2-benzothiazyl sulfonamide; FTIR: Fourier transform infrared.

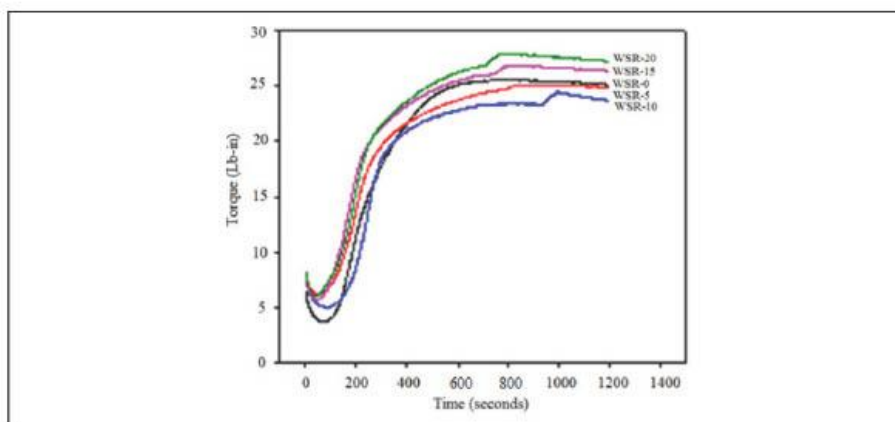


Figure 8. Cure curves for WSR with various contents of SAPC.

WSR: water-swellable rubber; SAPC: superabsorbent polymer composite.

groups ($-OH$) from indigenous HEC and amides when treated with alkaline base transformed into acid functional groups in the molecules. Thus, the rate of vulcanization was retarded.²² After curing region, the ODR curves of WSR with 15 and 20 phr SAPC showed higher moduli than

Table 2. Cure characteristics (t_{s1} , t_{c90} , CRI, M_L , M_H , and $M_H - M_L$) of WSR with and without SAPC.

Case	t_{s1}	t_{c90}	CRI	M_L	M_H	$M_H - M_L$
WSR-0	2.03	7.46	18.41	3.64	25.39	21.75
WSR-5	1.47	8.54	14.14	6.21	25.12	18.91
WSR-10	1.55	8.41	14.57	5.01	23.81	18.80
WSR-15	1.29	8.37	14.12	5.73	26.91	21.18
WSR-20	1.22	9.04	12.78	5.98	27.92	21.94

WSR: water-swellable rubber; SAPC: superabsorbent polymer composite; CRI: cure rate index.

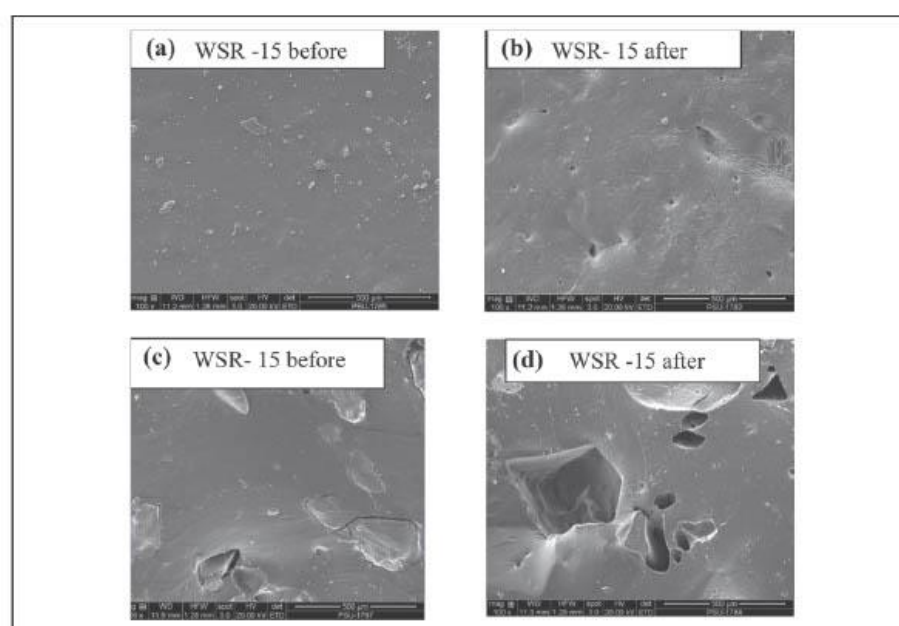


Figure 9. SEM micrographs of WSR with 15 phr SAPC: (a and b) surface and (c and d) cross section before and after immersion in water (fracture images; magnification $\times 20,000$; scale bar 500 μm).

WSR: water-swellable rubber; SAPC: superabsorbent polymer composite; SEM: scanning electron microscope.

unfilled WSR. On the other hand, the torques of WSR-5 and WSR-10 showed lower value of modulus than that without SAPC. With increased addition of SAPC, it was found that the t_{s1} , t_{c90} , M_L , and M_H were independent from further addition of SAPC. It is interesting to note that the cure characteristics obtained from ODR did not correlate with the cross-link density from the swelling test. The reason was that the swelling test probably confined solely in the cross-link occurred in rubber phase, which was different for ODR that generally mentioned to overall systems of cross-linking.

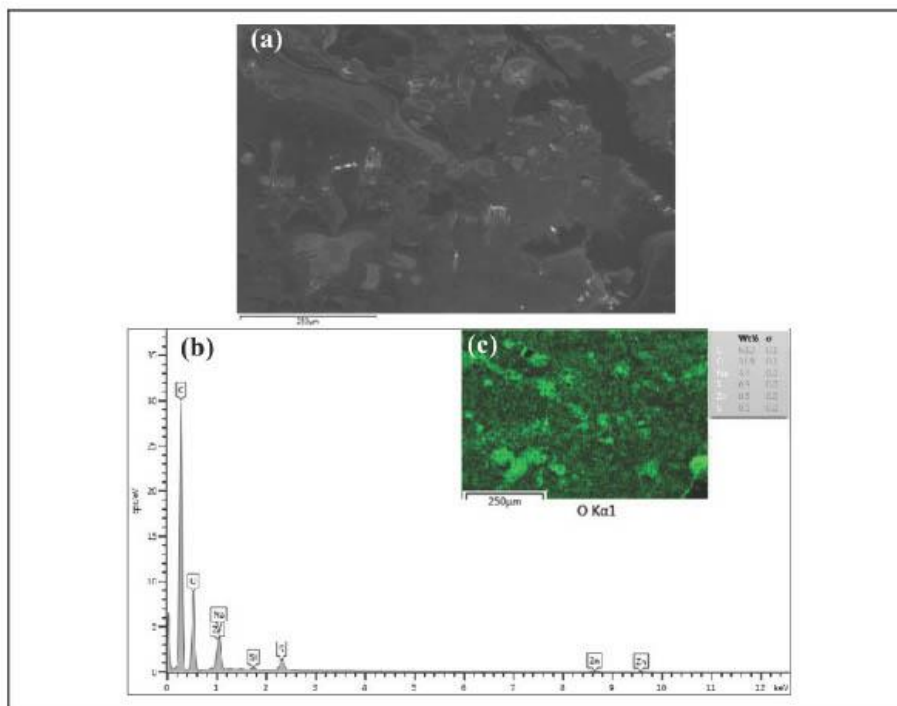


Figure 10. SEM micrographs of WSR with 15 phr SAPC: (a) surface (fracture images; magnification $\times 250$; scale bar 250 μm) and (b and c) SEM/EDX of WSR with X-ray mapping of O. WSR: water-swellaable rubber; SAPC: superabsorbent polymer composite; SEM: scanning electron microscope; EDX: energy-dispersive X-ray.

Morphological property

Figure 9 depicts SEM micrographs of the WSR containing 15 phr SAPC. It was clearly seen that the WSR images, after having an immersion in water, both surface Figure 9(b) and cross section Figure 9(d) are existing the vestiges due to the removal of SAPC. Poor dispersion before and the detachment of SAPC after immersion in water are seen in this sample. The loss of SAPC by immersion in water suggests that the bonding of SAPC to the matrix was very poor. The poor dispersion of SAPC along with the weak bonding also reduced tensile strength and elongation at break.

Figure 10 shows the SEM micrographs of WSR with 15% SAPC (Figure 10(a)) presented that the fracture surfaces of WSR showed fine dispersion with irregular shapes and sizes of particles in the rubber. The EDX analysis was also executed to establish the dispersion of SAPC in WSR (Figure 10(b) and (c)) and the X-ray mapping of O the bright green bars over the darker green background showed the distribution of O in the rubber matrix.

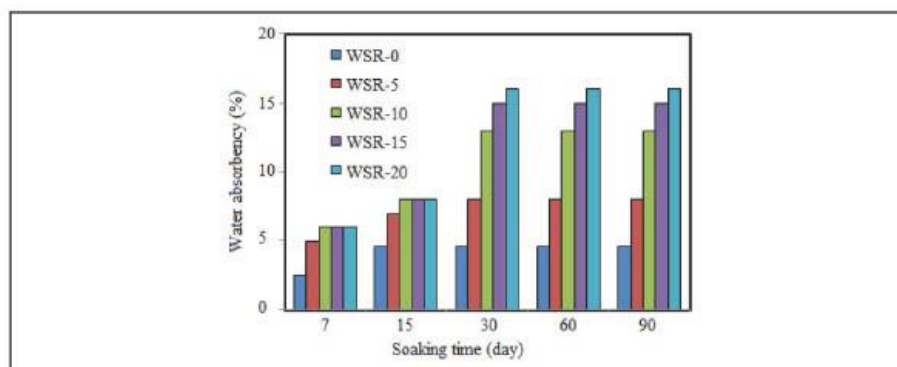


Figure 11. Second water absorbency of WSR with various SAPC loadings and soaking times. WSR: water-swellable rubber; SAPC: superabsorbent polymer composite.

Figure 11 shows the second water absorbency of WSR with various contents of SAPC for different soaking times. The WSR with 20 phr SAPC content had 16% second water absorbency while the first was 34% (2.13-fold difference). The loss of absorbency was due to the loss of SAPC from WSR during first immersion, as seen in SEM micrographs and in weight loss.

Conclusions

1. WSR was successfully prepared by mechanical blending of ENR with 50% oxirane ring (ENR-50) as the rubber matrix and SAPC as the dispersed water-absorbing filler, associated also with an activator, accelerator, and cross-linking agent.
2. The SAPC was first synthesized by grafting copolymerization of PAM onto HEC backbones with association of bentonite clay composites. The compounding was carried out in an internal mixer (Brabender Plasticorder) at 40°C, 60 r/min rotor speed, and 80% fill factor.
3. The first and second water absorbencies of WSR increased with SAPC content, but the second water absorbency was much lower than the first due to the loss of SAPC from WSR during first immersion. The weight loss increased with SAPC content.
4. The mechanical properties, tensile strength, and elongation at break decreased with increasing the SAPC contents, while modulus had an opposition. The morphology of the blends after water immersion clearly evidenced the loss of dispersing SAPC from WSR, which negatively affected the second water absorbency, tensile strength, and elongation at break.

Declaration of conflicting interests

The author(s) declared no potential conflicts of interest with respect to the research, authorship, and/or publication of this article.

Funding

The author(s) disclosed receipt of the following financial support for the research, authorship, and/or publication of this article: This work was financially supported by Graduate School Prince of Songkla University.

ORCID iDAjaman Adair  <https://orcid.org/0000-0001-9786-8831>**References**

1. Wang B, Liu Z, Liao S, et al. Preparation and properties of water-swellaable natural rubber vulcanizates. *Mater Res Innov* 2015; 19(8): 198–203.
2. Wang C, Zhang G, Dong Y, et al. Study on a water-swellaable rubber compatibilized by amphiphilic block polymer based on poly(ethylene oxide) and poly(butyl acrylate). *J Appl Polym Sci* 2002; 86(12): 3120–3125.
3. Park JH and Kim D. Preparation and characterization of water-swellaable natural rubbers. *J Appl Polym Sci* 2001; 80(1): 115–121.
4. Vudjunga C, Chaisuwana U, Pangana U, et al. Effect of natural rubber contents on biodegradation and water absorption of interpenetrating polymer network (IPN) hydrogel from natural rubber and cassava starch. *Energy Procedia* 2014; 56: 255–263.
5. Saijun D, Nakason C, Kaesman A, et al. Water absorption and mechanical properties of water-swellaable natural rubber. *Songklanakar J Sci Technol* 2009; 31(5): 561–565.
6. Khongthong S and Fungchonlajit N. Water swollen natural rubber. *Walailak J Sci Tech* 2008; 5(1): 67–75.
7. Nakason C, Nakaramontri Y, Kaesaman A, et al. Synthesis and characterization of water swellaable natural rubber vulcanizates. *Eur Polym J* 2013; 49: 1098–1110.
8. Wang G, Li M and Chen X. Effects of fillers on mechanical properties of a water swellaable rubber. *J Appl Polym Sci* 1999; 72(4): 577–584.
9. Liu C, Ding J, Zhou L, et al. Mechanical properties, water-swelling behavior, and morphology of water-swellaable rubber prepared using crosslinked sodium polyacrylate. *J Appl Polym Sci* 2006; 102(2): 1489–1496.
10. Zhang Z, Zhang G, Li D, et al. Chlorohydrin water-swellaable rubber compatibilized by an amphiphilic graft copolymer. II. Effects of PVA-g-PBA and CPA on water-swelling behaviors. *J Appl Polym Sci* 1999; 74(13): 3145–3152.
11. Zhang G, Zhang Z, Xie F, et al. Chlorohydrin water swellaable rubber compatibilized by an amphiphilic graft copolymer. I. Synthesis and characterization of compatibilizer PVA-g-PBA. *J Appl Polym Sci* 2000; 75(8): 977–986.
12. Zhang Z, Zhang G, Wang C, et al. Chlorohydrin water swellaable rubber compatibilized by an amphiphilic graft copolymer. III. Effects of PEG and PSA on water- swelling behavior. *J Appl Polym Sci* 2001; 79(14): 2509–2516.
13. Ren W, Zhang Y, Peng Z, et al. Investigation on the water swelling properties of chlorinated polyethylene modified by in situ formed sodium acrylate. *Polym Test* 2004; 23(7): 809–816.
14. Nnadi F and Brave C. Environmentally friendly superabsorbent polymers for water conservation in agriculture lands. *J Soil Sci Environ Manage* 2011; 2(7): 206–211.
15. Akhter J, Mahmood K, Malik KA, et al. Effect of hydrogels amendment on water storage of sandy loam and loam soils and seedling growth of barley, wheat and chickpea. *Plant Soil Environ* 2004; 50(10): 463–469.
16. He P, Zhang Y and Hu R. Synthesis and swelling properties of grafting-type and crosslinking-Type water-swellaable elastomers. *J Appl Polym Sci* 2007; 104: 2637–2642.
17. Adair A, Kaesaman A and Klinpituksa P. Superabsorbent materials derived from hydroxyethyl cellulose and bentonite: Preparation, characterization and swelling capacities. *Polym Test* 2017; 64: 321–329.

18. Lopez-Manchado MA, Herrero B and Arroyo M. Preparation and characterization of organoclay nanocomposites based on natural rubber. *Polym Int* 2003; 52: 1070–1077.
19. Du A, Peng Z, Zhang Y, et al. Water swelling rubber prepared by in situ formed sodium acrylate in EVM. *Elastom Plast* 2003; 56(6): 316–321.
20. Othman AB and Lye CB. Effect of pH coagulation and sulphuric acid as a coagulant on natural rubber properties. *J Rubb Res Inst Malaysia* 1980; 28(3): 109–118.
21. Ahmed K, Nizami SS, Raza NZ, et al. Cure characteristics, mechanical and swelling properties of marble sludge filled EPDM modified chloroprene rubber blends. *Adv Mater Phys Chem* 2012; 2: 90–97.
22. Wang G, Li M and Chen X. Preparation and water-absorbent properties of a water-swellaable rubber. *J Appl Polym Sci* 1998; 68(8): 1219–1225.
23. Heideman G, Datta RN, Noordermeer JWM, et al. Influence of zinc oxide during different stages of sulfur vulcanization elucidated by model compound studies. *J Appl Polym Sci* 2005; 95: 1388–1404.
24. Arroyo M, Lopez-Manchado MA, Valentin JL, et al. Morphology/behavior relationship of nanocomposites based on natural rubber/epoxidized natural rubber blends. *Compos Sci Technol* 2007; 67: 1330–1339.
25. Hamzah R, Abu Bakar M, Khairuddean M, et al. A structural study of epoxidized natural rubber (ENR-50) and its cyclic dithiocarbonate derivative using NMR spectroscopy techniques. *Molecules* 2012; 17: 10974–10993.

Appendix C: Article 3**Influences of neutralization of superabsorbent hydrogel from hydroxyethyl cellulose on water swelling capacities****Influences of neutralization of superabsorbent hydrogel from hydroxyethyl cellulose on water swelling capacities**

Cite as: AIP Conference Proceedings **1868**, 020012 (2017); <https://doi.org/10.1063/1.4995098>
Published Online: 04 August 2017

Ajaman Adair, Pairote Klinpituksa and Azizon Kaesaman



View Online



Export Citation

ARTICLES YOU MAY BE INTERESTED IN

[Morphological effect on swelling behaviour of hydrogel](#)

AIP Conference Proceedings **1584**, 153 (2014); <https://doi.org/10.1063/1.4866123>

[Superabsorbent hydrogel composite based on copolymer cellulose/poly \(vinyl alcohol\)/CNT](#)

AIP Conference Proceedings **1729**, 020046 (2016); <https://doi.org/10.1063/1.4946949>

[The effect of monomer types and loading on the characterization and absorption of superabsorbent polymer based on waste polystyrene foam](#)

AIP Conference Proceedings **1985**, 030019 (2018); <https://doi.org/10.1063/1.5047177>

Influences of Neutralization of Superabsorbent Hydrogel from Hydroxyethyl Cellulose on Water Swelling Capacities

Ajaman Adair^{1,a}, Pairote Klinpituksa² and Azizon Kaesaman¹

¹*Department of Rubber Technology and Polymer Science, Faculty of Science and Technology, Prince of Songkla University, Pattani 94000 Thailand.*

²*Department of Science, Faculty of Science and Technology, Prince of Songkla University, Pattani 94000 Thailand.*

^a Corresponding author : nadair1969@gmail.com

Abstract. In this research, superabsorbent hydrogels were synthesized by graft copolymerization of hydroxyethyl cellulose (HEC) and polyacrylamide (PAM) under the initiation of potassium persulfate (KPS). The polymer networks were constructed using *N,N'*-methylenebisacrylamide (MBA), and the reaction was performed in an aqueous solution. The extent of grafting products was evaluated from grafting efficiency (%GE) and percentage of add-ons at HEC/AM ratios of 1: 10. The water swelling capacities, in terms of swelling capacity and weight loss, of resultant superabsorbent polymers (SAPs) after solvent extraction were determined for swelling behaviors. The result showed that the SAP had poor water absorption of approximately up to 23 g/g. To enhance swelling capacity of SAPs, an alkaline hydrolysis was done by using two types of alkaline bases, i.e., 2 M NaOH and 2 M KOH solution. The obtained treatment SAPs were neutralized by washing with distilled water and 0.5 M HCl until the liquors pH was nearly 7. They were found that the treatment SAPs showed the highest water absorption up to 317 g/g. Influences of various fluids pH values ranging between 4 and 10, on water swelling capacities of SAPs were also investigated. Under optimal pH value, the highest water absorptions of SAP was 382 g/g. To confirm the grafting reaction of PAM onto HEC backbone, FT-IR analysis was used. The results revealed absorption bands of the HEC backbone and new absorption bands from the grafted copolymer. Furthermore, the FT-IR spectrum was proved that washing with distilled water can alter the chemical functional group of SAPs.

INTRODUCTION

The functional materials that can absorb and retain a large amount of fluid comparing to its weight, namely hydrogel or superabsorbent polymers (SAPs). They were basically described as a loose three dimensional network structures of hydrophilic polymer chains [1, 2]. In the 1980s, water absorption materials were derived from cellulosic or fiber-based products. Logical choices were tissue paper, cotton, sponge, and fluff pulp. These types of materials had low water absorption capacity up to 20 times their initial weight.

In the 1960s, the water conservation materials were firstly invented by the United States Department of Agriculture for soils amendment. They worked hard and developed a polymer based on the grafting of polyacrylonitrile onto starch backbone. This new material can absorb a large of water more than 400 times its weight without releasing liquid fluid even under high pressure. The SAPs were originally synthetic crosslinked polyacrylic acid and polyacrylated derivatives of petroleum products which have a tendency to increase the cost endlessly. They are able to absorb large quantities of water without dissolving, even exceeding 1,000 fold of their dry weight [3].

Because of its excellent swelling behaviors, the SAPs have prompted much attention both fields of academic and industries to produce for diverse utilizations. For example they are widely proposed for horticultural purposes over the last five decades with the idea to improve water availability for plants [4]. Several possible applications of SAPs have been described corresponding applications such as in disposable baby diapers, in agriculture as a soil amendment [5], in controlled release of drugs as a carrier [6], in coal dewatering [7,8], in waste water treatment [9], in cosmetic and absorbent pads [10], and in gel electrolyte membranes [11]. According to their structure, SAPs were

definitely divided into three main types, namely natural polymers (polysaccharide derivatives), semi-synthetic polymers (cellulosic primitive derivatives), and synthetic polymers [12]. Most of the commercial SAPs are synthetic polyacrylate-based products, non degradable and considered as potential pollutants for the environments. Because of large attention in environmental protection issues, biodegradable SAPs have stood up interest for potential application in various fields. Although all types of SAP have no direct threat to human life, systematical disposal of synthetic SAPs waste is a source of environmental pollutants [13, 2]. This problem has prompted polymer technologist to produce SAP that reduce the need to have an actual disposal system. The naturally occurring SAPs are attractive route due to their unique renewability and biodegradability. Amongst them, polysaccharides have been employed due to availability in large feedstock, renewability and biodegradability. Hydroxyethyl cellulose (HEC) is modified cellulose with abundant reactive hydroxyl groups, they can be grafted with hydrophilic vinyl monomers to produce materials with excellent properties [14].

In this work, Hydroxyethyl cellulose was finely used to prepare SAP by grafting copolymerization with polyacrylamide, via solution radical polymerization. The aim of this study was to investigate the main factors that affect the swelling capacity of SAP including types of alkaline hydrolysis treatment and neutralization condition after alkaline treatment. Water swelling capacities of obtained SAPs were determined under the different pH values in range of 4-10. FTIR determination was utilized to characterize and confirm successful graft copolymerization.

EXPERIMENTAL

Materials

Hydroxyethyl cellulose (HEC) (92% purity), Merck KGaA Corporate (Germany); acrylamide (AM) for synthesis (99% purity) Merck K GaA Corporate (Germany); potassium persulfate (KPS) assay (99% purity, radical initiator), Ajax Finechem; N,N'-methylenebisacrylamide (MBA) (98% purity, crosslinker), Fluka (Switzerland); Bentonite, Sigma Aldrich, (USA); sodium hydroxide (99% purity), Fluka (Switzerland).

Preparation of SAP

The reaction took place under nitrogen gas atmosphere and HEC was firstly dried in a hot air oven to constant weight, 12.0 g was dissolved in 400 mL of distilled water in a four-neck reactor, equipped with a mechanical stirrer, nitrogen gas channel, condenser and dropping funnel. They were at ambient temperature and stirred at 100 rpm for 30 minutes until slurry forming and ensure that oxygen gas, which would rapidly form radicals, clearly removed. The slurry was continuously heated to 60° C and kept constant for 30 minutes. Subsequently, 10.0 g of KPS as initiator (0.3 mol/100 g HEC) was added and stirred continuously for 10 minutes to exactly generate radicals onto HEC backbone. To prevent immediately undesired reaction, the temperature was decreased to 50° C then the solution of 120 g AM with MBA crosslinker (0.1 mmol/100 g HEC) in dropping funnel was further added, the temperature was raised to 70° C to initiate the actual reaction. This reaction temperature was constantly kept until the graft copolymerization reaction absolutely archived.

Purification of grafted copolymer

The crude product in gel form was cut into small pieces and subjected to Soxhlet extraction for 24 hrs using acetone, and using 40% ethanol/water as the solvents, to remove the homopolymer (PAM), and unreacted AM, respectively. The percentage of grafting efficiency (%GE) and percentage of add-on were calculated using equations (1) and (2) [15].

$$\text{Grafting efficiency}(\%) = \frac{M_2 - M_0}{M_1 - M_0} \times 100 \quad (1)$$

$$\text{Add-ons}(\%) = \frac{M_1 - M_0}{M_2} \times 100 \quad (2)$$

Where M_0 , M_1 and M_2 are the masses (in gram) of initial HEC backbone, HEC-g-PAM sample before extraction of homopolymer, and after extraction of homopolymer, respectively.

Alkaline treatment

Two types of alkaline base i.e., NaOH and KOH, were used to hydrolyze SAP. The resultant grafted copolymer with amide form had poor water swelling capacity of approximately up to 23 g/g. To improve the swelling capacity of the SAPs, approximately 50 g of grafted copolymer was transferred into round bottle reactor and treated separately with 1.0 L of 2 M NaOH solution and 1.0 L of 2 M KOH solution, stirred at 100 rpm, temperature at 70° C for 120 minutes. The final concentration of purified grafted copolymer in both type alkaline solution were calculated as percentage (w/w) of the total mass. The obtained SAPs were neutralized by washing three times with distilled water and 0.5 M HCl until the liquors pH was nearly 7. The treated SAPs were tested for water swelling capacity.

Measurements of swelling capacity and weight loss of SAP

For swelling capacity measurements, the dried powdery SAP of approximately 0.2 g in a tea bag was immersed in distilled water (pH=7), allowed to reach swelling equilibrium, the resultant SAPs that gave the highest water absorption was chosen for testing at various pH values ranging from 4 to 10 at room temperature and the final state was measured to determine the degree of water absorption (S_w) using equation (3). When measurement percentage of weight loss (% L_w), the swollen state SAP was dried to unchange and determine using equation (4) [9].

$$S_w = \frac{W_2 - W_1}{W_1} \quad (3)$$

$$L_w(\%) = \frac{W_1 - W_2}{W_1} \times 100 \quad (4)$$

Where W_1 and W_2 denote the weights of the sample before and after water absorption and W_3 are the dried weight of sample after first water absorption.

Measurements deswelling of SAP

For the deswelling measurements, the SAP equilibrium swollen in each various pH values of aqueous solution (ranging from 4-10) were transferred and placed on watch glass at ambient temperature (29° C) for 48 hrs. The weight change of SAPs was measured gravimetrically after time rested. The water retention was calculated in terms of the percentage of water retention (WR%) by using equation (5) [16].

$$WR(\%) = \frac{(W_t - W_d)}{(W_e - W_d)} \times 100 \quad (5)$$

Where W_d is the weight of the dry SAP, W_e and W_t denote the weights of the swollen SAP at equilibrium and deswollen SAP at time t, respectively.

RESULTS AND DISCUSSION

Infrared spectroscopy

FTIR analysis was utilized to confirm grafting copolymerize of PAM onto HEC backbone by comparison of all FTIR spectra. Figure 1 showed both the FTIR spectrum of HEC backbone and HEC-g-PAM, it was found that some important absorption peaks of HEC were changed after grafted copolymerization. The FTIR of HEC showed broad band absorption around 3560-3320 cm^{-1} was assigned to -OH stretching vibrations with hydrogen bonding and the

strongest absorption peak at 2879 cm^{-1} was ascribed to $-\text{O}-\text{H}$ bending vibrations. The intense bands around 1020 cm^{-1} was ascribed to $-\text{C}-\text{OH}$ stretching vibrations of HEC [17, 18]. After graft copolymerization, the broad band around $3560\text{--}3320\text{ cm}^{-1}$ had slightly exchanged due to $\text{N}-\text{H}$ of amide stretching vibrations emerging as a shoulder band at 3195 cm^{-1} for the graft copolymer. In addition, for HEC-g-PAM the absorption peaks at 1020 cm^{-1} and 2879 cm^{-1} had disappeared and new absorption bands substituted at 1667 and 1120 cm^{-1} were assigned to $-\text{C}=\text{O}$ stretching vibrations of amide functional group and asymmetric stretching vibrations of ether $\text{C}-\text{O}-\text{C}$ in graft copolymer [19]. Besides of this, the broad band of HEC-g-PAM was emerged strongly at 1443 cm^{-1} due to combining PAM CH_2 bending vibrations.

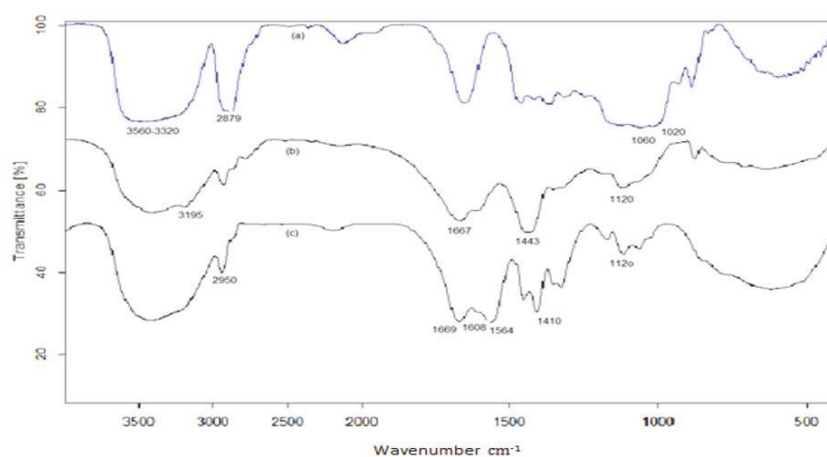


Figure 1. FTIR spectra of (a) HEC, (b) HEC-g-PAM and (c) HEC-g-PAM after hydrolysis alkaline treatment and washing with distilled water

After alkaline hydrolysis, and washing for three times with distilled water, new absorption peaks, especially the fingerprint region, were observed. From figure 2 it can be seen that dominant absorption peaks at 1410 cm^{-1} were assigned to $-\text{C}-\text{OH}$ bending vibrations of carboxylic groups which was directly emerged interchangeable carboxylate group. The changes attributed to the stretching of $\text{C}-\text{O}-\text{H}$ and the region assigned to stretching of $\text{C}-\text{O}-\text{C}$ confirmed successful PAM moieties graft copolymerized onto HEC backbone.

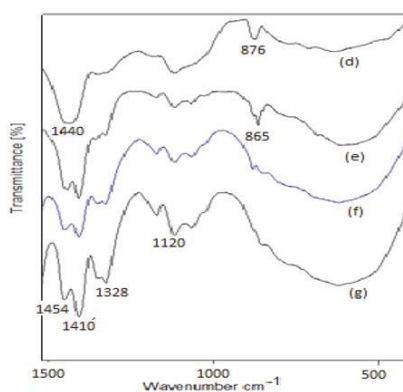


Figure 2. FTIR spectra of (d) HEC-g-PAM and HEC-g-PAM after alkaline treatment were affected by wash cycles with distilled water: (e) one washing, (f) two washings, or (g) three washings.

The effect of types of alkaline treatment and neutralization on swelling capacities of SAP

Studies have showed that the ultimate swelling capacity of SAPs increases dramatically after alkaline treatment [2]. The results showed that the highest swelling capacities of SAP were found after alkaline treatment with 0.5 M NaOH and washing 2 times with distilled water (figure 3). This is due to introduction of alkaline ion, sodium or potassium into the polymer network and subsequent development of negatively charged carboxyl groups. These groups set up an electrostatic repulsion between negative charges which tends to expand the polymer network. In fact the presence of alkaline cation, usually Na^+ acts as an opposite factor for an exceedingly large electrostatic repulsion. The dissociated sodium carboxylate groups in polymer network increase osmotic pressure in polymer which was effectively increased swelling capacity of SAP.

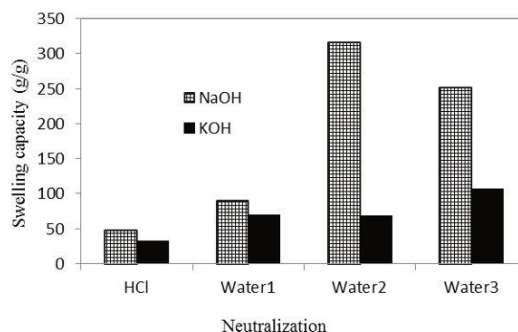


Figure 3. Swelling capacities of SAP after alkaline treatment with 0.5 M NaOH and 0.5 M KOH and neutralized with 0.5 M HCl and wash cycles with distilled water: 1 washing, 2 washings, or 3 washings.

The Effects of pH value on water swelling capacity

Research has indicated that water swelling capacity of SAPs was responsive to environmental pH [20]. So, the swelling behavior of the SAPs was investigated at various pH values ranging from 4 to 10 at ambient temperature. Figure 4. It can be clearly observed that pH value are influence swelling capacity of SAP, highest swelling capacity was found at pH solution 8 up to 382 g/g. This due to solutions containing a lot of ionic species (HCl and NaOH), as the swelling capacity of SAPs are decreased by ionic strength. At low pH, the swelling capacity decreases as its carboxylate group on the polymer network is protonated by HCl, leading the polymer becomes hydrophobic. At high pH, the swelling capacity also decreases by "charge screening effect" of excess Na^+ in the solution, which shields the carboxylate anions and prevents effective anion-anion repulsion. At pH=8, some of carboxylic acid groups are ionized and the electrostatic repulsion between COO^- groups causes an enhancement of the swelling capacity [21].

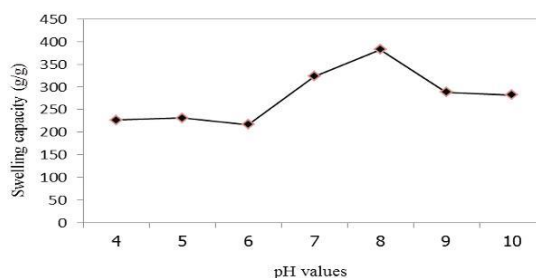


Figure 4. Swelling capacities of SAP measurement at different pH-values after alkaline treatment with 0.5 M NaOH and neutralized with distilled water.

The deswelling of SAP

The deswelling measurements of SAP was determined in terms of the percentage of water retention which of is amount of final water retaining in SAP, after equilibrium swollen in various pH solution and placed on watch glass at temperature of 29° C for 48 hrs. Studies have indicated that the deswelling response rate of the swollen SAP [22]. Figure 5 exhibited percentage of water retention, the result showed that pH value was not directly affected to deswelling of SAP. Some deviations observed can be ascribed to the fact that, as the gel swells it loses strength. As a result, the stresses imposed producing SAP fragmentation leading to erratic results.

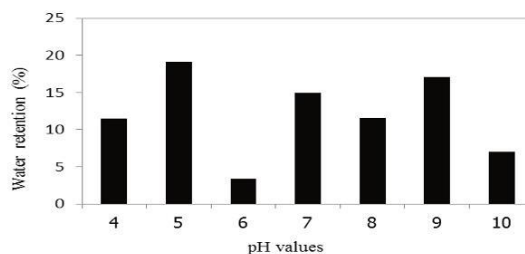


Figure 5. Water retention of SAP measurement after equilibrium swelling in each various pH values at room temperature and 48 hours

CONCLUSION

In summary, superabsorbent polymers were successfully copolymerized by graft copolymerization of polyacrylamide onto hydroxyethyl cellulose in the presence of crosslinker MBA using KPS as an initiator. The resulting SAPs produced at 1: 10 ratios of HEC : AM, was extensively characterized and determined for swelling behaviors including swelling capacity and water retention. The different types of alkaline treatment such as NaOH solution and KOH solution were investigated for swelling behaviors as important as neutralization system. It was found that the SAP with NaOH solution treatment and washing two times with distilled water exhibited highest water swelling capacity up to 317 g/g, while it was significantly increased water uptakes in solution of pH-8 up to 382 g/g. FT-IR determination was confirmed entirely grafted PAM onto HEC backbone. Furthermore FT-IR spectrum was proved that washing with distilled water can alter the chemical functional group of SAPs.

ACKNOWLEDGEMENTS

This work was supported and funded by the Faculty of Science and Technology, and Graduate School, Prince of Songkla University, Thailand and Faculty of Science Technology and Agriculture, Yala Rajabhat University, Thailand

REFERENCES

1. S. Kiatkamjornwong., *Sci. Asia*, **33**, 39-43, (2007).
2. C. Nakason, T. Wohming, A. Kaesaman, and S. Kiatkamjornwong, *Carbohydr. Polym.*, **81**, 348-357, (2010).
3. H. Wack, and J. Bertling, , *Noordwijkse Zee*, The Netherlands, April **18-20**, 1-9, (2007).
4. M. J. Zohuriaan-Mehr, and K. Kabiri, *Iranian Polym. J.*, **17** (6), 451-477, (2008).
5. G. Cannazza, A. Cataldo, E. D. Benedetto, C. Demitri, M. Madaghiele, and A. Sannino, *Water*, **6** (7), 2056-2069, (2014).
6. C. Chang, and L. Zhang, *Carbohydr. Polym.*, **84**, 40-53, (2011).
7. F. Peer, and T. Venter, *J. South African Institute of Mining and Metallurgy*. 403-410, (2003)
8. S. Devasahayam, M. Anas Ameen, T. Vincent Verheyen, and S. Bandyopadhyay, *Minerals*. **5**, 623-636, (2015).
9. W. Wang, J. Wang, Y. Kang, and A. Wang, *Composites: Part B*, **42**, 809-818, (2011).
10. R. H. Todd, and S. K. Daniel, *Progress and Challenges. Polym.*, **49**, 1993-2007, (2008).
11. M. A. Navarra, C. D. Bosco, J.S. Moreno, F. M. Vitucci, A. Paolone, and S. Panero. *Membranes*, **5**, 810-823, (2015).
12. R. L. Mikkelsen, *Nutr. Cycl. Agroecosy*, **38**(1), 53-59, (1994).
13. F. Nnadi, and C. Brave, *J. Soil Sci. and Environ. Manage.* **2**(7), 206-211, (2011).
14. S. B. Lin, L. H. Wu, K. D. Yao, K. Y. Cai, M. C. Xiao, and C. J. Jiang, *Compos. Interface*, **11**, 271-276, (2004).
15. D. Pathania, and R. Sharma, *Adv. Mater. Lett.*, **3**(2), 136-142, (2012).
16. X. Qi, W. Wei, J. Li, G. Zuo, X. Pan, T. Su, J. Zhang, and W. Dong, *Mol. Pharm.*, 1-42, (2017).
17. J. A. Heridia-Guero, J. A. Benitaze, E. Dominguez, I. S. Bayer, R. Cingolani, A. Athanassiou, and A. Heridia, *Spectroscopy. Asia*, **12**(4), 8-11, (2016).
18. S. C. Chen, Y. C. Wu, F. L. Mi., Y. H. Lin, L. C. Yu, and H. W. Sung, *J. Control. Release*, **96**, 285- 300, (2004)
19. E. S. Dragon, M. M. Lazar, M. V. Dinu, and F. Doroftei, *Chem. Eng. J.* **204-206**, 198-209, (2012).
20. F. Soleimani, and M. Sadeghi, *J. Biomater. Nanobiotechnol.*, **3**, 310-314, (2012).
21. F. Wu, Y. Zhang, L. Liu, and J. Yao, *Carbohydr. Polym.*, **87**, 2519- 2525, (2012).
22. Y. Dogu, and O. Okay, *J. Appl Polym. Sci.*, **99**, 37-44, (2005).

VITAE

Name Ajaman Adair

Student ID 6020330101

Educational Attainment

Degree	Name of Institution	Year of Graduation
Bachelor of Education	Srinakharinwirot University	1995
Master of Science	Prince of Songkla University	2001

Scholarship Awards during Enrolment

This Research was funded by Graduate school of Prince of Songkla University, Pattani Campus

Work – Position and Address (If Possible)

Asst. Prof. in Organic Chemistry and now being a Lecturer at Yala Rajabhat University in Cosmetic Science and Beauty Program, Faculty of Science Technology and Agriculture. 133 Tesbal 3 Road, Satang, Muang, Yala.

List of Publication and Proceeding (If Possible)

1. Superabsorbent materials derived from hydroxyethyl cellulose and bentonite: Preparation, characterization and swelling capacities
2. Water-swellaable rubber blend from epoxidized natural rubber and super-absorbent polymer composite
3. Influences of neutralization of superabsorbent hydrogel from hydroxyethyl cellulose on water swelling capacities